University of Southampton

Faculty of Environmental and Life Sciences

School of Biological Sciences

Novel Antibacterial Interventions against *Pseudomonas aeruginosa* Infections by targeting c-di-GMP and unravelling DSF Signalling Pathway.

by

Ying Hu

Thesis for the degree of Doctor of Philosophy

March 2024

University of Southampton

Abstract

Faculty of Environmental and Life Sciences

School of Biological Sciences

Doctor of Philosophy

Novel Antibacterial Interventions against *Pseudomonas aeruginosa* Infections by targeting c-di-GMP and unravelling DSF Signalling Pathway.

by

Ying Hu

Pseudomonas aeruginosa (*P. aeruginosa*) is an opportunistic bacterial pathogen causing acute and chronic infections in immunocompromised and hospitalized patients. Infections due to *P. aeruginosa* and other drug-resistant bacteria pose a major threat to healthcare systems worldwide and the development of new effective antibacterial agents is urgently needed. *P. aeruginosa* can also form biofilms that promote antibiotic tolerance and chronic infection, thereby posing additional major challenges for treatment.

P. aeruginosa regulates the production of virulence factors through N-acyl homoserine lactone and quinoline PQS signal-mediated quorum sensing and communicate between species through cis-2-unsaturated fatty acids of the diffusible signal factor (DSF) family. This thesis first focused on the DSF signalling mechanism of *P. aeruginosa* infection. In order to gain a deeper understanding of the communication regulatory mechanism of DSF signalling in *P. aeruginosa* infection, this work has focused on the role of the sensor kinase PA1396 in DSF perception. Further genomic analysis identified a gene encoding a response regulator, PA1397, upstream of PA1396, with a receptor domain and a DNA-binding domain. In order to systematically study the functions of DSF-related genes in *P. aeruginosa*, this study used a gene mutation and complementation strategy to mutate and complement the signalling orphan Hpt domains hptA, hptB, and hptC, and the results showed that these genes are highly active in *P. aeruginosa* and plays an important regulatory role in toxicity and motility, especially hptB. The functional role of the PA1397 gene and its interaction with DNA were further studied, and experiments proved that it may be involved in transcriptional regulation, suggesting its importance in DSF perception. Meanwhile, a comprehensive understanding of the signalling mechanisms of DSF perception in *P. aeruginosa* could provide valuable insights into the regulation of its virulence and facilitate the development of new therapeutic strategies. These findings lay the foundation for the development of antibacterial drugs against drug-resistant bacteria using signalling molecules as new pathways.

The second focus of this thesis was to determine the role of c-di-GMP, a signalling molecule that regulates its fitness, antibiotic resistance, and biofilm formation, on the ability of *P. aeruginosa* to cause infection in a co-culture model of infection using human bronchial epithelial cells. *P. aeruginosa* uses c-di-GMP to regulate the expression of a series of genes to adapt to different

environmental conditions, including antibiotic stress. Therefore, reducing intracellular c-di-GMP levels is considered a promising strategy to combat antibiotic-resistant *P. aeruginosa* infection. This paper also constructed and optimized the co-culture screening model to provide a physiologically realistic environment for the formation of bacterial biofilms, thereby improving the transferability of *in vitro* drug screening, and identified a promising compound that modulates c-di-MP levels and reduced virulence in the co-culture model.

Based on the above research contents, this thesis provides an important theoretical and experimental basis for the molecular regulation of *P. aeruginosa* infection and the development of antibacterial drugs by exploring the regulatory mechanisms of DSF and c-di-GMP signalling in *P. aeruginosa* infection. At the same time, research into new potential therapeutic drugs has also been carried out. These findings are of great significance for combating the challenge of drug-resistant bacteria and improving clinical treatment effects.

Table of Contents

Table of Contents ..... **i**

Table of Tables ..... **vii**

Table of Figures ..... **ix**

Research Thesis: Declaration of Authorship ..... **xiii**

Acknowledgements ..... **xv**

Definitions and Abbreviations ..... **xvii**

Chapter 1 Introduction **1**

1.1 *Pseudomonas aeruginosa* as an opportunistic human pathogen 1

1.1.1 Genome features of *Pseudomonas aeruginosa*. 1

1.1.2 Secretion system in *Pseudomonas aeruginosa*. 3

1.1.3 Biofilm formation in *Pseudomonas aeruginosa*. 4

1.1.4 Motility in *Pseudomonas aeruginosa*. 6

1.1.5 Antibiotic resistance in *Pseudomonas aeruginosa*. 7

1.2 Roles of signalling pathways in *Pseudomonas aeruginosa* 8

1.2.1 Quorum sensing of *Pseudomonas aeruginosa* 9

1.2.2 Two-component system of *Pseudomonas aeruginosa*. 10

1.2.3 C-di-GMP of *Pseudomonas aeruginosa* 11

1.2.3.1 C-di-GMP metabolism 11

1.2.3.2 C-di-GMP regulation of motility-sessility switch in *Pseudomonas aeruginosa.* 12

1.2.3.3 C-di-GMP plays diverse physiological roles in *Pseudomonas aeruginosa.* 13

1.3 Diffusion signal factor signalling in *Pseudomonas aeruginosa.* 15

1.3.1 The Diffusion signal factor family in bacteria 15

1.3.2 Diffusion signal factor mediated interspecies communication with *Pseudomonas aeruginosa.* 17

1.4 Infection models of *Pseudomonas aeruginosa* 19

1.4.1 *In vitro* models for studying *Pseudomonas aeruginosa* infections. 19

1.4.2 *In vivo* models for *Pseudomonas aeruginosa* infection. 21

1.5 The quest for novel antimicrobial compounds 22

1.5.1 Novel targets: The role of cyclic di-GMP signalling in *P. aeruginosa*. 23

1.5.2 The role of natural products in antibacterial drug discovery. 24

1.5.3 Screening assays as a tool for drug discovery. 25

1.6 Objectives and aims. 27

Chapter 2 Investigating the signal transduction mechanism of Diffusible signal factor perception in *Pseudomonas aeruginosa* 29

2.1 Abstract 29

2.2 Hypothesis 30

2.3 Materials and Methods 30

2.3.1 Bioinformatics analysis 30

2.3.2 Bacterial strains and cell culture conditions 30

2.3.3 DNA manipulation 32

2.3.4 Mutagenesis of *hptA*, *hptB* and *hptC* genes 36

2.3.5 Complementation of mutants Δ*hptA*, Δ*hptB* and Δ*hptC* 37

2.3.6 In *vitro* phenotype assays 38

2.3.7 Phenotype assays based on co-culture model. 39

2.3.8 Statistical Analysis 40

2.4 Results 41

2.4.1 Bioinformatics analysis of DSF signalling pathway 41

2.4.2 Construction of Δ*hptA*, Δ*hptB* and Δ*hptC* mutants 42

2.4.3 Construction of Δ*hptA*, Δ*hptB* and Δ*hptC* complementary genes 46

2.4.4 The mutants and complementary strains have no effect on growth. 49

2.4.5 The mutants have reduced swarming motility. 50

2.4.6 Human bronchial epithelial cell and *P. aeruginosa* co-culture biofilm model was constructed. 51

2.4.7 The mutants and complementary strains have affected on bacterial virulence during infection. 52

2.4.8 The impact of different mutations on human IL-6, IL-8, and TNF-α protein levels. 54

2.5 Conclusion and Discussion 56

Chapter 3 Differential Gene Expression and Protein-DNA Interaction Analysis Reveals the Regulatory Role of PA1397 in *Pseudomonas aeruginosa*.59

3.1 Abstract 59

3.2 Hypothesis 60

3.3 Materials and Methods 61

3.3.1 Bacteria collection 61

3.3.2 RNA extraction and DNA-free treatment 61

3.3.3 RNA sequencing and analysis 61

3.3.4 Statistical Analysis 62

3.3.5 Quantitative Real-Time PCR 62

3.3.6 Protein expression 65

3.3.7 Protein purification by affinity chromatography 65

3.3.8 Protein purification by centrifugation 66

3.3.9 Binding DNA preparation 66

3.3.10 Electrophoretic mobility shift assays 66

3.4 Results 68

3.4.1 RNA-Seq Data Analysis and Validation. 68

3.4.2 RNA-seq Analysis Reveals Differential Gene Expression Patterns in Mutant Genes. 71

3.4.3 The pathway enrichment analysis of RNA-seq 73

3.4.4 Validation of RNA-Seq Results by qRT-PCR. 74

3.4.5 Examination of Protein PA1397- DNA interaction by Electrophoretic mobility shift assays 76

3.5 Conclusion and Discussion 76

Chapter 4 Developing high-content screen assays to identify molecules that inhibit antibiotic-resistant bacterial infections. 79

4.1 Abstract 79

4.2 Hypothesis 80

4.3 Materials and Methods 80

4.3.1 Bacterial strains and culture conditions 80

4.3.2 Sources of small molecules libraries 81

4.3.3 Construction of the dual labelled bioreporter strain PA14-*lux* (pCdrA::*gfp*^{c}) 82
4.3.4 Bacterial cell-based screen model 82
4.3.5 Human bronchial epithelial cell-based screen model 83
4.3.6 Measurement of Growth, Intracellular c-di-GMP Level and LDH cytotoxicity level 83
4.3.7 Statistical Analysis 84
4.3.8 Dose-response test 84
4.3.9 Construction of the GFP tagged stain PA14-*gfp* 85
4.3.10 Co-culture Biofilm Assay 85
4.3.11 Confocal microscopy analysis 85
4.3.12 *Galleria mellonella* virulence assays 86
4.3.13 Statistical Analysis 86
4.4 Results 87
4.4.1 Construction of viability and c-di-GMP-responsive reporter 87
4.4.2 Development of a high-content bacterial cell-based screen 88
4.4.2.1 Quality control of the assay. 90
4.4.2.2 Hits from the first screen with an impact on bacterial growth. 93
4.4.2.3 Hits from the first screen influences c-di-GMP signalling. 95
4.4.2.4 Hit compounds confirmed by dose responds and the effect on biofilm formation. 97
4.4.3 Development of a high content co-culture cell-based screen 103
4.4.3.1 Quality control of the assay. 104
4.4.3.2 Initial screening to identify compounds that effect on bacterial growth. 107
4.4.3.3 Initial screening to identify compounds that modulate the c-di-GMP level. 109
4.4.3.4 Initial screening to identify compounds that inhibit cytotoxicity during infection. 111
4.4.3.5 6,7-Dihydroxycoumarin as a potential inhibitor selected by second screen model. 113
4.4.4 *Galleria mellonella* model treatment results 117
4.5 Conclusion and Discussion 119

Chapter 5 Final Conclusions and Future Work.....125

5.1 DSF signal transduction in *P. aeruginosa* 125

5.2 Small molecule screening and anti-biofilm 126

5.3 Future works.....127

5.3.1 Validating the recruited Hpt domain participate the signalling pathway. 127

5.3.2 Exploring the potential and structure optimization of esculetin as a potential Inhibitor 128

5.3.3 In-depth research and chemical structure analysis of the screened natural plant extracts.....128

Appendix A Supplementary information for chapter 2 129

A.1 Tables 129

A.1.1 %Cytotoxicity of mutations and complementary strains. 129

A.1.2 IL-6, IL-8 and TNF-α in response to *P. aeruginosa* bacteria in 16HEB cell cultures. 129

Appendix B Supplementary information for chapter 3 131

B.1 Tables 131

B.1.1 DEGs list. 131

B.2 R scripts182

Appendix C Supplementary information for chapter 4 186

C.1 Tables 186

C.1.1 Natural compounds list which effects on the bacterial growth selected from bacterial cell-based screen model 186

C.1.2 Natural product extracts list which effects on the bacterial growth selected from bacterial cell-based screen model 186

C.1.3 Natural compounds list which influence c-di-GMP level selected from bacterial cell-based screen model 187

C.1.4 Natural product extracts list which influence c-di-GMP level selected from bacterial cell-based screen model 187

C.1.5 Row data of the dose-response test for the "hits" selected from bacterial cell-based screen model 189

C.1.6 Output data of the quantified the 3D biofilm images 190

C.1.7 Natural compounds list which effects on the bacterial growth selected from human bronchial epithelial cell-based screen model 190

C.1.8 Natural product extracts list which effects on the bacterial growth selected from human bronchial epithelial cell-based screen model 191

C.1.9 Natural compounds list which influence c-di-GMP level selected from human bronchial epithelial cell-based screen model 192

C.1.10 Natural product extracts list which influence c-di-GMP level selected from human bronchial epithelial cell-based screen model 192

C.1.11 Natural compounds list which influence cytotoxicity level selected from human bronchial epithelial cell-based screen model 195

C.1.12 Natural product extracts list which influence cytotoxicity level selected from human bronchial epithelial cell-based screen model 196

C.1.13 Row data of the dose-response test for the 6,7-Dihydroxycoumarin 199

C.1.14 Output data of the quantified the 3D biofilm images for 6,7-Dihydroxycoumarin 199

C.1.15 %Inhibition of cytotoxicity for the hit compounds selected by first screen model 199

C.1.16 The Mortality percentage of the larvae at 16 hours after treating 200

C.2 Figure 200

Figure C.2.2 Validation of dual labeled reporter strain PA14-lux (pCdrA::*gfp*^{c}). (A) Relative Light Unit (RLU) of PA14, PA14-lux (pCdrA::*gfp*^{C}). (B) Relative GFP intensity of PA14, PA14-lux (pCdrA::*gfp*^{C}) and PA14-lux (pCdrA::*gfp*^{C}) grown under selection (antibiotics Amp and Gm), normalized to growth (RLU) and WT PA14. Note WT PA14 does not grow under selection.200

List of References 201

Table of Tables

Table 2.1 Strains and plasmids used in this study. 31

Table 2.2 Summary of primers used in this chapter. 33

Table 2.3 The PCR amplification reaction set-up. 34

Table 2.4 PCR amplification reaction conditions set-up. 35

Table 2.5 The enzyme digestion reaction set-up. 36

Table 3.1 DNase treatment reaction set-up. 61

Table 3.2 The components added for cDNA Synthesis. 62

Table 3.3 qRT-PCR reaction set-up. 63

Table 3.4 Summary of qrt-PCR primers. 63

Table 3.5 Thermocycling conditions for qRT-PCR (StepOnePlus, ThermoFisher, UK). 64

Table 3.6 Primers used in DNA probes constructed. 66

Table 3.7 Component of buffers used in the protein purification and EMSA. 67

Table 3.8 RNA concentration and integrity 68

Table 3.9 Data quality summary 69

Table 3.10 The Enrichment Pathway list 73

Table 4.1 Strains and plasmids. 83

Table 4.2 “Hits” list selected by bacterial cell-based screen model..... 99

Table of Figures

Figure 1.1 Circular map of the PA14 genome..2

Figure 1.2 Environmental factors that form biofilm formations..4

Figure 1.3 The basic pathway of c-di-GMP..12

Figure 1.4 An illustration of known c-di-GMP proteins controlling biofilm formation and dispersal in *P. aeruginosa*..13

Figure 1.5 *Xanthomonas campestris pv. campestris* and *Pseudomonas aeruginosa* utilize different sensor kinases to perceive DSF (diffusible signal factor) signals..18

Figure 2.1 Gene knockout of *P. aeruginosa* by recombining homology..37

Figure 2.2 Proposed signal transduction system involving PA1396-PA1397 in *P. aerugunosa*..42

Figure 2.3 Amplification of the ~400 bp upstream and downstream DNA fragments of *hptA*, *hptB* and *hptC*.43

Figure 2.4 Construction of suicide vectors for the deletion of *hptA, hptB* and *hptC*.44

Figure 2.5 Testing and validation of *htpC*, *htpA*, *htpB* deletion mutants.45

Figure 2.6 Amplification of complementation genes *hptA*, *hptB* and *hptC*.46

Figure 2.7 Confirmation of C*hptA*, C*hptB* and C*hptC* fragments inserted into sequencing vector pCR-TOPO.47

Figure 2.8 Confirmation of C*hptA*, C*hptB* and C*hptC* fragments inserted into sequencing vector pME6032Gm.48

Figure 2.9 Testing and validation of complementation strains C*hptA*, C*hptB* and C*hptC*48

Figure 2.10 Growth curve of *P. aeruginosa* strains. hours in M9 medium.50

Figure 2.11 Influence of these mutations (A) and complementary strains (B) on swarming motility.51

Figure 2.12 Confocal images from the co-culture model..52

Figure 2.13 Cytotoxicity assay with selected mutants..53

Table of Figures

Figure 2.14 ELISA assays were performed for human pro-inflammatory cytokines IL-8 and TNF-α, the dual functioning IL-6 in response to *P. aeruginosa* bacteria in 16HEB human bronchial epithelial cell cultures.. 55

Figure 3.1 (A) Gel imaging for all RNA samples. (B) Principal Component Analysis (PCA) plots for RNA-seq data in each genotype..... 70

Figure 3.2 (A)Volcano illustration. Venn diagram illustrating the significantly affected genes (B)between Δ*PA1396* and Δ*PA1397*, (C)between Δ*hptA*, Δ*hptB*, and Δ*hptC*.. 72

Figure 3.4 Comparison of relative fold changes between RNA-Seq and qRT-PCR results in mutants (A) Δ*PA1396*, (B) Δ*PA1396*, (C) Δ*hptA*, (D) Δ*hptB*, and (E) Δ*hptC* background..... 75

Figure 3.5 Binding of PA1397 to the PA_53410 promoter is modulated by the presence and absence of "CGCCGCTTC" motif.. 76

Figure 4.1 Bioluminescence and fluorescence expression in wildtype PA14 and PA14-lux (pCdrA::gfp^{C})..... 88

Figure 4.2 The bacterial cell-based screen assay setup. 89

Figure 4.3 Heatmap results for 96-well screening plate assays test.. 91

Figure 4.4 A: Representative heatmap results for one 96-well screening plate.. 92

Figure 4.5 Scatter plot by the value of Z-score from bacterial cell-based screen..... 94

Figure 4.6 Scatter plot by the value of %inhibition of GFP from bacterial cell-based screen.. 96

Figure 4.7 Representative results from a dose - response assay.. 98

Figure 4.8 Representative results from a confocal imaging and the Biovolume of each test.. 102

Figure 4.9 The co-culture human epithelial cell-based screen assay setup..... 104

Figure 4.10 Heatmap results for 96-well screening plate assays test.. 105

Figure 4.11 Representative heatmap results for one 96-well screening plate and the quality validation.. 106

Figure 4.12 Scatter plot by the value of Z-score from bacterial cell-based screen..... 109

Figure 4.13 Scatter plot by the value of %inhibition of GFP from co-culture human bronchial epithelial cell-based screen.. 111

Figure 4.14 Scatter plot by the value of %inhibition of cytotoxicity from co-culture human bronchial epithelial cell-based screen.. 113

Figure 4.15 Representative results from a dose-response assay.. 115

Figure 4.16 Confocal images and biovolume value of the hit from human bronchial epithelial cell-based screening.. 116

Figure 4.17 Effects of potential inhibitor 6,7-Dihydroxycoumarin combined with TB on 16-hour survival of waxworms.....118

Research Thesis: Declaration of Authorship

Print name: Ying Hu

Title of thesis: Novel Antibacterial Interventions against *Pseudomonas aeruginosa* Infections by targeting c-di-GMP and unravelling DSF Signalling Pathway

I declare that this thesis and the work presented in it are my own and has been generated by me as the result of my own original research.

I confirm that:

1. This work was done wholly or mainly while in candidature for a research degree at this University.
2. Where any part of this thesis has previously been submitted for a degree or any other qualification at this University or any other institution, this has been clearly stated.
3. Where I have consulted the published work of others, this is always clearly attributed.
4. Where I have quoted from the work of others, the source is always given. With the exception of such quotations, this thesis is entirely my own work.
5. I have acknowledged all main sources of help.
6. Where the thesis is based on work done by myself jointly with others, I have made clear exactly what was done by others and what I have contributed myself.
7. Part of this work has been published before submission.
   Hu Y, Webb JS and An S-q. 202. Host cellbased screening assays for identification of molecules targeting *Pseudomonas aeruginosa* cyclic di-GMP signalling and biofilm formation. Front. Microbiol. 14:1279922.

Signature: ..... Date:.....

Acknowledgements

I am deeply indebted to my supervisors, family, colleagues, and others who have supported me throughout my dissertation journey. While it is impossible to name everyone who contributed to my doctoral education, I would like to express my gratitude to those who provided essential assistance.

First and foremost, my heartfelt thanks go to my main supervisor, Prof. Jeremy S Webb, whose unwavering support, and guidance have been instrumental in shaping my doctoral career. Working under his mentorship has been an invaluable opportunity. His constant availability and encouragement during challenging times have been a source of light, guiding me through complexities. I am truly grateful.

I must also extend my gratitude to my co-supervisor, Dr. Shi-qi An. It was under her enlightened advice and professional support that I pursued my PhD study at the University of Southampton. Her dedication to providing an excellent project and guiding my experimental work wholeheartedly have been invaluable. Moreover, her assistance and companionship in personal matters have meant a great deal to me. Her support has been pivotal in ensuring the smooth progression of my entire PhD journey.

A special thank you to the wonderful team at Webb Labs: Joe, Cullum, Declan, Katie, Bhavik, Conor, Zhi-xiu, Kirsty, Liam, and Matt. Their constant help and the supportive work atmosphere have been a true blessing. Additionally, I extend my appreciation to Yu-ting, Si-yuan, Zi-jian, and Jiao-qi in this building for being such great friends and offering encouragement during our life.

Next, I would like to thank my sponsors, without whom I would not have been able to obtain my PhD. I would like to thank the China Scholarship Council and the University of Southampton Collaborative Scholarship Program for providing me with funding. Work on this project was supported by funding from the Wessex Medical Research and National Biofilms Innovation Centre (NBIC). Being a member of NBIC has been an honour, and I am grateful for all the learning opportunities it provided. The conferences shared a wealth of project results across various fields and offered valuable guidance at a business level, which will undoubtedly benefit my future career. I would like to express my thanks to Professor Jane Lucas for providing the human airway epithelial cells (16HEB 14o-cell).

Beyond academia, my family deserves special recognition. Their encouragement and love have been the foundation of my happiness and passion. Without the unwavering support from my parents and sisters, none of my accomplishments would have been possible. I am also deeply

thankful to my boyfriend Ben-yu Cao for his constant motivation and support throughout these four years. His persistence and belief in me have boosted my confidence significantly.

In conclusion, I owe a debt of gratitude to all those who have contributed to my academic and personal growth. Your support and encouragement have been invaluable, and I am forever thankful for the role you've played in shaping my journey.

Definitions and Abbreviations

CF .....Cystic Fibrosis

COPD .....Chronic Obstructive Pulmonary Disease

AET .....Antibiotic Eradication Therapy

T3SS .....Type III Secretion System

T1SS .....Type I Secretion System

T2SS .....Type II Secretion System

T5SS .....Type V Secretion System

T6SS .....Type VI Secretion System

T3SS .....Type III Secretion System

GAP .....GTPase Activating Protein

ADPRT.....Adenosine Diphosphate Ribosyl Transferase

PLA2 .....Phospholipase A2

iT3SS .....Injectisome Type III Secretion System

fT3SS .....Flagellum Type I Secretion System

COM .....Chronic Otitis Media

cAMP .....Cyclic Adenosine Monophosphate

C-di-GMP .....Bis-(3'-5')-cyclic Dimeric Guanosine Monophosphate

EPS .....Extracellular Polymeric Substance

QS.....Quorum Sensing

eDNA.....Extracellular DNA

T4P .....Type IV Pili

T4aP .....Type IVa

T4bP .....Type IVb

MDR .....Multiple Drug Resistance

DSF .....Diffusion Signal Factor

AHL .....N-acyl Homoserine Lactones

PQS..... *Pseudomonas* Quinolone Signal

IQS..... Integrated Quinolone Signal

3OC12-HSL..... N-(3-oxododecanoyl)-l-Homoserine Lactone

C4-HSL ..... N-butyryl-L-Homoserine Lactone

HHQ 2-heptyl-4-quinolone

TCS ..... Two-component System

HK..... Histidine Kinase

RR..... Response Regulator

ATP..... Adenosine Triphosphate

DGCs ..... Diguanylate Cyclase

PDE..... Phosphodiesterase

pGpG..... 5’-phosphoguanylyl-(3’-5’)-guanosine

BDSF..... Cis-2-dodecenoic acid

HPT..... Histidine Phosphate Transfer

REC..... Phosphoacceptor Receiver

HTH ..... Helix-Turn-Helix

AMPs..... Antimicrobial Peptides

HTS..... High Throughput Screening

HCS..... High Content Screening

NMR..... Nuclear Magnetic Resonance

HPLC..... High-Performance Liquid Chromatography

MS..... Mass Spectrometry

Au-NPs ..... Gold Nanoparticles

Se-NPs..... Selenium Nanoparticles

FBS ..... Fetal Bovine Serum

SDS..... Sodium Dodecyl Sulfate

EDTA ..... Ethylenediaminetetraacetic Acid

PCR..... Polymerase Chain Reaction

gDNA ..... Genomic DNA

SOE-PCR ..... Splicing by Overhang Extension- Polymerase Chain Reaction.

Gm ..... Gentamycin

OD_{600} ..... Optical Density at 600 nm

DMSO ..... Dimethyl Sulfoxide

ELISA ..... Enzyme-linked Immunosorbent Assay

SD ..... Standard Deviation

SMART ..... Simple Modular Architecture Research Tool

CLSM ..... Confocal Laser Scanning Microscopy

LDH ..... Lactate Dehydrogenase

WT ..... Wild Type

TNF-α ..... Tumor Necrosis Factor-alpha

IL-6 ..... Interleukin-6

IL-8 ..... Interleukin-8

TMH ..... Transmembrane Helix

RNA-Seq ..... RNA Sequencing

DEGs ..... Differentially Expressed Genes

PCA ..... Principal Component Analysis

qRT-PCR ..... Quantitative Reverse Transcription PCR

EMSA ..... Electrophoretic Mobility Shift Assay

FPKM ..... Fragments Per Kilobase of transcript per Million mapped reads

FDR ..... False Discovery Rate

cDNA ..... Complementary DNA

TEMED ..... N, N, N’,N’-Tetramethyl ethylenediamine

LB ..... Luria–Bertani

TB/Tb ..... Tobramycin

Amp ..... Ampicillin

Km ..... Kanamycin

Definitions and Abbreviations

Sp ..... Spectinomycin

PBS ..... Phosphate Buffered Saline

MAD ..... Median Absolute Deviation

Sub-MIC ..... Sub-minimal Inhibitory Concentration

Chapter 1 Introduction

1.1 *Pseudomonas aeruginosa* as an opportunistic human pathogen.

Pseudomonas aeruginosa (*P. aeruginosa*) is a Gram-negative bacterium that is heterotrophic and motile. It can thrive within a temperature range of 4-42°C, with optimal growth occurring at 37°C. Due to its wide-ranging metabolic adaptability and the strategic development of various cell-associated and secreted factors contributing to virulence and survival, this bacterium is commonly encountered in diverse environments, including soil, water, and plants, as well as within nearly any human or animal-affected setting. In humans, *P. aeruginosa* leads to severe infections, especially in individuals with weakened immune systems due to conditions such as cancer, as well as in patients who have suffered extensive burns or have cystic fibrosis (CF) (Wu *et al.*, 2014). The bacterium is capable of thriving both in environments with oxygen and those without, and it produces many virulence factors that contribute to its pathogenesis (Morita, Tomida and Kawamura, 2013). Its natural resistance to antibiotics makes it difficult to treat.

Regarded as an opportunistic pathogen in humans, *P. aeruginosa* triggers both acute and chronic infections among patients who have weakened immune systems or are hospitalized. It is one of the most common pathogens in various infections, associated with infection of patients with cystic fibrosis (CF), and patients suffering from severe burns, chronic wounds, chronic obstructive pulmonary disease (COPD), surface growth of implanted biomaterials, and major hosts on hospital surfaces and water systems (Breathnach *et al.*, 2012). In the absence of antibiotic intervention, an initial infection frequently transitions into a chronic state, resulting in severe inflammation that progressively damages the lungs and worsens the patient's clinical state (Taccetti *et al.*, 2020). Recent research emphasizes the critical nature of promptly initiating antibiotic eradication therapy (AET). Once a chronic infection takes hold, the eradication of *P. aeruginosa* becomes an incredibly challenging task (Döring, 2010).

1.1.1 Genome features of *Pseudomonas aeruginosa*.

The genome of *P. aeruginosa* is composed of a relatively sizeable circular chromosome (ranging from 5.5 to 6.8 Mb), containing between 5,500 to 6,000 open reading frames, which may vary depending on the strain's size (Klockgether, 2011). An analysis comparing 389 genomes across diverse *P. aeruginosa* strains reveals that a mere 17.5% are shared. This particular section of the genome constitutes the core of *P. aeruginosa* (De Smet *et al.*, 2017). A comparative study encompassing 494 complete genomes from the Pseudomonas genus includes 189 *P. aeruginosa*

strains. Their GC content lies within the range of 65.6 to 66.9% (with an average of 66.1%), while their protein count ranges from 5,500 to 7,352 (with an average of 6,192) (Nikolaidis *et al.*, 2020). Notably, PAO1 and PA14 (**Figure 1.1**) stand as two vital *P. aeruginosa* strains frequently used in laboratory settings. The large size of *P. aeruginosa*' s genome and its genetic complexity reflect its evolutionary adaptability, which enables it to thrive in a variety of niches. *P. aeruginosa* demonstrates an extensive capacity for transporting, metabolizing, and thriving on organic matter. Moreover, it enhances the ability to export compounds (such as antibiotics) through a large amount of protein secretion and efflux systems.

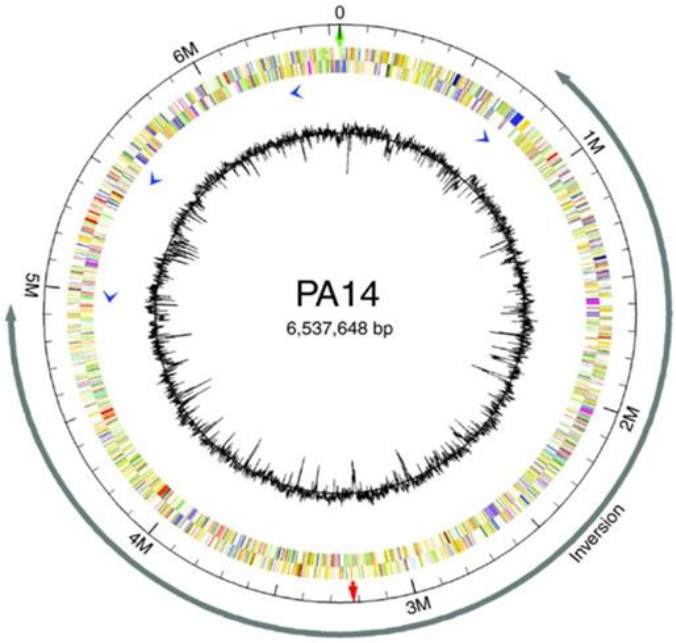

Figure 1.1 Circular diagram illustrating the PA14 genome structure, adapted from (Lee *et al.*, 2006). The outermost circle represents the chromosomal positions, with major ticks indicating 500 Kb increments and minor ticks denoting 100 Kb increments. Green and red arrows mark the probable replication origin and terminus, respectively. The positions and orientations of predicted genes are shown by rectangles in the next pair of circles; rectangles in the outer ring represent genes transcribed on the plus strand, while those in the inner ring indicate genes on the minus strand. Blue arrowheads indicated the positions and relative orientations of four ribosomal RNA gene clusters; the published PAO1 sequence contains an inversion (gray arrow) with respect to PA14 resulting from a presumptive recombination event between two of the rRNA clusters. The innermost ring displays the GC content, calculated for non-overlapping 1 Kb windows of the plus strand.

1.1.2 Secretion system in *Pseudomonas aeruginosa*.

Bacterial secretion systems are the protein complexes located on the cell membranes of bacteria, responsible for releasing various substances. Pathogenic bacteria utilize these systems to secrete their virulence factors, assisting them in invading host cells. There are at least eight distinct types specific to Gram-negative bacteria, and within *P. aeruginosa*, five of these types (T1SS, T2SS, T3SS, T5SS, and T6SS) have been identified and characterized (Filloux, 2011). Of these, the type III secretion system (T3SS) stands out as it plays a key role in host invasion by directly injecting toxins into eukaryotic cells. This system is particularly relevant in human pathogenesis and also significantly contributes to *P. aeruginosa*' s ability to colonize its host (Juan, Peña and Oliver, 2017; Jouault, Saliba and Touqui, 2022). *P. aeruginosa* employs two types of T3SS—injectisome (iT3SS) and flagellum (fT3SS)—to shuttle effector proteins into the host cell cytosol and ensure bacterial motility (Diepold and Armitage, 2015).

Four type III secretion (T3SS) effectors have been pinpointed within *P. aeruginosa*: ExoS, ExoU, ExoT, and ExoY. In comparison to the first two, ExoT and ExoY exhibit notably high detection rates (Ozer *et al.*, 2019). Both ExoS and ExoT feature a GTPase activating protein (GAP) domain along with an adenosine diphosphate ribosyl transferase domain (ADPRT) (Kaufman *et al.*, 2000), both of which induce apoptosis (Kaminski *et al.*, 2018). ExoU stands out as the most potent cytotoxin, significantly influencing *P. aeruginosa*' s cytotoxic behavior through its phospholipase A2 (PLA2) activity (Filloux, 2011; Jouault, Saliba and Touqui, 2022). This, in turn, correlates with unfavorable outcomes in severe pneumonia cases. ExoY, as an actin-activated nucleotidyl cyclase, can impact the actin cytoskeleton (Beckert *et al.*, 2014). Additionally, a few potential novel effectors have recently been suggested, including PemC, PemD, PemE, and PemF (Horna and Ruiz, 2021).

Recently, numerous studies have focused on the type VI secretion system (T6SS), a crucial component in interbacterial competition and a virulence determinant for certain Gram-negative bacteria, *P. aeruginosa* included. This system is recognized for transporting substances to both prokaryotic and eukaryotic target cells, finally causing damage. It's associated with bacterial antagonism and operates through the evolved VgrG2b spike protein in *P. aeruginosa* (Han *et al.*, 2019; Wood *et al.*, 2019; Hernandez, Gallegos-Monterrosa and Coulthurst, 2020). *P. aeruginosa* possesses three distinct T6SS: H1-T6SS, H2-T6SS, and H3-T6SS. The expression and function of these systems are influenced by environmental cues and are fine-tuned by modulators in many pathways (Sana, Berni and Bleves, 2016). The H3-T6SS in *P. aeruginosa* PA14 has been found to be negatively regulated by key global regulatory proteins related to oxidative and acid stress in bacteria, namely OxyR and OmpR. This particular system contributes to environmental adaptation by releasing an effector that promotes biofilm formation (Yang *et al.*, 2022).

1.1.3 Biofilm formation in *Pseudomonas aeruginosa*.

A biofilm is a complex, sessile microbial community that adheres to a surface in an aggregated form or embedding itself within a cellular matrix. Most bacteria have the capacity to attach to surfaces and form biofilms, allowing them to develop high resistance against antibiotics and the host's immune system. Research has outlined five distinct stages in biofilm development: (i) reversible attachment, (ii) irreversible attachment, (iii) microcolony, (iv) maturation, and (v) dispersal (Sauer *et al.*, 2002; Toyofuku *et al.*, 2016) (**Figure 1.2**). Biofilms influence numerous aspects of human life, including health, disease, industrial applications, bioremediation, and microbial fuel cells. Among these, the impact of biofilms on human health and disease is particularly significant and has attracted substantial attention. *P. aeruginosa* is a well-known biofilm former, recognized as one of the most severe pathogens responsible for biofilm-related issues in human hosts among the various microbial pathogens that form biofilms (Das *et al.*, 2016). Biofilm infections caused by *P. aeruginosa* are associated with a range of conditions, including pneumonia linked to cystic fibrosis, chronic wound infections, cases of chronic otitis media (COM), and infections connected to medical devices, among others.

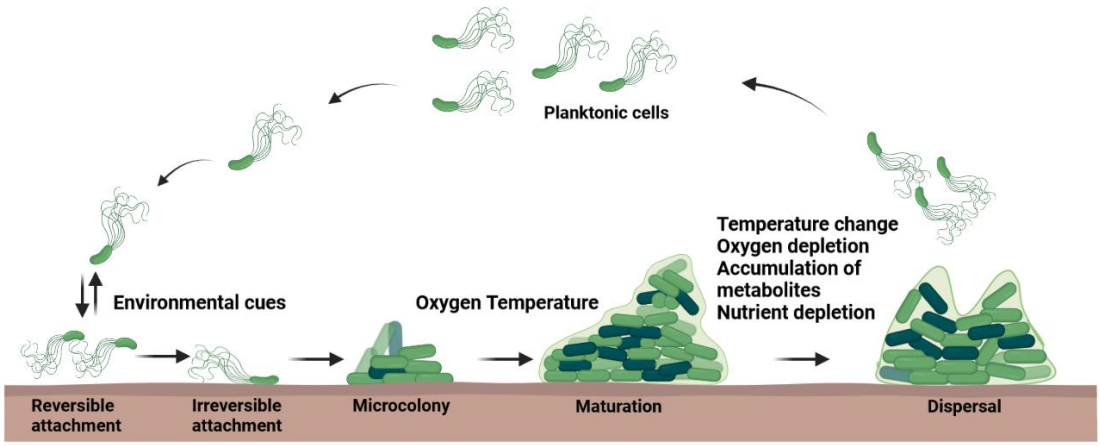

Figure 1.2 Environmental factors that form biofilm formations. The image illustrates the process of biofilm formation along with selected environmental factors that impact each stage of the process. These environmental cues play a pivotal role in modulating the concentration of second messengers, such as cyclic adenosine monophosphate (cAMP) and bis-(3'-5')-cyclic dimeric guanosine monophosphate (c-di-GMP), which in turn regulate various biofilm-associated elements like cellular appendages, surface proteins, extracellular polymeric substances (EPS), and cellular motility. Additionally, quorum sensing (QS) contributes to shaping the biofilm by exerting control over factors associated with the biofilm structure (Toyofuku *et al.*, 2016).

The biofilm is enveloped within a self-generated matrix of extracellular polymeric substances (EPS). This matrix plays a critical role in enhancing biofilm attachment to both living (biotic) and non-living (abiotic) surfaces, especially in challenging environmental conditions such as exposure to antibiotics and host immune responses (Ryder, Byrd and Wozniak, 2007, 2016). In the *P. aeruginosa* biofilm matrix, the primary components include polysaccharides, extracellular DNA (eDNA), proteins, and lipids (Thi, Wibowo and Rehm, 2020).

Alginate, Psl, and Pel are three key exopolysaccharides significantly involved in the adhesion, structure, and stability of biofilms. They have the function of protecting bacterial cells from antibiotics and human immunity (Wu *et al.*, 2014; Thi, Wibowo and Rehm, 2020). Alginate, a linear unbranched polymer comprising L-guluronic acid and D-mannuronic acid (Rasamiravaka *et al.*, 2015), has been identified to help to reduce biofilm susceptibility to antibiotic treatment and human antimicrobial defences (Pier *et al.*, 2001; Rasamiravaka *et al.*, 2015). Notably, it stands as a primary virulence factor in *P. aeruginosa*' s role in CF lung infections. The CF lung environment can induce an excess of alginate production, leading to the encapsulation of mucinous *P. aeruginosa*, contributing to declining lung function and associated lung lesions (Hentzer *et al.*, 2001; Pier *et al.*, 2001).

Both Psl and Pel can function as primary polysaccharide components within the biofilm matrix of non-mucoid strains. Psl consists of a neutral pentasaccharide composed of D-mannose, L-rhamnose, and D-glucose (Byrd *et al.*, 2009; Thi, Wibowo and Rehm, 2020). This polysaccharide plays a role in initial attachment and mature biofilm formation, which is advantageous for biofilm communities. It also contributes to maintaining structural stability in mature biofilms (Ma *et al.*, 2009; Ghafoor, Hay and Rehm, 2011). Additionally, Psl serves as a signal that activates two diguanylate cyclases, SiaD and SadC, leading to the production of the intracellular secondary messenger molecule c-di-GMP. Higher concentrations of c-di-GMP result in thicker and more robust biofilms (Irie *et al.*, 2012). Pel, on the other hand, is a glucose-rich cationic polysaccharide polymer. Its synthesis machinery is encoded by a seven-gene operon (pela-F) identified through mutagenesis screening for the loss of membrane formation in *P. aeruginosa* PA14 (Friedman and Kolter, 2004). The glucose-rich matrix material required for biofilm formation in *P. aeruginosa* PA14 is produced by the pel gene. Pel also contributes to maintaining cell-cell interactions within PA14 biofilms and enhancing resistance to aminoglycoside antibiotics within biofilm populations (Colvin *et al.*, 2011).

Extracellular DNA (eDNA) holds significant importance as a component of biofilms, produced by cell lysis releasing DNA into the surrounding environment. The presence of eDNA enhances the stability of biofilms. Furthermore, eDNA contributes to the twitching movement of bacteria and

can serve as a source of nutrients for bacterial cells during periods of starvation (Brindhadevi *et al.*, 2020). In *P. aeruginosa*, the release of eDNA is important for *P. aeruginosa* biofilm development, and the degradation of eDNA by exogenously added DNase leads to the dispersal of *P. aeruginosa* biofilms (Kim and Lee, 2016). For instance, eDNA that accumulates in the lung mucosa of individuals with cystic fibrosis (CF) can lead to the acidification of biofilms, rendering *P. aeruginosa* more resistant to aminoglycoside antibiotics (Sarkar, 2020).

1.1.4 Motility in *Pseudomonas aeruginosa*.

P. aeruginosa exhibits three different modes of motility, which include pilus-dependent twitching, flagellum-dependent swimming, and flagellum- and pilus-dependent swarming (Amina, 2017). Twitching motility is a mechanism for surface movement employed by *P. aeruginosa* to colonize and explore abiotic and host surfaces. It involves a sequence of processes including extension, tethering, and retraction of type IV pili (T4P) (Filloux, 2014; Mattick, 2002). T4P represents one of the most prevalent surface structures found in bacteria and archaea, serving purposes such as adhesion, movement, DNA uptake, and pathogenesis. Interestingly, T4P is among the first factors identified through genetic screenings as crucial for *P. aeruginosa* biofilm formation (Twomey *et al.*, 2012). T4P are categorized into two main subfamilies: Type IVa (T4aP) and Type IVb (T4bP). Of these, the fully functional T4aP plays a key role in biofilm construction (Conrad *et al.*, 2011). Every sequenced *P. aeruginosa* genome contains T4aP, whereas T4bP is present in strains that possess *P. aeruginosa* pathogenicity island PAPI-1 or associated elements (Burrows, 2012). *P. aeruginosa* serves as a model for comprehensive genetic and functional analyses of twitch motility, contributing to the identification of mutants with impaired twitching abilities (Mattick, 2002).

Swimming and swarming motility are controlled by flagella. Swimming motility occurs in a liquid environment and is promoted by the flagellum, while swarming takes place on a semi-solid surface (with 0.4 to 1.0% agar) and requires specific nitrogen and carbon sources (Murray and Kazmierczak, 2008; Yang *et al.*, 2017). In *P. aeruginosa*, the polar flagellum is essential for both swimming and swarming motility. This flagellum consists of distinct parts: the cap, hook, filament, and basal body (Ha and O'Toole, 2015). The hook and filament are polymer structures, each made up of a single repeating protein. The helical filament is composed of FliC, while the hook is formed by FlgE (Berg, 2003). The flagellar motor includes essential components such as FliG, FliM, and FliN, in conjunction with the rotor proteins MotA and MotB. FliG, FliM, and FliN serve as protein switches within the rotor. MotA and MotB are responsible for proton movement, regulating the rotation of the flagellum and the associated rotor proteins (McBride, 2008). Swimming motility holds significant importance as a virulence factor in *P. aeruginosa*. It facilitates the rapid spread of pathogens from the initial infection site to various tissues, leading to deeper infections (Z. Liu *et*

al., 2022). Additionally, swimming motility plays a role in biofilm formatio (Watnick and Kolter, 2000). T Swarming motility enables bacteria to quickly colonize surfaces, forming biofilms. This process is influenced by environmental and physiological factors, including the availability of carbon and nitrogen sources (Skerker and Berg, 2001). Swarming occurs under conditions resembling the semi-viscous environment of the human lung mucosal surface. As a result, it holds clinical relevance in acute or initial lung infections (Winstanley, O'Brien and Brockhurst, 2016; Coleman *et al.*, 2020). Coleman et al. (2020) observed that *P. aeruginosa* demonstrates reversible antibiotic resistance during swarm movement, potentially indicating a survival strategy. This ability to swiftly colonize may contribute to establishing infections in the lungs.

1.1.5 Antibiotic resistance in *Pseudomonas aeruginosa*.

Antibiotic resistance presents a worldwide health crisis. Antibiotics are medications used to both prevent and treat bacterial infections. When bacteria develop the capacity to withstand drugs intended to eliminate them, they acquire resistance. This phenomenon seriously threatens our ability to effectively manage common infectious diseases, making more and more infections difficult to treat. The most important categories of antibiotic resistance evovle as intrinsic resistance, acquired resistance, cross-resistance, multi-drug resistance, and various other forms of resistance. Mechanisms contributing to antibiotic resistance include alterations in antibiotics, enzymatic neutralization, reduced permeability of inner and outer membranes, an active pumping system, and the adoption of alternative metabolic pathways (Hasan and Al-Harmoosh, 2020). *P. aeruginosa* exhibits a high degree of physiological flexibility and significant antibacterial ability. However, due to its resistance to a diverse range of antibiotics, eradicating *P. aeruginosa* infections becomes extremely challenging (Tran *et al.*, 2014). The World Health Organization (WHO) has identified *P. aeruginosa* as a bacterium necessitating urgent development of novel antibiotics for effective infection management (WHO, 2017). Intrinsic, acquired, and adaptive resistance are the major mechanisms employed by *P. aeruginosa* to counter antibiotic assaults (Pang *et al.*, 2019).

Intrinsic resistance includes the inherent mechanisms that specific microorganisms employ to inhibit the action of antimicrobial agents (Blair *et al.*, 2015). In the case of *P. aeruginosa*, its intrinsic resistance mechanisms involve expelling antibiotics out of the cell through efflux systems, limiting the permeability of the outer membrane, and producing antibiotic-inactivating enzymes (Breidenstein, de la Fuente-Núñez and Hancock, 2011). This intrinsic resistance arises from reduced cell envelope permeability that hampers antibiotic uptake, working in conjunction with multidrug resistance (MDR) efflux pumps and antibiotic-inactivating enzymes (e.g., β-lactamase) that curtail antibiotic effectiveness (Alvarez-Ortega *et al.*, 2011).

Acquired resistance is acquired through mutations or horizontal gene transfers, granting access to resistance genes that render the microorganism challenging to eliminate (Henrichfreise *et al.*, 2007; Pang *et al.*, 2019). In *P. aeruginosa*, mutational modification of target sites and mutations causing overexpression of antibiotic-inactivating enzymes both promote antibiotic resistance. The modification of the quinolone target sites is a characterized example (Bruchmann *et al.*, 2013). Mutations leading to antibiotic-inactivating enzyme overexpression, such as mutations in the β-lactamase-inducing gene *ampC* and gain-of-function mutations in ampD, result in heightened β-lactamase production, thereby elevating resistance (Torrens *et al.*, 2019; Q. Liu *et al.*, 2022). Bacteria can acquire antibiotic resistance genes through horizontal gene transfer from the same or different bacterial species. Aminoglycosides and β-lactams are among the reported resistance genes acquired by *P. aeruginosa* (Breidenstein, de la Fuente-Núñez and Hancock, 2011; Pang *et al.*, 2019).

Adaptive resistance refers to the increased ability of bacteria to against antibiotic attacks due to alterations in gene and/or protein expression resulting from exposure to the environment (Ferrières and Clarke, 2003). In a study by Santiago Sandoval-Motta and Maximino Aldana (2016) adaptive resistance was proposed to enable cells to survive long-term exposure to low-concentration antibiotics. With a gradual increase in antibiotic concentrations, cells develop more robust mechanisms for antibiotic resistance. Adaptive resistance can also arise due to biofilm formation and swarming, which pose significant concerns in the clinical context of *P. aeruginosa*, often leading to persistent and recurring infections in patients with cystic fibrosis (Mulcahy *et al.*, 2010; Breidenstein, de la Fuente-Núñez and Hancock, 2011).

Traditional antibiotic treatment for *P. aeruginosa* infections is progressively losing its effectiveness due to the rise in multidrug-resistant strains. As a result, the creation of novel antibiotics and innovative treatment approaches has become particularly important. Given the constraints of established methods, there has been a surge in focus on novel therapeutic tactics in recent years. These include but are not confined to quorum sensing inhibition, vaccination strategies, and phage therapy. (Pires *et al.*, 2015; Reuter, Steinbach and Helms, 2016; Hoggarth *et al.*, 2019; Killough, Rodgers and Ingram, 2022; Xie *et al.*, 2022).

1.2 Roles of signalling pathways in *Pseudomonas aeruginosa*

P. aeruginosa, like many other bacteria, uses a variety of signalling pathways to sense and respond to changes in its environment. These pathways allow the bacteria to coordinate gene expression and cellular behaviour, and can play important roles in virulence, biofilm formation, and other processes. Among the key signalling pathways in *P. aeruginosa* are quorum sensing (QS),

a two-component system (TCS), and the secondary messenger bis-(3', 5')-cyclic dimeric guanosine (c-di-GMP) (Hentzer *et al.*, 2003; Valentini and Filloux, 2016a; Sultan, Arya and Kim, 2021). Additionally, *P. aeruginosa* can also sense the diffusible signal factor (DSF) to modulate various virulence factors, including biofilm formation, motility, and exopolysaccharide production.

1.2.1 Quorum sensing of *Pseudomonas aeruginosa*.

Quorum sensing (QS) is a cell-cell communication process. It controls gene transcription based on cell density and it plays a significant role in pathogenicity and virulence. QS can also create a collection of virulence factors that enhance the ability of *P. aeruginosa* to cause disease (Rutherford and Bassler, 2012). Virulence factors generated by QS in *P. aeruginosa* consist of pyocyanin, proteases, elastase, rhamnolipids, swarming motility, lectin, and toxins. Pyocyanin is a part of blue redox-active pigment, and it not only modulate c-di-GMP messenger and extracellular polymeric substance (EPS), but also regulate eDNA to influence biofilm development (Meirelles and Newman, 2018). Rhamnolipids also contribute to biofilm growth under certain conditions (Reis *et al.*, 2011). Elastase, also known as LasB, is a extracellular virulence factor, playing a important role in controlling infections caused by *P. aeruginosa* (Szamosvári *et al.*, 2016).

In *P. aeruginosa*, there are four distinct QS systems: LasR-LasI, RhlR-RhlI, the Pseudomonas quinolone signal (PQS), and the integrated quinolone signal (IQS). Among these, the LasR-LasI system and the RhlR-RhlI system are two fully characterized N-acyl homoserine lactone (AHL) QS systems (Smith and Iglewski, 2003). The LasR-LasI QS system gets activated by N-(3-oxododecanoyl)-l-homoserine lactone (3OC12-HSL), which is produced by LasI. This activation leads to LasR becoming an active transcription factor, triggering the expression of virulence-related genes (Bottomley *et al.*, 2007). Within the RhlR-RhlI system, RhlI generates the AHL N-butyryl-L-homoserine lactone (C4-HSL). This molecule complexes with RhlR, enabling it to regulate the expression of virulence genes (Dai *et al.*, 2019). The PQS system operates through the molecule 2-heptyl-3-hydroxy-4-quinolone, which is synthesized by the autoinducer synthase-PqsABCDH. PqsR functions as the receptor for this system, binding to both PQS and its biosynthetic precursor 2-heptyl-4-quinolone (HHQ) (Pesci *et al.*, 1999; Azam and Khan, 2019). The IQS system involves an autoinducer synthase, AmbBCDE, responsible for producing 2-(2-hydroxyphenyl)-thiazole-4-carbaldehyde. However, further research is needed to determine the precise role and receptor of this system. Importantly, it's worth noting that it is not difficult to find many overlaps in the regulators from the research reports. This suggests that certain genes can be activated by multiple regulators (Wagner, Gillis and Iglewski, 2004; Schuster and Greenberg, 2007).

1.2.2 Two-component system of *Pseudomonas aeruginosa*.

The Two-component system (TCS) is a signal transduction mechanism used by bacteria to sense various stimuli and adapt to changing environmental conditions. It consists of two proteins, including an inner membrane-spanning sensor histidine kinase (HK) and a cytoplasmic response regulator (RR) (Hirakawa *et al.*, 2020). The HK usually contains a histidine phosphotransferase domain and an adenosine triphosphate (ATP) binding domain. These elements allow it to perceive external stimuli such as osmotic pressure, pH, antibiotics, host factors, or nutrients. Consequently, it regulates the signalling pathway and undergoes an autophosphorylation reaction. This reaction transfers a phosphoryl group from ATP to a specific histidine residue (Gao and Stock, 2009). Subsequently, the phosphoryl group is transferred to an aspartate residue in the receiver domain of the RR. This activation prompts the output domain of the RR to bind to specific DNA sequences in the promoter regions of target genes. This binding can either activate or repress the transcription of these genes (Galperin, 2006).

Due to the large genome of *P. aeruginosa*, its adaptability, and the wide range of environments and hosts it can survive in, certain genes are dedicated to regulatory networks, and Two-component systems (TCS) play a vital role within these networks. There are many TCSs in *P. aeruginosa* regulated with motility, biofilm formation, pyocyanin, and cytotoxins (Sultan, Arya and Kim, 2021). One of these TCSs is AlgZ-AlgR, which controls the synthesis and export of alginate, a crucial component of the *P. aeruginosa* biofilm matrix. The response regulator AlgR controls the transcription of genes involved in alginate biosynthesis (Intile *et al.*, 2014). Another TCS in *P. aeruginosa* is PilS-PilR, which plays a key role in regulating the expression of type IV pili (Kilmury and Burrows, 2018). PilR, acting as a response regulator, binds to the DNA near the promoter region of pilA—a gene responsible for encoding the major structural subunit of type IV pili in *P. aeruginosa*. This binding activates the transcription of pilA (Kilmury and Burrows, 2018). The FleS-FleR TCS is implicated in regulating the H1-T6SS in *P. aeruginosa*. In the wild-type strain, H1-T6SS expression and activity are inhibited due to high c-di-GMP levels. Repression of H1-T6SS depends on the transcription factor FleQ (Zhou *et al.*, 2022). The PhoP-PhoQ is another TCS that playing roles in the detection of Mg^{2+} levels, cationic peptide resistance, and pathogenesis (McPhee *et al.*, 2006). Under conditions of limited Mg^{2+} growth, the oprH-phoP-phoQ operon is regulated by the PhoP-PhoQ system, which also plays a role in both resistance to cationic antimicrobial peptides and polymyxin B and virulence (Macfarlane, Kwasnicka and Hancock, 2009).

Of course, there are several unexplained TCSs that hold key roles in *P. aeruginosa*. Overall, TCSs are critical for *P. aeruginosa* to adapt to diverse environments, compete with other bacteria, and cause infections. Understanding the two-component system in bacteria like *P. aeruginosa* is

crucial for developing novel strategies to combat bacterial infections and design innovative antimicrobial agents.

1.2.3 C-di-GMP of *Pseudomonas aeruginosa*.

Second messengers play a critical role in intracellular signal transduction within bacteria. C-di-GMP stands out as a pivotal bacterial second messenger that regulates numerous essential processes, such as motility, biofilm formation, and virulence (An *et al.*, 2014). It was unexpectedly found by Benziman and colleagues 35 years ago during research on cellulose biosynthesis. They discovered that it acts as an allosteric activator of cellulose synthase in the bacterium *Acetobacter xylinum* (Ross *et al.*, 1987). Several publications have already provided detailed descriptions of the history behind the discovery of c-di-GMP (Ross, Mayer and Benziman, 1991; Amikam, Weinhouse and Galperin, 2014; Zhao *et al.*, 2019). C-di-GMP plays a pivotal role in the transition between the lifestyles of biofilm-forming bacteria and solitary, motile cells (Valentini and Filloux, 2016a). The synthesis or degradation of c-di-GMP can facilitate certain signal transmissions within bacteria.

1.2.3.1 C-di-GMP metabolism

C-di-GMP is synthesized by a protein exhibiting diguanylate cyclase (DGC) activity that combines two molecules of GTP. DGCs contain a GGDEF amino acid motif (**Figure 1.3**). The degradation of c-di-GMP is influenced by proteins with phosphodiesterase (PDE) activity. PDEs exist in two types: those with EAL domains or HD-GYP domains. EAL phosphodiesterases convert c-di-GMP into 5'-phosphoguanylyl-(3'-5')-guanosine (pGpG), which then undergoes sequential hydrolysis to form 2 GMP molecules, primarily facilitated by oligoribonucleases (Orr *et al.*, 2015). Frequently, GGDEF and EAL domains coexist within the same multi-domain protein (Romling, Galperin and Gomelsky, 2013). The genome of *P. aeruginosa* encodes over 40 enzymes responsible for maintaining intracellular c-di-GMP levels in balance (Ha and O'Toole, 2015). Among these enzymes, 17 feature the GGDEF domain, 16 possess both GGDEF/EAL domains, 5 carry only the EAL domain, and 2 have the HD-GYP domain (Kulesekara *et al.*, 2006).

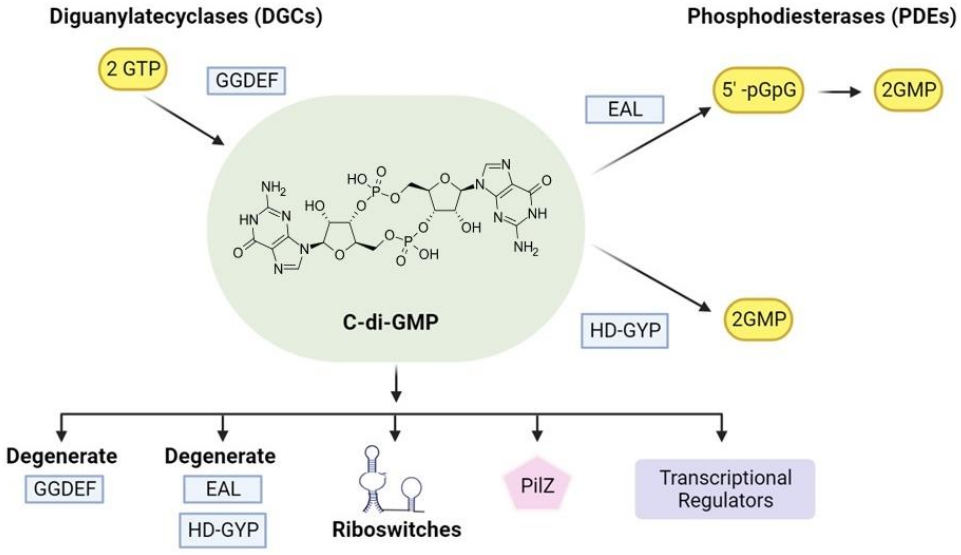

Figure 1.3 The basic pathway of c-di-GMP. C-di-GMP is produced by DGCs featuring a conserved GGDEF motif, while its degradation is facilitated by PDEs that possess either an EAL or HD-GYP motif. Receptor protein domains binding to c-di-GMP fall into five classes: degenerate GGDEF and EAL/HD-GYP, Riboswitches, PilZ, and transcriptional regulators.

1.2.3.2 C-di-GMP regulation of motility-sessility switch in *Pseudomonas aeruginosa.*

P. aeruginosa is an opportunistic pathogen, and its capacity to form biofilms within communities enhances its resistance, thus heightening the challenge of treatment. The transition from a planktonic to a biofilm lifestyle is intricate, necessitating multiple regulatory mechanisms. The primary regulator in this process is c-di-GMP, a key post-transcriptional signal that controls various factors crucial to biofilm formation. It is a nearly ubiquitous second messenger found in various bacteria, primarily responsible for controlling the motility-sessility switch. *P. aeruginosa* can sense many specific signals that affect the formation and dispersion of biofilms by regulating c-di-GMP, as shown in the figure, including QS signals, NO & nitrosative stress, glutamate, Oxygen limitation and sub-inhibitory antibiotic concentrations. (Sauer *et al.*, 2002; Davies and Marques, 2009) (**Figure 1.4**). The physiological roles of c-di-GMP in *P. aeruginosa* includes biofilm formation, motility and the production of EPS (Santos, 2012).

C-di-GMP regulates several cellular functions, such as modulating transcription factors or directly interacting with noncoding RNA molecules (riboswitches) to control gene expression, as well as allosterically regulating protein function and enzyme activity (Valentini and Filloux, 2016a). These regulations are establishing through molecular components consisting of various c-di-GMP binding receptors or c-di-GMP effector molecules. In *P. aeruginosa*, numerous c-di-GMP receptors

and effectors have been identified. For instance, PelD functions as a c-di-GMP receptor, and its expression and binding to c-di-GMP are connected to the production of Pel polysaccharide (Lee *et al.*, 2007).

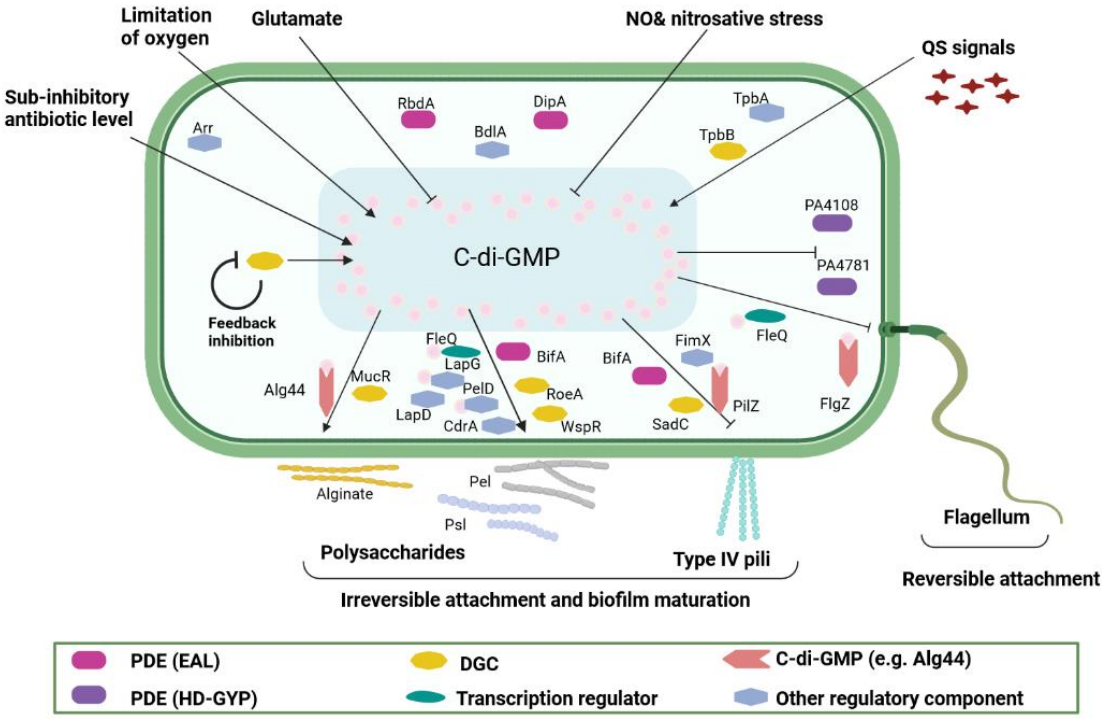

Figure 1.4 An illustration of known c-di-GMP proteins controlling biofilm formation and dispersal in *P. aeruginosa*. C-di-GMP regulates the formation and diffusion of biofilms in *P. aeruginosa* through a variety of different mechanisms involving different turnover enzymes and effectors that affect flagellar movement, twitching movement, attachment, and production of extracellular polysaccharides. (→) is shown as activation and (--|) mean inhibition (An and Ryan, 2016).

1.2.3.3 C-di-GMP plays diverse physiological roles in *Pseudomonas aeruginosa.*

C-di-GMP holds a crucial function in *P. aeruginosa*, controlling numerous cellular processes ranging from motility and biofilm formation to virulence and exopolysaccharide production (Simm *et al.*, 2004; Römling, Gomelsky and Galperin, 2005; Tischler and Camilli, 2009).

P. aeruginosa exhibits various modes of motility, such as swimming, swarming, and twitching. *P. aeruginosa*' motility require the flagella and twitching motility utilizes type IV pili. Flagellar motility is regulated by c-di-GMP at multiple levels (D'Argenio *et al.*, 2002). Among the regulators involved, AmrZ, previously recognized as AlgZ, functions as a transcription factor in *P. aeruginosa*.

It not only triggers alginate production but also serves as a positive regulator for Type IV pili biogenesis and twitching motility. Notably, in mucoid, nonmotile *P. aeruginosa* strains, AmrZ acts as a negative regulator of flagellum biosynthesis by repressing the flagellar master regulator FleQ. However, in nonmucoid strains, the deletion of AmrZ has no impact on flagellin synthesis (Baynham *et al.*, 2006; Tart, Blanks and Wozniak, 2006; Juan, Peña and Oliver, 2017). Among them, the transcription factor FleQ activates the synthesis of flagellar genes when the concentration of c-di-GMP is low. Flagellar gene transcription will be repressed when transcription of biofilm matrix components is activated by the c-di-GMP bound form of FleQ (Claudine and Harwood, 2013). Additionally, study show that the swarming motility of *P. aeruginosa* PA14 is promoted by PDE BifA and inhibited by DGC SadC (Kuchma *et al.*, 2007; Merritt *et al.*, 2007).

A study unveiled a robust correlation between hyper-biofilm formation and elevated intracellular c-di-GMP levels. This was achieved through an analysis of phenotypes linked to mutations in putative DGC and PDEA-encoding genes within *P. aeruginosa* (Kulasekara *et al.*, 2005). Pervious investigations have indicated that strains of *P. aeruginosa* exhibit reduced biofilm formation under GGDEF and EAL domain protein knockdown conditions, whereas overexpression augments biofilm development (Kulasekara *et al.*, 2005). The transcription factor BrlR has been identified as a contributor to colistin and tobramycin resistance in biofilms. It shows an enhanced interaction with DNA in the presence of c-di-GMP, functioning as an activator of multidrug efflux pumps (Liao, Schurr and Sauera, 2013). Furthermore, an additional study demonstrated GTP's ability to inhibit the PDE activity of the phosphodiesterase Arr in *P. aeruginosa*, thereby inhibiting the induction of tobramycin-mediated biofilm responses (Hoffman *et al.*, 2005). Usually, Research is focused on understanding the potential of reducing c-di-GMP levels, thereby preventing biofilm proliferation, and thus enhancing the treatment of diseases such as bacterial infections. Both NO and glutamate have been identified as agents capable of dispersing biofilms by actively reducing intracellular c-di-GMP levels. Notable regulatory components in biofilm dispersion include proteins from the GGDEF-EAL family, namely DipA, RbdA, MucR, and NbdA (Li *et al.*, 2013, 2014) and the GGDEF proteins NicD (Morgan *et al.*, 2006) and GcbA (Petrova, Cherny and Sauer, 2015) are both regulated with biofilm dispersion.

The intricate interplay between virulence and biofilm formation in *P. aeruginosa* underscores the significant involvement of c-di-GMP in the modulation of virulence. This is particularly evident through its impact on type III secretion systems, where the deletion of HD-GYP domains leads to impaired secretion of the ExoS effector protein. Furthermore, the observed distinct cytotoxicity patterns in *P. aeruginosa* mutant strains towards CHO cells shed light on the indirect role of c-di-GMP in governing cytotoxicity. Notably, strains like RocR, FimX, and PvrR, which lack cytotoxicity, contrast with WspR that exhibits partial cytotoxicity. That suggests c-di-GMP indirectly regulates

cytotoxicity by positively influencing Type III secretion systems while negatively impacting type IV pili (Kulesekara *et al.*, 2006; Rudzite *et al.*, 2023). In *P. aeruginosa*, the type Vb secretion system, which relies on the adhesin CdrA, is regulated by c-di-GMP through the GGDEF-EAL composite protein LapD and the associated protease LapG. Furthermore, *P. aeruginosa* virulence is influenced by the DGC YfiN or TpbB (Jacob G. Malone, 2012, Richard B. Cooley, 2016).

The three principal exopolysaccharides synthesized by *P. aeruginosa*, namely Pel, Psl, and alginate, are all subject to the influence of c-di-GMP. Transcriptionally, Pel production experiences positive regulation by c-di-GMP through the activation of the DGC WspR (Hickman, Tifrea and Harwood, 2005). Moreover, Pel polysaccharides undergo post-translational regulation mediated by the GGDEF c-di-GMP receptor PelD (Jennings *et al.*, 2015). E Elevated levels of c-di-GMP, generated by two distinct diguanylate cyclases (DGCs), have been observed to induce increased Psl production in *P. aeruginosa* (Irie *et al.*, 2012). Within the same context, the DGC SadC collaborates with the hydratase OdaA and the dioxygenase OdaI in a concerted manner to regulate alginate production. Notably, the synthesis of c-di-GMP by SadC is governed by an oxygen-dependent mechanism (Schmidt *et al.*, 2016). Furthermore, the GGDEF/EAL protein MucR, functioning as an active DGC, also contributes to the orchestration of alginate biosynthesis (Hay, Remminghorst and Rehm, 2009).

1.3 Diffusion signal factor signalling in *Pseudomonas aeruginosa.*

P. aeruginosa, recognized as a pathogenic bacterium capable of causing various infections, poses a particular threat to individuals with weakened immune systems. A key mechanism enabling *P. aeruginosa*' s survival and pathogenicity lies in its capacity to sense and response to its environment through an intricate network of signalling pathways. Among these intricate pathways, the diffusible signal factor (DSF) signalling system has been shown to play a key role in regulation of virulence, biofilm formation, and antibiotic resistance. In recent times, an increasing interest has been directed towards unravelling the molecular underpinnings of DSF signalling within *P. aeruginosa*. This aims to furnish novel strategies for the management of bacterial infections.

1.3.1 The Diffusion signal factor family in bacteria

Bacteria can produce signals of various structural categories. In the plant pathogen Xanthomonas campestris, the diffusion signal factor (DSF) was first described, with its signal molecule characterized as a cis-unsaturated fatty acid. Used to identify extracellular degrading enzymes and EPS in plant pathogens *Xanthomonas campestris* pv*. campestris* (*Xcc*). The unrelated bacteria

Burkholderia cepacia and *P. aeruginosa* produce the structurally related molecules (Boon *et al.*, 2008; Deng *et al.*, 2016). Signals involving these DSF family members not only contribute to the bacterial virulence, biofilm formation and antibiotic resistance of these important human pathogens, but also involve interspecies and interspecies signalling, which can regulate the behaviour of other non-signalling microorganisms (Ryan and Dow, 2008). Wang et al. (2020) developed an effective method for screening highly active DSF-degrading microorganisms and the results revealed the molecular basis of efficient DSF to explain the gift of bacteria and proposed to control infectious diseases caused by DSF-dependent bacterial pathogens useful genetic and biological control agents (Wang, Liao and Chen, 2020). The DSF from *Xcc* is characterized as cis-11-methyl-dodecenoic acid (Wang *et al.*, 2004). A key structural feature for the activity is the cis-unsaturated double bond position. This structural motif is regarded signature for signals from the DSF family. Multiple DSF family signals were detected in *Bccholderia cepacia complex* (*Bcc*) and Xanthomonas spp bacteria. Among them, *Bcc* has become the main opportunistic pathogen for immunocompromised individuals, especially patients with cystic fibrosis. And constitute most of the strains that can be spread and popular, with high toxicity (Isles *et al.*, 1984). Multiple DSF family signals have been identified in bacteria within the *Bcc* and in *Xanthomonas spp*. These Bcc bacteria: *Burkholderia lata*, *B. cenocepacia*, *B. vietnamiensis*, *B. dolosa* and *B. ambifaria* produce cis-2-dodecenoic acid (BDSF), while *B. multivorans*, *B. stabilis*, *B. anthina* and *B. pyrrocinia* also synthesise cis, cis-11-methyldodeca-2,5-dienoic acid, a new member of the Signal molecules DSF-like family (Deng *et al.*, 2010). DSF regulates biofilm formation, motility, and virulence through the two-component system RpfC/RpfG (Barber *et al.*, 1997; Slater *et al.*, 2000; Wang *et al.*, 2004).

RpfC is a sophisticated sensor kinase in xanthomonads, featuring distinct domains such as a sensory input domain, a histidine kinase (HK) domain, a CheY-like two-component receptor domain, and a C-terminal histidine phosphate transfer (HPT) domain (**Figure 1.5**) (Slater *et al.*, 2000; Ryan *et al.*, 2006, 2010). The RpfC–RpfG system in *Xcc* is extensively studied. RpfG, on the other hand, consists of a phosphoacceptor receiver (REC) domain and an HD-GYP domain, which functions as a phosphodiesterase responsible for the degradation of the second messenger cyclic di-GMP (**Figure 1.5**). Upon phosphorylation, RpfG becomes activated as a cyclic di-GMP phosphodiesterase. The ensuing changes in the cellular level of cyclic di-GMP influence the synthesis of virulence factors (Dow *et al.*, 2003).

1.3.2 Diffusion signal factor mediated interspecies communication with *Pseudomonas aeruginosa.*

Microbes interact with each other and can sense non-self-generated signals, among which various interspecies communication can be mediated by sensing DSF signalling molecules to influence the behaviour of organisms growing in polymicrobial communities. The exchange of signals between different species can result in changes to factors that impact the virulence or persistence of bacterial pathogens, as well as affecting the growth of advantageous microbial populations. *P. aeruginosa* is a widely concerned multidrug-resistant pathogens. Many CF patients infected *P. aeruginosa* are simultaneously co-infected with *Burkholderia cenocepacia* (*B. cenocepacia*) and/or *Stenotrophomonas maltophilia* (*S. maltophilia*) (Ryan and Dow, 2008; He *et al.*, 2023). Cis-2-dodecenoic acid (BDSF), one of the DSF-family signals was firstly identified in *B. cenocepacia* which affect the biofilm formation, swarming motility, and virulence (Deng *et al.*, 2012; Deng, Lim, *et al.*, 2013). The communication between *P. aeruginosa* and *B. cenocepacia* was mediated by the BDSF, the research has found the transcriptional level of QS regulator genes *rhlR*, *pqsR*, and *lasR* in *P. aeruginosa* were decreased when exogenously added BDSF and without significantly influence on *P. aeruginosa* growth. BDSF can also inhibit the T3SS genes expression and QS system in *P. aeruginosa* (Deng, Boon, *et al.*, 2013). *S. maltophilia* can synthesis the DSF due to it has *rpf* gene cluster (Fouhy *et al.*, 2007). *P. aeruginosa* can sensing DSF which produced by *S. maltophilia* to influences the biofilm architecture in *S. maltophilia–P. aeruginosa* cocultures. Study have shown that the polymyxin tolerance in *P. aeruginosa* biofilms were significantly enhanced when added the DSF to the co-culture system with *P. aeruginosa* and human CF-derived lung epithelial cells (Twomey *et al.*, 2012).

DSF family sensing and transduction into bacteria requires sensor kinases found in the cell's plasma membrane, for example RpfC is a complex sensor kinase. Sensor kinases that recognize DSF family signals in *P. aeruginosa* indicate that changes in the number-limiting pathway are related to the perception of DSF signalling molecules. Although *P. aeruginosa* cannot produced DSF signalling directly, the identification of PA1396 clearly shows the diversity of the signal sensing system of the DSF family (Ryan *et al.*, 2010). An et al. also demonstrated that DSF and cis-unsaturated fatty acid analogues improve *P. aeruginosa*' s resistance to several antibiotics, including polymyxin, nalidixic acid and tobramycin (An *et al.*, 2019). This process requires the participation of PA1396. As a sensor kinase, PA1396 has significant amino acid similarity with the input domain of RpfC and the N-terminus of DSF family signals (Ryan and Dow, 2008). An et al. demonstrated that DSF sensing requires two of the five transmembrane helices of the PA1396 input domain, and the binding of DSF is associated with enhanced PA1396 auto phosphorylation (An *et al.*, 2019). PA1397, a response regulator containing a CheY-like receptor domain and a

helix-turn-helix (HTH) DNA-binding domain, is thought to be a possible partner of PA1396 (**Figure 1.5**). Not only that, Twomey et al. (2012) found that DSF-mediated intermediate interactions occur in CF lungs, such as enhancing the tolerance of cationic antimicrobial peptides of *P. aeruginosa* biofilms grown on human airway epithelial cells, they may effect of antibiotics on chronic *P. aeruginosa* infection (Twomey *et al.*, 2012).

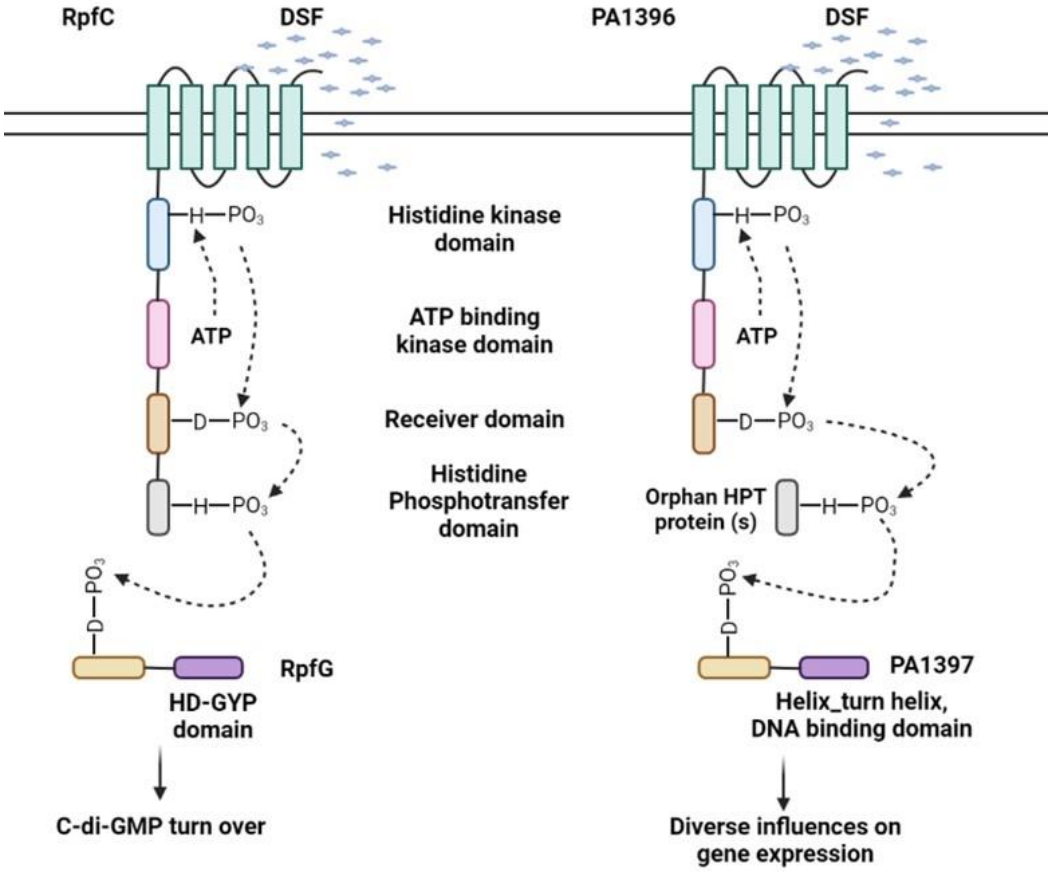

Figure 1.5 *Xanthomonas campestris pv. campestris* and *Pseudomonas aeruginosa* utilize different sensor kinases to perceive DSF (diffusible signal factor) signals. These sensors, along with their immediate signal transduction partners, (a) In Xcc, the sensor kinase RpfC interacts with RpfG. (b) In *P. aeruginosa*, the sensor kinase PA1396 is associated with PA1397, which is a hypothetical regulator of *P. aeruginosa* pathways. The latter acts as an interspecies sensor, sensing DSF signals produced by other species. In these sensor kinases, the letters "H" and "D" denote histidine and aspartic acid residues, respectively, which are involved in phosphorelay and phosphotransfer processes (Ryan and Dow, 2011; Ryan *et al.*, 2015).

1.4 Infection models of *Pseudomonas aeruginosa*

An increasing number of disease-causing bacteria are displaying multi-drug resistance, causing conventional antibiotics to become ineffectual in their therapeutic application. The need to explore and enhance alternative therapeutic approaches has become urgently. The combination therapy stands out as an emerging strategy to address the challenge of multiple drug resistance (MDR). This involves employing two types of interventions: a combination of antibiotics, and medications that target antibiotic resistance mechanisms, or a fusion of antibiotics with adjuvants. These innovative treatment methods have been anticipated as novel approaches for intervention (Tamma, Cosgrove and Maragakis, 2012). Nonetheless, an intricate relationship exists among the host, pathogens, and antibiotics, as discerned through the clinical manifestations of bacterial pathogenic infections. The innate immune system assumes a key role in combating bacterial infections. Therefore, strategic targeting of the host through reasonable combination therapy and appropriate antibacterial treatment of pathogens may inhibit antimicrobial resistance, thereby successfully treating and solving the problem of antimicrobial resistance infection, thereby overcoming some obstacle antibiotic treatment (Chiang *et al.*, 2018). In a common chronic infection state, bacteria are encapsulated in a biofilm structure, enabling them to withstand a variety of environmental attacks, including immune responses and antibacterial therapies. There have been many studies on the interaction between these molecules' *in vitro* experiments, but for the high efficiency and effectiveness of treatment, *in vivo* research and confirmation are very important.

1.4.1 *In vitro* models for studying *Pseudomonas aeruginosa* infections.

In vitro cell culture models involve the cultivation of cells within a laboratory environment, external to the organism. These models serve as valuable tools for investigating diverse facets of bacterial infections, including interactions between hosts and pathogens, bacterial virulence, and host immune responses. The utilization of these models presents several advantages, including the capacity to regulate experimental parameters, ensure reproducibility, facilitate accessibility, accommodate ethical considerations, and enable high-throughput screening. Various *in vitro* cell and tissue culture systems have been employed, encompassing epithelial cell cultures, macrophage cultures, neutrophil cultures, and organotypic tissue models.

A few studies have been performed to demonstrate the development of bacterial biofilms on cultivated epithelial cells, including Haemophilus influenzae and Mycobacterium avium biofilm formation on cultivated human airway cells and Salmonella enterica biofilm formation on HEp-2 liver cells (Boldrick *et al.*, 2002; Saga *et al.*, 2005). *P. aeruginosa* as an opportunity pathogen

caused many infections in the airway of patients with CF and other forms of bronchiectasis. The human airway epithelial cell culture is a very commonly used model system, which can be used to study *P. aeruginosa* infection in the lungs. There are several models to cultivate *P. aeruginosa* on human cells: 1) Monolayer cultures. In this model, a single layer of cells is grown on a flat surface, such as a petri dish or well plate. Monolayer cultures are commonly used to study host-pathogen interactions and the effects of bacterial toxins on host cells. 2) Co-culture models. This model involves the adaptation of biofilm flow cell equipment (usually used in biofilm research) to accommodate a single-layer glass cover glass that supports cell confluence. 3) Three-dimensional models. These models involve growing cells in a 3D structure, such as hydrogels or scaffolds, can more accurately mimic the microenvironment of host tissue, making them a more relevant tool for studying bacterial infections. The monolayer of cells is inoculated with *P. aeruginosa*, and then a peristaltic pump flows fresh medium through the cells (Moreau-Marquis *et al.*, 2010; De Bentzmann and Plésiat, 2011). The cell co-culture model allows the study of *P. aeruginosa* biofilm formation and biofilm cytotoxicity, as well as biofilm visualization.

There are also many cell culture model types of research using the ability of *P. aeruginosa* to adhere to host tissues, including but not limited to human airway epithelial cells (Di Paola *et al.*, 2017; Koeppen *et al.*, 2021), human oral epithelial cells (Geng *et al.*, 2017), human intestinal cells, pneumocyte Cells (Weichert *et al.*, 2013). In recent years, in vitro culture models of human epithelial cells have been widely used in various studies of *P. aeruginosa* infection. Through the study of the effectiveness of phage and ciprofloxacin alone and in combination in the treatment of *P. aeruginosa* infection in human airway epithelial cell line models, it was found that combining phage and ciprofloxacin can effectively treat *P. aeruginosa* infection and does not cause inflammation, making it a promising therapy for future clinical trials (Luscher *et al.*, 2020). By employing human lung epithelial cells as a model, it has been demonstrated that poly (acetyl, arginyl) glucosamine can effectively eliminate *P. aeruginosa* persister cells *in vitro*, without causing significant cytotoxicity at the concentrations tested. (Narayanaswamy *et al.*, 2018). A co-culture model of human bronchial epithelial cells and *P. aeruginosa* found that *P. aeruginosa*-derived flagellin induced the production of IL-6 and IL-8 in epithelial cells and found that corticosteroids were the most potent inhibitors which contributed to our understanding of the mechanisms behind the progression and exacerbation of COPD (Narayanaswamy *et al.*, 2018). Research on paraceratin and antimicrobial peptides (AMPs) in a co-culture model of human lung epithelial cells (A549) and *Pseudomonas aeruginosa* found effective antimicrobials, indicating the potential of keratin and AMPs for treating Pseudomonas infections in diseases such as cystic fibrosis (Oyardi, Savage and Guzel, 2022). Julien K. Malet et al. developed a model of *P. aeruginosa* infection in airway epithelium, allowing for the study of host-pathogen interactions

and bacterial factors involved in long-term intracellular persistence of *P. aeruginosa* in airway epithelial cells (Malet *et al.*, 2022). Overall, the use of *in vitro* human airway epithelial cell line models has proven to be a valuable tool in studying the efficacy of treatments for *P. aeruginosa* infections and has provided important insights into the pathogenesis of respiratory diseases and the development of novel therapies.

1.4.2 *In vivo* models for *Pseudomonas aeruginosa* infection.

At present, the use of invertebrate models makes the research of immune response to single infection flourish. For the study of the host, invertebrates are cheaper than ordinary rodents and pose a little moral challenge in model research. They are more effective and genetically easier to study. It is recognized that invertebrate and mammalian innate immune pathways have surprising homology and are recognized and activated by Toll signalling in humans and insects (Medzhitov, Preston-Hurlburt and Janeway, 1997). *In vivo* experiments are crucial for the clinical potential of novel antibiotic therapy. Animal models of inflammation caused by microbial infections like human pneumonia, and common biofilm bacteria, are established in mice and rats to track the body's immune response and the efficacy of antibiotic treatment (Høiby *et al.*, 2001; Mizgerd and Skerrett, 2008). Considering that these models are expensive and labour-intensive, and that mammals are under the control of ethics and strict rules, invertebrates are more used as an alternative model for microbiological research (O'Callaghan and Vergunst, 2010). The invertebrates, such as *Caenorhabditis elegans* (*C. elegans*) (Vasquez-Rifo *et al.*, 2019), *Galleria mellonella* (*G. mellonella*) (Cutuli *et al.*, 2019), *Drosophila melanogaster* (Stoltz *et al.*, 2008), or zebrafish (Clatworthy *et al.*, 2009) are commonly used to study host-pathogen interactions.

G. mellonella also known as larvae or waxworm used as a model of the host in microbiology has increased recently which has many advantages including low cost, high throughput due to the short lifespan, and similarities to mammalian innate immune response. The larvae as an *in vivo* model to study the antibiotics against gram-negative pathogens and related innate immunity without the adaptive response's influences (Kavanagh and Sheehan, 2018). Insect immunity relies on innate mechanisms including the prophenoloxidase system, defence proteins, and antimicrobial peptides. *G. mellonella* have numerous defence peptides with different properties in their hemolymph, which help fight off pathogens (Cytryńska *et al.*, 2007; Brown *et al.*, 2009). Certain larvae peptides and proteins, such as anionic peptide 2 and lysozyme, work together in the hemolymph to create a stronger antibacterial effect against Gram-negative bacteria (Zdybicka-Barabas *et al.*, 2012). Larvae can be infected with bacteria by injection, feeding, etc., and the infection status can be visually evaluated by observing the mortality, degree of melanisation, changes in gene expression, etc. *P. aeruginosa* as a typically gram-negative

pathogen, and many studies of infections caused by it have used the larvae model. Firstly, earlier studies have found that *P. aeruginosa* infection impairs the immune response of larvae, followed by high correlation between the results tested in the *C. mellonella* model and cytopathology assays using mammalian tissue culture systems (Madziara-Borusiewicz and Lysenko, 1971; Miyata *et al.*, 2003). The confirmation made more scientists choose to use this model for a series of studies on *P. aeruginosa* pathogenesis. which includes the role of the T3SS (Miyata *et al.*, 2003), evaluating antimicrobial agents (Zheng *et al.*, 2017; D'Angelo *et al.*, 2018; Naguib and Valvano, 2018), virulence factors (Tsai, Loh and Proft, 2016), and evaluate experimental phage therapy (Olszak *et al.*, 2015), etc. In addition, study found that the model can also distinguish different strains of *P. aeruginosa*, further confirming the role of the larvae model in the study of *P. aeruginosa* (Andrejko, Zdybicka-Barabas and Cytryńska, 2014).

In general, although the invertebrate model cannot fully simulate the real infection environment, the rapid reproduction of invertebrates meets the needs of multiple microorganisms for screening more mutants. Invertebrate models have been widely used to study *P. aeruginosa* infections due to their simplicity, low cost, and high throughput. The invertebrate models have proved to be valuable tools in understanding the molecular mechanisms underlying *P. aeruginosa* infection, play a very important role in the study between hosts and microorganisms, and have the potential to lead to the discovery of novel therapies against this important human pathogen.

1.5 The quest for novel antimicrobial compounds

The rapid development of bacterial resistance of clinically important antibiotics has become a serious threat to our ability to treat common infectious diseases, making more and more infections difficult to treat. Therefore, the discovery of new therapeutically interfering compounds has become very urgent. Small molecule screening can identify compounds that can regulate specific biological processes, so this method is usually used to develop small molecule drugs for further medical research. Nowadays, small molecule screening methods have become very common, and these specific compounds can be further modified to optimize their potential as drug candidates (Osipov *et al.*, 2019). Compared with the previous discovery through appropriate tests or the identification of active compounds in traditional drugs, small molecule screening methods have expanded the scope of screening and increased the possibility of developing new drugs. More and more bacteria are resistant to antibiotics, so the use of drugs based on changing signal molecules to reduce the pathogenicity of bacteria is more meaningful than directly changing the growth of bacteria (Rasmussen and Givskov, 2006).

1.5.1 Novel targets: The role of cyclic di-GMP signalling in *P. aeruginosa*.

Recently, interfering with the regulatory system of bacteria involved in virulence and disease through the intracellular second messenger c-di-GMP has become a promising target for effectiveness (Ryan, Tolker-Nielsen and Dow, 2012). The regulation and influence of bacteria by c-di-GMP have been explained in section 1.2.2 above, so we won't introduce too much here. Since c-di-GMP has a tentative effect on the formation of biofilms in bacteria, more and more research use interference and signal transduction strategies as control measures for biofilm infections. Recent studies suggest that altering c-di-GMP signalling could be used to either prevent the development of antibiotic-resistant illnesses or make them more sensitive to the immune system, or to provide effective treatment by co-administration of traditional antibiotics (Ryan, Tolker-Nielsen and Dow, 2012).

Several studies have identified molecules that can reduce the level of c-di-GMP in the body, including c-di-GMP signalling inhibitors in the screened molecular library, or reasonably involving diguanylate cyclase inhibitors, which are considered possible analogies of c-di-GMP (An and Ryan, 2016). Among them, Sambantha et al. tested a library of 66,000 compounds against *V. cholera* with transcriptional CdG reporter and identified N-(4-anilinophenyl) benzamide, 5-methoxy-2-[(4-methylbenzyl) and sulfanyl]-1Hbenzimidazole (Sambanthamoorthy *et al.*, 2012, 2014). To find possible c-di-GMP cyclase enzyme inhibitors, Lieberman et al. employed a distinct screening approach termed differential radial capillary action of ligand assay (Lieberman *et al.*, 2014). They tested a library of compounds that could disrupt PelD's (an enzymatically inactive GGDEF domain protein) interaction with 32P-c-di-GMP and discovered that the anti-cancer medication ebselen has such an activity. Ginger includes raffinose, which inhibits *P. aeruginosa* biofilms by lowering intracellular cyclic-di-GMP levels, resulting in a switch from non-motile (biofilm) to motile (planktonic) cells. The pathogen's growth is unaffected, implying that restricting cyclic-di-GMP could be a means to prevent biofilm development (Kim *et al.*, 2021). When in vitro, the artificial lowering of intracellular c-di-GMP in developing *P. aeruginosa* will result in a decrease in biofilm development and an increase in sensitivity to antimicrobial drugs (Christensen *et al.*, 2013). In 2016, Kushal N. Rugjee, et al. described a fluorescence-based high-throughput reporter gene detection method based on the previously developed GFP reporter gene measurement of c-di-GMP cell level and established that we can screen out small molecules that may regulate the level of c-di-GMP in *P. aeruginosa* cells and they also used this reporter gene to screen small molecules (Rugjee, An and Ryan, 2016). A high-throughput screening approach targeted c-di-GMP signalling was applied to identify small molecules that reduce c-di-GMP content in *P. aeruginosa*, whose activity depends on specific PDEs to induce the spread of *P. aeruginosa* biofilms (Andersen *et al.*,

2021). The previous research shows that the initiators that can inhibit c-di-GMP synthesis enzymes are effective against *P. aeruginosa* biofilm formation.

The c-di-GMP signalling pathway as one promising target for identifying antimicrobial drugs, which plays a crucial role in regulating bacterial virulence and biofilm formation. By targeting c-di-GMP, researchers can potentially develop new classes of antimicrobial drugs that can disrupt bacterial biofilms, prevent bacterial attachment to host cells, and enhance the immune response against bacterial infections. The study of c-di-GMP as a target for novel antimicrobial drugs provide new therapeutic options for the treatment of infectious diseases.

1.5.2 The role of natural products in antibacterial drug discovery.

Antibiotic overuse also aided the development of medication resistance, which could exacerbate the bacteria-infected sickness. To prevent bacterial and biofilm formation, innovative techniques other than antibiotics should be developed. Novel techniques to reducing biofilm development and QS, including natural compounds from plants, have been widely studied and published over the previous two decades. Antimicrobial and chemo preventive effects have been demonstrated in a variety of plant natural compounds (Tan and Vanitha, 2012). Due to their low cost and availability, natural products are used as medicine. They are chemically diverse with various bioactivities and are the most valuable sources of drug discovery and development (Shen, 2015). Evidence has accumulated suggesting natural compounds from plants have antibacterial and chemo preventive capabilities in the control of biofilm development. Plants used in traditional medicine, as well as marine invertebrates, insects, and vertebrate creatures on land, are being revived as possible sources of antimicrobials. Natural products, such as plants, minerals, and animals, have been extensively used for the treatment of various diseases. These products have also been a rich source of essential antibiotics, including well-known examples such as penicillin, streptomycin, and tetracycline (Uddin *et al.*, 2021). In fact, it is estimated that approximately 35 percent of all medicines developed to date have their origins in natural products (Calixto, 2019).

Many natural products have shown beneficial effects in the prevention and treatment of cancer and infectious diseases (Atanasov *et al.*, 2015). They treat cancer by exhibiting cytotoxic effects that attack macromolecules expressed by cancer cells, such as those in oncogenic signal transduction pathways, such as paclitaxel and eribulin mesylate in the treatment of breast cancer/metastatic breast cancer (Walsh and Goodman, 1999; Dyshlovoy and Honecker, 2018), and cytarabine in the treatment of leukemia, Vincristine provides effective agents against childhood leukemia (Khalifa *et al.*, 2019). Teixobactin is a newly discovered natural product that is effective against a variety of bacterial infections, such as in patients with methicillin-resistant

Staphylococcus aureus (Piddock, 2015; McCarthy, 2019). Darobactin is another recently discovered natural product that has shown promise as a potential new antibiotic (Imai *et al.*, 2019). Kanglemycin A, a natural ansamycin antibiotic, exhibits antibiotic properties against Gram-positive bacteria resistant to rifampicin as well as multidrug-resistant strains of Mycobacterium tuberculosis (Mosaei *et al.*, 2018). These findings clearly indicate that natural products hold great promise as innovative therapies. From Teixobactin and Darobactin, which exhibit potential as new antibiotics, to paclitaxel and cytarabine, which are cytotoxic agents used to treat different types of cancer, these natural products offer new possibilities for developing therapeutic treatments that have been challenging to use in the past. The diseases targeted by these treatments provide hope and emphasize the significance of ongoing research in this area.

The current pharmaceutical industry is equipped with proprietary libraries containing millions of compounds, showcasing the strength of reserves. These collections of compounds are commonly known as compound libraries and serve as the foundation for screening, which has emerged as a critical field for numerous companies (Holland‐Crimmin, Gosnell and Quinn, 2011). In the past, many medicines were extracted from natural products, most of which were plant extracts. At present, many small molecule libraries still have libraries of natural plant extracts. Recently, natural product libraries have been actively used in medicines Discovery. Correspondingly, some naturally known compounds are also popular in screening. These chemical libraries are commonly used for laboratory drug screening, drug discovery and target identification and other drug-related applications. They can also be used for high throughput screening (HTS) and high content screening (HCS).

1.5.3 Screening assays as a tool for drug discovery.

Screening assays are critical components in the process of drug discovery, as they enable scientists to identify potential therapeutic compounds. These assays are employed in the early stages of drug development to test a vast number of compounds for their ability to bind to specific target molecules, inhibit enzymes or signalling pathways, or affect certain biological functions. The purpose of these assays is to identify lead compounds that may have the potential to be developed into drugs. To do this, scientists use high-throughput screening (HTS) methods, which allow them to test hundreds or even thousands of compounds simultaneously (A, R and R. Radhakrishnan, 2011; Szymański, Markowicz and Mikiciuk-Olasik, 2012). These methods are designed to be rapid, reliable, and cost-effective. HTS plays a crucial role in the early stages of drug development. It is a critical component in the early stages of drug development. The process involves rapidly and efficiently screening large numbers of compounds to identify those that have the potential to be developed into drugs. HTS not only enables Nuclear Magnetic Resonance

(NMR)-based screening to identify compounds that bind to specific protein targets (Kumar and Clark, 2006), but also supports purity determination of screened compounds using techniques such as High-Performance Liquid Chromatography (HPLC) and HPLC- Mass Spectrometry (MS) (Ermer and Vogel, 2000; Gerber *et al.*, 2004). In recent years, a large amount of research has been carried out for drug discovery through high-throughput screening. MDM2 Inhibitor idasanutlin identified as a promising resensitizer of venetoclax-resistant neuroblastoma cell lines through HTS (Vernooij *et al.*, 2021). A HTS combining SDS-stimulated αSN aggregation with FRET was developed to identify derivatives of (4-hydroxynaphthalen-1-yl) sulfonamide as inhibitors of αSN aggregation and αSOs membrane permeabilization activity. Potential Inhibitor Potentially Affects Parkinson's Disease (Kurnik *et al.*, 2018). Ivacaftor as a medication used to treat cystic fibrosis, which was developed using HTS to identify compounds that target a specific mutant protein responsible for the disease (Sermet-Gaudelus, 2013). High-throughput screening is already heavily used, but due to the limitations of its single-effect measurement, an alternative screening modality-high content screening has also received attention.

High content screening (HCS) is a high-throughput screening technology based on cells and biological tissues, which can efficiently screen and analyse many biological samples. HCS technology is used in all aspects of modern drug discovery, from primary compound screening to early evaluation of ADME/toxicity properties and complex drug profiling. It has also been applied to stem cell biology research (Zanella, Lorens and Link, 2010). High content cellular imaging is a valuable tool for disease-relevant cell screening in early stages of drug discovery. The researchers developed a high-content screening assay to measure lysosomal and cytotoxicity. Known bacteriolysis-inducing drugs were identified and the anticancer drugs gefitinib, lapatinib, and dasatinib were found to cause bacteriolysis (Nadanaciva *et al.*, 2011). Developmental validation of high-content screening assays identifies cytoplasmic dynein-mediated glucocorticoid receptor translocation to the nucleus, such as 17-AAG, a benzoquinone ansamycin (Johnston *et al.*, 2012). HCS was also used to identify a method which combined the high content cell painting assay and the theta comparative cell scoring to measure the similarity of phenotypic response between breast cancer cell types that have genetic differences (Warchal *et al.*, 2020).

Screening assays are critical in drug discovery to identify potential therapeutic compounds by testing their ability to bind to targets or affect biological functions. HTS methods enable rapid and cost-effective testing of large numbers of compounds. HCS is another cell-based screening technology that efficiently screens and analyses many biological samples, used in drug discovery and stem cell research to identify potential drugs for diseases like cancer and cystic fibrosis.

1.6 Objectives and aims.

Many pathogenic bacteria use cell–cell signalling to regulate the expression of factors contributing to virulence. It is known that the opportunistic pathogen *P. aeruginosa* can participate in interspecies signalling mediated by DSF (diffusible signal factor) family signals. Sensing of these signals involves the histidine kinase PA1396 and leads to altered biofilm formation and increased tolerance to several antibiotics. A further understanding of the signal transduction mechanisms that underpin antibiotic resistant biofilm formation could suggest strategies for interference, with consequences for disease control. Additionally, as drug-resistant bacteria pose a major threat to healthcare systems worldwide, the new and effective antimicrobial drugs are urgently needed. *P. aeruginosa* infection is a bacterium known to cause acute and chronic infections in immunocompromised and hospitalized patients. C-di-GMP serves as a signalling molecule that regulates antibiotic resistance, biofilm formation, and virulence, allowing *P. aeruginosa* to control the expression of multiple genes.

The objectives of the study are:

1. To elucidate the molecular basis of DSF signalling in *P. aeruginosa* focusing on signal transduction involving the sensor kinase PA1396.
2. To optimize and validate a co-culture biofilm model that uses human bronchial epithelial cell and *P. aeruginosa*. The model will examine the impact of DSF signalling pathway on host-micro interaction and identify small molecules that influence *P. aeruginosa* viability and/or virulence during infection.
3. To explore the potential of targeting intracellular c-di-GMP as a strategy to combat antibiotic-resistant *P. aeruginosa* infections. Evaluate the effects of natural compounds on c-di-GMP levels, biofilm formation, and cytotoxicity in *P. aeruginosa*.
4. To design a high-content screening assay based on a co-culture model to screen natural products to identify potential small molecules that modulate c-di-GMP levels in bacteria, affecting *P. aeruginosa* biofilm formation and cytotoxicity.

Chapter 2 Investigating the signal transduction mechanism of Diffusible signal factor perception in *Pseudomonas aeruginosa*

2.1 Abstract

Pseudomonas aeruginosa is an opportunistic bacterial pathogen that causes acute and chronic infections. Its ability to grow in biofilm form poses significant challenges for treatment. The bacterium employs N-acyl homoserine lactones and the quinolone signal PQS as signalling molecules to regulate the production of virulence factors (Ng *et al.*, 2012; Chugani and Greenberg, 2014). Inhibition of these pathways through small molecules has been reported to decrease virulence factor synthesis. Gold nanoparticles (Au-NPs) and selenium nanoparticles (Se-NPs) have demonstrated the potential to effectively inhibit quorum sensing and virulence factors at low concentrations in *P. aeruginosa*, highlighting their efficacy as molecular-level inhibitors of both quorum sensing and virulence traits (Elshaer and Shaaban, 2021). In addition to intra-species signalling, *P. aeruginosa* engages in inter-species communication through the DSF family's cis-2-unsaturated fatty acids. This signalling mechanism can modify biofilm formation and enhance tolerance to various antibiotics.

This study focuses on investigating the signal transduction mechanism involved in the perception of DSF in *P. aeruginosa*. The sensor kinase PA1396 plays a role in sensing DSF and possesses the HK and receiver domains. Further analysis of the genomic region surrounding PA1396 reveals an upstream gene encoding a putative response regulator (PA1397) with the receiver domain and DNA binding domain. Notably, PA1396 differs from other proteins in the sensor kinase family as it lacks the Hpt domain. However, the analysis of the PAO1 genome identifies several orphan Hpt domains, namely hptA, hptB, and hptC. The goal of this study is to systematically study the functions of DSF-related genes in *P. aeruginosa* by using gene mutation and complementation strategies. Mutations and complementation of hptA, hptB, and hptC result in changes in cytotoxicity and swarming motility, indicating their involvement in the process. Additionally, the observed phenotypic similarities between PA1396 and PA1397 when mutated suggest a functional link between these two genes, potentially indicating a two-component system between them. A comprehensive understanding of the signal transduction mechanism underlying DSF perception in *P. aeruginosa* can offer valuable insights into the regulation of its virulence and contribute to the development of novel therapeutic strategies.

2.2 Hypothesis

It is hypothesized that PA1396 and PA1397, along with the orphan Hpt domains hptA, hptB, and hptC, play crucial roles in the signal transduction mechanism of Diffusible Signal Factor (DSF) perception in *P. aeruginosa*. Understanding the functional relationships among these proteins will provide valuable insights into the regulation of virulence factors and may unveil potential therapeutic targets against *P. aeruginosa* infection.

1. The presence of the receptor and DNA-binding domains in PA1397, along with its genetic proximity to PA1396, suggests a potential functional interaction between these two ptoteins. The similarities in phenotypic outcomes observed upon mutation of PA1396 and PA1397 indicate a potential functional link, possibly indicating the presence of a two-component system.
2. The absence of the Hpt domain in PA1396, unlike other sensor kinase family proteins, suggests that the orphan Hpt domains (hptA, hptB, and hptC) identified in the PAO1 genome may be involved in the DSF-sensing signal transduction process.
3. Mutating and complementing hptA, hptB, and hptC are expected to result in alterations in cytotoxicity and swarming motility, indicating their involvement in signal transduction mechanisms.

2.3 Materials and Methods

2.3.1 Bioinformatics analysis

We utilized the SMART bioinformatics platform to identify and annotate domain sequences of the PA1396 protein. Initially, we accessed the SMART website at http://smart.embl.de/, input the sequence of the target protein PA1396, and initiated the analysis process by clicking the "Submit" or "Search" button. Subsequently, we examined the analysis report to determine the crucial domains present in the protein and explored information about neighbouring genes.

2.3.2 Bacterial strains and cell culture conditions

The strains used in this study are found in **Table 2.1**, all of strains store at -80°C freezer. *P. aeruginosa* were routinely grown in Luria–Bertani (LB) medium. For growth curves, cells were also grown in M9 medium, which comprises M9 salts (5 X), 20% glucose (Merck Group), 1M MgSO4 (Fisher Scientific), 1M $CaCl_2$ (Fisher Scientific), H_2O. Human bronchial epithelial cell line 16HBE 14o- was a gift from Professor Jane Lucas (University of Southampton, UK) and was cultured in Gibco™ Minimum Essential Media (MEM, Merck) supplement with 10% fetal bovine serum (FBS)

(Merck Group), 2 mM L-glutamine (Merck Group) and Gibo™ Penicillin- streptomycin (50 U/mL penicillin, and 50 µg/mL streptomycin, Thermos Fisher Scientific) at 37 °C with 5% CO_2. In the co-culture biofilm model, Minimum Essential Medium Eagle (Thermo Fisher Scientific) supplemented with 2mM L-glutamine was used to wash cells before infection. And then 0.4% arginine (Merck Group) was added to the medium used for infection.

Table 2.1 Strains and plasmids used in this study.

Strains/Plasmids	**Relevant genotype or description**	**Source**
Strains		
E. coli		
DH5α	*E. coli* strain for constructing recombinant plasmids	This study
SM10	*E. coli* strain as conjugation donor	(Miller and Mekalanos, 1988)
pRK6000	*E. coli* fertile helper strain	(Bao et al., 1991)
pUX-BF13	*E. coli* helper strain carrying a transposase on a pUX plasmid	(Kessler, de Lorenzo and Timmis, 1992)
pUC18 - Tn7-*gfp*-StrepR	DH5α carrying Tn7-gfp-StrepR cassette on a pUC18 plasmid	Lab stock
P. aeruginosa		
PA14	Wild type	(Rahme *et al.*, 1995)
ΔPA1396(PA14)	*PA1396* deletion mutant	This study
*CPA1396(*PA14)	complementation strain	This study
ΔPA1397(PA14)	*PA1397* deletion mutant	This study
CPA1397(PA14)	complementation strain	This study
*Δhpt*A(PA14)	*hpt*A deletion mutant	This study
*Chpt*A(PA14)	complementation strain	This study
*Δhpt*B(PA14)	*hpt*B deletion mutant	This study
*Chpt*B(PA14)	complementation strain	This study
*Δhpt*C(PA14)	*hpt*C deletion mutant	This study
*Chpt*C(PA14)	complementation strain	This study
PA14-*gfp*	PA14 WT with chromosomal GFP tag	This study

PA14-*lux*	*luxCDABE*-tagged PA14	This study
PA14-*lux* (pCdrA::*gfp*^{C})	*luxCDABE*-tagged PA14 harboring plasmid pCdrA::*gfp*	This study
Plasmids		
pEX18Gm	Allelic exchange vector, Gm^{r}	(Hoang et al., 1998)
pME6032Gm	Vector for IPTG-inducible expression in *P. aeruginosa*, *lacI*^{Q}, Gm^{R}	Lab stock
pCR-TOPO	Cloning vector, Amp^{R} Kan^{R}	Invitrogen
p*ChptA*-TOPO	pCR-TOPO derivative carrying a copy of *hptA*	This study
p*ChptB*-TOPO	pCR-TOPO derivative carrying a copy of *hptB*	This study
p*ChptC*-TOPO	pCR-TOPO derivative carrying a copy of *hptC*	This study
p*ChptA*-pME6032Gm	pME6032 derivative carrying an IPTG-inducible copy of *hptA*	This study
p*ChptB*-pME6032Gm	pME6032 derivative carrying an IPTG-inducible copy of *hptB*	This study
p*ChptC*-pME6032Gm	pME6032 derivative carrying an IPTG-inducible copy of *hptC*	This study
p*hptA*up&down-TOPO	For make deletion mutant for *ΔhptA*	This study
p*hptB*up&down-TOPO	For make deletion mutant for *ΔhptB*	This study
p*hptC*up&down-TOPO	For make deletion mutant for *ΔhptC*	
pEX18Gm-*hptA*up&down	For make deletion mutant for *Δhpt*A	This study
pEX18Gm-*hptB*up&down	For make deletion mutant for *Δhpt*B	This study
pEX18Gm-*hptC*up&down m	For make deletion mutant for *Δhpt*C	This study
pCdraA::*gfp*^{C}	pUCP22Not-PcdrA-RBSII-*gfp*(Mut3)-T0-T1	(Rybtke *et al.*, 2012)
pUC18T-mini-Tn7T-*lux*-Gm	suicide vector for shuttling single copies of genes directly to the chromosome via a mini-Tn7 element; *aacC1* gene encoding gentamicin resistance marker on Tn7 element; contains oriT for mobilization; P1 integron promoter driving expression of *lux*CDABE; Amp^{r} Gm^{r}	(Damron *et al.*, 2013a)

2.3.3 DNA manipulation

Genomic DNA extraction. To extract genomic DNA, bacterial colonies were suspended in sterile water and incubated at 65°C for 15 minutes to disrupt cell walls. After centrifugation, the supernatant was removed, and the pellet was resuspended in a lysis buffer (40mM Tris-acetate

pH 7.8, 20Mm sodium acetate, 1mM Ethylenediaminetetraacetic acid (EDTA), 1% (M/V) Sodium dodecyl sulfate (SDS)). The mixture was supplemented with 5M NaCl and frozen for 20 minutes. Centrifugation separated the supernatant. Ethanol was added to the supernatant, followed by centrifugation to precipitate DNA. The supernatant was discarded, and the DNA pellet air-dried. The dried DNA pellet was reconstituted in sterile water for subsequent analysis.

PCR reaction, gel electrophoresis and PCR products purification. All the primers needed for this experiment have been designed and to be used as PCR amplification experiment (**Table 2.2**). The PCR amplification reaction system is fellow as **Table 2.3** and the PCR amplification reaction conditions in G-STORM are show in **Table 2.4**. 1% gel electrophoresis have been used to detect the quality of DNA. The gels were stained with 1X GelRed® Nucleic Acid Gel Stain (Biotium). Then the SYNGENE (GiBox) Gel image acquisition and analysis equipment have been used to collect electrophoretic band images.

The polymerase chain reaction (PCR) products were purified using the Qiaquick PCR purification kit (Qiagen) in accordance with established protocols. Initially, DNA was combined with buffer PB (ratio of 1:5), and the resulting mixture was loaded onto a purification column. Centrifugation was performed to facilitate the binding of the DNA to the column. Subsequently, the buffer PE, which contained added ethanol, was applied to the column. Centrifugation was carried out to remove any washing buffer. To elute and collect the purified DNA, sterile water was added to the central of column. The elution process facilitated the release of the purified DNA from the column, allowing it to be collected for subsequent analysis.

1% gel electrophoresis have been used to detect the quality of DNA. The gels were stained with 1X GelRed® Nucleic Acid Gel Stain (Biotium). Then the SYNGENE (GiBox) Gel image acquisition and analysis equipment have been used to collect electrophoretic band images.

Table 2.2 Summary of primers used in this chapter.

Primer Name	**Sequence**	**RE site***	**Purpose**
hptAUp-F	GGATCCTTTCCAACACATGCGCGT	BamHI	Forward primer for *Δhpt*A upstream fragment and *Δhpt*A fusion, and identifition
hptAUp-R	CTAGAGCCTCGCTTTCATACAGACTCC		Reverse primer for *Δhpt*A upstream fragment
hptADown-F	ATGAAAGCGAGGCTCTAGAGATCGGGC		Forward primer for *Δhpt*A downstream fragment
hptADown-R	AAGCTTTCTATAAGAGCCAGCAAC	HindIII	Reverse primer for *Δhpt*A downstream fragment and *Δhpt*A fusion, and identifition

ChptA-F	GAGCTCATGAAAGCGCTTGGTTCGGAA	SacI	Forward primer for C*hpt*A fragment and identifition
ChptA-His-R	GGTACCCTAGTGGTGGTGGTGGTGGTG GAGCCTTGCCAATTC	KpnI	Reverse primer for C*hpt*A fragment and identifition
hptBUp-F	GGATCCGCCCTGGAACATGGCGTC	BamHI	Forward primer for *Δhpt*B upstream fragment and *Δhpt*B fusion, and identifition
hptBUp-R	TCAGCGATACGCGGACATTCGATCGCT		Reverse primer for *Δhpt*B upstream fragment
hptBDown-F	ATGTCCGCGTATCGCTGAGGTTTTCGT		Forward primer for *Δhpt*B downstream fragment
hptBDown-R	AAGCTTGGTGCCAGGTAGAGCAGC	HindIII	Reverse primer for *Δhpt*B downstream fragment and *Δhpt*B fusion, and identifition
ChptB-F	GAGCTCATGTCCGCGCCGCATCTCGAT	SacI	Forward primer for C*hpt*B fragment and identifition
ChptB-His-R	GGTACCTCAGTGGTGGTGGTGGTGGTG GCGATAGCGCTGACG	KpnI	Reverse primer for C*hpt*B fragment and identifition
hptCUp-F	GAATTCCACCAAGGTCCTGGTCCT	EcoRI	Forward primer for *Δhpt*C upstream fragment and *Δhpt*C fusion, and identifition
hptCUp-R	CTATGACTTCGTTCGCATGGGATCCTC		Reverse primer for *Δhpt*C upstream fragment
hptCDown-F	ATGCGAACGAAGTCATAGCGTTGCGGG		Forward primer for *Δhpt*C downstream fragment
hptCDown-R	AAGCTTTTTCGTCGACTGGCTGCA	HindIII	Reverse primer for *Δhpt*C downstream fragment and *Δhpt*C fusion, and identification
ChptC-F	GAGCTCATGCGAACGTTCGACCTGACC	SacI	Forward primer for C*hpt*C fragment, and identification
ChptC-His-R	GGTACCCTAGTGGTGGTGGTGGTGGTG TGACTTCGCCGTGCC	KpnI	Reverse primer for C*hpt*C fragment, and identification
16S-F	GTAAAGCGTGCGTAGGTGGT		For conventional PCR amplification
16S-R	CTTTCGTGCCTCAGTGTCAG		For conventional PCR amplification

Table 2.3 The PCR amplification reaction set-up.

Reagent	**Volume**
2×Master Mix	10 μL
H_2O	8 μL
Primer F&R	1 μL
Template	1 μL

Table 2.4 PCR amplification reaction conditions set-up.

Temperature (°C)	**Time (min)**	
95	00:30	
95	00:30	×30 cycles
45-68	00:30	
68	00:30	
68	05:00	

Plasmid extraction and Gel extraction. Plasmid extraction utilized the QIAprep Spin Miniprep Kit (Qiagen, UK) according to standard protocols. The overnight culture underwent centrifugation, and the resulting pellet was resuspended in buffer P1 before being transferred to a microcentrifuge tube. Sequential additions of buffer P2 and buffer N3 followed by thorough mixing led to the formation of a precipitate. Centrifugation facilitated the pelleting of the precipitate. Subsequently, the plasmid-containing supernatant was applied to a spin column and centrifuged. The flow-through was discarded, and PE buffer (with added ethanol) was introduced. Two additional centrifugation steps were performed to ensure the removal of washing buffer. To elute and collect the purified DNA, sterile water was added to the centre of the column. This elution step effectively released the purified DNA from the column, enabling its collection for subsequent analysis.

DNA fragments were extracted from agarose gels using the MiniElute gel purification kit (Qiagen). Initially, plasmid was electrophoresed at 160V for 50 minutes in the gel. Following gel electrophoresis, the desired DNA band was precisely excised, ensuring maximum yield. The excised DNA band was then dissolved in buffer QG, using a 3:1 volume ratio. Incubation at 60 °C for approximately 10 minutes facilitated DNA dissolution. Subsequently, isopropanol was added in a 1:1 volume ratio to the dissolved DNA. The mixture was transferred to a spin column and centrifuged to bind the DNA. DNA and column were washed with PE buffer (with ethanol) and two centrifugation steps removed the washing buffer. Purified DNA was eluted and collected by adding sterile water to the column's center, effectively releasing it for subsequent analysis.

Enzyme digestion. Incubated the mixed system show in (**Table 2.5**) at 37°C for more than 2 hours, and 2 volumes ethanol then was added and centrifuge to precipitating. The supernatant was removed, and H_2O was added to dissolve.

Table 2.5 The enzyme digestion reaction set-up.

TOPO cloning. Gene cloning was conducted using the TOPO™ TA Cloning™ Kit (Invitrogen) according to the standard protocol. The salt solution and TOPO vector were kept on ice to maintain their stability and prevent degradation. PCR products (4 µL) were ligated with salt solution (1 µL) and TOPO vector (1 µL). After a 5-minute incubation at room temperature, the mixture was introduced into competent DH5α cells for diffusion. To ensure the integrity of bacterial cell membranes, the tube was transferred to ice. Subsequently, a brief heat shock at 45°C created temporary pores in the membranes, enhancing DNA uptake. LB medium was added to the tube to support the recovery and expression of the target genes in the transformed bacteria. Following a 1-minute centrifugation, the supernatant was removed, leaving 200 µL to resuspend the bacterial pellet. The resuspended mixture was plated on LB agar (under 35 µg/mL kanamycin) and incubated overnight at 37°C to allow colony formation. Colonies were picked and lysed in sterile water at 65°C for 15 mins, and PCR amplification was performed on the lysed samples. The PCR products were then confirmed through gel electrophoresis.

2.3.4 Mutagenesis of *hptA*, *hptB* and *hptC* genes

The construction of the mutant required the gene fragment to be ligated into the suicide vector, and the deletion construct was transferred to the *E. coli* cell and integrated into the *P. aeruginosa* chromosome through homologous recombination, as shown in (**Figure 2.1**). A pair of upstream and downstream primers (see primer list) have been designed for PCR amplification of the extracted total genomic DNA (gDNA). Performed PCR amplification reactions on the separately extracted upstream and downstream gDNA to amplify the target DNA fragments. The reaction conditions and reaction system were as above. The upstream and downstream amplified products have been mixed and diluted. Splicing by overhang extension (SOE)-PCR reaction was used to assemble and amplify the required mutant alleles and purify follow the step above. TOPO cloning technology was used to insert the fused and purified mutant alleles into the selected allele

exchange vector by adding 4 µL of product, 1 µL of TOPO vector and 1 µL of salt solution to in the PCR test tube. The colonies were plated, split, and the results of PCR verification were screened to identify the clones with the desired insert. The extracted plasmid was digested with BamHI/HindIII, then sent to Eurofins company for sequencing for double check. The plasmid and suicide vector have been connected by incubating the mixture of 4 µl pEX18Gm, 4ul plasmid, 1µl T4 DNA lygase, 1µl 10×buffer for T4 DNA ligase with 10 mM ATP overnight at room temperature, and then standard chemical transformation was used to transform the allelic exchange vector into a suitable donor *E. coli* strain. Then the plasmid of the bacteria strain which resistant Gentamycin (Gm) was extracted and transformed to the SM10. Then it is transformed into *P. aeruginosa* cells by mating the parents. Finally, the plasmid of the colony resistant to Gm and sucrose was extracted.

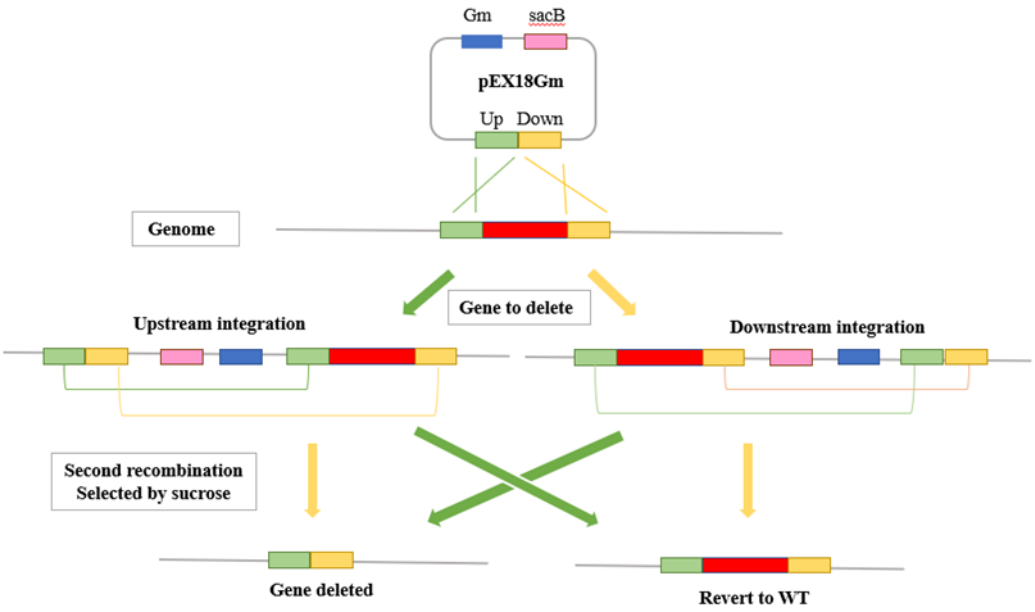

Figure 2.1 Gene knockout of *P. aeruginosa* by recombining homology. Firstly, primers specific to the genomic DNA sequence flanking the sequence cloned into the pEX18Gm vector were used for amplification, and the *E. coli* DH5α transformants containing the plasmid with the deleted allele were screened. The metalloid ploidy in which the deletion construct is integrated into the chromosome is then screened. After the second recombination, the deletion mutants were screened.

2.3.5 Complementation of mutants Δ*hptA*, Δ*hptB* and Δ*hptC*

A pair of primers (refer to the primer list) was designed for PCR amplification of the total gDNA extract. PCR amplification reaction was performed to amplify the target DNA fragment. The reaction conditions and system were the same as mentioned above. The purified product was

then subjected to the purification steps described earlier. The TOPO cloning technique was used to insert the purified mutant allele into the selected allele exchange vector. Plasmid extraction from successfully inserted colonies was validated using PCR, followed by further validation through restriction enzyme digestion. The extracted and purified plasmids were ligated into pME6032Gm. The plasmids were then transferred to *P. aeruginosa* by electroporation.

The culture of allele exchange vector-prepared strains (OD_{600} = 0.3-0.5) were centrifuged at 4°C, and the cell pellet was washed sequentially with equal volumes, 0.5 volumes, and 0.01 volumes of ice-cold 300 mM sucrose. After cooling the cells on ice for 30 minutes, up to 1 µg of plasmid DNA was added to the bacterial suspension, and the mixture was transferred to a pre-chilled, sterile 0.2 cm electroporation cuvette. Electroporation was performed at 1.8 kV, 25 µF. LB medium was added, and the cells were transferred to sterile tubes and incubated on a shaker at 37°C for 2 hours for plasmid expression. After incubation, the mixture was plated on LB agar supplemented with appropriate antibiotics. The plates were incubated at 37°C for detection. Finally, plasmids were extracted from successfully introduced colonies and validated by PCR.

2.3.6 In *vitro* phenotype assays

Growth curves assays. *P. aeruginosa* strains were incubated overnight. The optical density at 600 nm (OD_{600}) of the overnight culture was measured and adjusted to OD_{600}=0.01. Subsequently, the culture was added to each well of a 96-well plate, with six wells per sample and a control group containing only LB medium. The plate was placed in a reader and incubated for 24 hours, with OD_{600} measurements taken every 20 minutes to observe the growth curve.

A similar experiment was conducted using M9 minimal medium. The overnight culture pellet was resuspended in M9 medium, and the OD_{600} was adjusted accordingly. The culture was then divided into a 96-well plate, including a control group with only M9 medium. The plate was incubated for 48 hours, with readings taken every 40 minutes to observe the growth curve and collect data.

Swarming motility assay. The *P. aeruginosa* strains were cultured overnight until reaching an optical density of OD_{600} = 1. Swarming phenotypes of the *P. aeruginosa* strains were evaluated using 0.5% swarming agar, composed of 5g/L Eiken Agar, 5g/L Nutrient Broth, and 5g/L Glucose. For each plate, 2.5uL of the overnight *P. aeruginosa* culture was pipetted and spotted at the centre. The plates were then incubated at 37°C for 16-24 hours. The ability to swarm was determined by observing the spread of motility across the agar surface and measuring the distance of swarming from the central inoculation site.

2.3.7 Phenotype assays based on co-culture model.

Airway Epithelial Cell Thawing and Culture. 16HBE 14o- cells were thawed from liquid nitrogen and immediately placed in a 37°C water bath for approximately 1 minute to defrost. Once thawed, the cells were transferred directly into a tissue culture hood and gently mixed by flicking the tubes. They were then added to a new Falcon tube. Fresh complete media was pipetted up and down to mix with the cells, ensuring a final dimethyl sulfoxide (DMSO) concentration below 1% (Merck, UK). After a brief centrifugation, the cell pellet was resuspended in 10 mL of complete media in a T75 TC treated flask (SLS, UK) and incubated at 37°C with 5% CO_2. For epithelial cells, the media needed to be changed every two days, and typically, the cells reached >80% confluence after 5 to 7 days.

Co-culture Biofilm Assay. 16HBE 14o- cells were seeded in the 24/96 plate (Greiner, UK) or µ-Slide chamber slide (ibidi, Thistle Scientific). The cells are grown to form a confluent monolayer before being inoculated with *P. aeruginosa* strain (~ 2X 10^6 CFU). After incubating the slides for 1 hour at 37°C with 5% CO_2, the supernatant is removed and replaced with fresh medium supplemented with 2mM L-glutamine and 0.4% arginine. The slides are then incubated at 37°C with 5% CO_2 for 3.5~5 hours.

Confocal Microscopy Image Analysis. *P. aeruginosa* strain growing on a 16HEB monolayer can be visualized by Confocal microscopy imaging. For better imaging, the cells were stained with the CellBrite™ Orange Cytoplasmic Membrane Dyes (Excitation / Emission: 549/565 nm, Cambridge Bioscience) before being infected by bacteria. Confocal microscopy imaging for co-culture experiments was performed on an SP8 microscope (Lesia TSC) with a 63x (oil) lens. Images were processed using Image J65 with Fiji.66 Microscopy images shown in each figure are window-levelled in the same manner as one another.

Cytotoxicity assay methods. The CyQUANT™ LDH Cytotoxicity Assay, a fluorescence assay kit (1000 reactions, Fisher Scientific), was employed for this experiment. The bacterial strain infection steps were the same as those described in the co-culture experiment mentioned above. Two control groups, one with H_2O and the other with lysis solution, were added 45 minutes before the end of the incubation period. After the incubation, each sample medium (spontaneous LDH activity, maximum LDH activity, and compound-treatment LDH activity) were transferred to a 96-well flat-bottom plate containing with reaction mixture, with three replicates per sample. The plate was thoroughly mixed and incubated at room temperature, protected from light. Following incubation, stop solution was added to each well. Fluorescence was measured using an excitation wavelength of 560 nm and an emission wavelength of 590 nm. Cell toxicity percentage was calculated using the following formula:

$$\frac{-}{-} \qquad \textbf{(2.1)}$$

Enzyme-linked immunosorbent assay (ELISA). In this research, human interleukin-6 (hIL-6), interleukin-8 (IL-8), and tumor necrosis factor-alpha (TNF-alpha) ELISA kits (Invitrogen) were used. Co-culture supernatant samples were collected. For IL-6, standard, control, and cell culture samples groups have been set to corresponding wells, leaving chromogen blanks empty. The plate was incubated for 1 hour at room temperature with shaking. Solutions were gently aspirated and washed with 1X Wash Buffer three times. Anti-IL-6 conjugate was added to all wells, except chromogen blanks, followed by Solution A. After incubation and washing, Chromogenic TMB was added and incubated for 15 minutes. Stop Solution was added, and absorbance was read at 450nm.

For IL-8, standards were reconstituted and diluted. Then, 50µL of standards, controls, or cell culture samples were added to wells, followed by Biotin Conjugate solution (50µL). Chromogen blank wells were empty. The plate was incubated for 1 hour and 30 minutes. After washing four times, Streptavidin-HRP solution (100µL) was added, except for chromogen blanks. Further incubation and washing occurred. Stabilized Chromogen was added, incubated in the dark, and Stop Solution was added. Absorbance was read at 450nm.

For TNF-alpha, standard and blank wells received 150µL of distilled water, while sample wells received 100µL of distilled water supplemented with 50µL of cell culture samples. The plate was incubated on a shaker for 3 hours. After incubation, the wells were washed six times with 1X Wash Buffer, and the cleaning solution was removed. TMB Substrate Solution (100µL) was added to all wells, including blank wells. The plate was incubated in the dark. Stop Solution (100µL) was added. Absorbance was read at 450nm (optionally 620nm).

Average absorbance values were calculated, and a best fit curve was generated using standard absorbance values. Sample concentrations were determined from the curve.

2.3.8 Statistical Analysis

The experiments were conducted in triplicates to ensure robustness. The data were represented as the mean ± standard deviation (SD). To compare samples from two independent treatments, the student' t-test was employed either in a parametric or non-parametric manner. For comparing multiple samples. Statistical significance was defined as $p < 0.05$. The significance

levels were denoted as follows: * for $p < 0.05$, ** for $p < 0.01$. The figure legends provided details regarding the specific test methods and the number of biological replicates used in each analysis.

2.4 Results

2.4.1 Bioinformatics analysis of DSF signalling pathway

The *PA1396* gene encodes a probable two-component sensor of 540 amino acids with a histidine kinase phosphoacceptor (HK) domain (residues 179–244), histidine kinase domain (residues 288–399) and a C-terminal CheY-like receiver domain (residues 419–526) as revealed by SMART (Simple Modular Architecture Research Tool) analysis. This information suggests that PA1396 functions as a sensor kinase with the ability to receive signals and transduce them through phosphorylation events. Further examination of the genomic region surrounding PA1396 revealed an adjacent gene, PA1397, which encodes a putative response regulator. This finding suggests that PA1397 may potentially act as a signalling partner involved in the signal transduction process mediated by the PA1396 sensor kinase. The presence of these two genes in proximity on the chromosome suggests their functional relationship in a signalling pathway.

SMART is a web-based bioinformatics platform used for the recognition and annotation of protein domain sequences. Analysis of SMART on sensor kinase PA1396 and reaction regulator PA1397 was carried out. Interestingly, unlike other proteins in the sensor kinase family, PA1396 lacks a final Hpt domain. This type of sensor kinase is a sensor of the dual form, possessing a kinase and a receiver domain, but missing an Hpt domain. It is thought that sensor kinase missing Hpt domains can recruit them. In the PAO1 genome, several orphan Hpt domains have been identified and designated as Hpt domains A, B, and C. This observation suggests that PA1396 might be capable of recruiting one of these orphan Hpt domains to complete it signalling pathway. The evaluation of the response regulator PA1397 revealed that it contains two distinct domains: a receptor domain and a DNA binding domain. These domains indicate the potential involvement of PA1397 in receiving signals from PA1396 and subsequently binding to specific DNA sequences, potentially regulating gene expression.

Taken together, the combination of the PA1396 sensor kinase and the PA1397 response regulator, along with the possible recruitment of orphan Hpt domains, suggests their participation in a signal transduction pathway in *P. aeruginosa*. The detailed analysis of these protein domains and their genomic context provides valuable insights into the molecular mechanisms underlying signal sensing and response regulation in this bacterium (**Figure 2.2**).

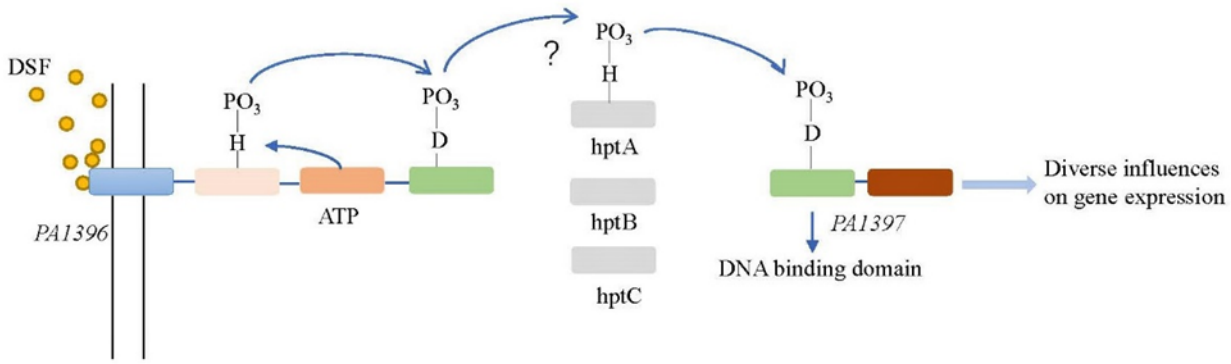

Figure 2.2 Proposed signal transduction system involving PA1396-PA1397 in *P. aerugunosa*. DSF perception involves the PA1396, the membrane-associated histidine kinase, which has no Hpt domain. PA1396 signal transduction involves autophosphorylation, phosphorelay, and phosphotransfer to the DNA-binding regulator PA1397 via orphan Hpt domain protein.

2.4.2 Construction of Δ*hptA*, Δ*hptB* and Δ*hptC* mutants

Construction of mutant alleles of *hptA*, *hptB* and *hptC*. In this experiment, the allelic exchange vectors to target *hptA*, *hptB* and *hptC* were constructed. To establish a deleted allele, three pairs of primers are needed for each gene. The primer pairs that amplify the upstream genomic region were hptAUp-F/R, hptBUp-F/R and hptCUp-F/R. The primer pairs for amplification of the downstream region were hptADown-F/R, hptBDown-F/R, and hptCDown-F/R. The primer pairs for fusion of upstream and downstream gene fragments were upstream F primer and downstream R primer.

Amplifying the upstream and downstream regions of *hptA*, *hptB* and *hptC* gene were carried out and the general size of the DNA fragment was ~400bp (**Figure 2.3A**). After purification these upstream and downstream fragments are fused to obtain the required mutant alleles by SOE-PCR. The fused PCR product was purified and run on a gel to confirm size (~800bp) (**Figure 2.3B**).

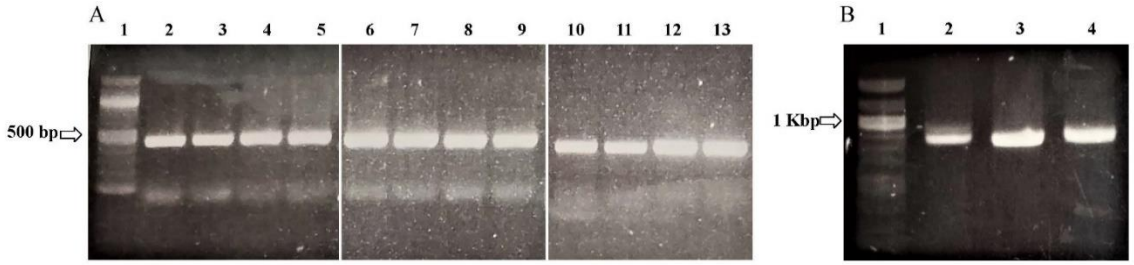

Figure 2.3 Amplification of the ~400 bp upstream and downstream DNA fragments of *hptA*, *hptB* and *hptC*. (A) Amplification of DNA fragments-the 400 bp upstream and downstream of *hptA*, *hptB* and *hptC*. Lane 1: 100 bp DNA Marker, lane 2, 3: Upstream fragment of *hptC,* lane 4, 5: Downstream fragment of *hptC*, lane6, 7: Upstream fragment of *hptA*, lane8, 9: Downstream fragment of *hptA*, lane10, 11: Upstream fragment of *hptB*, lane 12, 13: Downstream fragment of *hptB*. (B) Assembled allele with SOE-PCR. Lane 1: 100 bp DNA Marker, lane 2-4: Fused allele (~800bp) of *hptC*, *hptA* and *hptB* respectively.

Construction of allelic exchange vectors to target *hptA*, *hptB* and *hptC*. The constructed mutant alleles were inserted into the sequencing vector pCR-TOPO. To achieve this purified PCR products (~800bp) were ligated to pCR-TOPO vector and transformed into DH5α. Colonies that contain the pCR-TOPO were identified by blue/white screening and Km resistant selection. Validation of colonies was carried out by colony PCR using primer hptAUp-F/R, hptBUp-F/R and hptCUp-F/R to identify constructs contacting the mutant alleles (**Figure 2.4A**). The plasmids from the validated colonies were then extracted and digested with BamH I/Hind III. As shown in **Figure 2.4B**, several plasmids contacted the ~800bp assembled mutant alleles of *htpA,B,C*. These plasmids were sequenced for confirmation (Eurofins).

Once confirmed by sequencing these fragments were gel extracted and fragments ligated into the suicide vector pEX18Gm which was digested with BamHI/HindIII previously. The recombination plasmids were then transferred into DH5α which was grown on GM (1.5 µg/mL) containing plates. Gm resistant colonies were picked for colony PCR to validate plasmid uptake (**Figure 2.4C**). The pEX18Gm-*hptA*up&down, pEX18Gm-*hptB*up&down and pEX18Gm-*hptC*up&down plasmids were then extracted from validated colonies and transformed into SM10 for two parental conjugations.

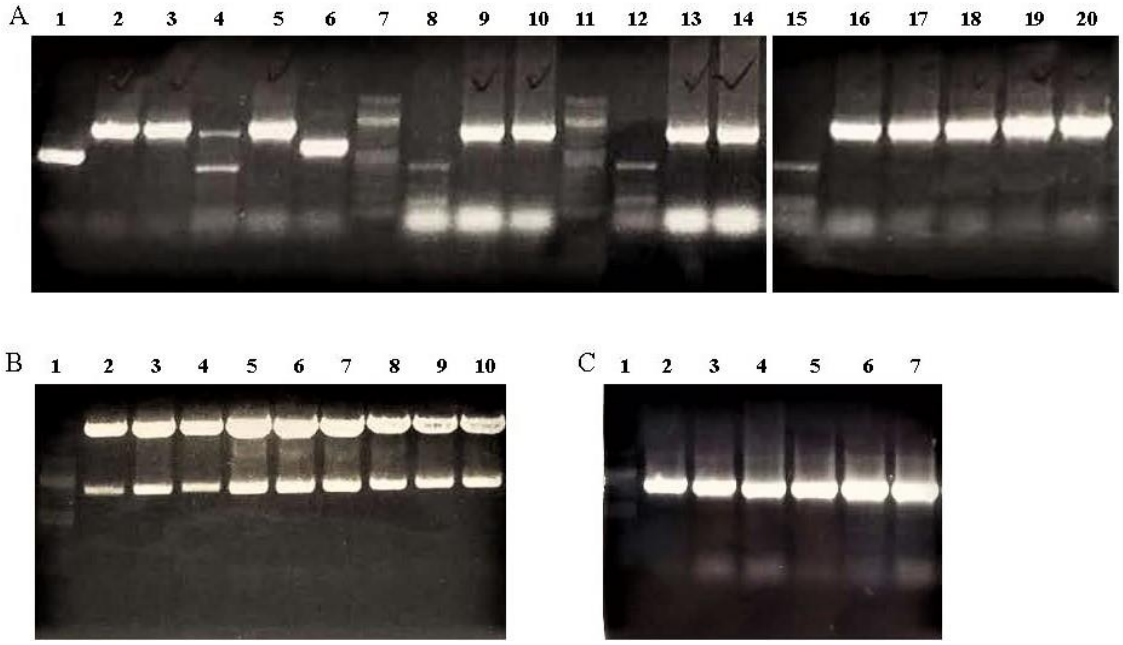

Figure 2.4 Construction of suicide vectors for the deletion of *hptA, hptB* and *hptC*. (A) Colony PCR of deletion alleles in sequencing vector pCR-TOPO. Lane 7, 11, 15: 100 bp DNA Marker, lane 1-6: ~800 bp fused up and down stream region of *hptC*, lane 8-10: ~800 bp fused up and down stream region of *hptA*, lane: 16-20: ~800 bp fused up and down stream region of *hptB*. (B) Digestion of pCR-TOPO with BamH Ⅰ /HindⅢ enzymes to confirm fragment. Lane 1: 100 bp DNA Marker, lane 2-4: p*hptC*up&down-TOPO, lane 5-7: p*hptA*up&down-TOPO, lane 8-10: p*hptB*up&down-TOPO. (C) Confirmation of transformation of suicide vector pEX18Gm into DH5α by colony PCR. Lane 1:100 bp DNA Marker, lane 2, 3: ~800 bp fused up and down stream region of *hptC,* lane 4, 5: ~800 bp fused up and down stream region of *hptA*, lane 6. 7: ~800 bp fused up and down stream region of *hptB.*

Merodiploids selection and sucrose-*sacB* counter-selection of deletion mutants. The transfer of the allelic exchange plasmid into *P. aeruginosa* was performed via biparental conjugation. Specifically, donor strains SM10 carrying deletion alleles of *htpA, htpB, htpC* were mated with recipient *P. aeruginosa* strain PA14. After mating, transformed *P. aeruginosa* cells were isolated from the conjugation mixture by plating on media containing Gm.

Selected Gm resistant strains were streaked onto a fresh Gm selection plate to avoid carryover contamination. Isolated colonies were then cultured in fresh LB medium at 37℃, 200rpm for approximately 2 hours before plating on LB agar plates containing 15% sucrose to select for colonies that have lost the integrated plasmid backbone containing *sacB*.

Sucrose-resistant colonies were analysed by PCR. Colonies were first tested using the complementation primer sets for *htpA, htpB, htpC*. As expected, the primers cannot amplify the complementation fragments of *htpA, htpB, htpC* when the genes are deleted from the genome, wild-type PA14 were used as control (**Figure 2.5A**). The genomic DNA of positive colonies were then extracted and further validated using upstream forward and downstream reverse primer sets for *htpA, htpB, htpC*. As shown in **Figure 2.5B**, the wild-type control generated an approximately 1200bp fragment (~400 upstream fragment + ~400 gene fragment + ~400 downstream fragment), while mutants only generated the ~800 bp fragment (~400 upstream fragment + ~400 downstream fragment). The deletions of *htpA, htpB, htpC* were also confirmed by sequencing.

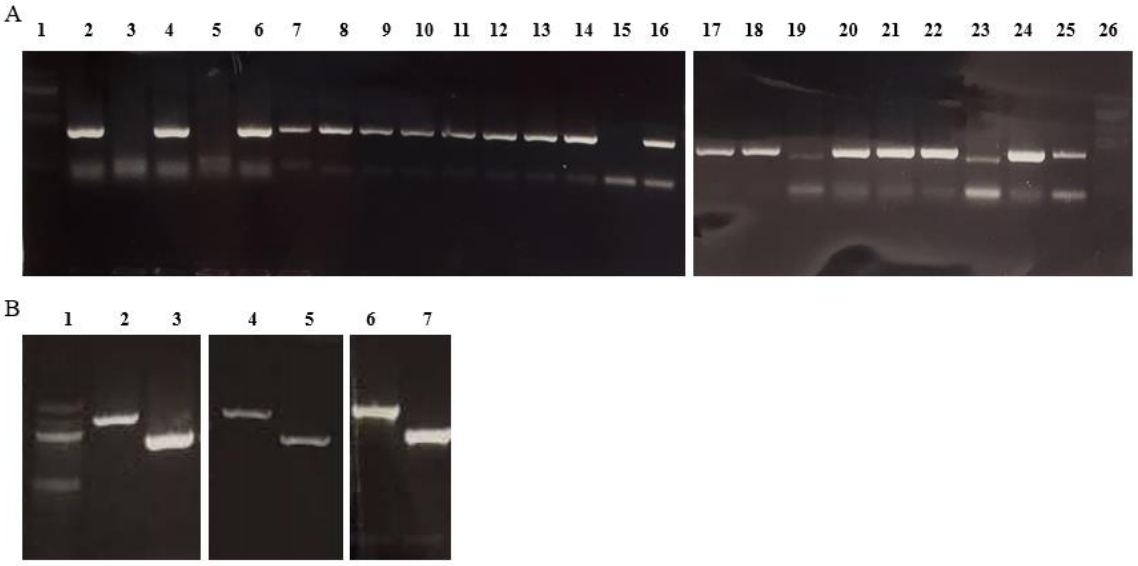

Figure 2.5 Testing and validation of *htpC*, *htpA*, *htpB* deletion mutants. (A) Confirmation of deletion of *htpC*, *htpA*, *htpB* by colony PCR. Lane 1, 26:100 bp DNA Marker, lane 3, 5, 15, 19, 23: Colony PCR confirming deletion of *htpC*, *htpA*, *htpB,* lane 2, 4, 6-14, 16-18, 20-22, 24: Strains that have reverted to WT, lane 7, 16, 25: WT control. (B) Confirmation of deletion of *htpC*, *htpA*, *htpB* using gDNA extracted from positive selected colonies. Lane 1: 100 bp DNA Marker, lane 2, 4 and 6 are WT control, lane 3: Δ*hptC*, lane 5: Δ*hptA*, lane 7: Δ*hptB.*

2.4.3 Construction of Δ*hptA*, Δ*hptB* and Δ*hptC* complementary genes

PCR amplification of complementary genes *hptA*, *hptB* and *hptC.* Complementary genes of *hptA*, *hptB* and *hptC* were amplified from *P. aeruginosa* strain PA14. This was achieved by designing three pairs of primers C*hptA*-F/R, C*hptB*-F/R and C*hptC*-F/ R to target *hptA*, *hptB* and *hptC* (**Table 2.2**). PCR was used to amplify the product and the amplified product was purified by the Qiaquick PCR purification kit and verified by gel electrophoresis (**Figure 2.6**).

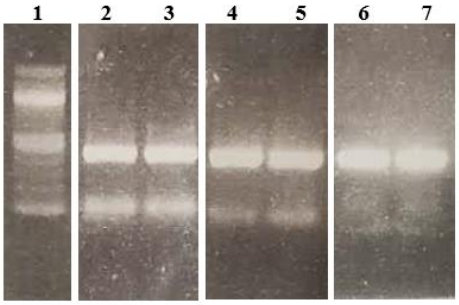

Figure 2.6 Amplification of complementation genes *hptA*, *hptB* and *hptC.* Lane 1: 100 bp DNA Marker, lane 2, 3: Complementation product C*hptC*, lane 4, 5: Complementation product C*hptA*, lane 6, 7: Complementation product C*hptB.*

Construction of plasmid for complementation of *hptA*, *hptB* and *hptC* mutants. The purified complementation products were cloned into the sequencing vector pCR-TOPO. The purified PCR products were ligated into pCR-TOPO vector and transformed into DH5α. Positive colonies were selected on Km agar plates with blue/white screening. Positive Km resistant white colonies were picked for further validation. Colony PCR was performed using primer C*hptA*-F/R, C*hptB*-F/R and C*hptC*-F/R to identify constructs containing target products and the results are shown in **Figure 2.7A**. The plasmids from of the validated selected colonies were then extracted and digested using SacI/KpnI to confirm insert. As shown in **Figure 2.7B**, we were able to cut the ~400bp complementation products of *hptA*, *hptB* and *hptC* back from the recombination plasmids. The inserts were further confirmed using DNA sequencing.

After gel extraction the complementation products were then ligated to vector pME6032Gm. The new constructs were then transferred into DH5α and selected on Gm agar plates. Gm resistant colonies were then picked for colony PCR and plasmids extracted for enzymatic digestion validation, as shown on **Figure 2.8A and B**. The validated plasmids p*hptA*-pME6032Gm, p*hptB*-pME6032Gm and p*hptC*pME6032Gm were then introduced to Δ*hptA*, Δ*hptB,* Δ*hptC* respectively by electroporation. Complementation strains were selected by Gm resistance and validated using colony PCR (**Figure 2.9**).

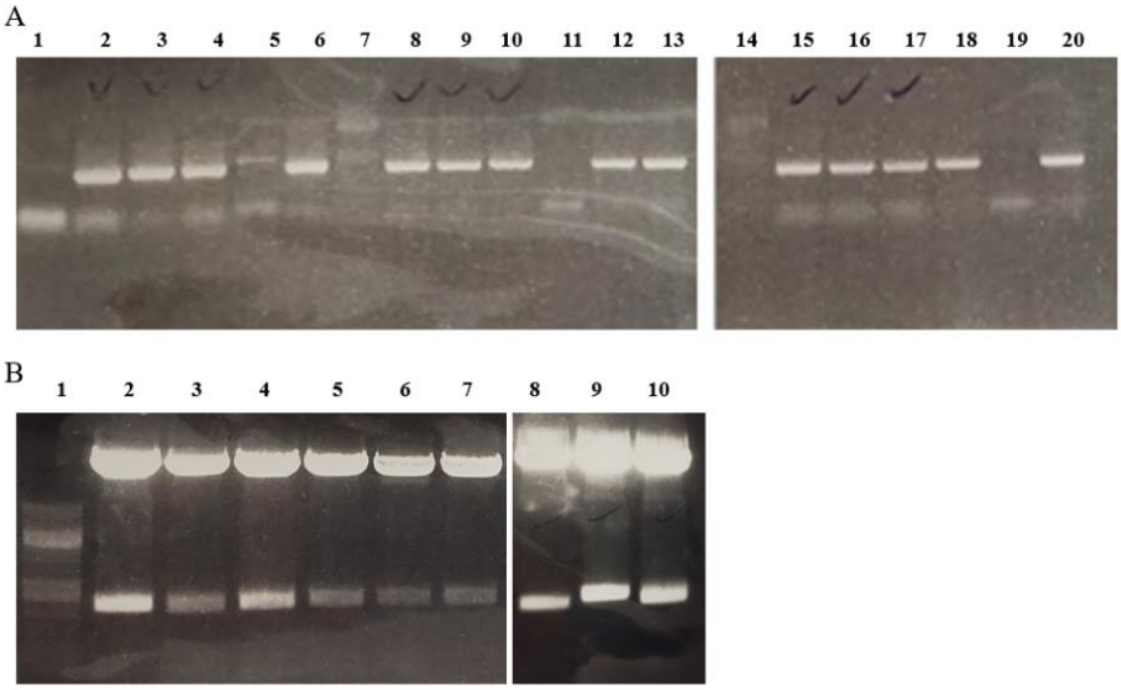

Figure 2.7 Confirmation of C*hptA*, C*hptB* and C*hptC* fragments inserted into sequencing vector pCR-TOPO. (A) Colony PCR to confirming insert. Lane 1 and 14: 100 bp DNA Marker, lane 2-6: pCR-TOPO containing C*hptC*, lane 8-13: pCR-TOPO containing C*hptA*, lane 15-20: pCR-TOPO containing C*hptB*. (B) Digestion of pCR-TOPO to confirm insert . Lane 1: 100 bp DNA Marker, lane 2-4: pCR-TOPO containing C*hptC* digested by SacI/KpnI, lane 5-7: pCR-TOPO containing C*hptA* digested by SacI/KpnI, lane 8-10: pCR-TOPO containing C*hptB* digested by SacI/KpnI.

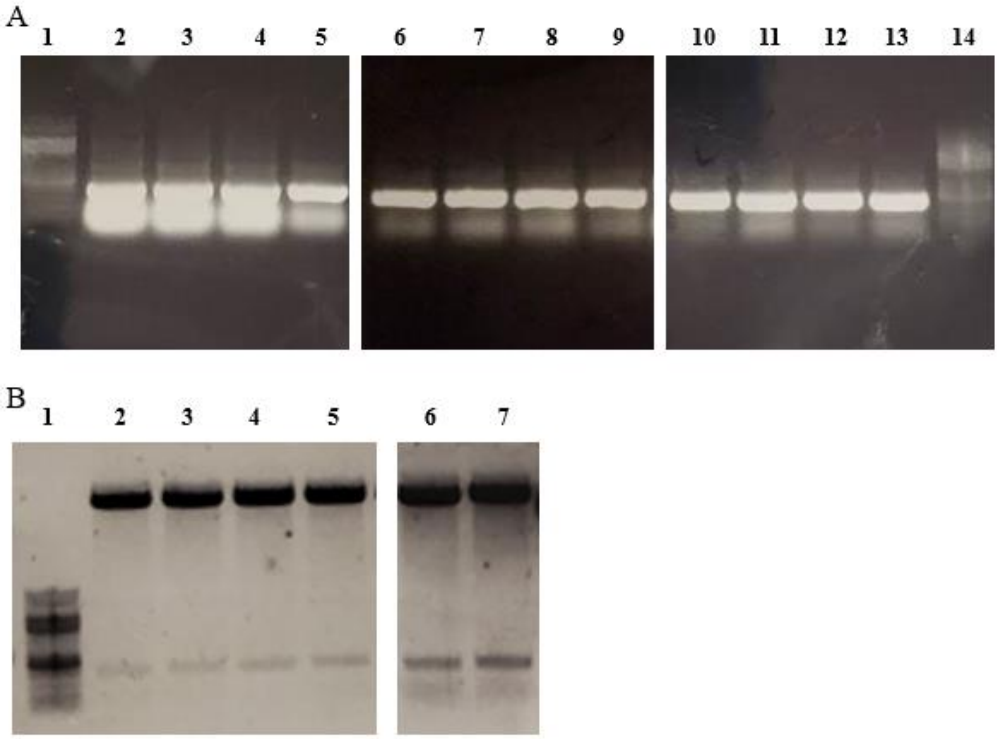

Figure 2.8 Confirmation of C*hptA*, C*hptB* and C*hptC* fragments inserted into sequencing vector pME6032Gm. (A) Colony PCR to confirming insert. Lane 1 and 14: 100 bp DNA Marker, lane 2-5: pME6032Gm containing C*hptC*, lane 6-9: pME6032Gm containing C*hptA*, lane 10-13: pME6032Gm containing C*hptB*. (B) Digestion of pME6032Gm to confirm insert. Lane 1, 100 bp DNA Marker, lane 2, 3: pME6032Gm containing C*hptC* digested by SacI/KpnI, lane 4, 5: pME6032Gm containing C*hptA* digested by SacI/KpnI, lane 6, 7: pME6032Gm containing C*hptB* digested by SacI/KpnI.

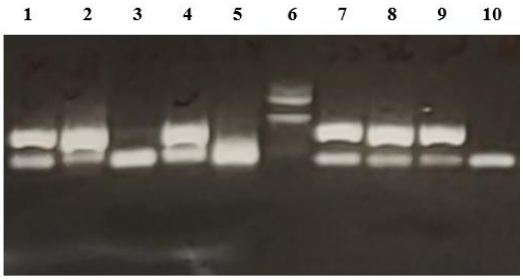

Figure 2.9 Testing and validation of complementation strains C*hptA*, C*hptB* and C*hptC*. Lane 6 and 12: 100 bp DNA Marker, lane 1-2: C*hptC*, lane 3: Δ*hptC*, lane 4: C*hptA*, lane 5: Δ*hptA*, lane 7-9: C*hptB*, lane 10: Δ*hptB.*

2.4.4 The mutants and complementary strains have no effect on growth.

To assess the potential impact of mutation and complementary strains on bacterial growth, we conducted comprehensive growth analyses for each strain in both LB rich medium and M9 minimal medium. We monitored the growth curves over a duration of 24 and 48 hours, measuring the optical density at 600 nm (OD_{600}) as an indicator of bacterial growth.

To ensure accurate interpretation of the growth data, we included blank controls for each medium to account for any background growth. Our results, as depicted in **Figure 2.10 A and B**, revealed that in LB medium, the growth curves for each strain exhibited no significant differences. This implies that the mutations introduced, and the expression of complementation genes did not exert any discernible influence on bacterial growth. In fact, the growth patterns observed remained remarkably consistent with those of the wildtype strain. Furthermore, our investigations in M9 medium, as illustrated in **Figure 2.10 C and D**, yielded similar outcomes. The growth curves of each strain exhibited comparable patterns, indicating that the mutations and expression of complementation genes did not induce any notable alterations in bacterial growth, resembling the behaviour of the wildtype strain. Based on these findings, we can conclude that the mutations and complementation genes examined in this study had no substantial impact on bacterial growth in either LB or M9 medium.

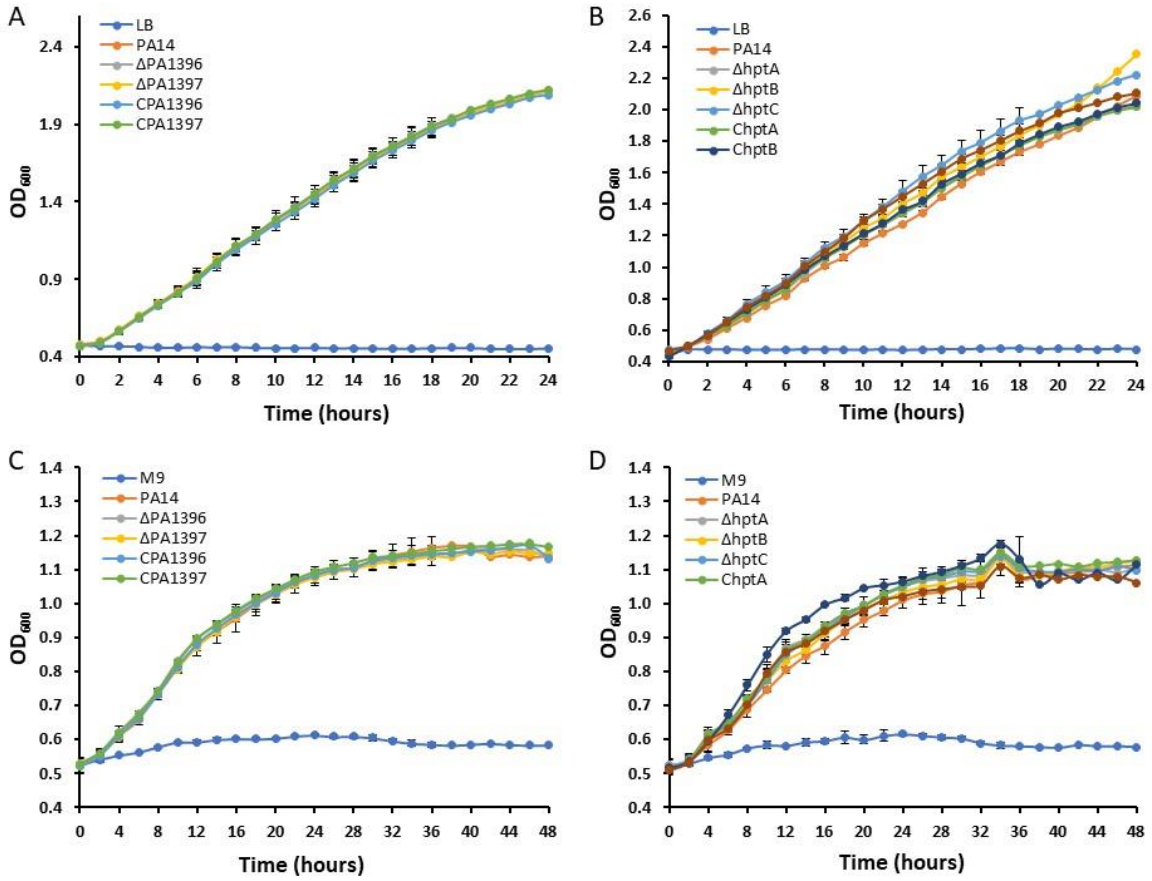

Figure 2.10 Growth curve of *P. aeruginosa* strains. (A) Strains Δ*PA1396*, C*PA1396*, Δ*PA1397* and C*PA1397* grown for 24 hours in LB medium. (B) Strains Δ*hptC*, C*hptC*, Δ*hptA*, C*hptA*, Δ*hptB* and C*hptB* grown for 24 hours in LB medium. The blank control of LB medium and the PA14 control are set at the same time for (A and B). (C) Strains Δ*PA1396*, C*PA1396*, Δ*PA1397* and C*PA1397* grown for 48 hours in M9 medium. (D) trains Δ*hptC*, C*hptC*, Δ*hptA*, C*hptA*, Δ*hptB* and C*hptB* grown for 48 hours in M9 medium. The blank control of M9 medium and the PA14 control are set at the same time for (C and D).

2.4.5 The mutants have reduced swarming motility.

We conducted extensive swarming motility tests on various mutants and complementation strains of *P. aeruginosa* bacteria associated with DSF (**Figure 2.11**). The results obtained in these tests provided valuable insights into the role of DSF-related genes in the swarming motility of *P. aeruginosa*. Comparing the mutants to the blank control strain PA14, we observed a significant reduction in swarming motility across all mutant strains. However, the extent of this reduction varied among the mutants, with Δ*hptA* and Δ*hptB* displaying a more pronounced effect, particularly Δ*hptB*. These results strongly indicate that the DSF-related genes play a crucial role in

facilitating the swarming motility of *P. aeruginosa*. Disruption or mutation of these genes can significantly impair the bacteria's ability to swarm.

Interestingly, when we performed complementary of the mutated genes by introducing their functional counterparts, we observed a remarkable restoration of swarming motility. The motility levels of the complementation strains closely resembled that of the blank control strain PA14. This observation highlights the significance of the DSF-related genes in governing swarming motility and further emphasizes their essential role in this process.

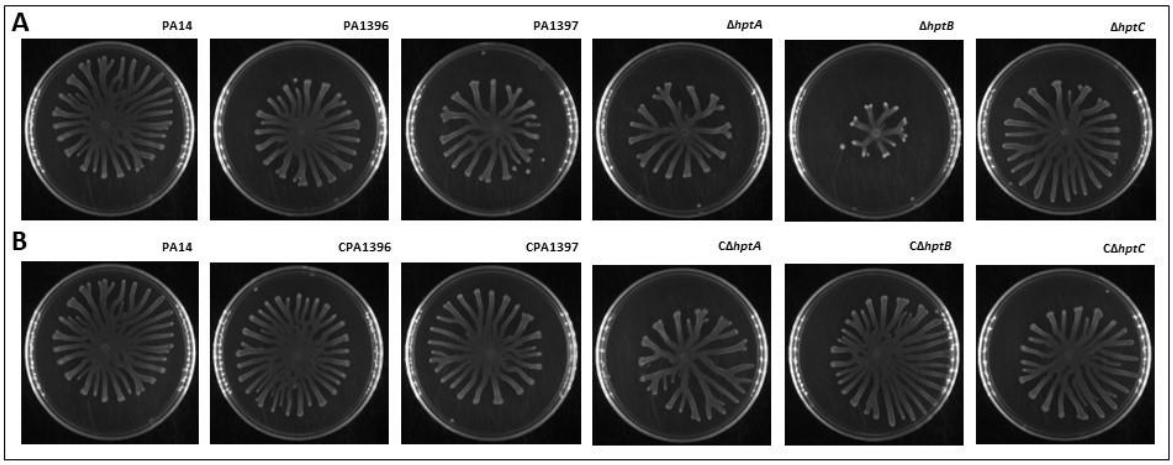

Figure 2.11 The motility of these mutations (A) and complementary strains (B) on 0.5% swarming agar.

2.4.6 Human bronchial epithelial cell and *P. aeruginosa* co-culture biofilm model was constructed.

To investigate the interaction between *P. aeruginosa* and human airway cells, we established a co-culture model system to study biofilm formation on epithelial cells. Specifically, we utilized 16HBE cells and cultured them in standard multiwell tissue culture plates, such as 24-well and 96-well plates, allowing them to form monolayers over a period of 3-4 days.

Following the formation of these monolayers, we inoculated them with the *P. aeruginosa* strain PA14. To assess biofilm formation, we employed confocal laser scanning microscopy (CLSM) to observe the interactions between the bacteria and the epithelial cells. The epithelial cells that were not infected by bacteria continued to grow and form confluent monolayers as a control (**Figure 2.12A**). Upon contact and infection with PA14, we observed a significant change in the behaviour of the cells. Within a timeframe of 3-5 hours, a substantial number of cells started to detach from the monolayers. This detachment was accompanied by the presence of PA14

bacteria wrapping around the cell surfaces, forming a biofilm (**Figure 2.12B**). This observation suggests that the interaction between PA14 and the airway cells leads to cell death, potentially induced by the bactericidal activity of the bacteria.

The findings from this co-culture model system demonstrate the ability of *P. aeruginosa* to form biofilms on epithelial cells, leading to detrimental effects on the airway cells. The wrapping of bacteria around the cell surface and subsequent cell death indicates the pathogenic nature of PA14 in the context of the airway environment.

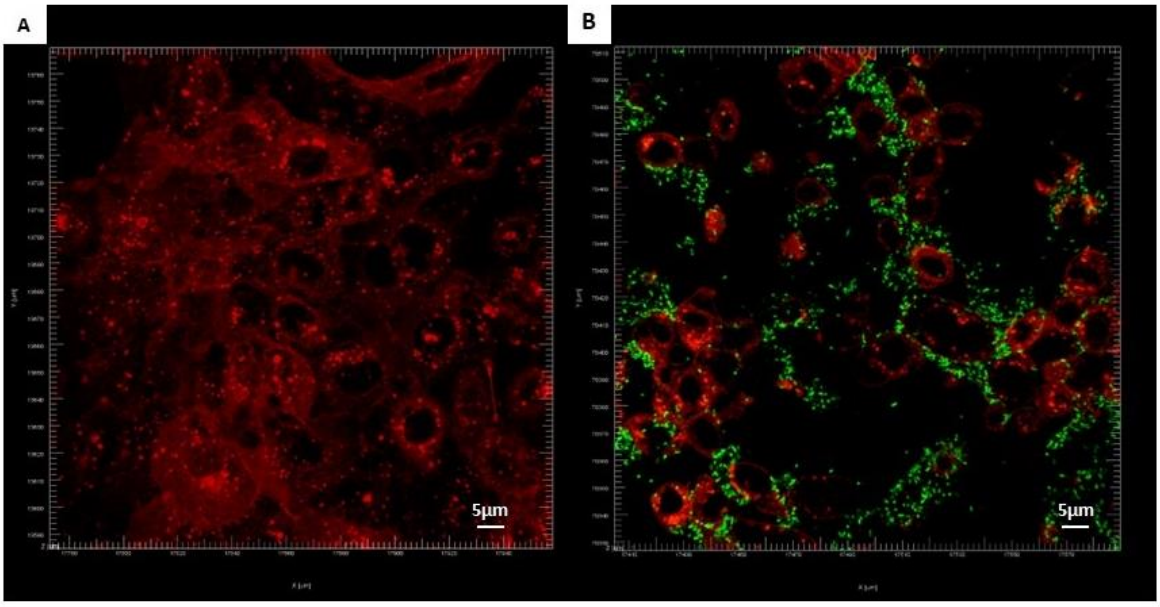

Figure 2.12 Confocal images from the co-culture model. (A) 16HBE airway cells only, without infection. (B) 16HBE airway cells after PA14 infection for 4 hours. Orange: human airway epithelial cell 16HBE stained by CellBrite™ cytoplasmic membrane dye, and green show the PA14 (GFP).

2.4.7 The mutants and complementary strains have affected on bacterial virulence during infection.

To assess bacterial cytotoxicity, we employed a quantification method based on the measurement of Lactate Dehydrogenase (LDH) released from the epithelial cells. Through multiple repeated experiments, we observed significant differences in bacterial infections within the 3.5 to 4-hour period. This allowed us to evaluate the cytotoxicity of various strains, including the wild-type, mutant, and complementation strains, by normalizing the data to the mean virulence of the wild-type strain.

By comparing the LDH release from 16HBE cells incubated with the wild-type strain PA14 and the mutant strains (Δ*PA1396*, CΔ*PA1396*, Δ*PA1397*, CΔ*PA1397*, Δ*hptA*, CΔ*hptA*, Δ*hptB*, CΔ*hptB*, and Δ*hptC*, CΔ*hptC*), we obtained insightful results (**Figure 2.13**). It is evident that all the mutant strains exhibited a significant reduction in cytotoxicity when compared to the wild-type strain. This finding suggests that this disruption of specific genes, leads to a diminished cytotoxic effect on the epithelial cells. When the mutated genes were complemented, we observed a less reduction (CΔ*hptA*, CΔ*hptB*, and CΔ*hptC*) or even normalization to PA14 (CΔ*PA1396* and CΔ*PA1397*) of cytotoxicity levels. The cytotoxicity levels of the complementation strains were higher than those of their respective mutant strains. This observation indicates that the reintroduction of the wild-type genes through complementation reverses the cytotoxic effects, either partially or completely, restoring or even surpassing the cytotoxicity levels observed in the mutant strains.

These results provide strong evidence that the genes under investigation play a crucial role in the cytotoxicity of *P. aeruginosa.* The reduction in cytotoxicity observed in the mutant strains suggests the involvement of these genes in the pathogenic mechanisms leading to cell damage. Moreover, the rescue or enhancement of cytotoxicity upon complementation highlights the essentiality of these genes in promoting cytotoxic effects.

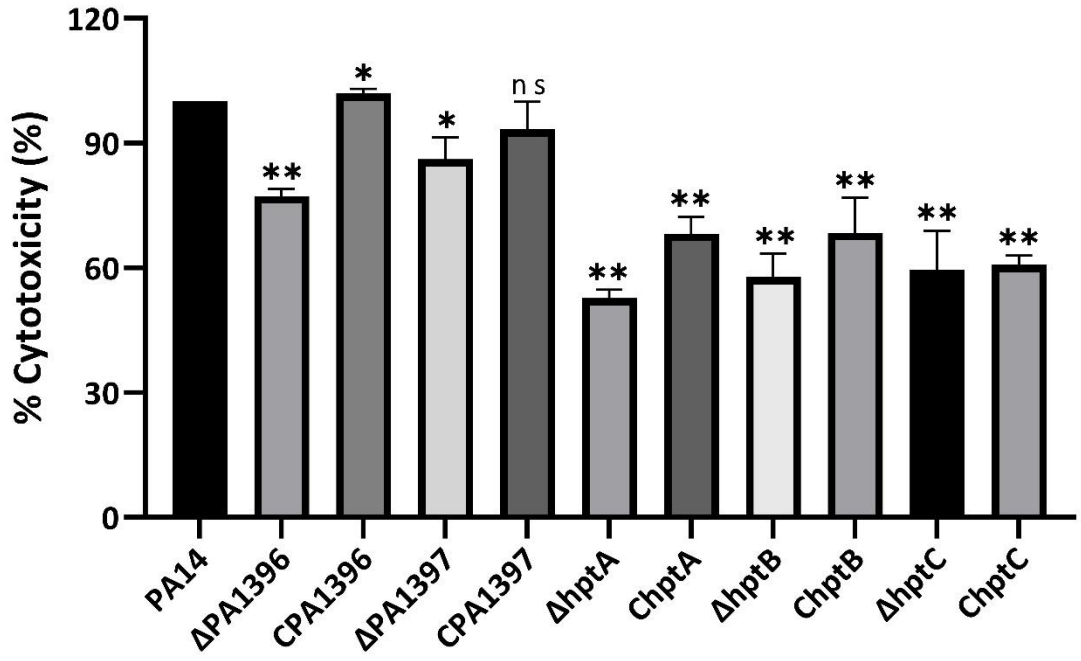

Figure 2.13 Cytotoxicity assay with selected mutants. The cytotoxicity test in the PA14, ΔPA1396, CΔ*PA1396*, Δ*PA1397*, CΔ*PA1397*, Δ*hptA*, CΔ*hptA*, Δ*hptB*, CΔ*hptB* and Δ*hptC*, CΔ*hptC* cells which have infected 16HBE cell. The mean values from three independent

experiments are shown with the error bars representing the standard deviation. (*p < 0.05; **p < 0.01).

2.4.8 The impact of different mutations on human IL-6, IL-8, and TNF-α protein levels.

To investigate the effects of different mutant strains on the levels of human interleukin-6 (IL-6), interleukin-8 (IL-8), and tumor necrosis factor-alpha (TNF-α), we utilized human bronchial epithelial cells and treated them with various strains of *P. aeruginosa* bacteria. The strains tested in this experiment included the wild-type strain PA14 as the control group, as well as the mutant strains Δ*PA1396*, Δ*PA1397*, Δ*hptA*, Δ*hptB*, and Δ*hptC*. We specifically focused on the levels of IL-6, IL-8, and TNF-α in response to these strains. Our results revealed distinct patterns of cytokine levels among the mutant strains compared to the control group.

In the IL-6 and IL-8 assays, the levels of these cytokines were significantly higher in the Δ*hptB* mutant strain compared to the PA14 WT group. On the other hand, the levels of IL-6 and IL-8 in the other mutant strains were lower than those in the control group (**Figure 2.14 A, B**). In the TNF-α assay, all mutant strains were higher than that in the control group, particularly in the case of Δ*PA1397* and Δ*hptA* (**Figure 2.14 C**).

Taken together, these findings suggest that the different mutant strains have distinct effects on the levels of IL-6, IL-8, and TNF-α in human bronchial epithelial cells. Notably, the Δ*hptB* mutant strain consistently exhibited higher levels of all three proteins compared to the control group, indicating a potentially important role of this mutant strain in modulating the human inflammatory response. These experimental results enhance our understanding of the relationship between mutant strains and protein levels, providing valuable insights into the association between mutant strains and disease processes.

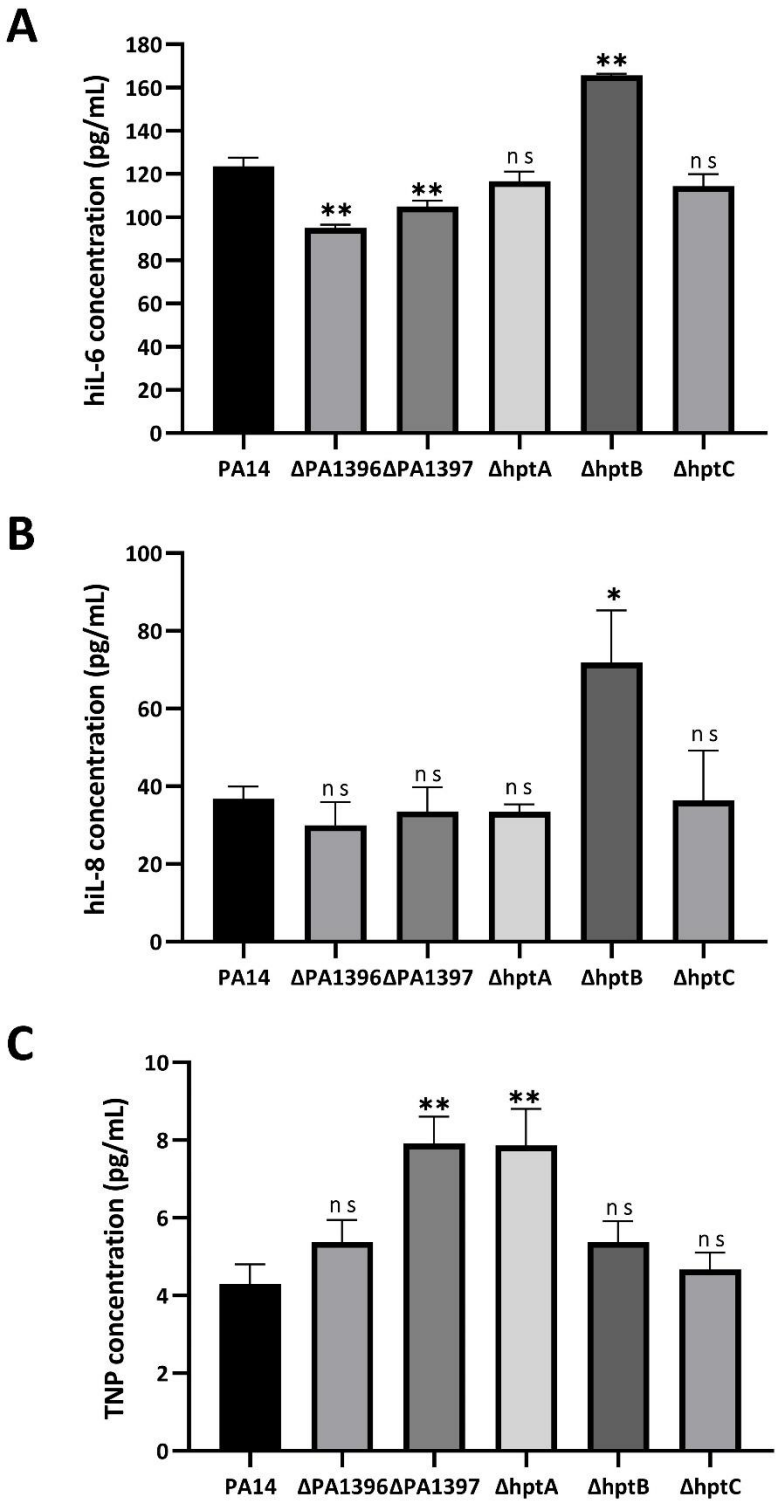

Figure 2.14 ELISA assays were performed for human pro-inflammatory cytokines IL-8 and TNF-α, the dual functioning IL-6 in response to *P. aeruginosa* bacteria in 16HEB 14o- human bronchial epithelial cell cultures. The proteins were measured 5 hours post-inoculation of the bacteria (n = 3). The mean values from three independent experiments are shown with the error bars representing the standard deviation. (*$p < 0.05$; **$p < 0.01$).

2.5 Conclusion and Discussion

Much work in the last ten years by a number of laboratories has shown that DSF family (cis-unsaturated fatty acid) signalling is found in many unrelated bacteria such as the plant pathogen X. campestris and opportunistic pathogens *B. cenocepacia*, *S. maltophilia*, and *P. aeruginosa* and regulates many phenotypes including virulence, formation of biofilms and antibiotic tolerance (Boon *et al.*, 2008; Deng *et al.*, 2016). More fascinating is the role that the DSF signal molecule appears to play in interspecies signalling. Unlike the *B. cenocepacia* and *S. maltophilia*, *P. aeruginosa* does not appear to produce DSF and BDSF but responds to these exogenous signals by modulation of biofilm formation and increased polymyxin tolerance (Ferrières and Clarke, 2003).

Previous work showed that in *P. aeruginosa* sensing of these signals involves the histidine kinase PA1396 and leads to altered biofilm formation and increased tolerance to a number of antibiotics and demonstrated that the transmembrane helix (TMH) IV and V of PA1396 input domain are required for DSF sensing (An *et al.*, 2019).

To further understand the signal transduction mechanism in *P. aeruginosa* following the perception of DSF, this work has focused on identifying the possible candidates involved with the sensor kinase PA1396. This study was carried out by using a bioinformatics approach, screening the chromosomal region surrounding PA1396 using KEGG. This identified a gene encoding a putative response regulator (PA1397) upstream of the gene encoding the sensor kinase (PA1396). These two genes are not in an operon together and appear to be divergently transcribed. Interestingly, studies showed that under various environmental conditions these genes are co-ordinately expressed and regulated suggesting a functional link (Ryan and Dow, 2011).

SMART analysis of the PA1396 domain identified five transmembrane helices input domain attached to a HAPTase domain, HK domain and a REC domain, but this sensor appeared not to encode an Hpt domain. This suggests that the sensor kinase must recruit a “solo” Hpt domain to function in a multiple step phosphorelay in order to activate the response regulator, PA1397 (Ryan and Dow, 2008).

To gain evidence of the functional link between these candidate genes, deletion mutations and complementation of hptA, hptB and hptC were generated. Initially, the growth curves of these strains were measured, confirming that these mutant and complemented genes had no significant impact on bacterial growth (**Figure 2.10**). Swarming motility, a surface-related movement behaviour, is crucial for the rapid spread, colonization, and biofilm formation of *P. aeruginosa* (Hou *et al.*, 2019). To emphasize the importance of DSF-related genes in the survival and spread of *P. aeruginosa*, swarming motility assays were conducted for all mutant and complemented

strains, revealing a significant effect of the mutant strains on the swarming motility of *P. aeruginosa* (**Figure 2.11A**). Specifically, the Δ*hptB* mutant strain showed a considerable decrease. However, substantial recovery of swarming motility was achieved through complementation with the mutant genes, reaching a level comparable to that of the wild-type strain (**Figure 2.11B**).

Furthermore, we investigated the impact of these mutant strains on the cytokine levels of human cells to uncover their roles in the pathogenicity of *P. aeruginosa*. Regarding cytotoxicity, this study assessed the impact of the strains on epithelial cells by quantifying their LDH cytotoxicity. The results demonstrated a significant reduction in cytotoxicity of the mutant strains compared to the wild-type strain (**Figure 2.13**). This suggests that the disruption caused by these mutant genes weakens the cytotoxicity of the strains against epithelial cells. Importantly, partial, or complete restoration of cytotoxicity levels was achieved through complementation with the mutant genes, indicating a reversal of cytotoxicity through reintroduction of the wild-type genes. These findings elucidate the critical role of DSF-related genes in the pathogenicity of *P. aeruginosa* and provide insights into their toxic mechanisms. Additionally, the impact of different mutant strains on cytokine levels (interleukin IL-6, IL-8, and tumor necrosis factor-α TNFα) in human bronchial epithelial cells was investigated. The results revealed varied effects of the mutant strains on cytokine levels compared to the wild-type strain (**Figure 2.14**). Notably, the Δ*hptB* mutant strain resulted in a significant increase in these levels. This suggests that different mutant strains have varying effects on cytokine levels in human bronchial epithelial cells, particularly highlighting the potential importance of the Δ*hptB* mutant strain in regulating inflammatory responses in the human body.

The findings of this study underscore the pivotal role of the hptB gene in shaping the phenotype of *P. aeruginosa*. In our results, the *ΔhptB* mutant strain exhibited a significant impairment in swarming motility, a surface-related behaviour crucial for the bacterium's rapid spread, colonization, and biofilm formation. Moreover, a substantial reduction in cytotoxicity against epithelial cells was observed in the absence of the hptB gene, highlighting its direct involvement in the pathogenicity of *P. aeruginosa*. Complementation with the hptB gene not only restored swarming motility but also partially or completely reinstated cytotoxicity levels, emphasizing the essential role of hptB in these processes. Additionally, the *ΔhptB* mutant strain elicited a noteworthy increase in cytokine levels in human bronchial epithelial cells, suggesting a regulatory role in modulating inflammatory responses. These comprehensive results collectively illuminate the multifaceted impact of the hptB gene on various phenotypic traits, providing valuable insights into its crucial contribution to the overall pathogenic behaviour of *P. aeruginosa*.

In recent *P. aeruginosa* research over the past two years, the hptB gene has emerged as a significant player. In one study led by Congcong Guan, it was revealed that the hptB gene regulates c-di-GMP signalling through the HptB/HsbR/HsbA/HsbD pathway, impacting biofilm formation and motility. The HptB pathway proved crucial for *P. aeruginosa*, as demonstrated by the restoration of biofilm formation upon hptB complementation. Additionally, in the study by Melanie Dostert and colleagues, the hptB gene, linked to the Gac-Rsm pathway, exhibited reduced fitness in a skin model, contrasting with the heightened fitness observed for the global transcriptional regulator mvaU in skin biofilms. Furthermore, in another context, the nitric oxide sensing protein NosP was found to inhibit the kinase NahK, which selectively phosphorylates HptB in the GacS MKN. Deletion of hptB resulted in reduced motility and virulence, suggesting its pivotal role in modulating *P. aeruginosa* phenotypes. Interestingly, mutations in hptB, along with ΔnahK and ΔretS, led to RsmA inactivation, resulting in increased pyocyanin production and enhanced biofilm formation, highlighting the unique regulatory role of HptB and its associated network components in controlling *P. aeruginosa* virulence factors (Guan *et al*., 2024; Dostert, 2023; Marshik *et al*., 2023). These studies and conclusions highlight its important contribution to the overall virulence and pathogenic behaviour of *P. aeruginosa*.

In summary, this study reveals the functions of DSF-related genes in *P. aeruginosa* and their impact on strain phenotypes. These genes play critical roles in regulating bacterial motility, cytotoxicity, and cytokine levels. Among them, it is noteworthy that PA1396 and PA1397 exhibit similar phenotypes when mutated, suggesting a functional link between these two genes, which may imply a two-component system (**Figure 2.2**) between them. However, as a possible response regulator, PA1397's function in regulating gene expression needs further study.

Chapter 3 Differential Gene Expression and Protein-DNA Interaction Analysis Reveals the Regulatory Role of PA1397 in *Pseudomonas aeruginosa.*

3.1 Abstract

Recently, the emergence of RNA sequencing (RNA-Seq) has empowered researchers with a powerful tool to explore transcriptional profiles and analyze gene expression in numerous organisms. By leveraging RNA-Seq, researchers can identify differentially expressed genes (DEGs) and perform expression analysis across various isolates. The application of RNA-Seq has enabled the measurement of transcript expression levels and facilitated in-depth investigations into molecular mechanisms (Trapnell *et al.*, 2012; Zhao *et al.*, 2019).

In this study, we focused on the role of the PA1397 gene in the regulation of *Pseudomonas aeruginosa* PA14 gene expression and protein-DNA interactions. The above section 2 has shown that PA1397 may be involved in the signal transduction process mediated by PA1396 sensor kinase by binding to specific DNA sequences as a signalling partner, thereby possibly regulating gene expression. Despite these hypotheses, its specific functions and regulatory targets remain largely unknown.

To further verify it, we conducted a series of experiments. First, we extracted RNA samples from mutant strains lacking the PA1396, PA1397, hptA, hptB, and hptC genes, followed by DNA removal to ensure the purity of the RNA samples. RNA samples were verified by gel electrophoresis and concentration determination. Next, we performed RNA sequencing (RNA-seq) analysis on these samples, using RNA-seq data from the exponential growth phase of *P. aeruginosa* PA14 as a control. The overall gene expression profile of the mutant strain was compared to the control to identify differentially expressed genes (DEGs). Subsequent analysis of differential gene expression revealed significant differences in gene expression patterns between mutants and controls. Principal component analysis (PCA) analysis confirmed clustering of the repeats and demonstrated distinct gene expression profiles of the mutants. Further analysis of the DEGs using KEGG pathway analysis revealed enrichment of specific pathways related to metabolism and bacterial adaptation. Due to Quantitative Reverse Transcription PCR (qRT-PCR)'s high specificity and sensitivity, it is widely used to study gene expression levels. We also have utilized real-time qRT-PCR to identify genes that regulated DSF perception in *P. aeruginosa*.

To gain insight into the functional role of PA1397 and its interaction with DNA, an electrophoretic mobility shift assay (EMSA) was performed. The results showed that PA1397 interacted with the promoter region of the PA_53410 gene, suggesting its possible involvement in transcriptional regulation. The binding affinity of PA1397 to DNA fragments is concentration-dependent, suggesting a dose-dependent regulatory mechanism.

Overall, this study aimed to elucidate the role of PA1397 in the regulation of *P. aeruginosa* PA14 gene expression and protein-DNA interactions. The results of this study contribute to our understanding of the regulatory mechanisms of *P. aeruginosa* gene expression and reveal the potential functions of PA1397 in bacterial adaptation and pathogenicity. Further studies of PA1397 and its regulatory targets will provide valuable insights into the pathogenesis of *P. aeruginosa* and may lead to the development of new therapeutic strategies against Pseudomonas infections.

3.2 Hypothesis

PA1396 and PA1397, as well as the orphan Hpt domains hptA, hptB, and hptC, are hypothesized to play critical roles in the signalling mechanism of diffusion signalling factor (DSF) perception in *Pseudomonas aeruginosa*. Through RNA-seq analysis of these genes, we can further understand the functional relationship between these genes, their role in signal transduction and their regulatory capabilities.

1. Given the observed interaction between PA1397 and PA1396 sensor kinases, it was hypothesized that PA1397 plays a key role in signal transduction. This interaction may involve specific DNA sequences as signalling partners that affect downstream gene expression events. Thus, PA1397 is expected to play a key role in coordinating transcriptional responses within *P. aeruginosa* PA14.
2. The influence of PA1396, PA1397 and the recruited HPT domain on the gene expression pattern exists and plays a role in multiple aspects.
3. PA1397 may act as a transcriptional regulator, binding to specific DNA sequences and affecting the initiation or repression of gene transcription, thereby regulating downstream cellular responses.

3.3 Materials and Methods

3.3.1 Bacteria collection

The overnight culture was diluted to 1:100 and was grown at 37°C with shaking (200 rpm) until the culture attains OD_{600} = 0.6-0.7. After centrifuging the culture, the bacteria pellets were resuspended in 0.5 mL of RNA protect (Qiagen, UK) and incubated at room temperature for 1 hour. Cell suspensions were centrifuged, the supernatant was discarded, and pellets were stored in a -80°C freezer.

3.3.2 RNA extraction and DNA-free treatment

The samples collected from 3.2.1 were thawed, and 400 µg/mL TE-lysozyme was added, and samples were incubated at room temperature for 5 minutes. The cells were homogenized utilizing a 20-gauge needle and syringe, and total RNA was isolated using RNeasy Mini Kit (Qiagen). To ensure the absence of DNA contamination in RNA samples, DNase treatment was performed using the DNA-free™ DNA Removal Kit (Thermo Fisher, UK). The effectiveness of DNase treatment was assessed by PCR with 16s Quick primers. Each PCR reaction set-up (**Table 3.1**).

Table 3.1 DNase treatment reaction set-up.

Reagent	Volume
Q5 Master Mix	10 µL
H2O	8 µL
Primer F&R	1 µL
Template (RNA)	1 µL

* gDNA, no template replacement RNA as a control group.

3.3.3 RNA sequencing and analysis

The Total RNA samples with DNase treatment triplicate replicates were used as input for library construction and subsequently sent to the company for sequencing using a paired-end strategy (2 × 150) on the Illumina NovaSeq 6000 platform following standard protocols (Novogene, Cambridge, UK).

The RNA-seq data underwent a comprehensive analysis within CLC Genomics Workbench 10.0, commencing with the importation of raw data. Pre-processing steps were meticulously executed, involving the removal of low-quality reads and adapter sequences to ensure data integrity. Subsequent to this, the quality-controlled reads were aligned to the reference genome utilizing either the STAR or HISAT2 alignment algorithms, with fine-tuning of alignment parameters to suit the specific characteristics of the dataset and reference genome. For quantification, an RNA-Seq experiment was set up to derive expression values, such as Fragments Per Kilobase of transcript per Million mapped reads (FPKM), providing normalized metrics accounting for transcript length and total mapped reads. Differential expression analysis was conducted using DESeq2 or EdgeR, employing stringent criteria for significance (adjusted FDR P-value < 0.05) to identify genes exhibiting significant upregulation or downregulation. Gene read counts were computed from the alignment results, and FPKM values from treatment and control replicates were harnessed to construct a Principal Component Analysis (PCA) plot, offering insights into sample relationships. Visualization tools included Venn diagrams for depicting gene overlaps across different conditions and volcano plots for visually discerning both fold change and statistical significance. In-depth analysis of differentially expressed genes considered those with an adjusted FDR P-value less than 0.05. Pathway enrichment analysis, a pivotal step, was carried out using R, and the corresponding R code for generating Gene Ontology terms is provided in Appendix B.2.1, enabling a thorough exploration of enriched biological pathways associated with the identified differentially expressed genes.

3.3.4 Statistical Analysis

The data were represented as the mean ± standard deviation (SD). To compare samples from two independent treatments, the student' t-test was employed either in a parametric or non-parametric manner. For comparing multiple samples. Statistical significance was defined as $p < 0.05$. The significance levels were denoted as follows: * for $p < 0.05$, ** for $p < 0.01$. The figure legends provided details regarding the specific test methods and the number of biological replicates used in each analysis.

3.3.5 Quantitative Real-Time PCR

The DNA-treated RNA was synthesized to complementary DNA (cDNA) utilising Revert Aid First Strand cDNA Synthesis Kit (Fisher scientific). Total 0.1ng-5µg RNA was combined with the Random Hexamer primer and was incubated at 65°C for 5 minutes and placed immediately on ice. The remaining reagents were added to the reaction, the conditions were listed (**Table 3.2**).

Table 3.2 The components added for cDNA Synthesis.

Reagent	Volume
RiboLock RNase Inhibitor	1 µL
Reaction Buffer (5X)	4 µL
10 mM dNTP Mix	2 µL
Revert Aid M-MuLV RT	1 µL

The first strand reaction was incubated at 25°C for 5 minutes followed by 42°C for 60 minutes, terminate the reaction by heating at 70°C for 5 min. Double check by run sample on a gel and PCR with 16s Quick primers.

Quantitative RT-PCRs were used to validate RNA-Seq data obtained in this study. Real-time PCR was performed using a PowerUp SYBR Green Master Mix kit (Thermo Fisher, UK) according to the manufacturer's instructions, the reaction set-up (**Table 3.3**). The constitutively expressed housing keeping gene, 16S rRNA was used as a reference to standardize all samples and replicates. Specific RT-PCR primers were used to amplify central fragments of approximately 200 bp in length from different genes., the gene primers (Merck, UK) selected from the RNA-Seq results were listed (**Table 3.4**), and the thermocycling conditions were followed (**Table 3.5**)

Table 3.3 qRT-PCR reaction set-up.

Reagent	Volume
PowerUp SYBR Green Master Mix	10 µL
H2O	8 µL
Primer F&R	1 µL
Template (RNA)	1 µL

Table 3.4 Summary of qrt-PCR primers.

Gene	Sequence (5'->3')	
PA14_03670	Forward primer	CGTGACCCTGCCGAACATTA
	Reverse primer	CGGCGACATGGTTGTATTCG
PA14_03680	Forward primer	CGTGCTCAATGGCTTGATCG
	Reverse primer	GATCTTGAAGCCGAGGTCGC

PA14_04180	Forward primer	CACCATCGTCAAGCGCATC
	Reverse primer	GTCGACTTCGCCGGTCAG
PA14_04270	Forward primer	CCGAGCCGTTTTCAATGTCC
	Reverse primer	TATCGAGCGCTCTTTCCAGG
PA14_06680	Forward primer	CCACTATCGCCTTGGCTACC
	Reverse primer	GTAGCCTTCGATCTCCGCTT
PA14_11670	Forward primer	CGTTTGCGTGACATCAACCT
	Reverse primer	GCCGACGTTCCACATCTCG
PA14_13770	Forward primer	ATCACCCTGTGGAACTACGC
	Reverse primer	CCACTCGTTGCGGAAGATCA
PA14_13780	Forward primer	GATGAACGATGACCTCGGCA
	Reverse primer	TGCATGTCGGAGGTGTTGAG
PA14_19490	Forward primer	CTCGCACCTGAAGTGGATCG
	Reverse primer	TAGGTGATGATCAGGCGCAC
PA14_29510	Forward primer	GCGGATACCCAGGTGAAGAT
	Reverse primer	TACAGGTAAGGCCGGTTCCA
PA14_52570	Forward primer	GACTCGTCGGGTCGGAGA
	Reverse primer	TCTTTCTGGATGCGCTGGTA
PA14_53410	Forward primer	CCAAGGGCTCCTTCTATCACT
	Reverse primer	CAGTGGTATTCGGGCTTTTCC
PA14_63150	Forward primer	GACCTGCTGGTGCTCGACAT
	Reverse primer	GAAGGGCTTGGTCAGGTAGTC
PA14_RS31465	Forward primer	CGAAACGTTCTGCATTCGCA
	Reverse primer	CCTCCTCGGTGAGAGCGATA

Table 3.5 Thermocycling conditions for qRT-PCR (StepOnePlus, ThermoFisher, UK).

Step	Temperature	Time	Cycles
Holding Stage			
UDG activation	50°C	2 minutes	1

Activation	95°C	2 minutes	1
Cycling Stage			
Denature	95°C	3 seconds	40
Anneal/extend	60°C	30 seconds	
Melt Curve Stage			
Denaturation	95°C	15 seconds	1
Annealing	60°C	1 minutes	1
High resolution melting	95°C	15 seconds	1

3.3.6 Protein expression

The *P. aeruginosa* PA1397 full length was inserted into the pMAL-c5x vector (An *et al.*, 2020), This vector facilitates the expression of a protein that incorporates both the maltose binding protein (MBP) tag at the N-terminal and the 6xHis tag at the C-terminal.

A 1-ml overnight culture of PA1397FLinframe-pMAL-c5x-His was employed to inoculate 500 mL of fresh LB medium supplemented with 50 µg/mL ampicillin in a 1 L culture flask. The flask was then incubated overnight at 37°C with shaking at 180 rpm until the culture reached an OD_{600} = 0.6 (~3 hours). Expression of the target protein was induced by adding 0.3 mM IPTG. The flask was further shaken at 160 rpm and maintained at 18°C for a duration of 24 hours. Following incubation, cells were harvested by centrifugation at 4000 rpm and 4°C for 30 minutes, and the supernatant was discarded. The cell pellets can be stored indefinitely at -80°C or utilized directly for protein purification.

3.3.7 Protein purification by affinity chromatography

The expressed protein cell pellets were resuspended in 30 mL of cold lysis buffer (**Table 3.6**) until a homogeneous mixture was achieved. Bacterial cells were lysed using sonication, and lysis was considered complete when the initially cloudy cell suspension turned translucent. The resulting lysate was then subjected to centrifugation at 16,000 rpm and 4°C for 30 minutes. The supernatant, which contained the desired protein, was carefully transferred to a fresh 50 mL centrifuge tube after centrifugation. To ensure purity, the supernatant was filtered through a 0. 4 µm filter and kept on ice.

For affinity chromatography purification, a HisTrap™ FF column (5 mL) in the ÄKTA protein purification system was employed. The column was initially washed with Wash buffer 1 (**Table 3.6**) to eliminate non-specifically bound DNA. Subsequently, Wash buffer 2 (**Table 3.6**) was used for a further wash. Elution of the target protein was carried out using Elution buffer 1 (**Table 3.6**) with a linear gradient, aiming for a final concentration of 50% Elution buffer 1. Protein-containing fractions were analyzed on a 12% polyacrylamide gel to visualize the protein bands. To accomplish this, the gel was incubated with InstantBlue stain for 5–10 minutes. Fractions containing the desired protein were pooled together. The resulting protein sample was then stored at 4°C.

3.3.8 Protein purification by centrifugation

Protein samples were transferred to 20 mL ultrafiltration spin columns (10,000 MWCO) and centrifuged at 4000 rpm at 4°C until a final volume of approximately 5 ml was reached. Exchange purification of polyproteins using Elution buffer 2 (**Table 3.6**), repeated addition of buffer and centrifugation several times until reaching replacement ratio of 1: 50. It should be noted that each centrifugation should not cause excessive protein precipitation. The final purified protein was electrophoresed on a 12% polyacrylamide gel. Visualization of protein bands is achieved by incubating the gel with Instant Blue stain for 5-10 min. Fractions containing protein were pooled together and concentrations were determined using BioRad DC Protein Assay Kit (Bio-Rad, UK).

3.3.9 Binding DNA preparation

The DNA probe was selected from the regulated genes with PA1397. It was synthesized or obtained by PCR amplification. The primers used in this reaction listed in (**Table 3.6**). The subsequently constructed DNA probes were cloned into the XX vector for sequencing verification.

Table 3.6 Primers used in DNA probes constructed.

Gene	Sequence (5'->3')
PA_53410P	Forward primer CGCCGCTTCCTTTCCTGTCTT
	Reverse primer CTTTCCTGTCTTGCGCCGGT
Variant PA14_53410	Forward primer CGTGCTCAATGGCTTGATCG
	Reverse primer GGAACGAGAGAATATGACCG

3.3.10 Electrophoretic mobility shift assays

The prepared DNA and protein were added in the same tube for binding reaction with 5X binding buffer (**Table 3.7**), each reaction include 20% 5X binding buffer, 40 ng DNA and different dose protein, supplement H_2O to final 10 μL-system. The reaction mixture was incubated at room

temperature for half an hour to forming a protein-DNA complex. Subsequent separation of protein-DNA complexes and free DNA probes by gel electrophoresis using a 5% polyacrylamide gel (10% 5XTBE (University of Southampton, UK), 5% 40% acrylamide stock (19:1, Merck, UK), 0.1% APS (10%, VWR, UK), N, N, N',N'-Tetramethyl ethylenediamine (TEMED, Thermofisher, UK) and H_2O), which have already pro-run. After running, the gel was stained by gel stain for 20 minutes. Finally, it was taken for an imaging to confirm the binding status.

Table 3.7 Component of buffers used in the protein purification and EMSA.

Component	**Final Conc.**	**Component**	**Final Conc.**
Lysis buffer		*5 X Binding buffer*	
Tris HCl (pH 8)	100 mM	Tris HCl (pH 8)	50 mM
NaCl	500 mM	KCl	250 mM
Imidazole (pH 8)	20 mM	MgCl2	10 mM
Glycerol	2%	EDTA	2.5 mM
TCEP-HCl	1 mM	DTT	0.5 Mm
AEBSF	0.1 mM	Triton-X100	0.50%
Lysozyme	1mg/mL	Glycerol	20%
Dnase	5 µg/mL		
Protease Inhibition	1 table		
Wash buffer 1		*Wash buffer 2*	
Tris HCl (pH 8)	100 mM	Tris HCl (pH 8)	100 mM
NaCl	2 M	NaCl	50 mM
Imidazole (pH 8)	20 mM	Imidazole (pH 8)	20 mM
Glycerol	2%	Glycerol	2%
TCEP-HCl	1 mM	TCEP-HCl	1 mM
AEBSF	0.1 mM	AEBSF	0.1 mM
Elution buffer 1		*Elution buffer 2*	
Tris HCl (pH 8)	100 mM	Tris HCl (pH 8)	10 mM
NaCl	500 mM	KCl	50 mM
Imidazole (pH 8)	500 mM	MgCl2	2 mM
Glycerol	2%	EDTA	0.5 mM
TCEP-HCl	1 mM	DTT	0.1 mM
AEBSF	0.1 mM	Triton-X100	0.10%
		Glycerol	4%

3.4 Results

3.4.1 RNA-Seq Data Analysis and Validation.

We performed DNA depletion on RNA samples extracted from the Δ*PA1396*, Δ*PA1397*, Δ*hptA*, Δ*hptB*, and Δ*hptC* genes, followed by validation through gel electrophoresis (**Figure 3.1A**) and concentration determination (**Table 3.8**). Subsequent quality checks confirmed the high quality of these samples (**Table 3.9**), meeting the requirements for further sequencing analysis. RNA-seq analysis was conducted on these samples, using RNA-seq data from the exponential growth phase of *Pseudomonas aeruginosa* PA14 as the control. To assess the consistency of biological replicates, principal component analysis (PCA) was performed on the RNA-seq data (**Figure 3.1B**). The PCA results demonstrated the expected clustering of the three replicates per treatment and clear separation. Specifically, the global gene expression profiles of Δ*PA1396* and Δ*PA1397* samples showed similarity and were closely aligned with the control group, while the Δ*hptA*, Δ*hptB*, and Δ*hptC* samples exhibited distinct differences and were distant from the control group.

Table 3.8 RNA concentration and integrity

Sample Name	Con. (ng/μL)	Integrity value
PA14_RNA_1	555	9.4
PA14_RNA_2	548	9.6
PA14_RNA_3	544	9.6
PA1396_RNA_1	580	9.1
PA1396_RNA_2	501	9.6
PA1396_RNA_3	566	9.4
PA1397_RNA_1	539	9.6
PA1397_RNA_2	526	9.6
PA1397_RNA_3	537	10
PA0033_RNA_1	502	9.7
PA0033_RNA_2	501	9.5
PA0033_RNA_3	507	9.7
PA0991_RNA_1	496	9.8
PA0991_RNA_2	493	9.8
PA0991_RNA_3	487	9.8
PA3345_RNA_1	466	9.6
PA3345_RNA_2	481	9.6
PA3345_RNA_3	479	9.4

Table 3.9 Data quality summary

Sample	Raw reads	Raw data	Effective (%)	Error (%)	Q20(%)	Q30(%)	GC (%)
PA14_RNA_1	17777166	2.7	99.7	0.03	97.69	93.84	63.07
PA14_RNA_2	14389704	2.2	99.82	0.02	98.49	95.58	63.07
PA14_RNA_3	15218570	2.3	99.78	0.03	97.64	93.62	63
PA1396_RNA_1	15949202	2.4	99.77	0.02	98.53	95.67	63.07
PA1396_RNA_2	22269348	3.3	99.72	0.03	97.62	93.71	63.03
PA1396_RNA_3	21943228	3.3	99.74	0.03	97.63	93.71	62.96
PA1397_RNA_1	17734390	2.7	99.63	0.03	97.52	93.47	62.92
PA1397_RNA_2	16972720	2.5	99.75	0.02	98.3	95.13	62.77
PA1397_RNA_3	19414396	2.9	99.64	0.03	97.68	93.85	62.82
PA0033_RNA_1	18383504	2.8	99.7	0.03	97.65	93.74	63.14
PA0033_RNA_2	18489150	2.8	99.69	0.03	97.67	93.78	63.1
PA0033_RNA_3	21060226	3.2	99.69	0.03	97.85	94.18	63.11
PA0991_RNA_1	25634852	3.8	99.33	0.03	97.8	94.14	63.85
PA0991_RNA_2	22469154	3.4	99.52	0.03	97.74	93.93	63.8
PA0991_RNA_3	19736848	3	99.49	0.03	97.75	93.96	63.82
PA3345_RNA_1	23362354	3.5	99.4	0.03	97.7	93.88	63.91
PA3345_RNA_2	24167994	3.6	98.62	0.03	97.71	93.93	63.89
PA3345_RNA_3	22490178	3.4	98.49	0.03	97.75	94.02	64.38

A

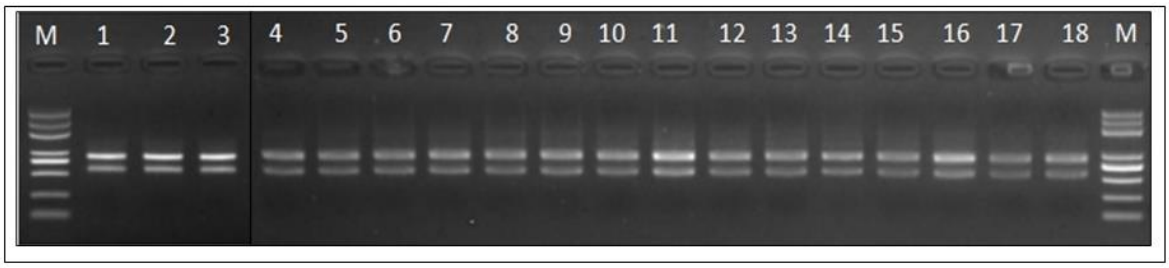

B

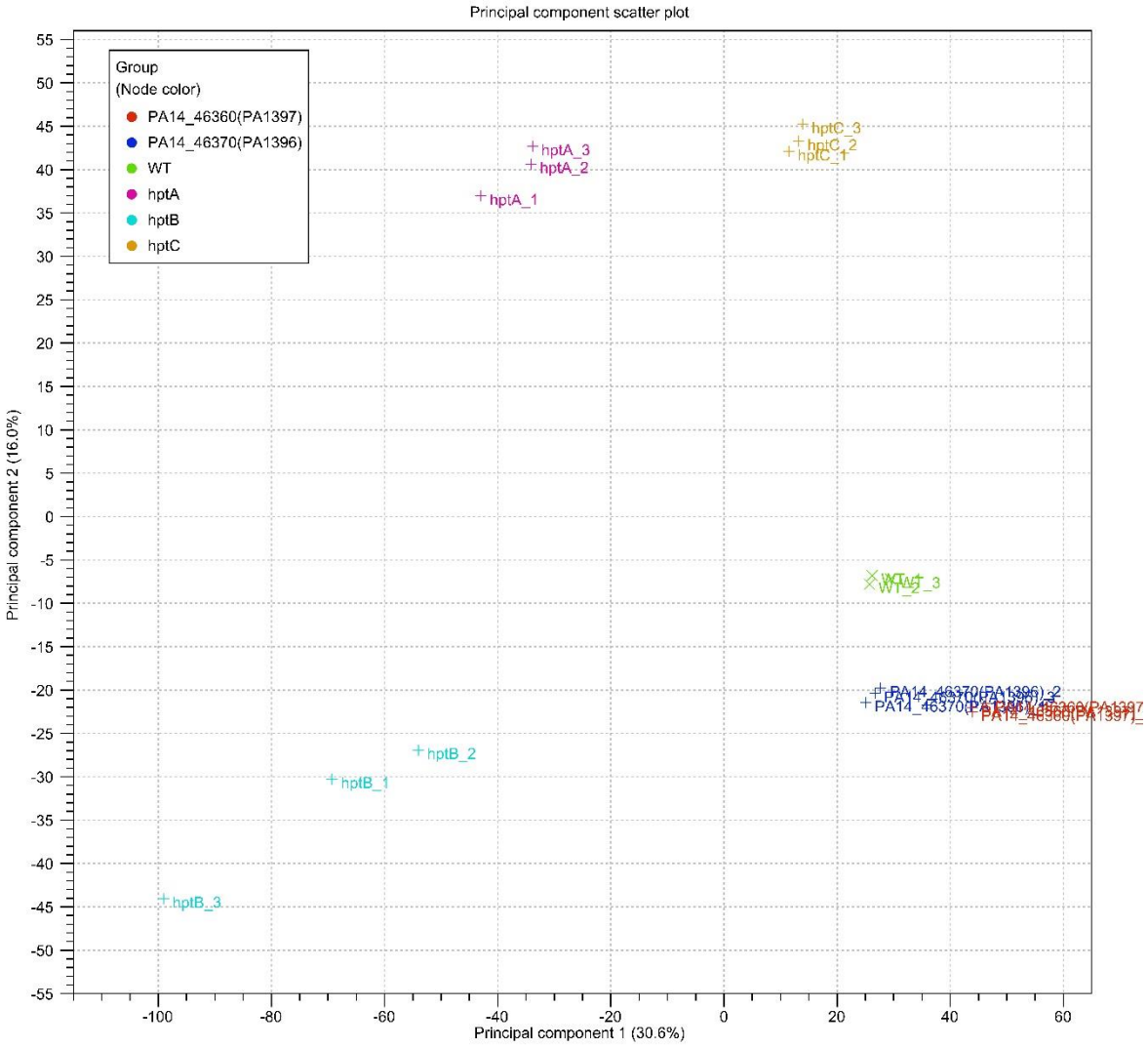

Figure 3.1 A: Gel imaging for all RNA samples. Lane M: Trans 2K Plus DNA ladder; Lane 1-18: RNA samples ranged in the upper table (1-18 loaded 1). B: Principal Component Analysis (PCA) plots for RNA-seq data in each genotype. Each sample have three biological replicates.

3.4.2 RNA-seq Analysis Reveals Differential Gene Expression Patterns in Mutant Genes.

Differential gene expression analysis was performed to compare the mutant gene samples with the control group, resulting in the detection of DEGs meeting the criteria of an absolute fold change greater than or equal to 1.5 and an adjusted P value less than or equal to 0.05 (**Figure 3.1C**). Compared with PA14, Δ*PA1396* exhibited significant differential expression in 12 genes, including 6 up-regulated genes and 6 down-regulated genes (**Figure 3.2A i**). The greatest increases were observed for the genes Δ*PA1902* (3.38-fold), which participate in multiple pathways, including Phenazine biosynthesis, Metabolic pathways, Biosynthesis of secondary metabolites, and Quorum sensing. Among them, Δ*LsfA*, which exhibits peroxidase activity, is crucial for *P. aeruginosa*-induced immunomodulation, enabling the host to overcome infection in its absence (Kaihami *et al.*, 2014). The most downregulated gene, Δ*XphA* (-2.59-fold) (Michel, Durand and Filloux, 2007), and the upregulated gene in Δ*PA1396* and Δ*PA1397*, Δ*PA2675* (2.38 and 1.82-fold), were strongly associated with *P. aeruginosa* type II secretion.

Compared to the 12 genes of Δ*PA1396* that showed different expression from PA14, a total of 127 genes exhibited altered expression levels in ΔPA1397 (**Figure 3.2A ii**). The regulons of ΔPA1396 and Δ*PA1397* overlap, with a total of 3 co-regulated genes (Figure 3.2B), consisting of 1 up-regulated and 2 down-regulated genes, and none of the genes showed the opposite change in Δ*PA1396* and Δ*PA1397*. These 2 downregulated genes, Δ*PA0320* and Δ*PA0327*, can affect Ca^{2+} homeostasis with pleiotropic effects, altering cluster motility, pyocyanin production, and tobramycin sensitivity (Guragain *et al.*, 2016).

The Δ*hptA* and PA14 comparison revealed 469 DEGs, consisting of 201 up-regulated genes and 268 down-regulated genes (**Figure 3.2A iii**). Likewise, Δ*hptB* and PA14 comparison exhibited 813 DEGs, with 638 genes up-regulated and 175 genes down-regulated (**Figure 3.2A iv**). Finally, Δ*hptC* and PA14 comparison identified 133 DEGs, including 90 up-regulated genes and 43 down-regulated genes (**Figure 3.2A v**). Detailed information regarding the DEGs can be found in **Appendix B.1.1**. To visually represent the continuously enriched or downregulated genes, a Venn diagram was constructed using the DEGs from the comparisons of Δ*PA1396*, Δ*PA1397*, Δ*hptA*, Δ*hptB*, and Δ*hptC* with the control group (**Figure 3B and C**).

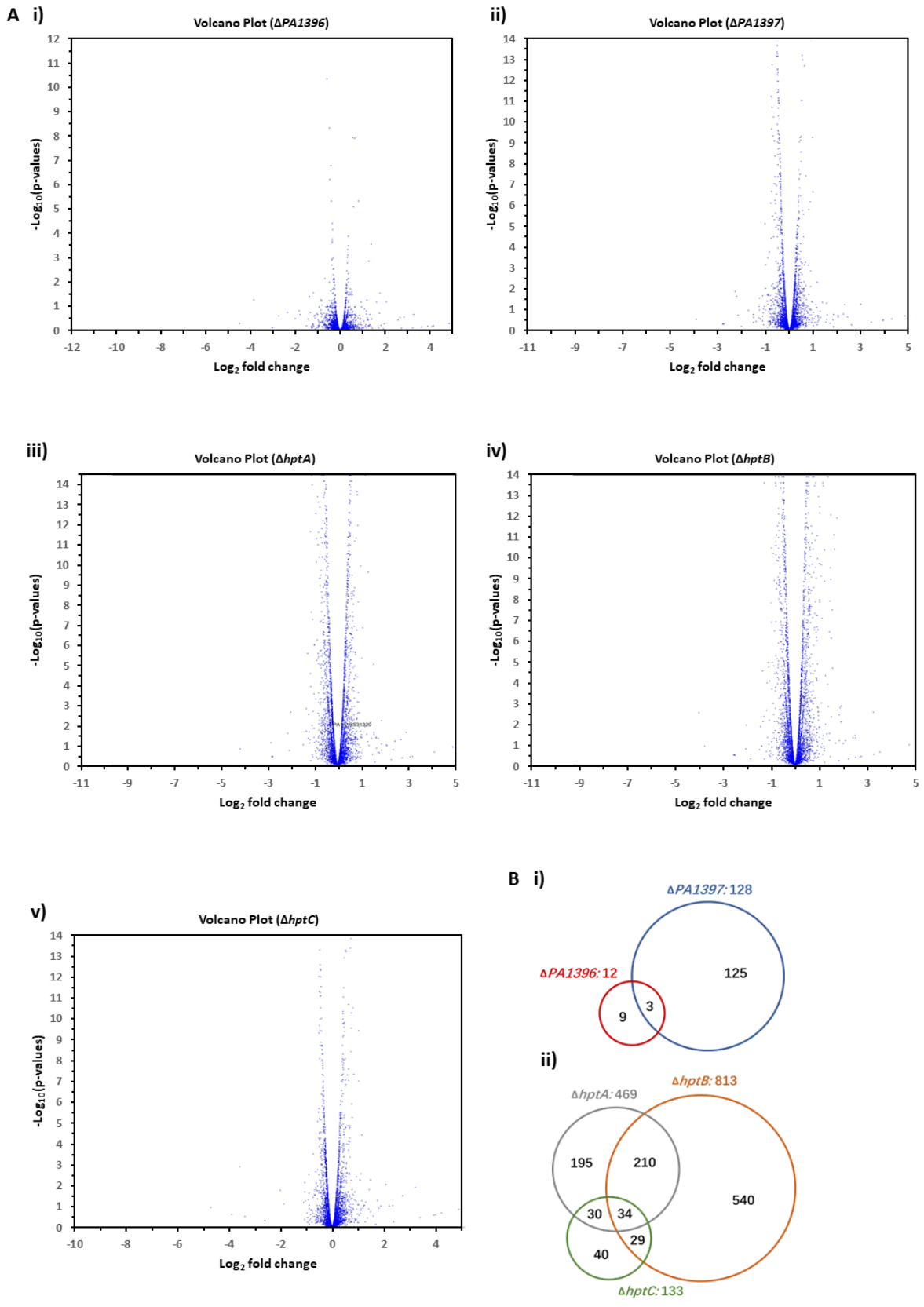

Figure 3.2 (A)Volcano illustration. The horizontal axis represents the degree of gene expression difference (log2 fold change). The vertical axis represents the statistical significance of the gene (-log10(P-value)). Each dot represents a gene whose position is determined by its expression

difference and statistical significance. Venn diagram illustrating the significantly affected genes (B)between Δ*PA1396* and Δ*PA1397*, (C)between Δ*hptA*, Δ*hptB*, and Δ*hptC*.

3.4.3 The pathway enrichment analysis of RNA-seq

To gain further insights into the functions of the differentially expressed genes, we conducted KEGG pathway analysis on the 1153 identified genes. As a result, we obtained a total of 161 differentially expressed genes that were associated with 9 KEGG pathways. The specific information can be found in **Table 3.10**.

Among the up-regulated genes, the up-regulated genes at Δ*hptA* mutant exhibited a strong enrichment only in the nitrogen metabolism pathway. This pathway showed the highest enrichment factor in Δ*hptC* mutant among all the up-regulated pathways. Notably, the Δ*hptB* mutant displayed the highest enrichment of up-regulated genes among all the mutants. The pathways with the largest number of up-regulated genes in the Δ*hptB* mutant was ABC transporter. Additionally, sulfur metabolism oxidative phosphorylation, and phenazine biosynthesis were found to be the most significantly enriched pathways. Regarding the down-regulated genes, the down-regulated genes at Δ*PA1396* mutant exhibited an enrichment in the bacterial secretion system pathway, which had the highest enrichment degree among all pathways. Interestingly, this pathway was also the only pathway enriched in down-regulated genes in the Δ*hptB* and Δ*hptC* mutants. Among the mutants, the Δ*hptB* mutant displayed the largest number of down-regulated genes.

Table 3.10 The Enrichment Pathway list

Count	Pathway name	Enrich facter	-log10p
Up-regulate genes			
hptA			
7	Nitrogen metabolism	5.66	3.81
hptB			
29	Sulfur metabolism	6.58	18.36
13	Phenazine biosynthesis	6.27	7.99
13	Oxidative phosphorylation	2.60	3.03
30	ABC transporters	1.71	2.81
hptC			
6	Sulfur metabolism	9.71	4.66
5	Phenazine biosynthesis	6.35	3.58
5	Oxidative phosphorylation	4.10	2.20
PA1397			
5	Two-component system	4.11	2.41

Down-regulate			
hptA			
6	Sulfur metabolism	4.66	2.84
hptB			
16	Bacterial secretion system	4.04	6.12
hptC			
4	Bacterial secretion system	9.706	3.247
PA1396			
1	Bacterial secretion system	20.20	1.31
PA1397			
7	Cationic antimicrobial peptide (CAMP) resistance	11.00	5.79
5	Amino sugar and nucleotide sugar metabolism	6.93	3.23
4	Nitrogen metabolism	5.55	2.29
5	Oxidative phosphorylation	4.06	2.17

3.4.4 Validation of RNA-Seq Results by qRT-PCR.

To validate the expression changes identified through RNA-Seq, we employed quantitative real-time reverse transcriptase PCR (qRT-PCR) analysis to assess the reliability of the RNA-seq expression data. A careful selection of genes representing a wide range of expression fold changes and diverse functional classes was made for this analysis.

Using qRT-PCR, we measured the relative expression levels of these selected genes in each mutant. Remarkably, the results obtained through qRT-PCR mirrored the differences in gene expression patterns observed in the transcriptome analysis (**Figure 3.3**). It is important to note that while the magnitude of gene fold change might have varied between the two datasets, the qRT-PCR results demonstrated similar trends of up- or down-regulation as observed in the RNA-seq data. This consistency between the two methods strongly supported the validity and accuracy of the RNA-seq expression data. The utilization of qRT-PCR as a complementary validation approach reinforces the robustness of our results and enhances the overall credibility of the gene expression profiling performed in this study.

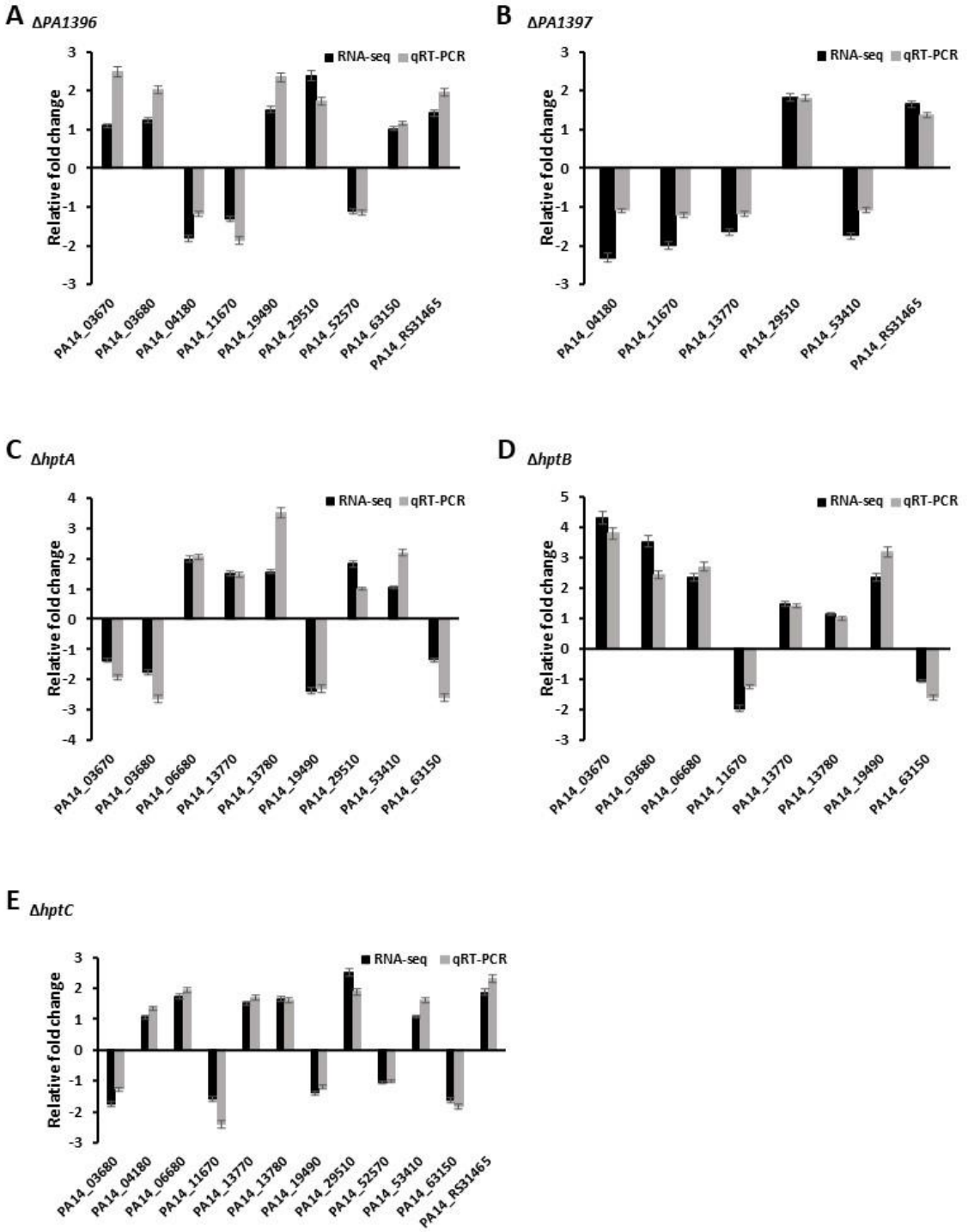

Figure 3.3 Comparison of relative fold changes between RNA-Seq and qRT-PCR results in mutants (A) Δ*PA1396*, (B) Δ*PA1396*, (C) Δ*hptA*, (D) Δ*hptB*, and (E) Δ*hptC* background. The Cts obtained for 16S rRNA amplifications run in the same plate were used to normalize all qRT-PCR results. Gene transcript levels were determined from standard curves. The reported values represent the mean and standard deviation of triplicate measurements.

3.4.5 Examination of Protein PA1397- DNA interaction by Electrophoretic mobility shift assays

We performed electrophoretic mobility shift analysis (EMSA) to demonstrate that PA1397 interacts with the PA_53410 promoter region. A dual tag expression construct of PA1397 (His6-MBP) and a tag alone (His6-MBP) as a control were generated, followed by protein purification by affinity chromatography and centrifugation. Purified double-tagged PA1397 fusion protein resulted in a shift in mobility when incubated with a DNA fragment spanning the PA1397 promoter (**Figure 3.4**). And with the increase of PA1397 protein concentration, the higher the degree of fusion with DNA. However, DNA fragments lacking the CGCCGCTTC motif did not change unless higher concentrations of protein were added, while the MBP tag alone did not bind to either DNA fragment (**Figure. 3.4**).

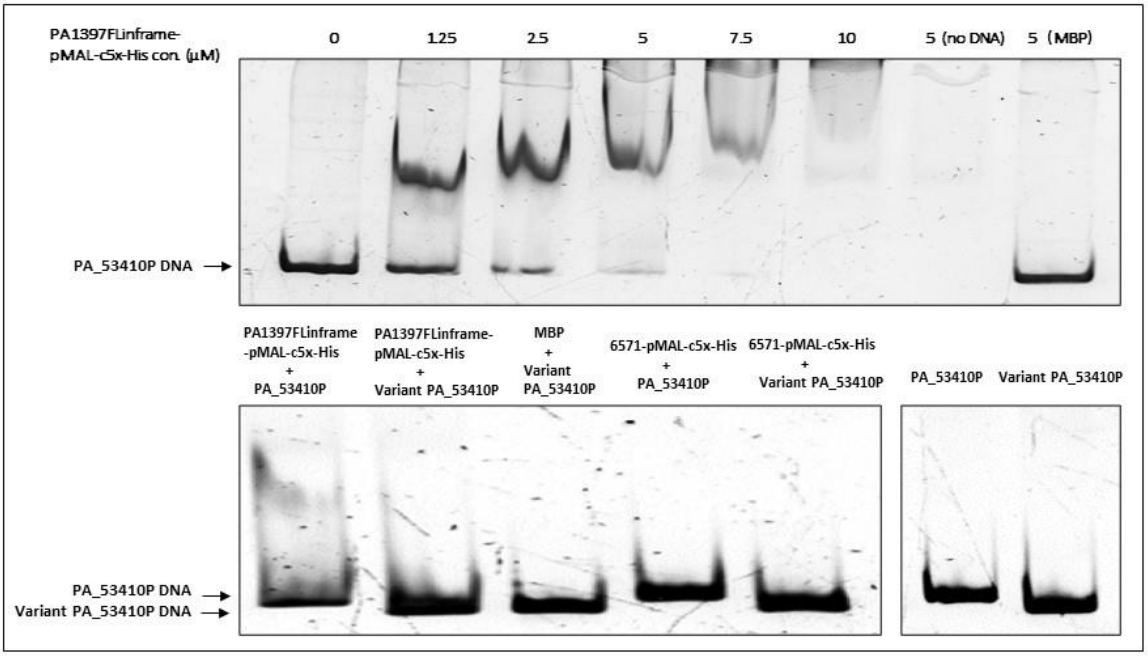

Figure 3.4 Binding of PA1397 to the PA_53410 promoter is modulated by the presence and absence of "CGCCGCTTC" motif. His-MBP tag alone and DNA fragment alone ware used as negative control in the assay.

3.5 Conclusion and Discussion

Quorum sensing is an important communication method between microorganisms, which assists bacteria to sense population density and regulate gene expression. The diffusible signal factor (DSF) signalling pathway is a transmembrane signalling system that regulates the expression of a

series of genes and affects the formation, movement, and interaction with host cells of biofilms. The regulatory mechanism and function of DSF signalling pathway have been confirmed in various bacteria, especially in pathogenic bacteria (Guo *et al.*, no date; Li *et al.*, 2019; Wang *et al.*, 2022). This study is aimed at the opportunistic infection bacteria *Pseudomonas aeruginosa*. In Chapter 2, we also mentioned that *Pseudomonas aeruginosa* senses DSF signals through PA1396 as a signal receptor, and PA1397 participates in this signal as a response regulator The process of transmission thereby regulates gene expression. Therefore, the findings in this chapter provide valuable insights into the role of PA1397 in the regulation of gene expression and protein-DNA interactions in *P. aeruginosa* PA14.

Through RNA-seq analysis and differential gene expression analysis, we observed that the mutant strains had different gene expression profiles compared with the control. Specifically, ΔPA1396 and ΔPA1397 samples showed similarities, further validating the conjecture in chapter 2 that these two genes function as a two-component system. Δ*hptA*, Δ*hptB*, and Δ*hptC* showed significant differences in gene expression compared to controls, suggesting that loss of these genes resulted in global changes in gene regulation.

This study of KEGG pathway analysis revealed the association between a series of differentially expressed genes and specific pathways in *P. aeruginosa* through KEGG pathway analysis. Notably, in the *ΔhptA* and *ΔhptB* mutants, the significant enrichment of the oxidative phosphorylation pathway suggests that the absence of these genes may impact the energy metabolism of the bacterium. Particularly in the *ΔhptB* mutant, the upregulation of genes in sulfur metabolism and ABC transporter pathways indicates a potentially crucial role of *ΔhptB* in regulating sulfur metabolism and substance transport. Furthermore, downregulated genes in the ΔPA1396 mutant were found to be enriched in the bacterial secretion system pathway, implying a key role of the ΔPA1396 gene in the secretion regulation of *P. aeruginosa*. It is noteworthy that this downregulation pattern was validated in the *ΔhptA* and *ΔhptB* mutants, emphasizing the importance of this pathway under different gene deletion conditions. The *ΔhptB* mutant exhibited the highest number of downregulated genes, suggesting a key function of the *ΔhptB* gene in maintaining normal gene expression levels. These findings provide crucial clues for further exploring the functions and biological significance of genes associated with these pathways in *P. aeruginosa*. Future research could delve into understanding the specific contributions of these pathways to bacterial survival, metabolism, and adaptability. Additionally, investigating their roles in pathophysiological processes such as *P. aeruginosa* infection and antibiotic resistance formation may pave the way for the theoretical foundation of novel therapeutic strategies to effectively combat infections and diseases associated with *P. aeruginosa*.

The electrophoretic mobility shift analysis (EMSA) provided further evidence of the interaction between PA1397 and the PA_53410 promoter region. The observed shift in mobility when the double tagged PA1397 fusion protein was incubated with the DNA fragment indicates a direct binding between PA1397 and the specific DNA sequence. The concentration-dependent fusion of PA1397 with DNA suggests that PA1397 may act as a transcription factor, modulating the transcription of target genes through its interaction with specific promoter regions. This finding highlights the potential role of PA1397 in gene expression regulation in *P. aeruginosa*.

The knowledge gained from this research has broader implications for the field of regulation of bacterial gene expression. The RNA-seq and differential gene expression analysis methods employed in this study can be used to study gene regulatory networks in other bacterial species. Understanding the mechanisms by which transcription factors such as PA1397 interact with DNA and regulate gene expression is critical for deciphering complex regulatory networks in bacteria and may have implications for the development of novel antimicrobial strategies targeting transcriptional regulation.

In conclusion, this study provides insight into the role of PA1397 in the regulation of gene expression and protein-DNA interactions in *P. aeruginosa* PA14. These findings contribute to our understanding of the regulatory mechanisms of *P. aeruginosa* gene expression and reveal the potential functions of PA1397 in bacterial adaptation and pathogenicity. Further research on PA1397 and its regulatory targets will deepen our understanding of *P. aeruginosa* pathogenesis and may provide new avenues for the development of therapeutics against *P. aeruginosa* infection. In addition, this study has important reference significance for more clearly exploring the signal transduction of DSF in *P. aeruginosa*. The recruited solo Hpt domains were also analyzed at the sub-ah transcriptional level, showing that their gene Significant effect on expression, especially of Δ*hptB*.

Chapter 4 Developing high-content screen assays to identify molecules that inhibit antibiotic-resistant bacterial infections.

4.1 Abstract

Drug-resistant bacteria pose a significant threat to global healthcare systems, and the need for new, effective anti-bacterial agents is urgent. This chapter focuses on *P. aeruginosa* infection, a bacterium that causes acute and chronic infections in immunocompromised and hospitalized patients. To address this issue, the chapter explores the potential of targeting the regulatory pathway of intracellular c-di-GMP, a signalling molecule that regulates antibiotic resistance, biofilm formation, and virulence. *P. aeruginosa* utilizes c-di-GMP to control the expression of a wide range of genes involved in its adaptation to different environmental conditions, including antibiotic stress. Therefore, reducing the intracellular levels of c-di-GMP has been proposed as a promising strategy to combat antibiotic-resistant *P. aeruginosa* infections (Ryan, 2013; Valentini and Filloux, 2016b). Additionally, the chapter emphasizes the importance of natural products as a potential source of new drugs due to their diverse chemical structures, low toxicity, and reduced risk of resistance (Dzobo, 2022).

For decades, drug screening models have played a critical role in identifying novel compounds with therapeutic potential. High-throughput screening (HTS) and high-content screening (HCS) are two widely used methods in drug discovery. In contrast, HCS involves screening smaller compound libraries with higher quality and diversity, thereby increasing the hit rate of bioactive compounds (Kang *et al.*, 2016). To optimize the screening process, the chapter presents two high-content screening models: one based on co-culturing human airway epithelial cells and *P. aeruginosa* and the other based on *P. aeruginosa* cells alone. The co-culture model provides a physiologically realistic environment for bacterial biofilm formation and enables the identification of natural compounds that modulate c-di-GMP levels and impact biofilm formation and cytotoxicity. This approach also improves the transferability of *in vitro* drug screening.

In this chapter, we screened 800 natural plant extracts and 200 natural compounds using the two high-content screening models mentioned above to identify potential inhibitors. Our goal was to discover small molecules that could modulate c-di-GMP levels in bacteria, influencing *P. aeruginosa* biofilm formation and cytotoxicity while minimizing effects on bacterial growth. Scalability and transferability are the primary concerns in our current study. Therefore, for the

potential compounds identified through bacterial cell-based screening models, we will focus on assessing scalability and transferability using the waxworm model for further verification.

4.2 Hypothesis

Discover natural compounds and natural plant products that can regulate *P. aeruginosa* biofilm formation and cytotoxicity by constructing and optimizing high-quality screening models targeting c-di-GMP.

1. Altering c-di-GMP signalling in *P. aeruginosa* bacteria can effectively combat antibiotic resistance. By regulating the level of c-di-GMP, it may affect the biofilm formation and virulence of bacteria, thereby weakening their drug resistance and pathogenicity.
2. Natural products may become a potential drug source for the treatment of *P. aeruginosa* infection. Natural products have a wide range of chemical structures and biological activities, which have potential advantages for the discovery of new compounds that can be transformed into effective drugs.
3. By constructing a high-quality screening model, natural compounds that regulate c-di-GMP and thus affect *P. aeruginosa* biofilm formation and cytotoxicity can be efficiently screened out. The co-culture model of human airway epithelial cells and *P. aeruginosa* can more realistically simulate the environment of bacterial biofilm formation.

4.3 Materials and Methods

4.3.1 Bacterial strains and culture conditions

The wild-type *P. aeruginosa* PA14 and other strains, plasmids used in this study are described in Table 2.1, all the strains store at -80°C freezer. For most experiments, *P. aeruginosa* strains were grown in Luria–Bertani (LB) medium. The antibiotics used were tobramycin (Tb), gentamicin (Gm), ampicillin (Amp), Kanamycin (Km), spectinomycin (Sp) and the concentrations used are indicated.

Minimum essential media supplement with 10% FBS, 2mM L-glutamine, 50U/mL penicillin and 50μg/mL streptomycin was used for culturing 16HBE 14o- cells. Minimum essential medium eagle supplement with 2mM L-glutamine and 0.4% arginine (Merck Group)) was used for the infection step when setting the co-culture model. In the high-content screen model based on bacterial cells only, the 5% LB (1:25 ratio with Phosphate Buffered Saline (PBS)) has been used.

Table 4.1 Strains and plasmids

Strains/Plasmids	Relevant information	Source/Reference
Strains		
E. coli		
DH5α	*E. coli* strain for constructing recombinant plasmids	Lab stock
SM10	*E. coli* strain as conjugation donor	(Miller and Mekalanos, 1988)
pUX-BF13	pUX-BF13 *E. coli* helper strain carrying a transposase on a pUX plasmid, amplicillin resistant	(Bao *et al.,* 1991)
pRK600	PRK 600 *E. coli* fertile helper strain, chloramphenicol resistant	(Kessler, de Lorenzo and Timmis, 1992)
P. aeruginosa		
PA14	Wild type	(Rahme *et al.*, 1995)
PA14-*lux* (pCdrA::*gfp*^{C})	*luxCDABE*-tagged PA14 harboring plasmid pCdrA::*gfp*	This study
PA14-*gfp*	PA14 WT with chromosomal GFP tag	This study
Plasmids		
pCdraA::*gfp*^{C}	pUCP22Not-PcdrA-RBSII-*gfp* (Mut3)-T0-T1	(Rybtke *et al.*, 2012)
pUC18T-mini-Tn7T-lux-Gm	Suicide vector for shuttling single copies of genes directly to the chromosome via a mini-Tn7 element; *aacC1* gene encoding gentamicin resistance marker on Tn7 element; contains oriT for mobilization; P1 integron promoter driving expression of *lux*CDABE; Amp^{r} Gm^{r}	(Damron *et al.*, 2013b)

4.3.2 Sources of small molecules libraries

The Puretitre natural compound library and the Phytotitre natural product extracts library purchased from Caithness Biotechnologies, UK were used in this work (http://www.caithnessbiotechnologies.com/puretitre.html). One library contains a collection of 200 compounds found in natural products used as traditional medicines, or as the basis of modern drugs. All of the compounds were maintained in DMSO. Another one is the natural product extract library. This library focuses on plants with a history and medicinal or association with health in man and with excellent diversity, including 367 unique species and 304 unique genera. The follow-up compounds used after the primary screen were also purchased from Caithness Biotechnologies, UK.

4.3.3 Construction of the dual labelled bioreporter strain PA14-*lux* (pCdrA::*gfp*^{C})

The growth and c-di-GMP levels in *P. aeruginosa* in different conditions were assessed using a *lux* reporter and a *gfp* reporter respectively. In order to create the dual-labelled reporter strain, WT PA14 was first tagged with the mini-Tn7 reporter construct from pUC18T-mini-Tn7T-*lux*-Gm by means of four-parental mating with *E. coli* DH5α harbouring the delivery vectors as donor strains and with *E. coli* strains harbouring pUX-BF13 and pRK600 as helper strains, as previously described (Damron *et al.*, 2013a). Then the plasmid-based reporter pCdrA::*gfp*^{C} (Rybtke *et al.*, 2012) was introduced into the lux-labelled background strains by electroporation.

For further confirmation, the *P. aeruginosa* WT PA14 and the selected strain are cultured in LB medium at 37°C overnight in a shaker. The overnight culture is adjusted to the final concentration to OD_{600}=0.01. *P. aeruginosa* WT PA14, or the selected strain in combination with Ampicillin (final concentration: 0.1mg/mL) have been transferred to a 96-well plate (SLS, UK). After incubating the plate for 24 hours at 37°C, the BMG CLARIOstar multi-mode microplate reader was used to measure the value of OD_{600}, GFP and bioluminescent value.

4.3.4 Bacterial cell-based screen model

The single colony of PA14-*lux* (pCdrA::*gfp*^{C}) strain was incubated overnight in LB medium supplemented with Amp (100 µg/mL) and Gm (5 µg/mL) antibiotics. A subculture was prepared by diluting the overnight culture with fresh LB medium to OD_{600} =1 and further diluted with 5% LB medium at a 1:25 ratio.

To establish negative controls (0% inhibition), 195 µL of the subculture was supplemented with 5 µL DMSO. For positive controls (100% inhibition), 195 µL of the subculture was supplemented with 5 µL of DMSO and 0.4 µL of a 25 mg/mL Tb solution (final concentration of 50 µg/mL). They were individually added to eight wells of TC-treated flat bottom clear black 96-well microplates (SLS, UK). For small molecule screening, the remaining wells were filled with 195 µL of the prepared subculture per well. Subsequently, 5 µL of a distinct small molecule compound (at a concentration of 10 mM) or a product extract (at a concentration of 10 mg/mL) was added to each well, resulting in a final concentration of 250 µM for the compound or 250 µg/mL for the product extract. To maintain optimal conditions, the microplate was securely sealed with a vented lid seal and placed in an incubator at 37°C for a duration of 6 hours.

4.3.5 Human bronchial epithelial cell-based screen model

The overnight culture of PA14-*lux* (pCdrA::*gfp*^{C}) strain was subjected to centrifugation, and the resulting cell pellet was carefully resuspended in Minimum Essential Medium Eagle supplemented with 2 mM L-glutamine and 0.4% arginine. Subsequently, a subculture was prepared by diluting the resuspended culture with the same medium to achieve OD_{600} = 0.01.

In accordance with the procedure described in section 4.3.5, the negative control, positive control, and small molecule screening wells were prepared using this subculture. Each of these samples was individually added to TC-treated flat bottom clear black 96-well microplates that had been previously seeded with 16HBE 14o- cells. The microplates were sealed with air-permeable cover seals and incubated at a temperature of 37 °C with 5% CO_2 for a duration of 1 hour. Following the initial hour of incubation, carefully replace fresh medium into each well, and the microplates were further incubated for 3.5 hours in a 37 °C CO_2 incubator.

To assess the cytotoxicity of the human bronchial epithelial cells, the CyQUANT™ LDH Cytotoxicity Assay-Fluorescence Kit (Invitrogen, UK) was employed. The sample culture from each well was transferred to another 96-well plate containing the Reagent Stock Solution in each well. Subsequently, the plate was incubated at room temperature for 10 minutes while being protected from light. Following the 10-minute incubation, the Stop Solution was added to each well containing the samples.

4.3.6 Measurement of Growth, Intracellular c-di-GMP Level and LDH cytotoxicity level

Approximately 30 minutes before spectrophotometric measurement, pre-warm the plate reader to 37 °C to avoid condensation. Create a protocol for measuring OD_{600} and GFP (Excitation max 470-15nm, Emission max 515-20nm, with a setting of 10 flashes per well and a settling time of 0.3 sec. Focal height is 8.2mm) and bioluminescence (Emission max 580-80nm, choose the spiral avg. and 4mm diameter of wells' scan, with a setting of 0.86s for measurement interval time and a settling time of 0.3 sec. Focal height 17.5mms) and LDH cytotoxicity (Excitation max 560nm, Emission max 590nm, with a setting of 10 flashes per well and a settling time of 0.3 sec. Focal height is 8.2mm). Setting up the "Double orbital" shake mode (300rpm, the 20s) before plate reading. The highest value well was selected to adjust the gain. Export data after reading using excel for further analysis.

4.3.7 Statistical Analysis

For analysing the data, the software KNIME has been used to obtain the value of Z-score to screen the potential antibiotic molecules. Based on the HTS pipeline provided by KNIME's official website, adapted to the actual situation of this research.
(https://hub.knime.com/jordi/spaces/Public/latest/HTS%20pipeline~AY4qLEx7XG0mgfx3/)

In addition, the robust Z' value can be calculated to test the quality of each plate by the formula:

$$\text{robust z}' = 1 - \frac{3(\text{MAD}_\text{n} + \text{MAD}_\text{p})}{|\text{median}_\text{n} - \text{median}_\text{p}} \quad \textbf{(4.1)}$$

*MAD (Median Absolute Deviation) is an estimate of standard deviation, p is the positive control and n is the negative control. Note: An assay with a robust Z' greater than or equal to 0.5 is considered as an excellent assay.

To calculate %inhibition of the intracellular level of c-di-GMP using the formula:

$$\%\ \text{Inhibition}_\text{GFP} = 100\% \times \left(1 - \frac{(\text{Xi}_\text{GFP} - \text{median}_{\text{p(GFP)}}/(\text{Xi}_{\text{OD600}} - \text{median}_{\text{p(lux)}})}{(\text{median}_{\text{n(GFP)}} - \text{median}_{\text{p(GFP)}})/(\text{median}_{\text{n(lux)}} - \text{median}_{\text{p(lux)}})}\right) \quad \textbf{(4.2)}$$

* Xi_{GFP} is the iterated GFP value of each sample well. % InhibitionGFP > 0, c-di-GMP inhibitor.

% InhibitionGFP < 0, c-di-GMP promoter.

To calculate %inhibition of the intracellular level of cytotoxicity using the formula:

$$\%\ \text{Inhibition}_\text{Cytotoxicity} = 100\% \times \left(1 - \frac{(\text{Xi}_\text{GFP} - \text{median}_{\text{p(\%Cytotoxicity)}})}{|\text{median}_{\text{n(\%Cytotoxicity)}} - \text{median}_{\text{p(\%Cytotoxicity)}}|}\right) \quad \textbf{(4.3)}$$

* Xi%cytotoxicity is the %cytotoxicity value of each sample well (use the formula above).

A threshold has been set for hit detection.

4.3.8 Dose-response test

The selected hit compounds were further tested by a 10-point dose-response assay with a top 2 mM and two-fold dilution series. All experiments were performed three times. Results are expressed as mean value ± standard deviation (SD). IC50 calculations were erformed using the built-in algorithms for dose-response curves with variable slope using GraphPad Prism software (version 9).

4.3.9 Construction of the GFP tagged stain PA14-*gfp*

The PA14, pRK6000, pUX-BF13, and pUC18-Tn7-*gfp*-StrepR strains were cultured in LB medium and incubated overnight at 37°C with shaking at 180 rpm. The overnight culture of the receptor strain PA14, the helper strains pRK6000 and pUX-BF13, and the donor strain pUC18-Tn7-*gfp*-StrepR were collected in the same tube in turn (the ratio is 2:1:1:2). These bacterial pellets were resuspended in LB medium to ensure thorough mixing, and then inoculated on PIA plate supplemented with Sp (800 μg/mL) for overnight incubation to screen for PA14- *gfp* binding strains. The PA14- *gfp* strain was visually confirmed under a microscope, exhibiting a green fluorescence signal.

4.3.10 Co-culture Biofilm Assay

The co-culture biofilm formation assay used in this study is based on the ability of *P. aeruginosa* to adhere and form biofilms on human airway epithelial cells grown in culture, as previously described (Moreau-Marquis *et al.*, 2010). 16HBE14o- cells were seeded in μ-Slide 8 Well Chamber Slide (ibidi, Thistle Scientific). The cells were grown to form a confluent monolayer before being inoculated with PA14-*gfp*, *P. aeruginosa* WT PA14-*gfp* strain alone (~ 2×10^6 CFU), or in combination with tobramycin (final concentration: 1000 μg/mL), the test compound 6,7-Dihydroxycoumarin (final concentration: 207 μM), or 6,7-Dihydroxycoumarin plus tobramycin. After incubating the slides for 1 hour at 37°C with 5% CO_2, the supernatant was removed and replaced with fresh medium supplemented with 0.4% arginine. The slides were then further incubated at 37°C with 5% CO_2 for 5 hours. The integrity of the airway epithelial cells and the development of GFP-labelled *P. aeruginosa* biofilms at the apical surface of airway epithelial cells were visualized by confocal microscopy.

4.3.11 Confocal microscopy analysis

Bacterial cell-based screen model. The development of *P. aeruginosa* biofilms after incubation for 6 hours were visualized by Leica (SP8) confocal microscope equipped with a 63X oil objective (Imaging and Microscopy Centre, University of Southampton). To visualized by confocal microscopy, the LIVE/DEAD® BacLight™ Bacterial Viability Kit (ThermoFisher, UK) was used to stain the live (excitation/emission: 480/500 nm) and dead (excitation/emission: 490/635 nm) bacterial cells.

Human bronchial epithelial cell-based screen model. The integrity of the airway epithelial cells and the development of GFP-labelled *P. aeruginosa* biofilms were visualized by Leica (SP8) confocal microscope equipped with a 63X oil objective (Imaging and Microscopy Centre,

University of Southampton). The 16HBE cells were pre-stained with CellBrite™ Orange Cytoplasmic Membrane Dyes (excitation/emission: 549/565 nm, Cambridge Bioscience). Biofilms formed by GFP-tagged PA14 strain were observed by monitoring the GFP fluorescence.

Leica LAS AF software (Imaging and Microscopy Centre, University of Southampton) was used for the visualization and processing of three-dimensional (3D) image data. Quantitative analyses of image stacks were performed using the IMARIS software package (Bitplane) Oxford Imaging, UK). At least XXX image stacks from each of three independent experiments were used for each analysis.

4.3.12 *Galleria mellonella* virulence assays

Galleria mellonella were purchased from Blades Biological Ltd. UK) and stored wood chippings at 15°C in darkness to prevent pupation. Larvae weighing 300 ± 30 mg with no cuticle discoloration were selected. Ten healthy larvae per treatment and controls were used per experimental parameter. All experiments were performed indecently on three separate occasions. In the pathogenicity studies, ten larvae were inoculated through the last left pro-leg into the hemocoel using a 25 µL syringe (Merck Group) with 10 µL of PBS-washed WT PA14 culture (approximately $1X10^3$ CFU/mL). One hour after inoculation, larvae were treated with either tobramycin (final concentration: 1mg/Kg), the test compound 6,7-Dihydroxycoumarin (final concentration: 200mg/Kg), or the compound plus tobramycin. Larvae inoculated with PBS were utilized as controls. The injected larvae were placed in Petri dishes containing filter paper and were incubated at 37°C. Mortality, cuticle discoloration, and responses to touch were recorded 16 hours post-treatment. All experiments were performed independently on three separate occasions.

4.3.13 Statistical Analysis

The data were represented as the mean ± standard deviation (SD). To compare samples from two independent treatments, the student' t-test was employed either in a parametric or non-parametric manner. For comparing multiple samples. Statistical significance was defined as $p < 0.05$. The significance levels were denoted as follows: * for $p < 0.05$, ** for $p < 0.01$. The figure legends provided details regarding the specific test methods and the number of biological replicates used in each analysis.

4.4 Results

4.4.1 Construction of viability and c-di-GMP-responsive reporter

In order to identify compounds that potentially modulate the c-di-GMP signalling during infection *Pseudomonas aeruginosa* reference strain PA14, we established a co-culture-based screening assay. We constructed a dual-labelled reporter strain that allowed the library of natural compounds to be screened for their effects on both modulation of bacterial c-di-GMP signalling and growth during infection. WT PA14 strain was first tagged with the mini-Tn7 reporter construct from pUC18T-mini-Tn7T-*lux*-Gm by means of four-parental mating with *E. coli* DH5α harbouring the delivery vectors as donor strains and with *E. coli* strains harbouring pUX-BF13 and pRK600 as helper strains, as previously described (Damron *et al.*, 2013a). Then the plasmid-based reporter pCdrA::*gfp*^{C} (Rybtke *et al.*, 2012) was introduced into the lux-labelled background strains by electroporation, generating the dual-labelled reporter strain named PA14-lux (pCdrA::*gfp*^{C}) (**Table XX**). The experimental strain PA14-*lux* (pCdrA::*gfp*^{C}) and the control strain WT PA14 were cultivated in Luria-Bertani (LB) medium. Bioluminescence and GFP fluorescence were measured using a multimode microplate reader. **Figure 4.1A** illustrates that WT PA14 exhibited background-level bioluminescence, whereas PA14-*lux* (pCdrA::*gfp*^{C}) displayed an elevated bioluminescent signal. As seen in **Figure 4.1B** the baseline reference is set by the GFP expression of the WT PA14 strain, represented as 100%. Without antibiotic treatment, the dual-labelled reporter strain PA14-*lux* (pCdrA::*gfp*^{C}) exhibits similar GFP expression to the WT strain due to low c-di-GMP levels, resulting in low cdrA::*gfp* transcription. However, the addition of Ampicillin (con.) and Gentamicin (con.) induces a significant increase in GFP expression in PA14-*lux* (pCdrA::*gfp*^{C}), surpassing the WT strain by over 20%. Sub-minimal inhibitory concentration (sub-MIC) antibiotic exposure has been shown to enhance biofilm formation, elevate cyclic-di-GMP levels, and subsequently promote increased cdrA::*gfp* transcription through heightened c-di-GMP levels within the bacteria (Nolan and Behrends, 2021). These results indicate that the reporter can be used to monitor *P. aeruginosa* strain viability and drug-induced changes in c-di-GMP levels.

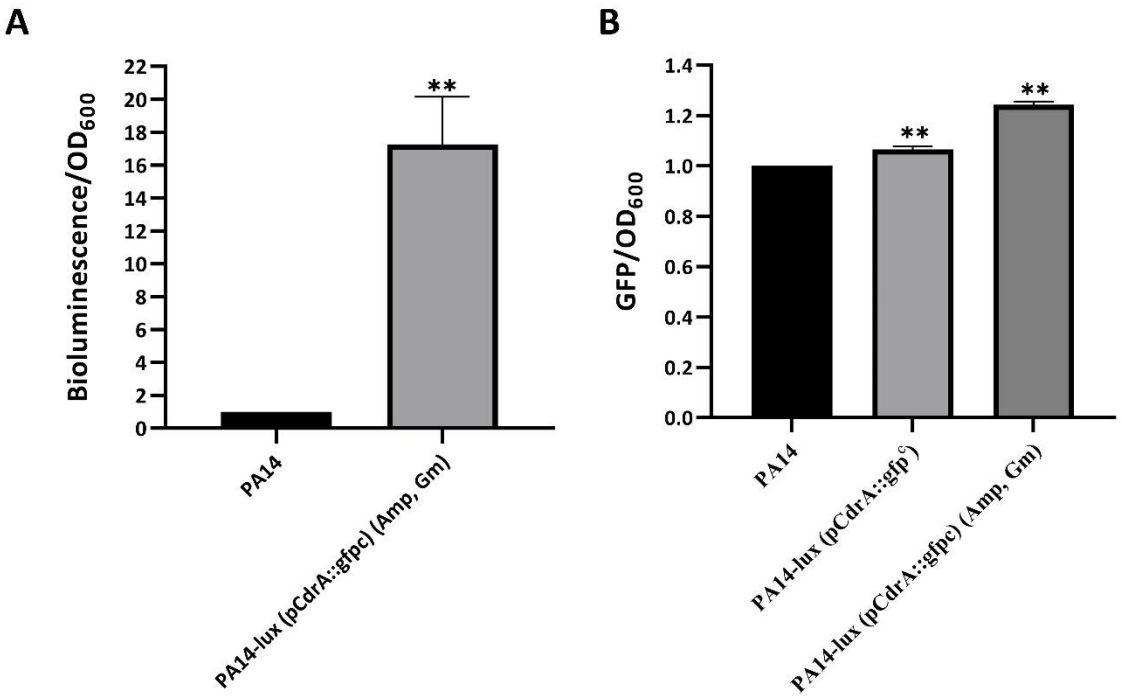

Figure 4.1 Bioluminescence and fluorescence expression in wildtype PA14 and PA14-lux (pCdrA::*gfp*^{C}). (A) Bioluminescence expression level in strains PA14, and PA14-lux (pCdrA::*gfp*^{C}) grown under selection (antibiotics Amp and Gm). Note wildtype PA14 does not grow under selection. (B) GFP expression level in strains PA14, PA14-lux (pCdrA::*gfp*^{C}) and PA14-lux (pCdrA::*gfp*^{C}) grown under selection (antibiotics Amp and Gm). Note wildtype PA14 does not grow under selection.

4.4.2 Development of a high-content bacterial cell-based screen

The *P. aeruginosa* bacterial cell-based model was used to screen small molecules for inhibition of the cellular c-di-GMP level and bacterial growth (**Figure 4.2A)**. The *P. aeruginosa* PA14-*lux* (pCdrA::*gfp*^{C}) constructed as described in section 4.3.1 was incubated into plates with test compounds, tobramycin (a positive control) or DMSO (a negative control), according to the layout shown in **Figure 4.2B**. After incubation, the value of GFP, Bioluminescence, OD_{600} were read by plate reader.

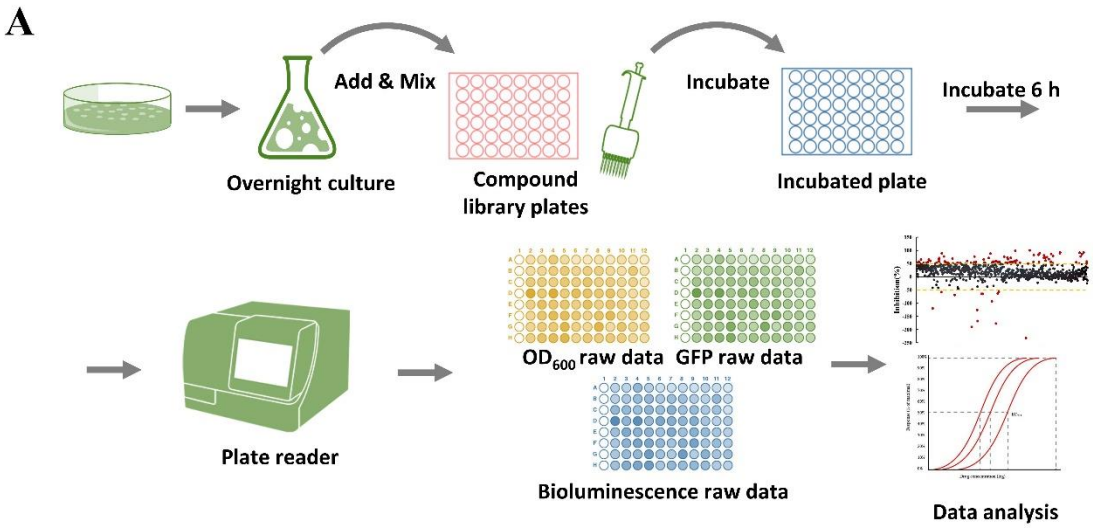

B

	1	2	3	4	5	6	7	8	9	10	11	12
A												
B												
C												
D												
E												
F												
G												
H												

Figure 4.2 The bacterial cell-based screen assay setup. (A) The bacterial colonies of *P. aeruginosa* were grown overnight in the LB starter culture. After diluting to the required concentration, inoculate bacteria, small molecules, and control group. The plate was incubated for 6 hours, and then the OD_{600}, bioluminescence, and GFP values were measured. Using these readings, compounds that affect c-di-GMP cellular levels can be identified. (B) A 96-well plate layout used for small molecule screening assay. The natural compounds and natural product extracts from library (blue) are aliquoted into wells A1-H10. The positive control (red) consisting of tobramycin sulfate and DMSO is added to wells A11-H11. The negative control (green) containing a final concentration of DMSO only is added to wells A12-H12.

4.4.2.1 Quality control of the assay.

The quality of the high-content screen model has been thoroughly validated. **Figure 4.3 A**, **B**, **C** displays representative heatmap results obtained from the 96-well screening plate assays, and this validation test was repeated three times for robustness. To evaluate the screening assay's performance, robust Z' values for each element were calculated using **Equation 4.1** and depicted in **Figure 4.3 D**. For phenotypic screening, an excellent value falls between 0.5 and 1.0, acceptability is within the range of 0 to 0.5, and values below 0 are considered unacceptable. Remarkably, all the robust Z' values obtained in this study exceed 0.5.

The high-content screen model was employed to screen a total of 800 natural product extracts and 200 natural compounds. Thirteen 96-well plates (labelled as CB01-CB10 for natural compounds and NC01-NC03 for natural product extracts) were utilized for this purpose. As mentioned earlier, the luminescence, GFP, and OD_{600} values of each screening plate were measured. **Figure 4.4 A** presents representative heatmap results from one of the 96-well screening plates. These heatmaps provide a clear and intuitive visualization of the effects of certain small molecules on bacterial growth (bioluminescence) and c-di-GMP levels (GFP). The heatmap color scale ranges from hot (red) to cold (blue), indicating low to high luminescent/GFP values, respectively. Lower bioluminescence or GFP values compared to the negative control signify inhibition of growth or c-di-GMP levels, while higher values indicate promotion of growth or c-di-GMP levels.

The robust Z' values for all the screening plates were calculated using Equation 4.1 and are illustrated in **Figure 4.4 B**. Notably, all the values fall within the range of 0.75 to 0.97, indicating that all the screening plates yielded high-quality and excellent assay results. Consequently, all the plate results are deemed acceptable. These robust Z' values ensure the obtained data from this experiment possess high reliability and are suitable for subsequent analysis.

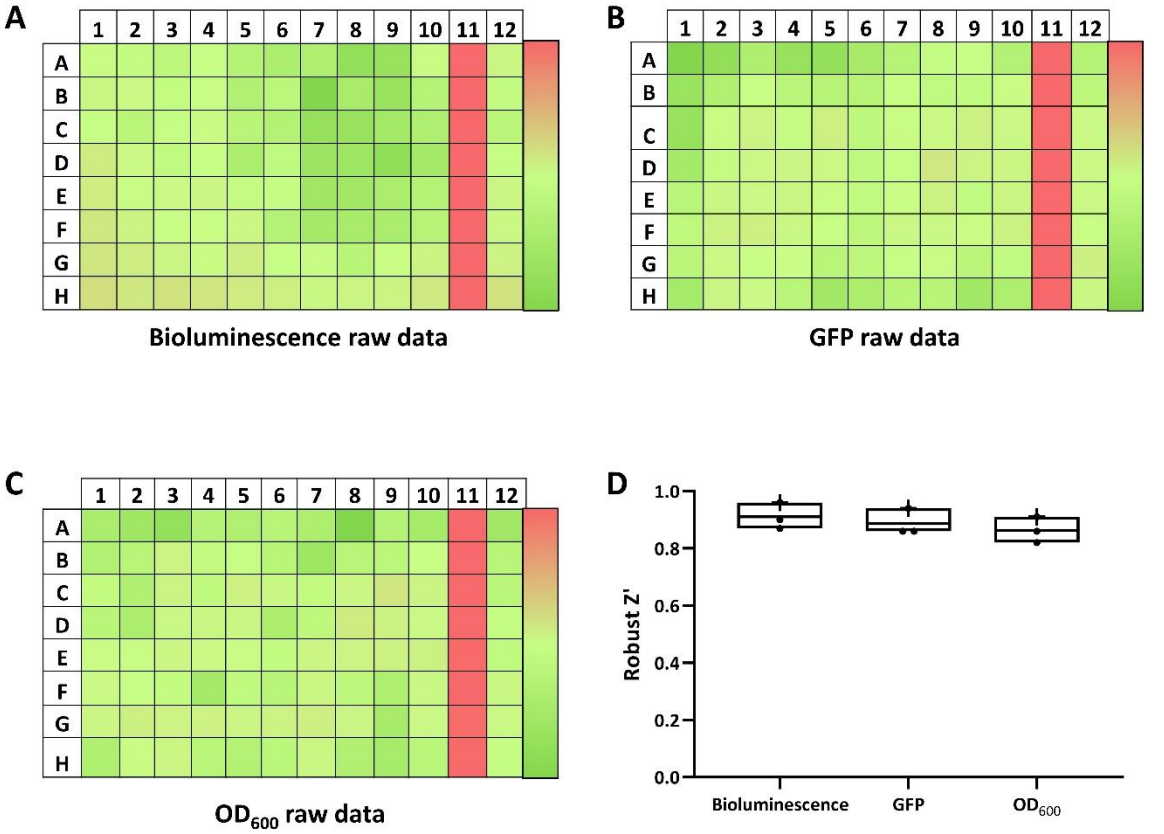

Figure 4.3 Heatmap results for 96-well screening plate assays test. A colour gradient heat map, with hot (Red: positive control) to cool (Green: negative control) colours indicating low to high values, has been applied to the well values. For test assay, there are no small molecules test. The heatmap of A, B and C show the representative raw data of bioluminescence, GFP and OD_{600} respectively for a 96-well plate. D show the robust Z' 3 times repeat test for the assay. The value of robust Z' greater than or equal to 0.5 is considered as an excellent assay, between 0.5-1.0 is considered as a marginal assay.

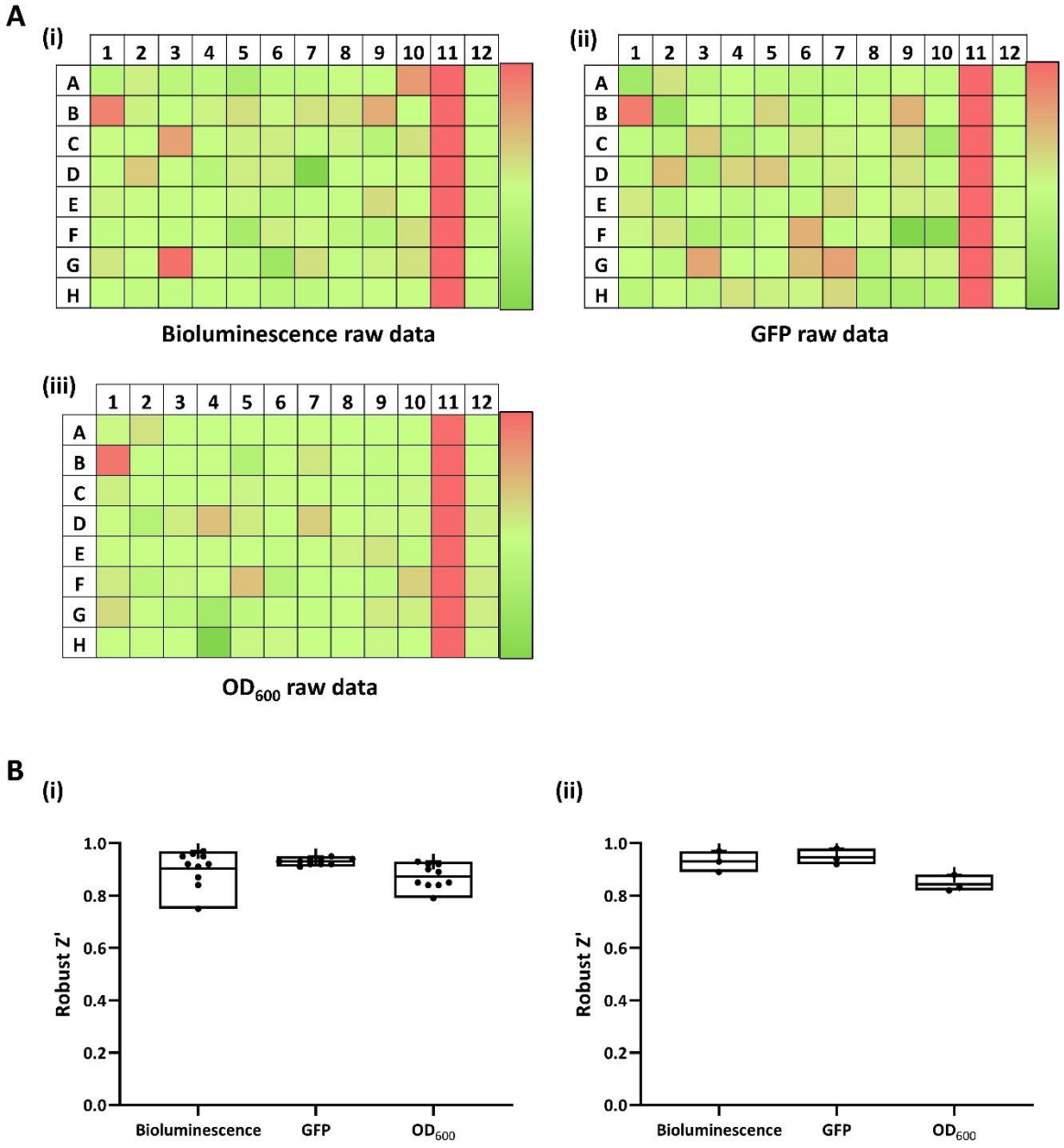

Figure 4.4 A: Representative heatmap results for one 96-well screening plate. The representative results for the bacterial cell based. A colour gradient heat map, with hot (Red: Lux=11000, GFP=200000 or OD600=0.1) to cool (Green: Lux=60, GFP=42000 or OD600= 3) colours indicating low to high values, has been applied to the well values. B: Robust Z' calculated for assays validation from the bacterial cell-based and Assay quality. Using natural product extraction (i) and natural compound (ii) and libraries.

4.4.2.2 Hits from the first screen with an impact on bacterial growth.

The HST workflow provides an effective means of visualizing the processed data through an interactive table linked to a scatter plot. To identify hit compounds, a Z-score threshold of ±2 has been carefully chosen. By utilizing the colour manager, hit compounds and non-hit compounds are assigned specific colours, enhancing the clarity of the scatter chart. In **Figure 4.5**, the hit compounds are denoted by red dots, enabling easy identification and analysis.

Based on the obtained analytical data, we discovered that 17 natural compounds have a discernible impact on the growth of *P. aeruginosa*. Among these compounds (**Appendix D 1.1**), 4 of them exhibit potential as promoters, effectively stimulating bacterial growth. On the other hand, 13 compounds demonstrate inhibitory effects, impeding the growth of *P. aeruginosa*. Notably, during the screening process, we identified 6 antibiotics, including well-known ones like chloramphenicol and erythromycin. The natural product extracts were divided into two distinct libraries based on the extraction methods employed: polar (aqueous) and non-polar (dichloromethane) solvent extracts. Among the polar solvent extracts, a total of 19 extracts were found to promote the growth of *P. aeruginosa*, providing potential candidates for further investigation. In the case of the non-polar solvent extracts, 9 extracts demonstrated the ability to enhance the growth of *P. aeruginosa*, while 10 extracts exhibited inhibitory effects, effectively impeding bacterial growth (**Appendix D 1.2**).

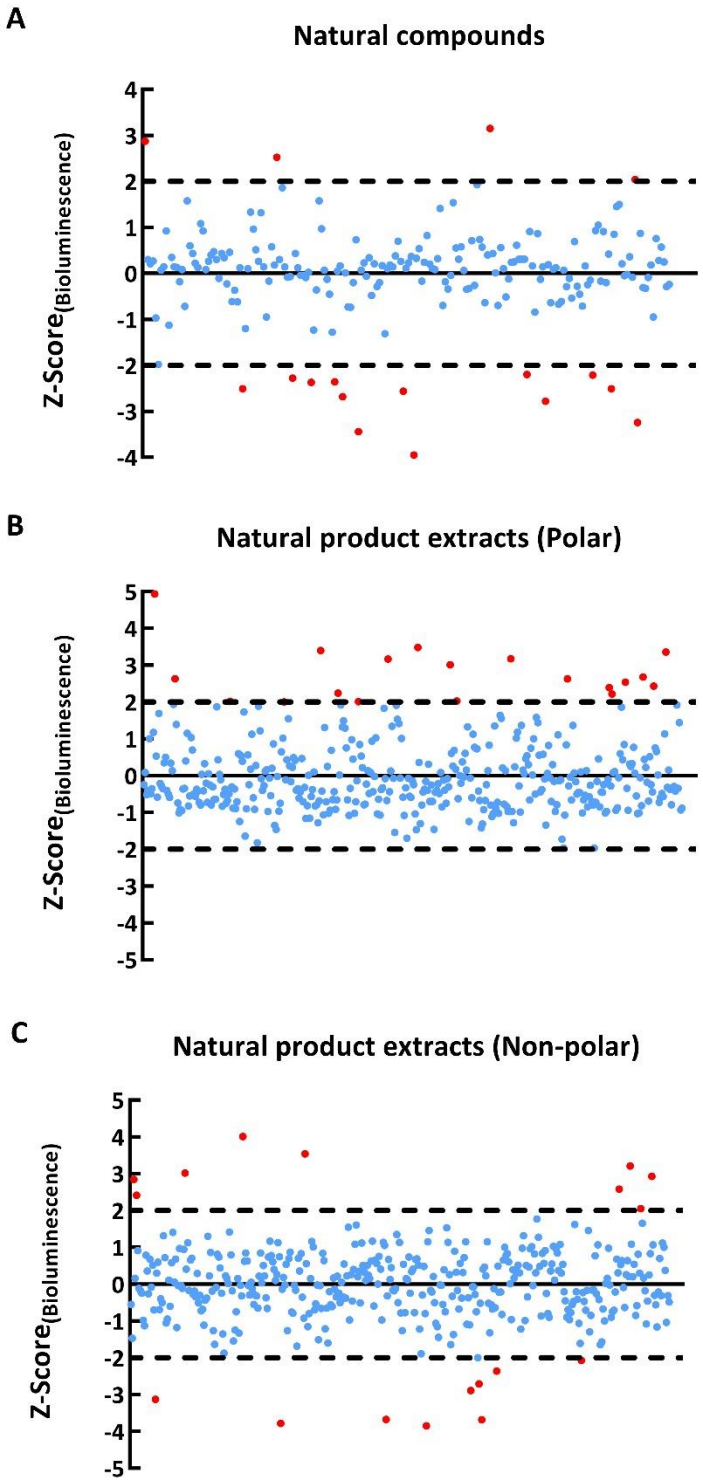

Figure 4.5 Scatter plot by the value of Z-score from bacterial cell-based screen. The natural compounds and natural product extracts (polar and non-polar) Z-score value (Bioluminescence) are for (A) Natural compounds. (B) Natural product extracts (polar). (C) Natural product extracts (non-polar). For all scatter plot, the cut-off threshold is ±2, red plots represent hit compounds or extracts selected by threshold. Blue plots represent non-hit compounds or extracts within the selected threshold.

4.4.2.3 Hits from the first screen influences c-di-GMP signalling.

To identify small molecules capable of modulating c-di-GMP levels, we employed **Equation 4.2** to calculate the inhibition rate. The GFP values were normalized to bioluminescence, allowing us to select specific c-di-GMP levels for regulation without influencing bacterial growth. The inhibition percentage was calculated using **Equation 4.2**, and the resulting inhibition data were visualized in a scatter plot (**Figure 4.6**). A +50% cut-off was applied to determine hit small molecules, which are represented by red dots in the plot. These potential hits indicate their potential ability to regulate intracellular c-di-GMP levels.

From the measurement results, we were able to identify target small molecules, in terms of c-di-GMP modulation, 8 compounds demonstrated inhibitory effects on c-di-GMP, with 4 of them not significantly impacting the growth of *P. aeruginosa* (**Appendix D.1.3**). This suggests that these specific compounds may have the ability to regulate c-di-GMP levels without adversely affecting bacterial growth. Similarly, the natural product extracts were categorized into polar (aqueous) and non-polar (dichloromethane) solvent extract libraries based on the extraction methods employed. Among the polar solvent extracts, 74 extracts displayed inhibitory effects on c-di-GMP, out of which 56 extracts did not significantly affect the growth of *P. aeruginosa*. In the case of non-polar solvent extracts, 4 extracts exhibited potential inhibition of c-di-GMP, with 2 of them having no effect on bacterial growth (**Appendix D.1.4**).

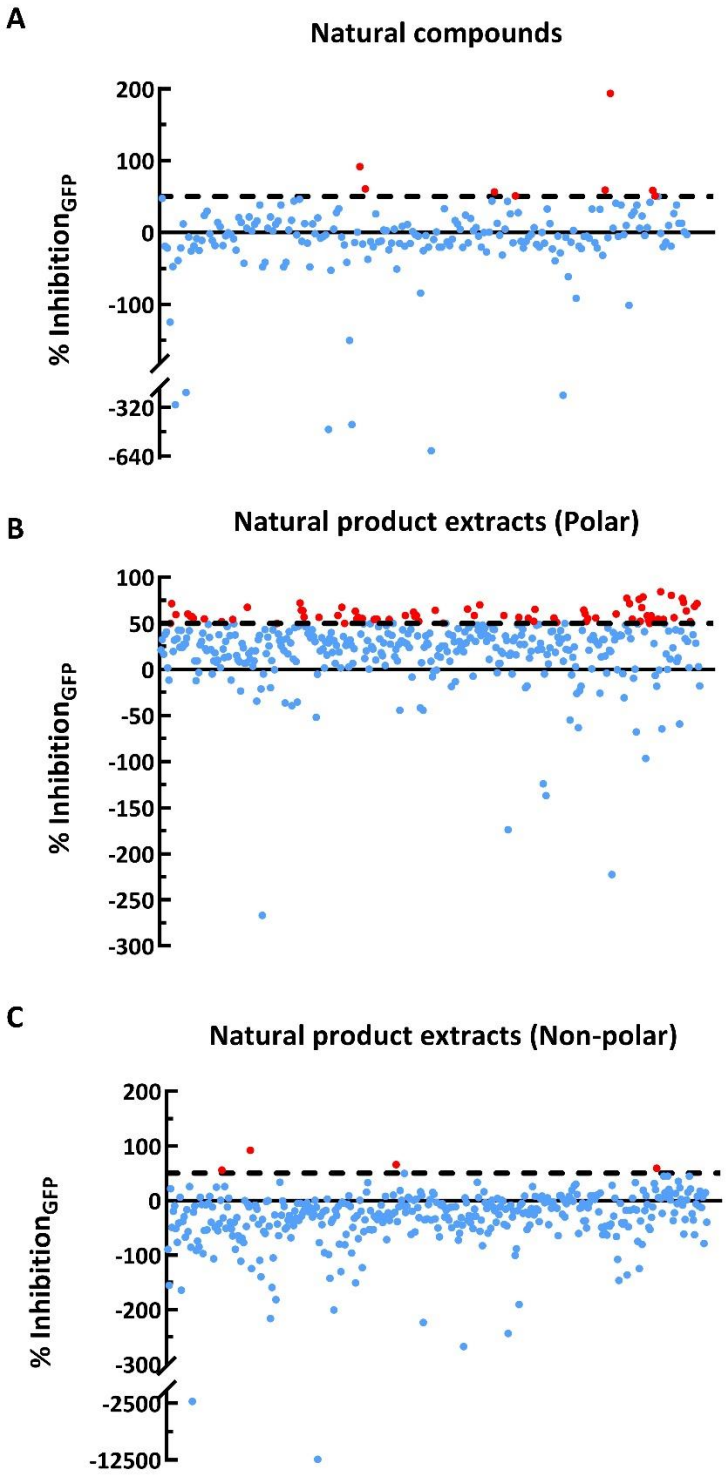

Figure 4.6 Scatter plot by the value of %inhibition of GFP from bacterial cell-based screen. The %inhibition GFP value of all natural compounds and natural product extracts (polar and non-polar) have been calculated. (A) Natural compounds. (B) Natural product extracts (polar). (C) Natural product extracts (non-polar). For all scatter plot, the cut-off threshold is +50%, red plots represent hit compounds or extracts selected by threshold. Blue plots represent non-hit compounds or extracts within the selected threshold.

4.4.2.4 Hit compounds confirmed by dose responds and the effect on biofilm formation.

When completing the screening and analysis of all natural product extracts and natural compounds, we proceeded to design additional experiments to investigate potential hits from the natural compound library. Specifically, we focused on compounds that exhibited inhibition of c-di-GMP levels without significantly affecting the growth of *P. aeruginosa*. In accordance with these criteria, four compounds were selected, which are listed in **Table 4.2**.

To further evaluate the selected hit compounds, we conducted a 10-point dose-response assay with a maximum concentration of 2 mM and a two-fold dilution series. By analysing the dose-response curves, we calculated the IC_{50} values, which indicate the concentration at which the compounds exert 50% inhibition. Notably, three of the compounds, namely myricetin, resveratrol, and ellagic acid, displayed a significant trend in their inhibition rates relative to the concentration. **Figure 4.7** illustrates the fitting of a four-parameter logistic function to the data (**Appendix D.1.5**), allowing us to determine the IC50 values for each compound. Myricetin, resveratrol, and ellagic acid, identified as potential hits from the bacterial cell-based screen, exhibited IC_{50} values of 320 µM, 210 µM, and 11 µM, respectively. These findings highlight the concentration at which these compounds are effective in inhibiting c-di-GMP levels as measured by the $\%Inhibition_{GFP}$.

Table 4.2 "Hits" list selected by bacterial cell-based screen model.

NC Name	MWt	$\%Inhibition_{GFP}$ (normalized lux)	$Z\text{-}score_{lux}$
Myricetin	302.24	50.9%	-0.699
Magnolol	266.32	56.3%	1.930
Resveratrol	228.24	59.0%	-0.254
Ellagic acid	302.19	60.6%	-0.729

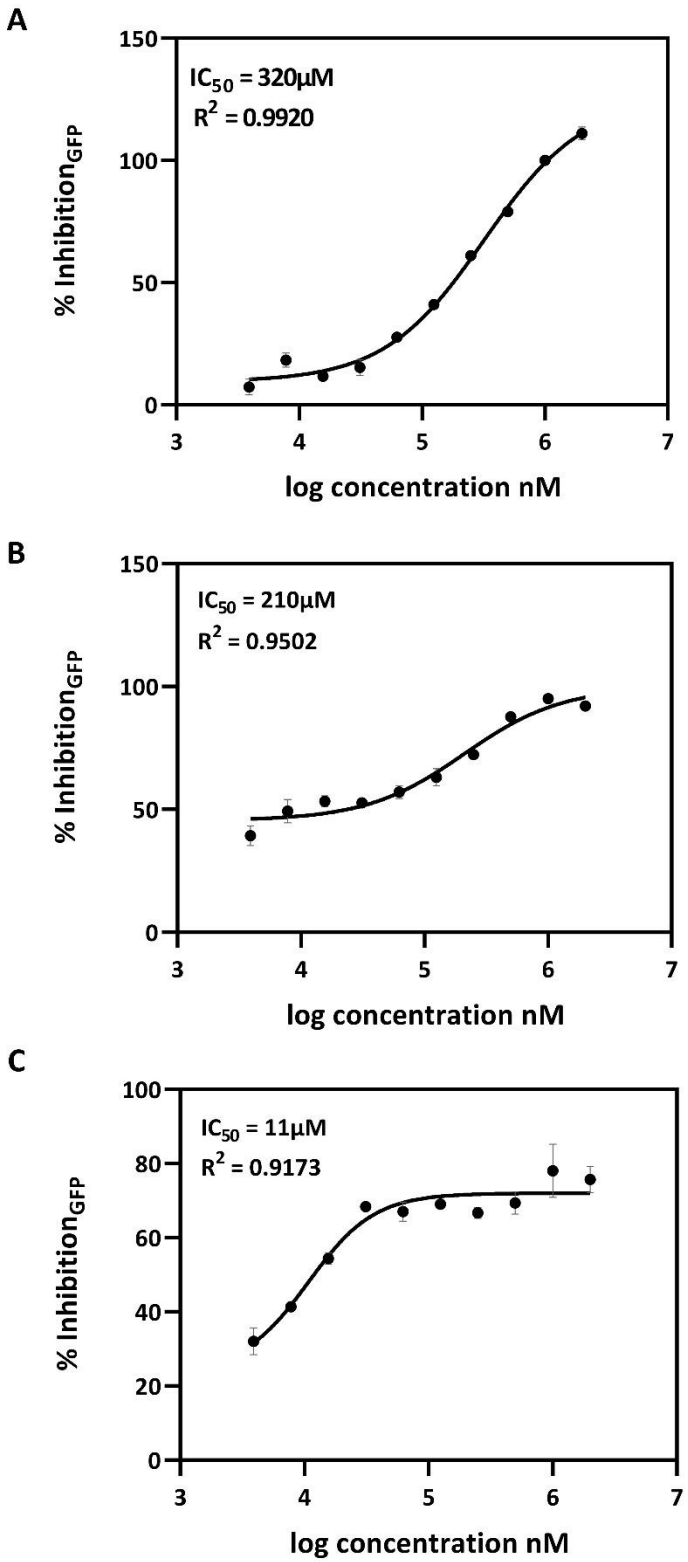

Figure 4.7 Representative results from a dose - response assay. Three compounds (potential c-di-GMP inhibitors: A: myricetin, B: resveratrol and C: ellagic acid) identified from previous screens are further tested in a 10-point dose-response assay with a top concentration of 2 mM and two-fold dilution series. Fitting a four-parameter logistic function to the data yielded IC_{50} values of 320 µM, 210 µM and 11 µM respectively.

We identified three natural compounds, myricetin, resveratrol, and ellagic acid, which exhibited conditional trends in dose-response on *P. aeruginosa* c-di-GMP level. To further validate the inhibitory effects of these compounds, we examined confocal imaging to visualize their effects on biofilm formation. As shown in **Figure 4.8 A(i)**, **B(i)**, and **C(i)**, representative images were taken for each group, including a wild-type control with PA14 bacteria only, a group treated with TB, a group treated with TB and compound, and a group treated with compound only. Binding of each of the hits to the antibiotic TB significantly inhibited biofilm formation compared to the TB control, with no significant changes observed compared to the wild-type control only.

To calculate biofilm biomass, we quantified the 3D biofilm images using IMARIS software (**Appendix D.1.6**). The live/total biovolume values (**Figure 4.8 A(ii), B(ii),** and **C(ii)**) showed a significant reduction in biofilm biovolume for each compound after antibiotic TB as well as compound and TB combination treatment, with the combined effect being more pronounced. The total biovolume (**Figure 4.8 A(iii)** and **B(iii)**) for myricetin and resveratrol showed the same trend. However, it is noteworthy that the total biovolume of ellagic acid was higher under the combined treatment than after antibiotics and ellagic acid alone (**Figure 4.8 C(iii)**). Overall, these results suggest that myricetin and resveratrol may be potential compounds for inhibiting *Pseudomonas aeruginosa* biofilm formation, while the effect of ellagic acid may be more complex and require further investigation. Further studies are needed to fully understand the mechanisms behind these effects and to explore the potential clinical applications of these compounds as treatments for *P. aeruginosa* infections.

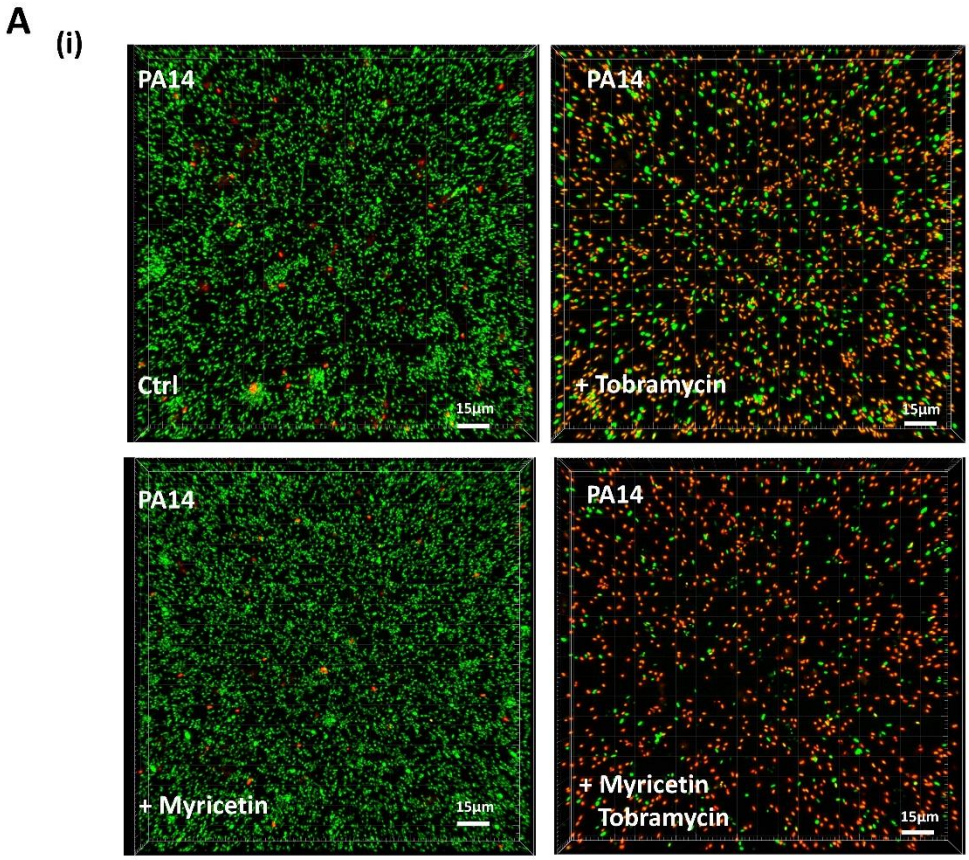
A
(i)
PA14
Ctrl
15µm
PA14
+ Tobramycin
15µm
PA14
+ Myricetin
15µm
PA14
+ Myricetin
Tobramycin
15µm

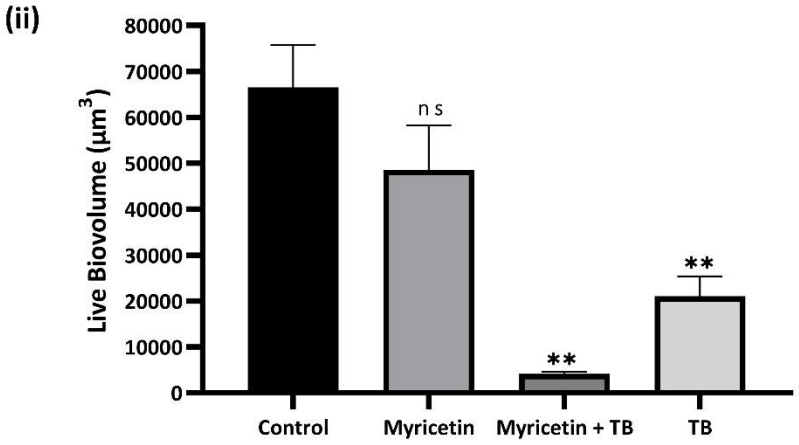
(ii)
Live Biovolume (µm3)
80000
70000
60000
50000
40000
30000
20000
10000
0
n s
**
**
Control
Myricetin
Myricetin + TB
TB

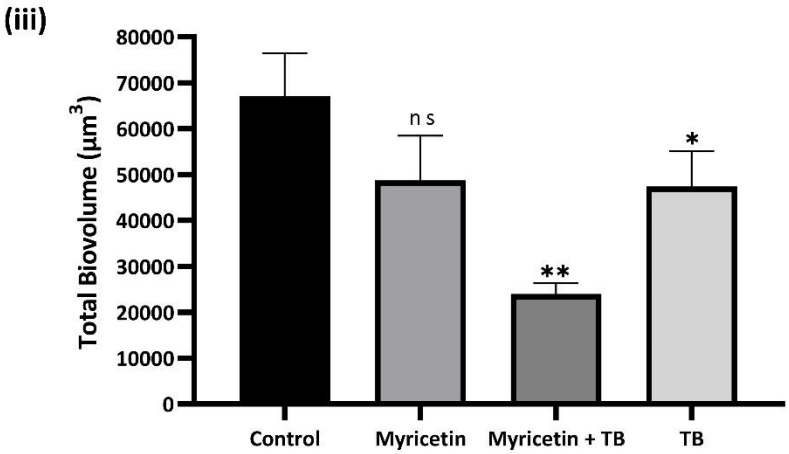
(iii)
Total Biovolume (µm3)
80000
70000
60000
50000
40000
30000
20000
10000
0
n s
**
*
Control
Myricetin
Myricetin + TB
TB

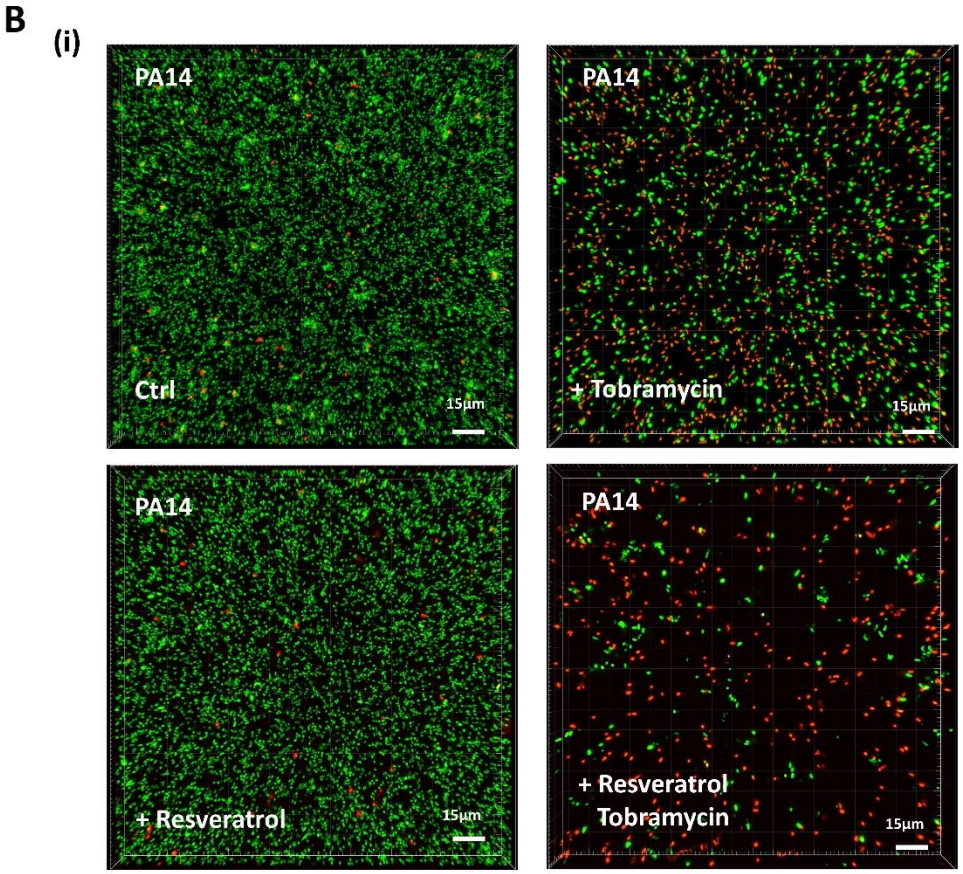
B
(i)
PA14
Ctrl
15µm
PA14
+ Tobramycin
15µm
PA14
+ Resveratrol
15µm
PA14
+ Resveratrol
Tobramycin
15µm

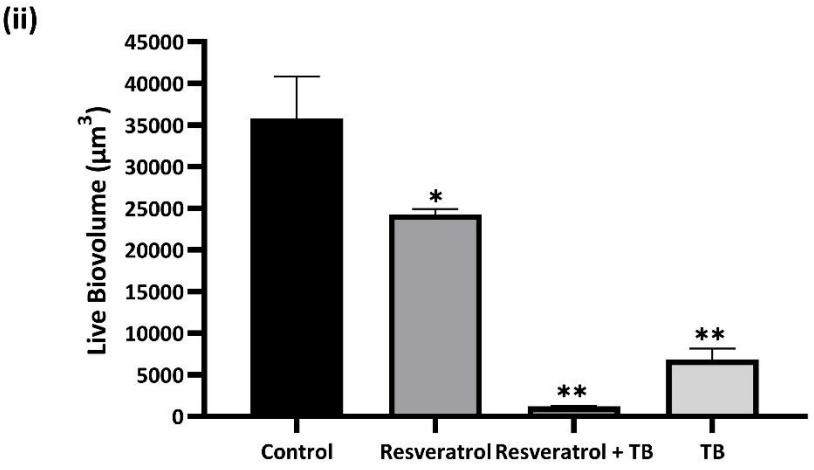
(ii)
Live Biovolume (µm3)
45000
40000
35000
30000
25000
20000
15000
10000
5000
0
*
**
**
Control
Resveratrol
Resveratrol + TB
TB

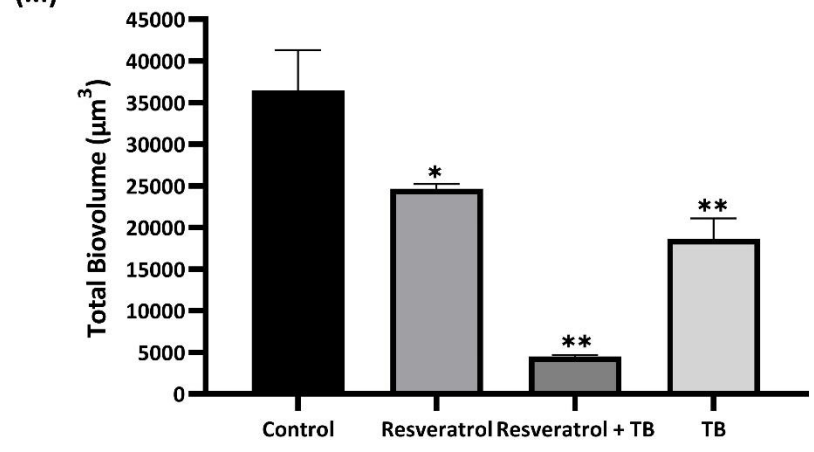
(iii)
Total Biovolume (µm3)
45000
40000
35000
30000
25000
20000
15000
10000
5000
0
*
**
**
Control
Resveratrol
Resveratrol + TB
TB

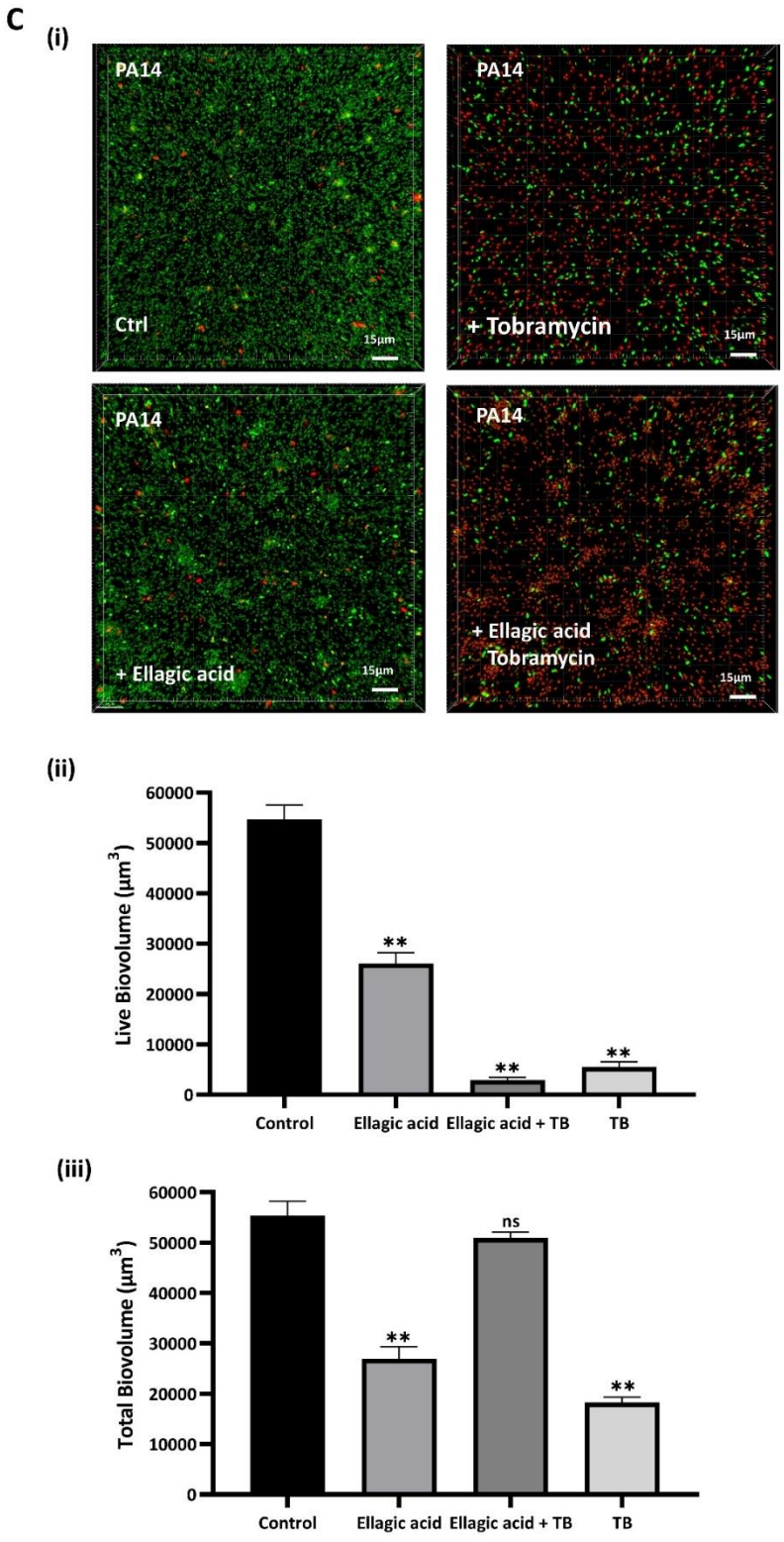

Figure 4.8 Representative results from a confocal imaging and the Biovolume of each test. Three compounds (potential c-di-GMP inhibitors: A: myricetin, B: resveratrol and C: ellagic acid) identified from previous screens are further tested in a confocal imaging. (i) Representative imaging for each compound with four groups of control, TB, compound, and TB+ compound. (ii) Live biovolume and (iii) total biovolume. (*$p < 0.05$; **$p < 0.01$).

4.4.3 Development of a high content co-culture cell-based screen

The human bronchial epithelial cell-based co-culture with *P. aeruginosa* was used to screen small molecules for inhibition of virulence (measured as loss of cytotoxicity to human cells), modulation of the cellular c-di-GMP level and inhibition of bacterial growth (**Figure 4.9A)**. The *P. aeruginosa* PA14-*lux* (pCdrA::*gfp*^{C}) constructed as described in section 4.3.1 was inoculated into plates seeded with 16HBE cells together with test compounds, tobramycin (a positive control) or DMSO (a negative control), according to the layout shown in **Figure 4.9B**. After infection, read the GFP, Bioluminescence, OD_{600} first, then collect the supernatant of each well evenly, and perform the LDH cytotoxicity experiment in a new 96-well plate according to the same layout and read the value. The output data show the value of the OD_{600} for bacterial was affected by the 16HBE cells, so we used the bioluminescence value to exhibit the growth ability.

A

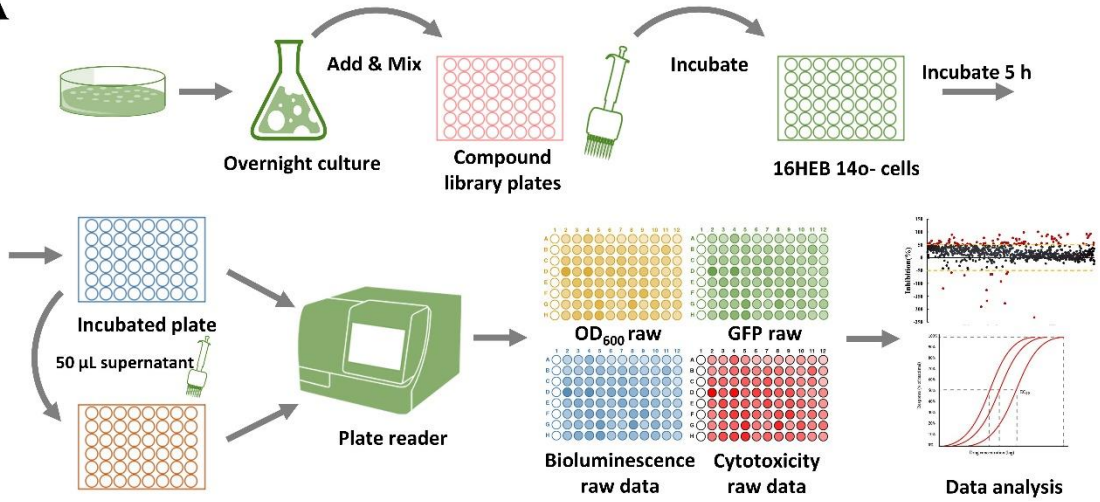

B

	1	2	3	4	5	6	7	8	9	10	11	12
A												
B												
C												
D												
E												
F												
G												
H												

Figure 4.9 The co-culture human epithelial cell-based screen assay setup. (A) The bacterial colonies of *P. aeruginosa* were grown overnight in the LB starter culture. Use cell culture medium to resuspend the bacterial and diluting to the required concentration, inoculate bacteria, small molecules, and control group with the 96-well plate which already have human epithelial cells evenly attached to the bottom of each well. The plate was incubated for 1 hour, and then change all supernatant to cell culture medium, and incubate further 3.5 hours, then the OD_{600}, bioluminescence, and GFP values were measured. The supernatant will be used for cytotoxicity testing, using these readings, compounds that affect cytotoxicity levels can be identified. (B) A 96-well plate containing with 16HEB 14o- cell layout. XXX

4.4.3.1 Quality control of the assay.

The quality of the co-culture high-content screen model has been thoroughly validated. **Figure 4.10 (A, B,** and **C)** presents representative heatmap results for the 96-well screening plate assays, and this validation test was repeated three times. Assay quality is measured by Robust Z'. An excellent range for phenotypic screening is between 0.5 and 1.0, while values between 0 and 0.5 are considered acceptable. Values below 0 are deemed unacceptable. The robust Z' values for bioluminescent, red cytotoxicity and GFP are calculated according to the formula provided in Material & Methods (**Figure 4.10D**). (Here only positive/negative controls are used for Robust Z' calculation- 3 replicates). As they are all above 0.5 (average 0.96, 0.87 and 0.66 respectively) **Figure 4.10D**, the assay quality was deemed robust.

A total of 800 natural product extracts and 200 natural compounds were screened using this model, utilizing a total of 13 96-well plates (Natural compound: NC01-NC03, natural product extract: CB01-CB10). **Figure 4.11A** presents representative heatmap results for one of the 96-well screening plates. It is evident and visually apparent that some of these small molecules have an impact on bacterial growth (bioluminescence), c-di-GMP levels (GFP), and virulence (cytotoxicity). The heatmap illustrates a colour change from hot (red) to cold (blue), indicating the range of bioluminescent/GFP/%Cytotoxicity values from low to high, which can be interpreted as meaningful. In comparison to the negative control, lower bioluminescent/GFP/%Cytotoxicity values signify inhibition of growth or c-di-GMP levels, respectively, while higher values indicate promotion of growth, c-di-GMP levels, or %Cytotoxicity, respectively.

To assess the quality of each screening plate, robust Z' values were calculated using **Equation 4.1**, as shown in **Figure 4.11B**. Robust z' values were calculated to determine the assay's response

window for bioluminescent, GFP, and %Cytotoxicity measurements. The average values obtained were 0.82, 0.72, and 0.53, respectively (**Figure 4.11B**). These values demonstrate the reliability and consistency of the screening procedure. Based on the robust quality of the assay, we proceeded to further analyse the acquired data.

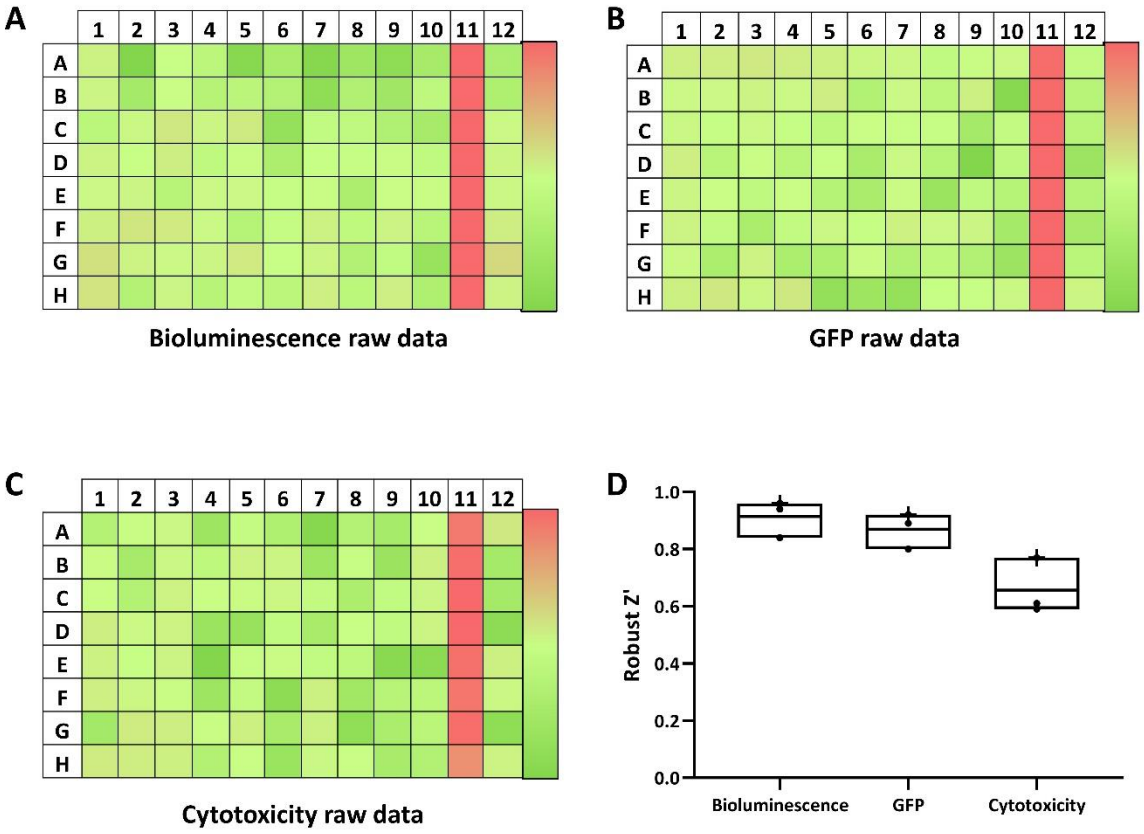

Figure 4.10 Heatmap results for 96-well screening plate assays test. A colour gradient heat map, with hot (Red: positive control) to cool (Green: negative control) colours indicating low to high values, has been applied to the well values. For test assay, there are no small molecules test. Assay quality. The value of robust Z' greater than or equal to 0.5 is considered as an excellent assay, between 0.5-1.0 is considered as a marginal assay.

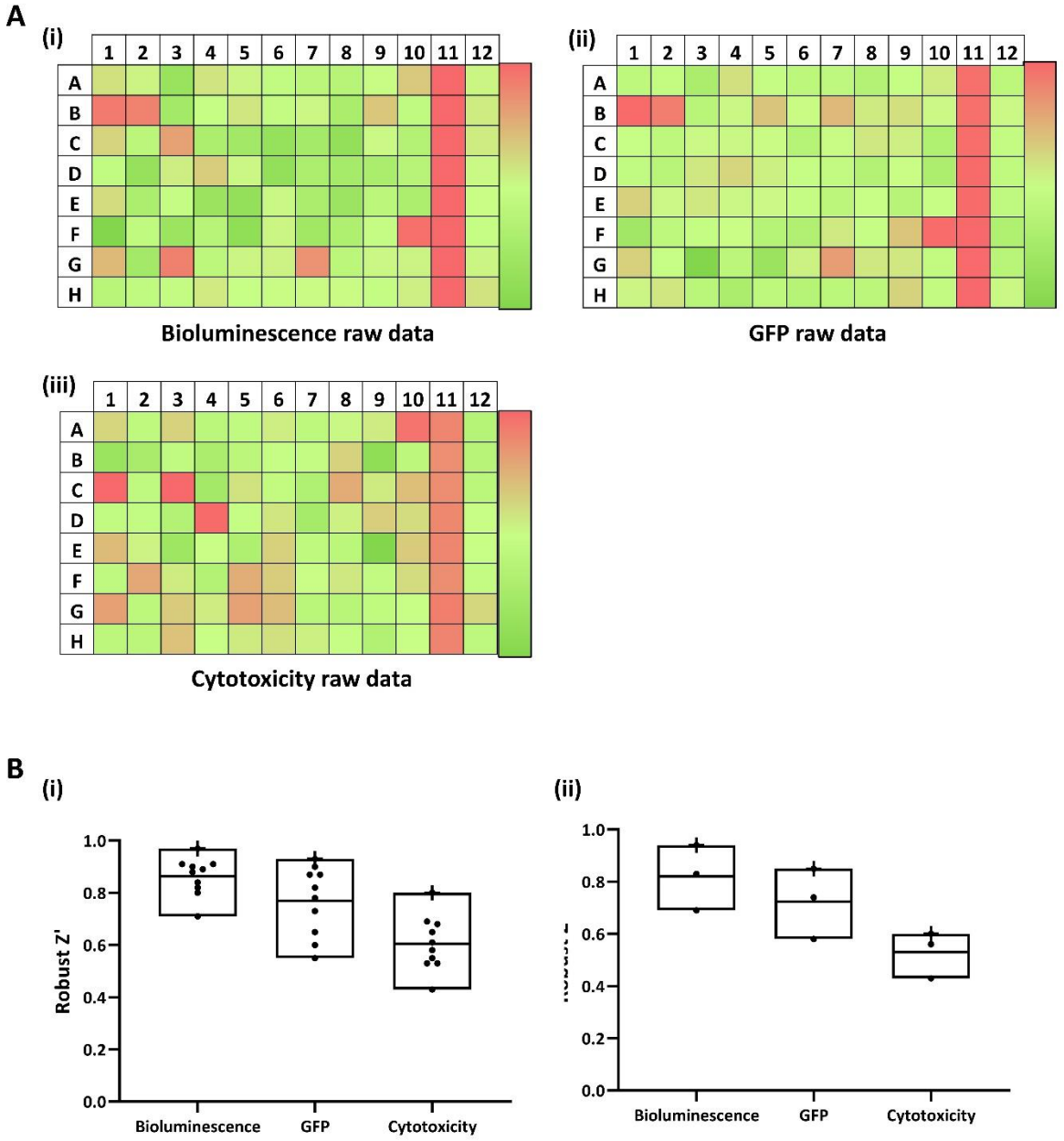

Figure 4.11 Representative heatmap results for one 96-well screening plate and the quality validation. (A) The representative results for the human bronchial epithelial cell based. A colour gradient heat map, with hot (Red: Lux=15000, GFP= 250000, Cytotoxicity= 250000) to cool (Lux=50, GFP=49000 or Cytotoxicity= 23000) colours indicating low to high values, has been applied to the well values. (B) Robust Z' calculated for assays validation from the bacterial cell-based and Assay quality. Using Puretitre natural compound and natural product extraction libraries.

4.4.3.2 Initial screening to identify compounds that effect on bacterial growth.

Similar to the bacterial cell-based screen, a Z-score threshold of ±2 has been selected to identify hit compounds. The results, presented in **Figure 4.12**, reveal that 16 different natural compounds have an impact on the growth of *P. aeruginosa* (**Appendix D.1.7**). Among these compounds, one shows potential as a growth promoter, while 15 compounds inhibit the growth of *P. aeruginosa* (**Figure 4.12A**). Notably, erythromycin and doxycycline hyclate, which are antibiotics that have already been discovered, are among the compounds exhibiting growth inhibition effects.

Regarding polar solvent extracts, two kinds of extracts promote the growth of *P. aeruginosa*, while 16 polar solvent extracts demonstrate potential as growth inhibitors (**Figure 4.12B**). As for non-polar solvent extracts, four types of extracts promote the growth of *P. aeruginosa*, whereas 14 kinds of extracts inhibit its growth (**Figure 4.12C**) (**Appendix D.1.8**).

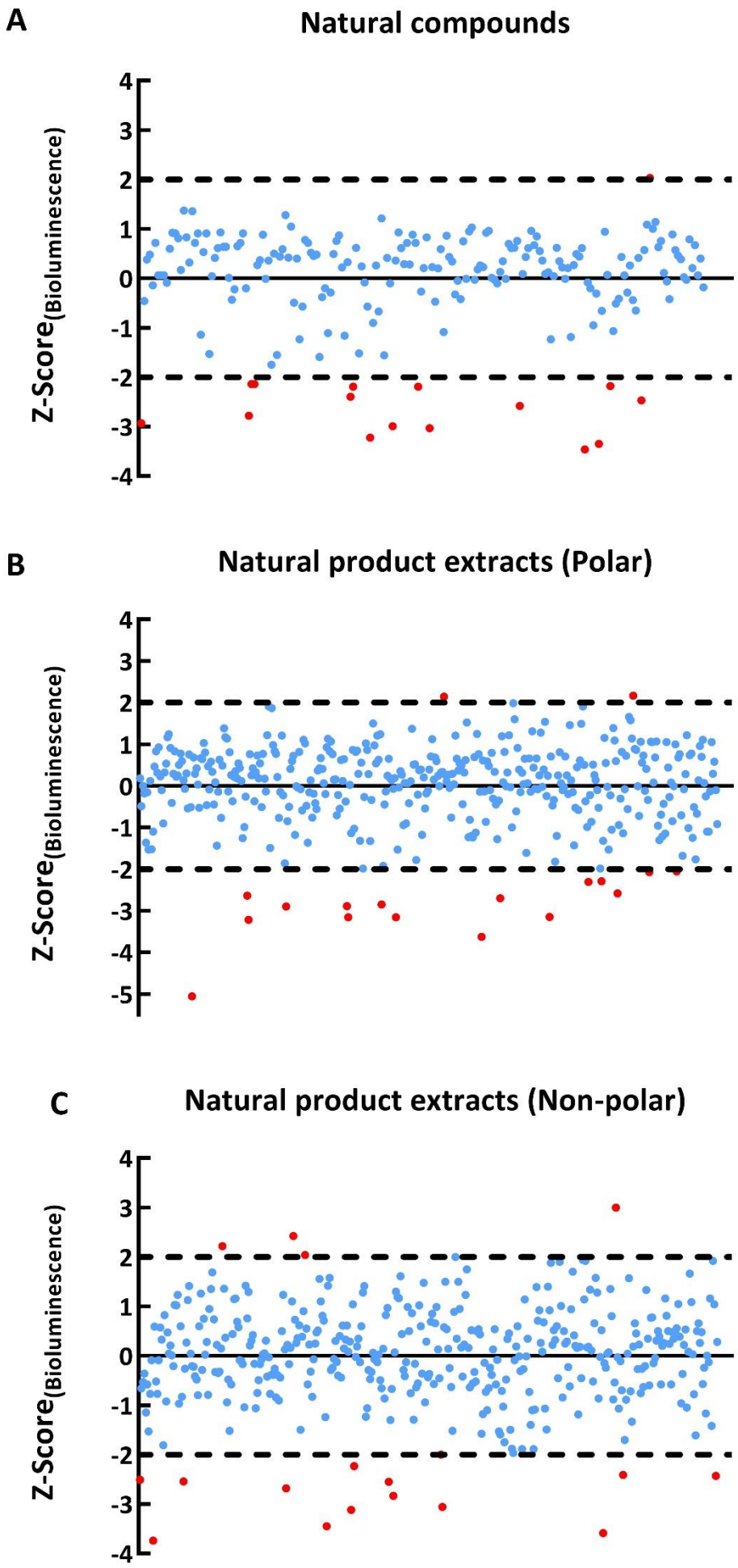
A
Natural compounds
Z-Score(Bioluminescence)
4
3
2
1
0
-1
-2
-3
-4
B
Natural product extracts (Polar)
Z-Score(Bioluminescence)
4
3
2
1
0
-1
-2
-3
-4
-5
C
Natural product extracts (Non-polar)
Z-Score(Bioluminescence)
4
3
2
1
0
-1
-2
-3
-4

Figure 4.12 Scatter plot by the value of Z-score from bacterial cell-based screen. The natural compounds and natural product extracts (polar and non-polar) Z-score value (Bioluminescence) are for (A) Natural compounds. (B) Natural product extracts (polar). (C) Natural product extracts (non-polar). For all scatter plot, the cut-off threshold is ±2, red plots represent hit compounds or extracts selected by threshold. Blue plots represent non-hit compounds or extracts within the selected threshold.

4.4.3.3 Initial screening to identify compounds that modulate the c-di-GMP level.

The % inhibition of intracellular c-di-GMP level (GFP) are calculated by the formulae provided in **Equation 4.2**. All GFP values were normalized to bioluminescence to ensure that the selection of compounds regulating c-di-GMP levels with limit effect on bacterial growth. Scatter plots of these values from individual wells are depicted in **Figure 4.13**. A ±50% cut-off was applied to identify potential hit small molecules, which are denoted by red dots. From the measurement results, target small molecules can be selected, and the hits (red plots) identified in **Figure 4.13** may possess the ability to regulate intracellular c-di-GMP levels.

Regarding c-di-GMP levels, 11 compounds were found to promote c-di-GMP, out of which 7 did not significantly affect the growth of *P. aeruginosa* (**Appendix D.1.9**). Additionally, 7 compounds were observed to inhibit c-di-GMP, with 4 of them having no significant impact on the growth of *P. aeruginosa* (**Figure 4.13A**). The natural product extracts were categorized into polar (aqueous), and non-polar (dichloromethane) solvent extract libraries based on the different extraction methods employed. For polar solvent extracts, 78 extracts were found to promote c-di-GMP, with 67 of them having no significant effect on the growth of *P. aeruginosa* (**Figure 4.13B**). On the other hand, 4 extracts were observed to inhibit c-di-GMP while not significantly affecting bacterial growth. In the case of non-polar solvent extracts, 49 extracts were found to promote c-di-GMP, and out of these, 38 had no effect on bacterial growth. On the other hand, one extracts were observed to inhibit c-di-GMP while not significantly affecting bacterial growth. (**Figure 4.13C**) (**Appendix D.1.10**).

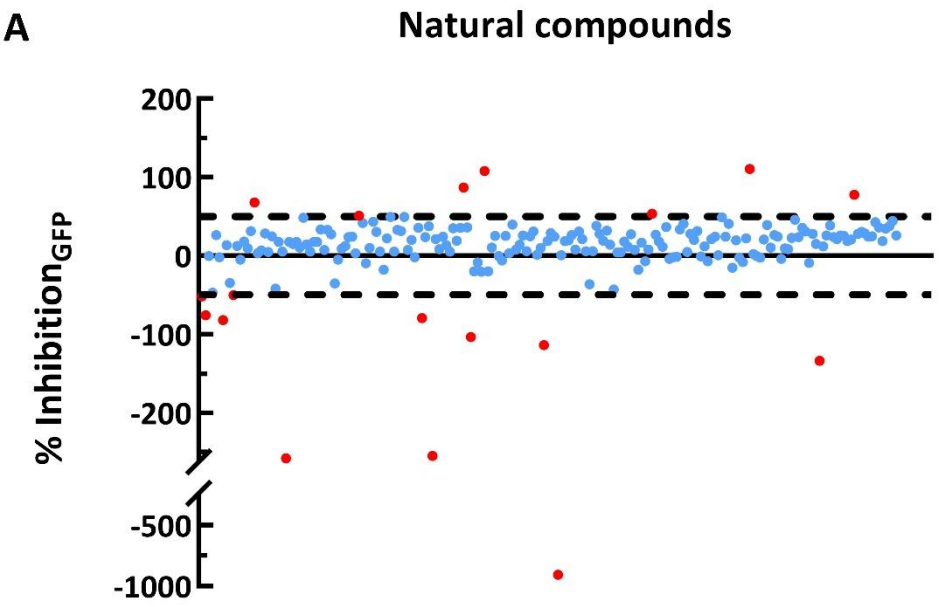
A
Natural compounds
% Inhibition GFP
200
100
0
-100
-200
-500
-1000

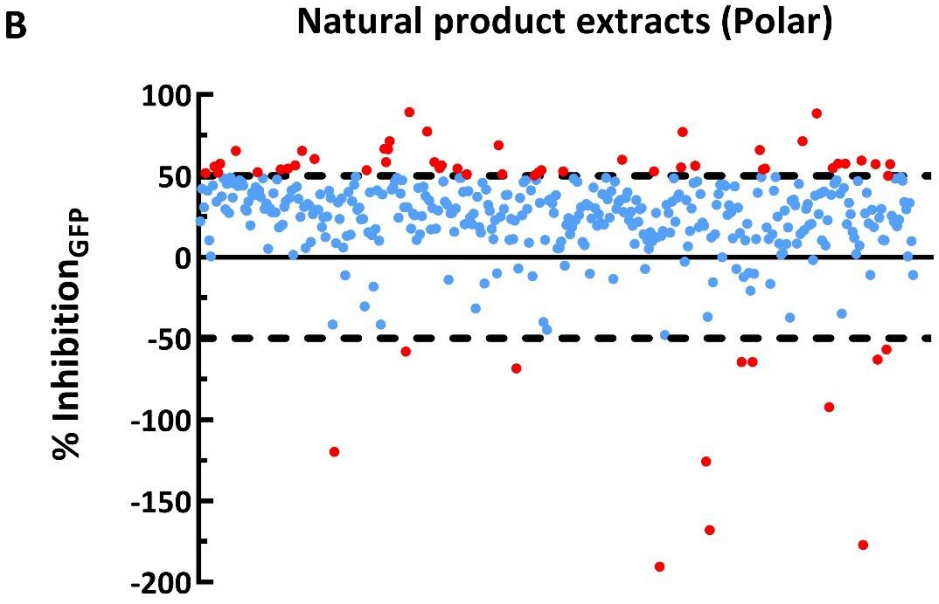
B
Natural product extracts (Polar)
% Inhibition GFP
100
50
0
-50
-100
-150
-200

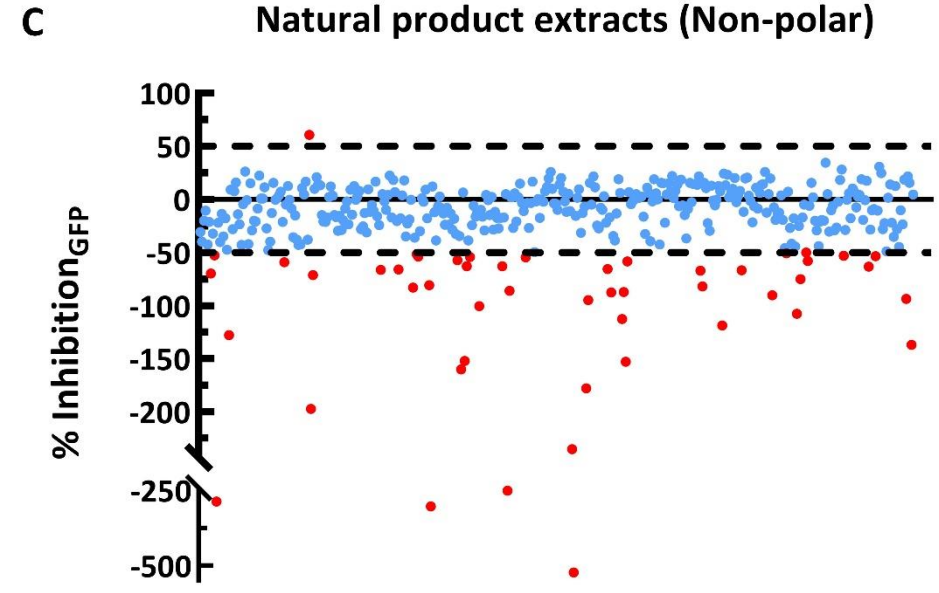
C
Natural product extracts (Non-polar)
% Inhibition GFP
100
50
0
-50
-100
-150
-200
-250
-500

Figure 4.13 Scatter plot by the value of %inhibition of GFP from co-culture human bronchial epithelial cell-based screen. The $\%inhibition_{GFP}$ value of all natural compounds and natural product extracts (polar and non-polar) have been calculated. (A) Natural compounds. (B) Natural product extracts (polar). (C) Natural product extracts (non-polar). For all scatter plot, the cut-off threshold is ±50%, red plots represent hit compounds or extracts selected by threshold. Blue plots represent non-hit compounds or extracts within the selected threshold.

4.4.3.4 Initial screening to identify compounds that inhibit cytotoxicity during infection.

To enhance the screening process and capture a more comprehensive understanding, this study introduced a co-culture human bronchial epithelial cell-based model. By incorporating tool strains in combination with the co-culture biofilm model, we aimed to identify potential small molecules that can effectively modulate the host response during infection. To evaluate the impact of these molecules, we performed cytotoxicity tests to assess the viability of human bronchial epithelial cells. To quantify %Cytotoxicity, we employed **Equation 2.1**. Subsequently, these values were normalized to the negative control to determine the percentage of inhibition of %cytotoxicity, employing **Equation 4.3**. The resulting inhibition data were then plotted on a scatter plot, represented as **Figure 4.14**. In order to identify hit small molecules, a cut-off of +50% was selected on the plot. Those compounds that surpassed this threshold were considered potential hit small molecules and were denoted as red dots on the scatter plot.

The hits highlighted in **Figure 4.14** exhibited potential in regulating co-culture cytotoxicity, suggesting their efficacy in countering the deleterious effects of infection. Specifically, the study found that 30 compounds demonstrated significant inhibition of cytotoxicity, indicating their potential as therapeutic candidates (**Figure 4.14A**) (**Appendix D.1.11**). Among these compounds, 26 did not display any adverse effects on bacterial growth, suggesting their specificity in targeting host response without impacting microbial proliferation. To further explore potential therapeutic sources, natural product extracts were divided into polar (aqueous) and non-polar (dichloromethane) solvent extracts libraries using distinct extraction methods. Within the polar solvent extracts, two compounds exhibited inhibition of cytotoxicity, with one of them not affecting bacterial growth (**Figure 4.14B**). In contrast, the non-polar solvent extracts demonstrated more extensive effects, with a total of 115 extracts displaying cytotoxicity inhibition. Among these, 109 extracts did not impact bacterial growth (**Figure 4.14C**) (**Appendix D.1.12**).

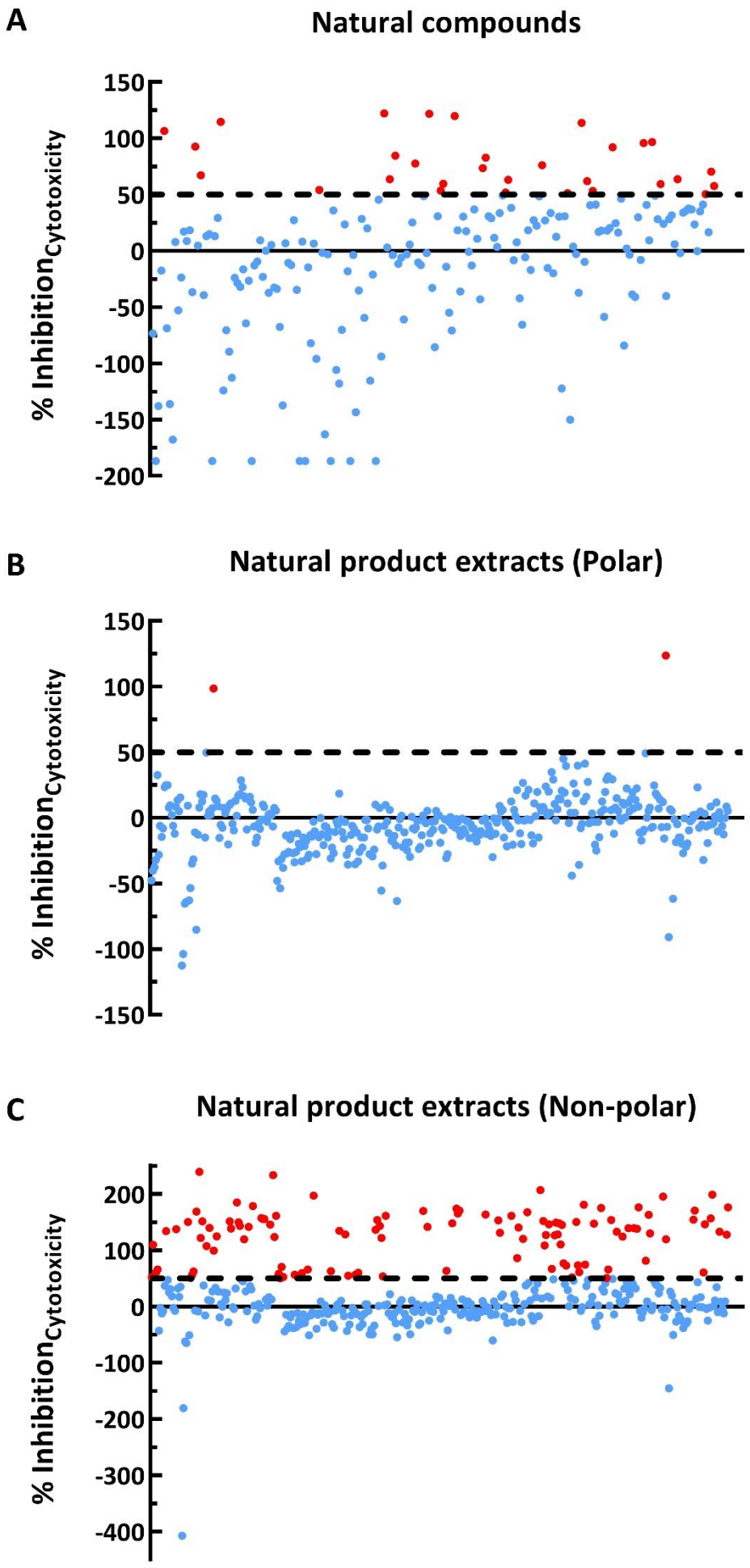
A
Natural compounds
% Inhibition Cytotoxicity
150
100
50
0
-50
-100
-150
-200
B
Natural product extracts (Polar)
% Inhibition Cytotoxicity
150
100
50
0
-50
-100
-150
C
Natural product extracts (Non-polar)
% Inhibition Cytotoxicity
200
100
0
-100
-200
-300
-400

Figure 4.14 Scatter plot by the value of %inhibition of cytotoxicity from co-culture human bronchial epithelial cell-based screen. The $\%inhibition_{cytotoxicity}$ value of all natural compounds and natural product extracts (polar and non-polar) have been calculated. (A) Natural compounds. (B) Natural product extracts (polar). (C) Natural product extracts (non-polar). For all scatter plot, the cut-off threshold is +50%, red plots represent hit compounds or extracts selected by threshold. Black points represent non-hit compounds or extracts within the selected threshold.

4.4.3.5 6,7-Dihydroxycoumarin as a potential inhibitor selected by second screen model.

In the co-culture human bronchial epithelial cell-based model screen, our objective was to identify compounds that could attenuate the virulence of *P. aeruginosa* on human airway epithelial cells during infection by influencing the bacteria's c-di-GMP level. Through careful analysis of the screening results and comparison of the hits identified by the three experimental groups, we discovered that only one out of the 200 natural compounds possessed this unique ability. This compound was identified as 6,7-Dihydroxycoumarin, which demonstrated the capacity to reduce both the c-di-GMP level and cytotoxicity, while exhibiting no discernible effect on bacterial growth.

Selected hit 6,7-Dihydroxycoumarin was further tested by **10-point** dose-response analysis with a top concentration of 2 mM and a two-fold dilution series (**Appendix D.1.13**). IC_{50} values were calculated from dose-response curves for 6,7-dihydroxycoumarin as 109 µM for inhibition of GFP levels and 207 µM for inhibition of cytotoxicity (**Figure 4.15A and B**, respectively).

A

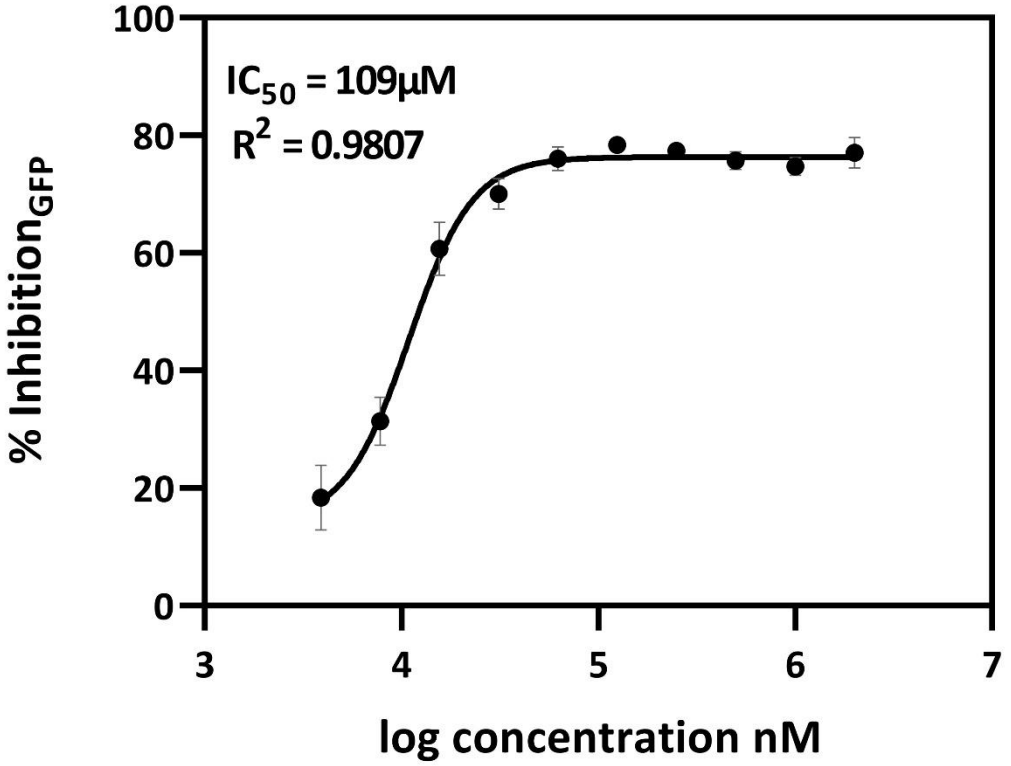
IC50 = 109µM
R2 = 0.9807
% InhibitionGFP
log concentration nM

B

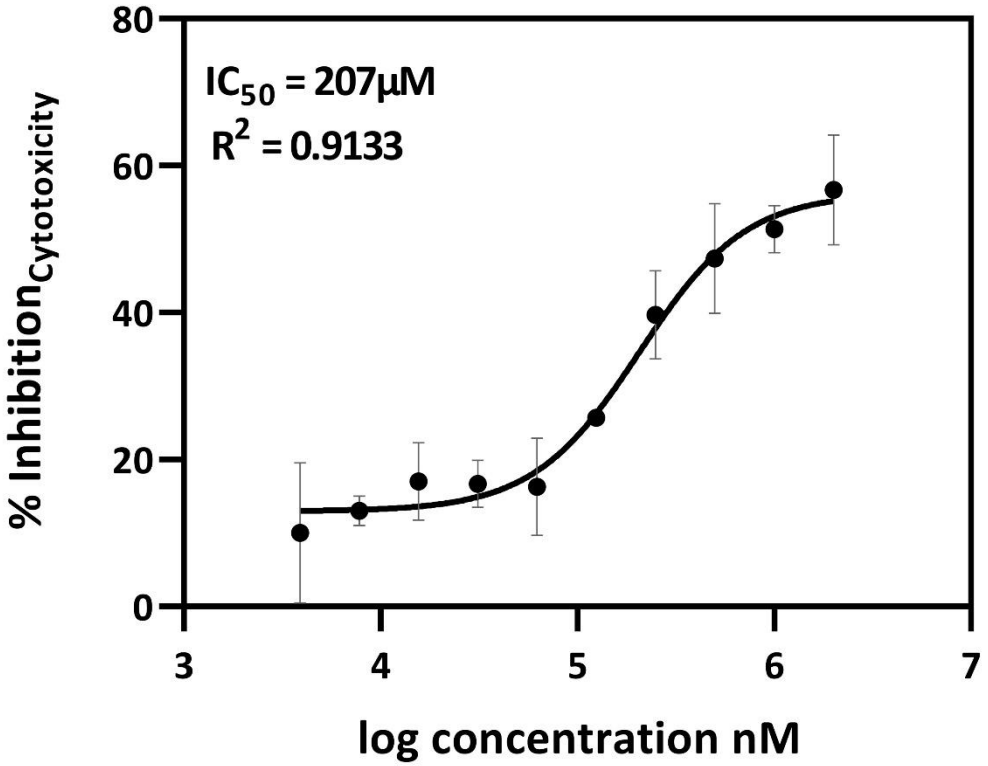
IC50 = 207µM
R2 = 0.9133
% InhibitionCytotoxicity
log concentration nM

Figure 4.15 Representative results from a dose-response assay. The compound 6,7-Dihydroxycoumarin as a potential c-di-GMP and virulence inhibitor identified from previous screen is further tested in a 10-point dose-response assay with a top concentration of 2 mM and two-fold dilution series for A: $\%Inhibition_{GFP}$, B: $\%Inhibition_{Cytotoxicity}$. Fitting a four-parameter logistic function to the data yielded IC50 values of 320 µM and 193 µM respectively.

We examined if 6,7-Dihydroxycoumarin interferes with biofilm formation using a co-culture system in which *P. aeruginosa* biofilms were allowed to form on epithelial cells. 16HBE14o- cells were seeded in µ-Slide 8 Well Chamber Slide (ibidi, Thistle Scientific). The cells are grown to form a confluent monolayer before being inoculated with GFP-tagged, *P. aeruginosa* WT PA14 strain alone (~ 2×10^6 CFU), or in combination with tobramycin (final concentration: 1000 µg/mL), the test compound 6,7-Dihydroxycoumarin (final concentration: 207 µM), or 6,7-Dihydroxycoumarin plus tobramycin. The integrity of the airway epithelial cells and the development of GFP-labelled *P. aeruginosa* biofilms at the apical surface of airway epithelial cells were visualized by confocal microscopy and biofilm biomass was quantity by the Imaris software.

As expected, the addition of tobramycin resulted in a significant reduction in biofilm biomass. When 6,7-Dihydroxycoumarin was added alone, it also caused a reduction in biofilm development (**Figure 4.16**), although not to the same extent as in the presence of tobramycin. However, at a concentration of 207 µM, 6,7-Dihydroxycoumarin further decreased biofilm formation in the presence of tobramycin (**Figure 4.16**). In the µ-chambers, 16HBE14o- cells treated with the wild-type strain exhibited compromised membrane integrity, leaving large empty spaces (**Figure 4.16A**). In contrast, cells treated with 6,7-Dihydroxycoumarin in conjunction with tobramycin maintained their morphology. These results align with the cytotoxicity data, as cells treated with the wild-type strain exhibited high lactate dehydrogenase (LDH) levels, while cells treated with 6,7-Dihydroxycoumarin in conjunction with tobramycin showed a significant reduction in LDH levels (**Figure 4.16C**).

These results suggest that compound 6,7-Dihydroxycoumarin has the potential to be used in combination with antibiotics to reduce the toxicity of *P. aeruginosa* to human airway epithelial cells and significantly reduce biofilm formation. Further studies are needed to fully understand the mechanisms behind these effects and to explore the potential clinical application of 6,7-Dihydroxycoumarin as a treatment for *P. aeruginosa* infection.

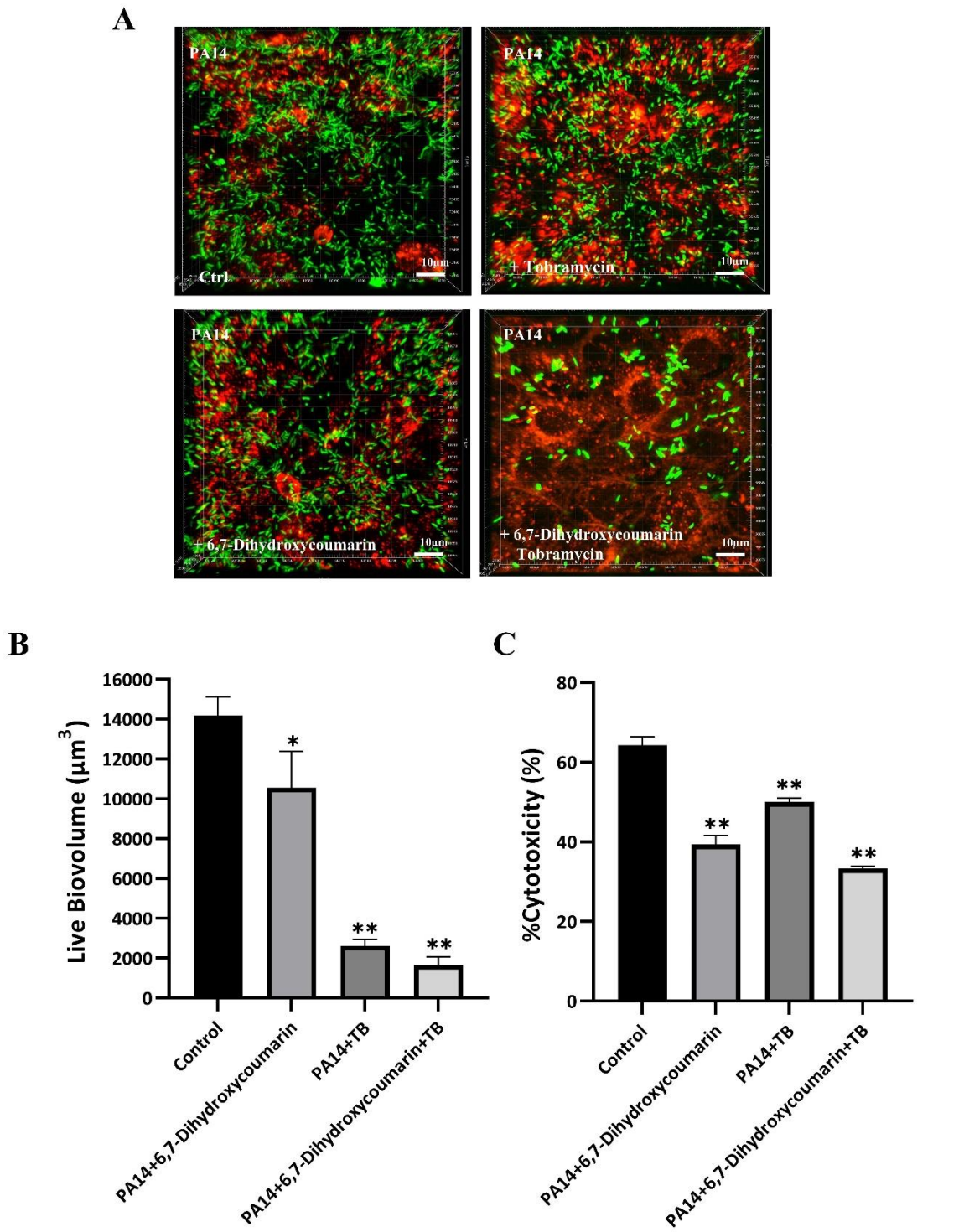

Figure 4.16 Confocal images and biovolume value of the hit from human bronchial epithelial cell-based screening. The potential c-di-GMP and cytotoxicity inhibitor compound 6,7-Dihydroxycoumarin is further tested in a confocal imaging. A: representative imaging for 6,7-Dihydroxycoumarin with four groups of control, TB, 6,7-Dihydroxycoumarin, and TB+ 6,7-Dihydroxycoumarin. B: total biovolume value. (*$p < 0.05$; **$p < 0.01$).

4.4.4 *Galleria mellonella* model treatment results

Given that the three hits identified from the bacterial cell-based screening model did not show a significant reduction in toxicity during the co-culture model screening experiments (**Appendix 1.15**), our focus shifted only to investigating potential inhibitors of 6,7-Dihydroxycoumarin that were screened by the co-culture model effects on larvae. Before conducting the larval experiment, we examined whether 6,7-Dihydroxycoumarin could directly influence human cells using the LDH cytotoxicity test to estimate cytotoxicity. The results showed that 6,7-Dihydroxycoumarin alone had little effect on the toxicity of the cells with a percentage reduction in LDH level of 2.1% (**Appendix C.2.1**).

The effect of 6,7-Dihydroxycoumarin on the efficacy of tobramycin treatment was further evaluated in the *Galleria mellonella* infection model. Larvae were inoculated with WT PA14 culture and subsequently treated with PBS, tobramycin (1mg/Kg), 6,7-Dihydroxycoumarin (200mg/Kg), or a combination of both. Mortality, cuticle discoloration, and response to touch were recorded 16 h post-treatment. Control larvae infected with *P. aeruginosa* and treated with PBS exhibited 100% mortality, which was reduced to 80% by tobramycin treatment. However, the addition of 6,7-Dihydroxycoumarin to tobramycin resulted in a greater reduction in mortality compared to tobramycin alone (**Figure 4.17**). Treatment with 6,7-Dihydroxycoumarin alone did not show a decrease in mortality.

Altogether, the findings from both in vitro and in vivo experiments indicate that the combination of 6,7-Dihydroxycoumarin with antibiotic treatment effectively reduces resistance of *P. aeruginosa*. These results highlight the potential of 6,7-Dihydroxycoumarin as an adjunct therapy to enhance the effectiveness of antibiotics against *P. aeruginosa* infection.

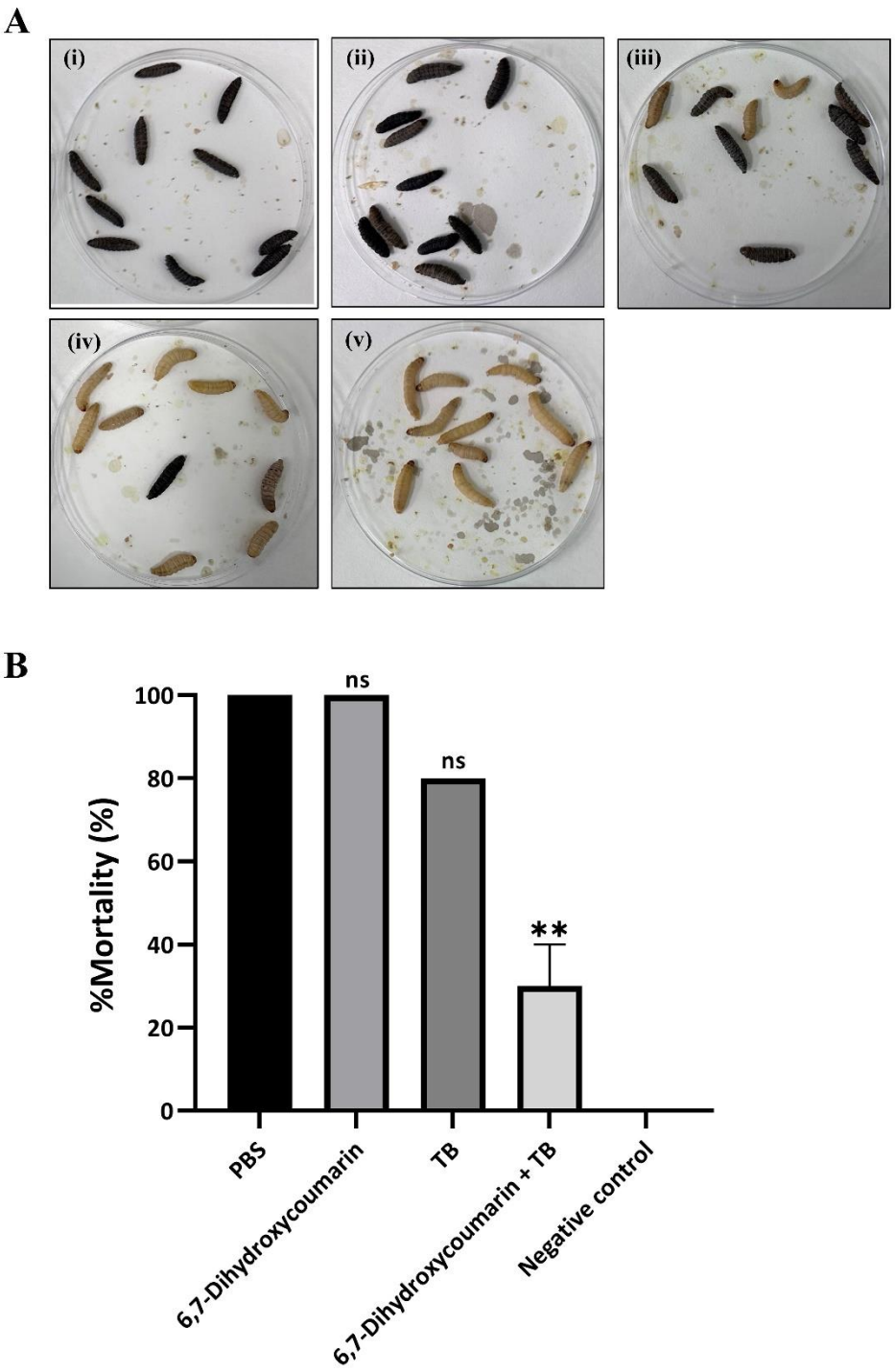

Figure 4.17 Effects of potential inhibitor 6,7-Dihydroxycoumarin combined with TB on 16-hour survival of waxworms. (A) waxworms in different groups: a) control, b) TB, c) 6,7-Dihydroxycoumarin, d) 6,7-Dihydroxycoumarin + TB. (B) The waxworms in different groups. Values are expressed as mean ± SD.

4.5 Conclusion and Discussion

The rapid emergence of bacterial resistance to antibiotics is a global concern, posing a significant threat to healthcare systems worldwide. In response to this urgent issue, researchers have been exploring new strategies to identify efficient anti-bacterial agents. One promising approach is targeting regulatory pathways that utilize intracellular Bis-(3',5') cyclic di-guanylate (c-di-GMP) as a second messenger. C-di-GMP is present in nearly all bacteria and plays a vital role in regulating various processes, including antibiotic resistance, biofilm formation, and virulence. Manipulating c-di-GMP levels through interference with associated signalling pathways holds great potential to reduce biofilm formation or enhance the susceptibility of biofilm bacteria to antibiotics.

We first employed a high-throughput screening model based on *P. aeruginosa* to investigate the impact of 17 natural compounds on bacterial growth. Among them, 4 compounds were identified as potential enhancers, while 13 compounds exhibited inhibitory effects on growth, including 6 antibiotics that have been identified and studied in previous studies, including Azomycin (Belanger *et al.*, 2020; Ulloa and Sakoulas, 2022), Chloramphenicol (Idowu *et al.*, 2019; Mohammed and Ali, 2021), Doxycycline Hyclate (Brown *et al.*, 2022; Huygens *et al.*, 2023), Erythromycin (Ramirez *et al.*, 2022; Yazdanian *et al.*, 2023), Rifampicin (Chaudhary *et al.*, 2022; Mahamad Maifiah *et al.*, 2022), Tetracycline hydrochloride (Anisa *et al.*, 2021; ALTUN *et al.*, 2023). This also verifies the reliability of our model. Additionally, the solvent compositions of natural product extracts displayed different effects on the growth of *P. aeruginosa*. These discoveries contribute to our understanding of potential therapeutic agents and pave the way for targeted research against *P. aeruginosa* infections. However, in this study we focused more on compounds that regulate c-di-GMP levels, we successfully identified small molecules capable of modulating c-di-GMP levels without adversely affecting *P. aeruginosa* growth. These findings offer insights into the potential application of these molecules as regulators of c-di-GMP, aiding in the control and management of *P. aeruginosa* infections.

Through further experiments and dose-response analyses, we determined three compounds—myricetin, resveratrol, and Ellagic acid—as potential inhibitory compounds in the natural compound library. We found that these three natural compounds all had certain effects on *P. aeruginosa* in some previous reports. Myricetin was reported a lot before as an anticancer, antioxidant, anti-inflammatory, antibacterial and antiviral (Wang *et al.*, 2010; Devi *et al.*, 2015; Semwal *et al.*, 2016). In a study by Jayaraman et al., (2010) on the in vitro activity and interaction of antibiotic and phytochemical combinations against *P. aeruginosa*, myricetin was also reported to show synergy with sulfamethoxazole. In addition, myricetin showed better interaction with the QS protein of *P. aeruginosa*, showing considerable inhibitory effect on its biofilm (Ghosh *et al.*,

2022). Resveratrol as a QS inhibitor (Ayerbe-Algaba *et al.*, 2019) also has anti-inflammatory, anticancer, and antimicrobial activities (Vasavi *et al.*, 2017). Resveratrol enhances the activity of colistin against multiple colistin-resistant strains in vitro, combined treatment with resveratrol and colistin was reported to effectively treat the topical bacterial infection caused by MDR *P. aeruginosa* (Cannatelli *et al.*, 2018; Qi *et al.*, 2022; Vitro *et al.*, 2023). Ellagic acid was proven to have significant antioxidant and antibacterial activity. Studies have found that extracts containing ellagic acid significantly inhibited biofilm formation and QS-dependent virulence factors in *P. aeruginosa* (Rather, Gupta and Mandal, 2021). In addition, ellagic acid and sulfamethoxazole also showed a synergistic mode of action in infection studies against *P. aeruginosa* (Jayaraman *et al.*, 2010).

These compounds displayed concentration-dependent inhibition of c-di-GMP levels without significant impact on *P. aeruginosa* growth. Determining their IC_{50} values provided valuable insights into the efficacy of these compounds in modulating c-di-GMP levels (**Figure 4.8**). These findings contribute to the development of potential therapeutic candidates for controlling *P. aeruginosa* infections and warrant further research in bacterial signalling and drug discovery fields. Our results suggest that myricetin and resveratrol hold promise as potential compounds to inhibit *P. aeruginosa* biofilm formation. However, the role of Ellagic acid appears more complex and requires further investigation. Additional research is necessary to fully understand the underlying mechanisms responsible for these effects and explore the potential clinical applications of these compounds in treating *P. aeruginosa* infections.

To investigate the effects of compounds on c-di-GMP levels and their potential as modulators of biofilm formation, antibiotic resistance, and virulence, we further developed a co-culture model using bronchial epithelial cells. In this way we hoped to mimic the complex interactions between bacterial biofilms and host cells, providing an insight into bacterial behaviour and biofilm formation during the infection process. One notable advantage of the developed screening method is its scalability. The ability to scale up the assay allows for the screening of a large number of compounds, increasing the chances of identifying potential inhibitors or modulators of c-di-GMP levels. This scalability is crucial for efficiently screening compound libraries and expanding the scope of potential therapeutic interventions.

The screening results indicate the impact of various natural compounds, including antibiotics like Doxycycline Hyclate and Erythromycin, on *P. aeruginosa* growth. Additionally, certain small molecules and natural extracts regulated c-di-GMP levels without affecting bacterial growth significantly. These findings emphasize the potential of these compounds as modulators of the c-di-GMP signalling pathway in *P. aeruginosa* infection. By combining a co-culture system based on

human bronchial epithelial cells, this study introduced a more complex experimental model. It identified small molecules that modulate host responses during infection and inhibit cytotoxicity.

Through this screening model, we ultimately focused on reducing *P. aeruginosa* virulence to human bronchial epithelial cells by modulating c-di-GMP levels without significantly affecting the growth of bacterial. A single natural compound, 6,7-dihydroxycoumarin, that can reduce c-di-GMP levels and cytotoxicity. 6,7-dihydroxycoumarin also known as esculetin, is a naturally occurring compound derived mainly from the Chinese herbal medicine *Fraxinus rhynchophylla* Hance. It displays a broad spectrum of pharmacological activities, including antioxidant, anti-inflammatory, anticancer, antidiabetic, neuroprotective, cardiovascular protective properties, and potent antibacterial effects (Zhang, Xie and Li, 2022).

Research into the antibacterial and anti-biofilm potential of esculetin has yielded promising results across multiple bacterium types. In one study, esculetin significantly inhibited quorum sensing (QS) and biofilm formation in *Aeromonas hydrophila*. Different concentrations of esculetin (25, 50, and 100μg/ml) were shown to reduce the production of protease and hemolysin, impair biofilm formation, and attenuate swarming motility. The anti-biofilm activity of esculetin was confirmed using confocal laser scanning microscopy and scanning electron microscopy. Gene expression analysis revealed downregulation of genes positively related to QS and biofilm formation, and upregulation of a gene (litR) negatively related to biofilm formation. The alteration in gene expression aligned with the phenotypic changes, indicating the potential of esculetin as a QS inhibitor for *A. hydrophila* (Sun *et al.*, 2021). In addition to its effects on *A. hydrophila*, synthetic derivatives of esculetin, specifically 6,7-dihydroxycoumarin-5-carboxylates (DHCou and 4-Me-DHCou), have shown effective antibiofilm activity against *Staphylococcus aureus* and *Candida albicans*. Interestingly, these compounds lack the cytotoxic activity associated with parent 6,7-dihydroxycoumarins such as esculetin and 4-methylesculetin (Zscherp *et al.*, 2023). Esculetin also displays significant antibacterial activity against the phytopathogen *Ralstonia solanacearum* and *E. coli* O157:H7, a common cause of hemorrhagic colitis (Lee *et al.*, 2011; Yang *et al.*, 2016). It seems to damage the bacterial cell membrane and inhibit biofilm formation, most likely by repressing key virulence genes. These findings suggest potential applications of esculetin in anti-virulence strategies for managing bacterial infections.

However, despite these promising results, the therapeutic use of esculetin is somewhat hampered by its low oral bioavailability, linked to its extensive metabolism through glucuronidation. Despite this limitation, the potential of esculetin for treating a range of conditions, from bacterial infections to chronic diseases like cancer, diabetes, and neurodegenerative disorders, is increasingly recognized. The methodology we developed is

adaptable to other infection models. Biofilm-related infections can occur in various host tissues and organs, necessitating the investigation of different contexts. By replicating the co-culture model with different host cell types, we can examine the effects of c-di-GMP modulators on biofilm formation and antibiotic susceptibility in diverse settings. This adaptability enhances the generalizability and translational potential of our findings, allowing for a broader application in combating bacterial infections.

It is noteworthy that our exploration of potential molecules, including ellagic acid, myricetin, and resveratrol, was initially conducted using a bacterial cell-based screen model. In this context, these compounds were assessed for their impact on virulence, aiming to identify promising candidates for further investigation. However, when transitioning to a human airway epithelial cell-based screening, a distinct shift in outcomes was observed. Specifically, ellagic acid, myricetin, and resveratrol exhibited increased toxicity or negligible changes in the virulence assay of the co-culture model. The $\%Inhibition_{cytotoxicity}$ results were -115.4%, -16.9%, and 2.0%, respectively. This discrepancy strongly suggests that the bacterial mechanism undergoes alteration upon co-cultivation with host cells, emphasizing the co-culture model's closer representation of the bacterial infection state.

In light of these discoveries, our research focuses seamlessly transitioned towards the co-culture model, a setting that offers a more physiologically relevant milieu for comprehending the bacterial response during interactions with host cells. The deliberate choice to explore molecules capable of concurrently reducing cytotoxicity and c-di-GMP levels within this specific model underscores the significance of targeting factors that intricately influence both bacterial virulence and host cell response. This strategic pivot towards the co-culture model aligns seamlessly with our overarching goal of unravelling the nuanced dynamics of bacterial infections and identifying potential therapeutic interventions adept at mitigating cytotoxicity while modulating key signalling pathways.

In conclusion, directing our attention to regulatory pathways involving c-di-GMP emerges as a promising strategy in the battle against antibiotic-resistant bacteria. The utilization of a co-culture model, incorporating bronchial epithelial cells, provides a robust platform for a comprehensive examination of biofilm interactions with host cells. The scalability inherent in our screening method facilitates the exploration of extensive compound libraries, leading not only to the identification of potential c-di-GMP modulators like 6,7-Dihydroxycoumarin but also expanding the scope of our understanding. Moreover, the adaptability of this methodology to various infection models enhances its applicability in addressing biofilm-related infections across diverse host environments. The continued research and development rooted in these findings hold

substantial promise for contributing to the creation of innovative therapeutic interventions against antibiotic-resistant bacteria.

This study encountered several noteworthy limitations that warrant discussion. Firstly, in the screening process of the natural plant extract library, we confronted challenges during subsequent dose analysis. The coloration of the plant extracts emerged as a significant factor influencing the plate reader's ability to accurately read data pertaining to bioluminescence, GFP, and LDH cytotoxicity. This colour interference introduced a level of complexity in interpreting the obtained data, thereby raising concerns about the reliability of our assessments and conclusions. The impact of colour variations on the plate reader readings underscores the need for careful consideration and standardization in future screenings, with a focus on minimizing potential confounding factors.

Moreover, a critical limitation stems from the lack of clarity regarding the specific molecular structures extracted from natural plants. The identification and characterization of these structures are essential for a comprehensive understanding of the mechanisms underlying the observed biological activities. The absence of detailed molecular information poses constraints on the depth of our analysis and limits the potential for elucidating the precise pathways and interactions involved. Future investigations should prioritize efforts to unveil the molecular constituents of the natural plant extracts employed in this study, thereby enhancing the robustness and depth of our findings. Addressing these limitations is imperative for refining our methodologies and ensuring the reliability and applicability of the insights derived from our research.

Chapter 5 Final Conclusions and Future Work

5.1 DSF signal transduction in *P. aeruginosa*

This research presented in the first two chapters of this thesis sheds light on the DSF signalling pathway in various bacteria, particularly *Pseudomonas aeruginosa*, and its potential implications in bacterial pathogenesis and antibiotic resistance. The DSF signalling pathway has been found to regulate important phenotypes such as virulence, biofilm formation, and antibiotic tolerance in multiple bacterial species, including opportunistic pathogens like *X. campestris*, *B. cenocepacia*, *S. maltophilia*, and *P. aeruginosa*. This pathway appears to play a fascinating role in interspecies signalling, influencing bacteria's behaviour in response to exogenous signals.

The discovery of the histidine kinase PA1396 as a key sensor receptor for DSF signals in *P. aeruginosa*, along with the identification of the putative response regulator PA1397, unveils a potential two-component system. This potential two-component system has been mentioned in previous publications (Dow *et al.*, 2003; Chen *et al.*, 2004; Ryan *et al.*, 2008). Biofilm formation linked to high c-di-GMP levels, low levels promote motility (e.g., pilus-dependent). In *P. aeruginosa*, PA1397 phosphorylated by PA1396, forming a TCS. DSF phosphorylate PA1397 via PA1396, affecting gene expression for polymyxin resistance and stress tolerance without altering c-di-GMP (Ryan *et al.*, 2008; Ryan, 2013; Adrian and Löffler, 2016; An and Ryan, 2016; Guła *et al.*, 2018).

The coordinated expression and regulation of these two genes under various environmental conditions suggest a functional link, implicating them in *P. aeruginosa*' s complex regulatory network. The distinctive structure suggests that PA1396 recruits a "solo" Hpt domain to function in a multiple step phosphorelay, ultimately activating the response regulator PA1397. Understanding the signal transduction mechanism in *P. aeruginosa* following the perception of DSF is a critical step in deciphering the complex regulatory pathways and gene expression networks that govern bacterial behaviour.

This study not only provides insights into the functionality and regulation of DSF-related genes in *P. aeruginosa* but also reveals potential therapeutic targets against bacterial infections. We constructed deletion and complementation mutants for three Hpt-coding genes, Δ*hptA*, Δ*hptB*, and Δ*hptC*, in *P. aeruginosa* and conducted a series of phenotype experiments to elucidate their significant impacts on bacterial motility, cytotoxicity, and cytokine levels. Particularly, the Δ*hptB* mutant showed a remarkable reduction in swarming motility and toxicity, highlighting its

importance in *P. aeruginosa* survival, dissemination, colonization, and biofilm formation, emphasizing its role in pathogenicity.

Although our study uncovers the influence of these three genes in *P. aeruginosa*, their direct association with the potential two-component system PA1396 and PA1397 remains unclear. The existing literature provides a certain reference value, which coincides with the *hptB* highlighted in this study, which is very important for future research. HptB functions as an intermediary protein in *P. aeruginosa* PAO1. Transcriptomic analysis of the *hptB* knockout mutant revealed changes in the expression of motility-related genes (Bhuwan *et al.*, 2012). Earlier studies have suggested the presence of a distinct phosphotransfer pathway connecting the sensor kinase PA1611 to HptB and then to PA3346, which potentially plays a role in the regulation of twitch motility, biofilm formation, and other processes (Lin *et al.*, 2006). In the SagS-HapZ two-component system of *P. aeruginosa*, HapZ binding to SagS inhibits phosphotransfer to the downstream protein HptB in a c-di-GMP-dependent manner. Through structural modeling and NMR titration, a buried hydrophobic interface and potentially specific hydrogen bonding residues involved in the REC SagS-HptB interaction. These findings elucidate the specific recognition of SagS by HptB (Xu *et al.*, 2016).

5.2 Small molecule screening and anti-biofilm

The DSF signalling pathway is a key regulator of bacterial behaviour and virulence and has been implicated in antibiotic resistance and biofilm formation. We then constructed a high-content screening model to develop natural compounds that can alleviate bacterial infection and ameliorate existing antibiotic resistance by targeting c-di-GMP signalling, which is known to be regulated by DSF signalling in many bacteria.

The emergence of bacterial resistance to antibiotics is a global problem with major implications for healthcare systems worldwide. To address this issue, researchers are exploring new strategies for identifying effective antimicrobial agents. One promising approach involves targeting regulatory pathways using the intracellular messenger molecule c-di-GMP. This molecule is found in most bacteria and plays a key role in processes as diverse as antibiotic resistance, biofilm formation and virulence. Controlling c-di-GMP levels by interfering with related signalling pathways showed the potential to reduce biofilm formation and enhance bacterial susceptibility to antibiotics.

In this study, we performed high-throughput screening using *P. aeruginosa* to develop natural compounds as potential inhibitors. We first identified potential growth enhancers and inhibitors, including several antibiotics, validating the reliability of their model. In addition, certain

compounds were found to modulate c-di-GMP levels without adversely affecting bacterial growth. Through further experiments, myricetin, resveratrol, and ellagic acid were identified as potential inhibitory compounds, offering hope for controlling *P. aeruginosa* infection.

The study also developed a co-culture model using bronchial epithelial cells to mimic the complex interactions between bacterial biofilms and host cells. The model helps assess the effects of compounds on biofilm formation, antibiotic resistance, and virulence. Importantly, a compound named esculetin was identified as a potential modulator of c-di-GMP, reducing bacterial virulence without significantly affecting growth. The compound has been verified *in vitro* and *in vivo* experiments, and its combined treatment with antibiotics can effectively reduce the drug resistance of *P. aeruginosa*. These results highlight the potential of esculetin as an adjuvant therapy to enhance the effectiveness of antibiotics against *Pseudomonas aeruginosa* infection.

Together, these studies contribute to a more complete understanding of *P. aeruginosa* pathogenesis and provide potential therapeutic targets to combat antibiotic-resistant infections. The identification of potential c-di-GMP modulators and their effect on the pathogenicity of *P. aeruginosa* opens new possibilities for the development of targeted therapies against antibiotic-resistant bacteria. The co-culture model with bronchial epithelial cells introduces a more comprehensive approach to study bacterial behaviour during infection and evaluate potential therapeutic interventions. Although challenges remain, the results of this study pave the way for further research and development in the fields of bacterial signalling and drug discovery. Future research may lead to the optimization and clinical translation of potential therapeutic candidates, contributing to global efforts to combat antibiotic resistance and bacterial infections.

5.3 Future works

Based on the existing research and findings, a series of future works can be carried out in depth, which will help to better understand the role of signalling in bacterial infection and develop more new natural potential drugs to combat the major problem of antibiotic resistance.

5.3.1 Validating the recruited Hpt domain participate the signalling pathway.

As we described in chapter2 and chapter3, we found that the recruited solo Hpt domain, hptA, hptB and hptC all affect the motility, virulence, and other factors of *Pseudomonas aeruginosa* to a certain extent. In future work, phosphorylation can be used to verify that these three Hpt domains are individually or partially involved in the signal transduction of the entire DSF, which will induce DSF signal transduction for *P. aeruginosa* to affect biofilm formation, virulence, etc.

5.3.2 Exploring the potential and structure optimization of esculetin as a potential Inhibitor

Exploring the synergistic effect of esculetin as a c-di-GMP modulator with more existing antibiotics may help in the fight against antibiotic-resistant infections. Combination therapy may enhance the effectiveness of antibiotics and reduce the likelihood of bacterial resistance. It is also possible to gain insight into how the co-culture model affects biofilm formation and antibiotic sensitivity in different infection settings by extending the co-culture model to include different host cell types and tissues. Given the low oral bioavailability of escin, follow-up efforts could be devoted to structural optimization to improve its pharmacokinetic properties and enhance its potential as a therapeutic agent. Synthesis of derivatives with improved bioavailability could lead to more effective treatments.

5.3.3 In-depth research and chemical structure analysis of the screened natural plant extracts.

In the future, in-depth research on the screened natural plant extracts can be conducted to address the effect of color on plate reader readings and ensure accurate measurement of its effect on bacterial growth. It may involve the use of correction methods or the development of new measurement techniques. For potential inhibitors that meet the screening requirements, conduct chemical structure analysis, use mass spectrometry, nuclear magnetic resonance and other techniques to understand their mechanism of action on bacteria, and provide reference for the synthesis of similar molecules. More importantly, conduct cytotoxicity experiments and in vivo model studies to ensure its safety and reliability in clinical applications. In addition, the combined application of plant extracts and existing antibiotics can be further explored to seek possible synergistic effects, enhance the ability of antibacterial agents to kill drug-resistant strains, and reduce the risk of drug resistance.

Through the above future work, we will further understand the antibacterial potential of natural plant extracts, provide a scientific basis for the development of new antibacterial drugs, and provide solutions to the problem of antibiotic resistance.

Appendix A Supplementary information for chapter 2

A.1 Tables

A.1.1 %Cytotoxicity of mutations and complementary strains.

Gene Name	%Cytotoxicity		
PA14	100.0%	100.0%	100.0%
ΔPA1396	78.8%	77.6%	75.3%
CPA1396	100.8%	102.9%	102.2%
ΔPA1397	80.0%	89.2%	89.2%
CPA1397	90.2%	100.9%	88.9%
*Δhpt*A	54.6%	50.6%	53.1%
*Chpt*A	65.2%	66.7%	72.8%
*Δhpt*B	63.8%	57.1%	52.7%
*Chpt*B	58.9%	75.3%	71.1%
*Δhpt*C	66.2%	63.5%	48.9%
*Chpt*C	58.7%	63.1%	60.5%

A.1.2 IL-6, IL-8 and TNF-α in response to *P. aeruginosa* bacteria in 16HEB cell cultures.

PA14	*ΔPA1396*	*ΔPA1397*	*ΔhptA*	*ΔhptB*	*ΔhptC*
hiL-6 concentration (pg/mL)					
118.82	93.53	106.47	114.71	166.47	120.00
126.47	95.29	106.47	113.53	165.29	114.12
125.29	96.47	101.76	121.76	165.29	108.82
hiL-6 concentration (pg/mL)					
33.53	32.67	39.21	32.54	57.36	49.70
39.70	23.04	34.52	35.63	83.90	35.38
37.23	34.15	26.86	32.30	74.27	24.02
hiL-6 concentration (pg/mL)					
4.72	5.28	8.38	8.94	5.14	5.14
4.44	5.99	8.24	7.25	5.99	4.58
3.73	4.86	7.11	7.39	5.00	4.30

Appendix B Supplementary information for chapter 3

B.1 Tables

B.1.1 DEGs list.

Gene Name	hptA	hptB	hptC	PA1396	PA1397	Gene annotation
PA0012					1.54	hypothetical protein
PA0019		-1.57				peptide deformylase
PA0032a		-1.70				putativedioxygenase
PA0033	1.91	1.51				putative histidine phosphotransfer domain
PA0039	-1.51					conserved hypothetical protein
PA0042		-1.62				hypothetical protein
PA0044		-2.72				exoenzyme T
PA0051	1.56	1.58				potential phenazine-modifying enzyme
PA0058		1.60				putative protein-disulfide isomerase
PA0059		-1.62				osmotically inducible protein OsmC
PA0072		1.54				TagS1/putative permease
PA0073		1.63				TagT1/putative ATP-binding component of ABC transporter
PA0092		1.54				Tsi6/hypothetical protein
PA0097	1.53	1.77				conserved hypothetical protein
PA0107	1.90					cytochrome C oxidase assembly protein
PA0108	1.53	1.79				cytochrome c oxidase subunit III
PA0109	-1.61					conserved hypothetical protein
PA0122	-1.55					putative hemolysin
PA0125	-2.40	-1.69				putative transcriptional regulator
PA0127	-1.58	-1.68				putative lipoprotein
PA0128	-2.37	-2.24				hypothetical protein

PA0146	-1.57	-1.56				hypothetical protein
PA0153	-1.56					protocatechuate 3,4-dioxygenase subunit beta
PA0155	-1.56					transcriptional regulator PcaR
PA0165		-1.50				putative outer membrane protein
PA0170		1.73				hypothetical protein
PA0171	-1.56					conserved hypothetical protein
PA0174	1.93	3.70				putative chemotaxis protein
PA0175		2.09				chemotaxis protein methyltransferase
PA0176		1.98				chemotaxis transducer
PA0177		1.69				putative purine-binding chemotaxis protein
PA0178		2.04				putative two-component sensor
PA0184	1.61	2.11				putative BC-type transporter, ATP-binding component
PA0185		1.69				putative permease of ABC transporter
PA0191		1.72				putative transcriptional regulator
PA0192		1.94				TonB-dependent receptor
PA0193		1.57				putative alkylsulfatase
PA0195		2.06				putative NAD(P) transhydrogenase, subunit alpha part 1
PA0197	1.72	1.75				putative TonB protein
PA0198	1.58	2.14				transport protein ExbB
PA0199	1.59					transport protein ExbD
PA0200		-1.76				conserved hypothetical protein
PA0201		1.54				putative esterase
PA0209		2.13			-1.68	putative Triphosphoribosyl-

						dephospho-CoA synthetase
PA0210			-2.03			malonate decarboxylase delta subunit
PA0211		2.70				malonate decarboxylase beta subunit
PA0212		2.32				malonate decarboxylase gamma subunit
PA0213	1.93	3.48				phosphoribosyl-dephospho-CoA transferase
PA0214		1.91				epsilon subunit of malonate decarboxylase
PA0219	-1.66					aldehyde dehydrogenase
PA0239		-1.59				putative permease
PA0250	-1.66	-1.64				putative CBS domain
PA0251	-1.51	-1.66				hypothetical protein
PA0261	1.54	1.71				hypothetical protein
PA0263	-2.16	-2.68				secreted protein Hcp
PA0263		2.31				secreted protein Hcp
PA0276	-1.71					putative membrane protein
PA0277					1.59	putative putative Zn-dependent protease with chaperone function
PA0278		1.61				putative membrane protein
PA0279		1.52				putative transcriptional regulator, ArsR family
PA0280		3.38				sulfate transport protein CysA
PA0281		4.30	-1.50			sulfate transport protein CysW
PA0282	-1.76	3.53	-1.75			sulfate transport protein CysT
PA0283		3.33				sulfate-binding protein precursor
PA0284		3.35				conserved hypothetical protein
PA0295	-1.84					probable periplasmic polyamine binding

						protein
PA0320	-2.54	-5.14		-1.81	-2.31	conserved hypothetical protein
PA0327		-1.99		-1.51	-1.87	putative transcriptional regulator
PA0346		-1.53				hypothetical protein
PA0351	-1.52	-1.82				putative phosphoesterase
PA0359	-1.54					conserved hypothetical protein
PA0363	-1.60	-1.57				phosphopantetheine adenylyltransferase
PA0365		1.66				conserved hypothetical protein
PA0384		-1.51				hypothetical protein
PA0393		1.50				pyrroline-5-carboxylate reductase
PA0398	-1.60	-1.58				putative membrane protein
PA0399		1.63				cystathionine beta-synthase
PA0433		-1.55				conserved hypothetical protein
PA0436		-1.50				transcriptional regulator
PA0441	-1.56	-1.88				phenylhydantoinase
PA0443					-1.94	putative permease for cytosine/purines, uracil, thiamine, allantoin
PA0446		1.53				putative acyl-CoA transferase
PA0456	-2.07	-2.96				putative major cold shock protein
PA0457	1.57					conserved hypothetical protein
PA0459					-1.71	putative ClpA/B protease ATP binding subunit
PA0471					1.83	putative transmembrane sensor
PA0472		-1.51			2.10	putative RNA polymerase sigma-70 factor, ECF

						subfamily
PA0481	-1.69					hypothetical protein
PA0507	1.50					putative acyl-CoA dehydrogenase
PA0509	1.81	2.03	1.82			putative c-type cytochrome
PA0510	1.93	2.63	1.60			putative uroporphyrin-III c-methyltransferase
PA0511	2.11	2.79	1.94			heme d1 biosynthesis protein NirJ
PA0512	1.97	2.36	1.72			heme d1 biosynthesis protein NirH
PA0513	1.67	2.66	1.74			heme d1 biosynthesis protein NirG
PA0514	1.79	2.74	1.66			heme d1 biosynthesis protein NirL
PA0515	1.77	2.35	1.73			heme d1 biosynthesis protein NirD
PA0516		1.57			-1.62	heme d1 biosynthesis protein NirF
PA0517	1.66	1.89			-1.69	putative c-type cytochrome precursor
PA0520		-1.95				regulatory protein NirQ
PA0521	1.86					cytochrome c oxidase subunit
PA0522	2.26					hypothetical protein
PA0523		-2.43				nitric-oxide reductase subunit C
PA0524	2.17					nitric-oxide reductase subunit B
PA0525	2.92		1.65			putative dinitrification protein NorD
PA0531	1.68					putative glutamine amidotransferase
PA0534		1.65				putative oxidoreductase

PA0535		1.76				putative transcriptional regulator, Cro/CI family
PA0540	-1.65					putative membrane protein
PA0547	-1.50					putative transcriptional regulator, ArsR family
PA0560		-1.56				putative metal-dependent hydrolase
PA0563		-1.52				conserved hypothetical protein
PA0578	1.61					hypothetical protein
PA0586	1.50	1.66				putative sporulation protein
PA0587		1.53	1.53			conserved hypothetical protein
PA0588		1.50				putative protein kinase
PA0593		1.58				pyridoxal phosphate biosynthetic protein PdxA
PA0597	1.58					putative nucleotidyltransferase
PA0612	1.96	1.86				putative zinc finger protein
PA0627			-2.35			putative phage protein X
PA0648		1.54				hypothetical protein
PA0653	-1.64	-1.65				putative redox protein
PA0665	1.50					HesB-like domain
PA0668.1		2.22	1.77			16S ribosomal RNA
PA0668.1		2.22	1.82			16S ribosomal RNA
PA0668.1		4.66				16S ribosomal RNA
PA0668.4		2.65	1.56			23S ribosomal RNA
PA0668.4		2.78	1.67			23S ribosomal RNA
PA0668.4	1.51	2.92	1.55			23S ribosomal RNA
PA0668.4	1.79	3.74				23S ribosomal RNA
PA0672					1.94	heme oxygenase
PA0673	-1.87	-1.83				hypothetical protein
PA0674		-1.72				hypothetical protein
PA0675		-2.06				probable sigma-70 factor, ECF subfamily
PA0676	1.88	1.89				probable

						transmembrane sensor
PA0677			1.72		1.67	probable type II secretion system protein
PA0684			-17.75			probable type II secretion system protein
PA0693		1.67				transport protein ExbB2
PA0697	2.20					hypothetical protein
PA0708	-1.53					probable transcriptional regulator
PA0713	-2.26	-2.27				conserved hypothetical protein
PA0724	-1.60					conserved hypothetical protein
PA0725	-2.61					conserved hypothetical protein
PA0727	-1.77					conserved hypothetical protein
PA0728	-1.67	-1.81				putative bacteriophage integrase
PA0728	1.64		1.60			putative integrase
PA0734			1.56			hypothetical protein
PA0747		-1.50				probable aldehyde dehydrogenase
PA0755		-1.66				probable porin
PA0779		5.38				probable ATP-dependent protease
PA0788		1.62	1.75			conserved hypothetical protein
PA0788a		-1.65				conserved hypothetical protein
PA0802			-1.71			hypothetical protein
PA0805	-1.66	-2.07				hypothetical protein
PA0808	-1.52	-1.97				hypothetical protein
PA0812		1.65	1.55			hypothetical protein
PA0824	1.77					hypothetical protein
PA0835					-1.77	phosphate acetyltransferase
PA0837		-1.53				peptidyl-prolyl cis-trans isomerase SlyD
PA0839		-1.57			-1.75	probable transcriptional

						regulator
PA0840					-1.74	probable oxidoreductase
PA0853		1.54				probable oxidoreductase
PA0865		-1.74				4-hydroxyphenylpyruvate dioxygenase
PA0867	-1.98	-1.80				lysozyme inhibitor
PA0871		-1.64				pterin-4-alpha-carbinolamine dehydratase
PA0878					-1.52	hypothetical protein
PA0879		-1.67				probable acyl-CoA dehydrogenase
PA0881					-2.34	putative protein involved in propionate catabolism
PA0905	-2.83	-2.10				RsmA, regulator of secondary metabolites
PA0908	-1.66	-1.57				hypothetical protein
PA0909		2.13				hypothetical protein
PA0915	-1.54		-1.66			conserved hypothetical protein
PA0929		-2.32			2.06	two-component response regulator
PA0930					1.61	two-component sensor
PA0931		-1.53				siderophore receptor protein
PA0937	-1.61	-1.91				conserved hypothetical protein
PA0939	1.62	1.51				hypothetical protein
PA0957	-1.57					hypothetical protein
PA0960					1.55	conserved hypothetical protein
PA0978		-1.51				possible transposase
PA0982	1.52					Putative protein-disulfide isomerase
PA0984					1.55	colicin immunity protein
PA0988		-1.55				hypothetical protein
PA0989		-1.66				hypothetical protein
PA0995		-1.58				methylated-DNA--protein-cysteine

						methyltransferase
PA1023					-1.87	probable short-chain dehydrogenase
PA1026	-1.50					hypothetical protein
PA1035		-1.71				conserved hypothetical protein
PA1041		1.59				probable outer membrane protein precursor
PA1042		1.53				conserved hypothetical protein
PA1053	-1.50	-1.58				conserved hypothetical protein
PA1066	-1.56					probable short-chain dehydrogenase
PA1076	-1.90	-1.93				hypothetical protein
PA1077		-1.61				flagellar basal-body rod protein FlgB
PA1079		-1.56				flagellar basal-body rod modification protein FlgD
PA1134	1.52		1.59			hypothetical protein
PA1136	1.77					probable transcriptional regulator
PA1138		-1.65				probable transcriptional regulator
PA1141		1.51				probable transcriptional regulator
PA1146		-1.71				probable iron-containing alcohol dehydrogenase
PA1147	1.83					probable amino acid permease
PA1153		1.59				hypothetical protein
PA1168	-1.89					hypothetical protein
PA1172			1.56			cytochrome c-type protein NapC
PA1176		1.65				ferredoxin protein NapF
PA1178		-1.77			-1.57	PhoP/Q and low Mg2+ inducible outer membrane prote
PA1183	2.09					C4-dicarboxylate

						transport protein
PA1187	-1.73					probable acyl-CoA dehydrogenase
PA1189	-1.57	-2.43	-1.71			putative peptidase, SprT family
PA1196					-1.57	putative transcriptional regulator
PA1199	-1.53	-1.93				putative lipoprotein
PA1210		-1.51				putative pirin protein
PA1212		1.74				putative MFS transporter
PA1213		2.05				putative clavaminic acid synthetase
PA1214		1.83				putative sparagine synthase
PA1215		1.60				putative AMP-binding enzyme
PA1217		1.66				putative 2-isopropylmalate synthase
PA1218					-2.11	conserved hypothetical protein
PA1219	1.86	1.94	2.38			conserved hypothetical protein
PA1221	1.66	1.66				putative AMP-binding enzyme
PA1228	-1.68					conserved hypothetical protein
PA1238	1.65					putative outer membrane component of multidrug efflux pump
PA1245		1.58				conserved hypothetical protein
PA1246		1.63				alkaline protease secretion protein AprD
PA1251	1.72	2.36				putative methyl-accepting chemotaxis transducer
PA1255	1.67					putative proline racemase protein
PA1282		1.62				putative major facilitator superfamily (MFS) transporter

PA1284	1.53		1.54		1.55	putative acyl-CoA dehydrogenase
PA1285	-1.86					putative transcriptional regulator, MarR family
PA1287		-1.57				putative glutathione peroxidase
PA1298	-1.53					conserved hypothetical protein
PA1310	1.56					2-aminoethylphosphonate:pyruvate aminotransferase
PA1313		-1.78				putative MFS transporter
PA1317					-1.81	cytochrome o ubiquinol oxidase subunit II
PA1318					-1.60	cytochrome o ubiquinol oxidase subunit I
PA1319					-2.18	cytochrome o ubiquinol oxidase subunit III
PA1320		1.84				cytochrome o ubiquinol oxidase subunit IV
PA1321		2.20				cytochrome o ubiquinol oxidase protein CyoE
PA1322			1.81			putative TonB-dependent receptor
PA1340		2.03				putative permease of ABC transporter
PA1341		1.75				putative permease of ABC transporter
PA1346					-1.67	putative lysine decarboxylase
PA1351					-1.59	putative sigma-70 factor, ECF subfamily
PA1355	-2.74					conserved hypothetical protein
PA1356		1.97				conserved hypothetical protein
PA1363		-1.71			1.52	putative sigma-70 factor, ECF subfamily

PA1367	-1.50					putative phenazine biosynthesis protein
PA1374		-1.74				putative transcriptional regulator
PA1377		-1.61				putative acetyltransferase
PA1395				2.59		hypothetical protein
PA1398					1.94	hypothetical protein
PA14_01130		1.60				hypothetical protein
PA14_03330		1.83				hypothetical protein
PA14_03360		1.68				conserved hypothetical protein
PA14_07480		1.77				putative reverse transcriptase
PA14_10070		1.89				putative zinc-dependent oxidoreductase
PA14_10080	-1.65	-1.63				hypothetical protein
PA14_10090		1.52				possible LysR family transcription regulator
PA14_10980		-1.50				hypothetical protein
PA14_11350		1.53				hypothetical protein
PA14_13200	2.35		1.90			conserved hypothetical protein
PA14_13220	-1.76	-2.05				possible protein-tyrosine-phosphatase
PA14_14310	-1.82				1.93	putative transcriptional regulator
PA14_14550		-1.50				hypothetical protein
PA14_15445	1.78	1.76				mercury resistance protein
PA14_15500		-1.58				possible oriT-binding protein, TraK
PA14_15510		-1.58				oriT-binding protein, TraJ
PA14_15560	-1.53	-1.75				hypothetical protein
PA14_15650	-1.52					conserved hypothetical protein
PA14_15750		1.73				conserved hypothetical protein
PA14_19930		2.20				conserved hypothetical protein
PA14_22190	-1.65	-2.07				hypothetical protein

PA14_22230	7.74	8.27				hypothetical protein
PA14_22240	2.42					hypothetical protein
PA14_22530					-1.84	putative glutathione S-transferase
PA14_22880		1.66				putative Fe-S protein
PA14_23380		1.50				UDP-N-acetyl-D-mannosaminuronate dehydrogenase
PA14_26200		2.58				putative transcriptional regulator
PA14_27990		-1.98				putative sialidase
PA14_28540		-3.35				hypothetical protein
PA14_28830		1.61				conserved hypothetical protein
PA14_28980			-2.33			Possible Fe2+-dicitrate sensor
PA14_29330		1.52				hypothetical protein
PA14_29375		-1.65				PA14_29375
PA14_29575	-1.51	-2.28				hypothetical protein
PA14_30980	-2.11	-2.17				hypothetical protein
PA14_31100					-5.33	putative plasmid partitioning protein
PA14_31160			2.27			hypothetical protein
PA14_31930	2.17					hypothetical protein
PA14_33300		1.59				hypothetical protein
PA14_33310		1.99				hypothetical protein
PA14_33320		2.38				hypothetical protein
PA14_35720	-1.89					hypothetical protein
PA14_35730	-1.70					hypothetical protein
PA14_35770		1.83				hypothetical protein
PA14_35780	1.51	1.87				hypothetical protein
PA14_35970		-2.01			-2.03	Probable Acyl-CoA dehydrogenase
PA14_41575		-2.04				ECF sigma factor SigX
PA14_46610		1.53				hypothetical protein
PA14_48450		1.67				putative peptidyl-arginine deiminase
PA14_48490	-1.69					putative peptidylarginine deiminase
PA14_48500	-1.71					putative transcriptional regulator
PA14_49030	-1.83					hypothetical protein

PA14_49510		-1.52				immunity protein S3I structureal gene
PA14_49870		-1.71				probable peptide deformylase
PA14_51520		-1.61				SpcU
PA14_51530		-1.80				ExoU
PA14_51570		1.57				hypothetical protein
PA14_52120		-1.68				hypothetical protein
PA14_54460	1.51	1.57				conserved hypothetical protein
PA14_55000		-1.97				possible ABC-type transporter, periplasmic component
PA14_56970	1.91					conserved hypothetical protein
PA14_58730		-1.76				type IV pilin structural subunit
PA14_58970					-1.81	putative phage protein
PA14_58980	3.25	4.95				conserved hypothetical protein
PA14_58990			1.69			Putative DNA helicase
PA14_59000		2.25				conserved hypothetical protein
PA14_59010	3.76					conserved hypothetical protein
PA14_59030		7.47	13.22			hypothetical protein
PA14_59130		1.52				conserved hypothetical protein
PA14_59190		-1.50				hypothetical protein
PA14_59340		1.61				type IV B pilus protein
PA14_59400		1.74				conserved hypothetical protein
PA14_59430		1.88				conserved hypothetical protein
PA14_59470	-2.01	-1.93				hypothetical protein
PA14_59490		1.69				conserved hypothetical protein
PA14_59500		1.53				hypothetical protein
PA14_59520		1.71				hypothetical protein
PA14_59530		1.69				conserved hypothetical protein
PA14_59700		1.57	1.66			conserved hypothetical protein

PA14_59770			1.53			putative two component response regulator
PA14_59790	-1.83	-1.50				two component response regulator
PA14_59850		1.69	1.81		-1.75	putative candidate type III effector Hop protein
PA14_59860		3.63	2.14			type III effector Hop protein
PA14_59880			1.52		1.63	conserved hypothetical protein
PA14_59890		1.79	1.62			conserved hypothetical protein
PA14_59910			1.50			conserved hypothetical protein
PA14_59980		-1.79				hypothetical protein
PA14_60190		1.84				clpB protein
PA14_61110	1.52					conserved hypothetical protein
PA14_67900		1.66				conserved hypothetical protein
PA14_RS01390	-1.52	-1.50				
PA14_RS02080		1.55				
PA14_RS06215	1.77		1.86			
PA14_RS06250	1.52	1.82				
PA14_RS11995		1.86				
PA14_RS12590	2.12					
PA14_RS12655	-1.53	-1.71				
PA14_RS12715	9.21	8.11				
PA14_RS12730	3.03					
PA14_RS12755	-1.57	-1.94				
PA14_RS12790	-1.61	-1.88				
PA14_RS13380		-2.50				
PA14_RS15095		1.55			-1.68	

PA14_RS18020	2.11	5.49	1.73			
PA14_RS18680		-1.65				
PA14_RS18890		1.61				
PA14_RS21810	-1.64					
PA14_RS22255		-1.50				
PA14_RS24145			3.32			
PA14_RS24600		-1.59				
PA14_RS25835	1.52	1.69				
PA14_RS29940	-1.68	-2.05				
PA14_RS30445	-2.23					
PA14_RS30465	-1.53					
PA14_RS30470		-1.68				
PA14_RS30650		-1.56				
PA14_RS30830	-1.64	-1.86				
PA14_RS30830	-1.57					
PA14_RS31075	2.70					
PA14_RS31165	-1.50					
PA14_RS31200	-5.07	-28.23				
PA14_RS31320		-1.78				
PA14_RS31365		-1.94				
PA14_RS31430		-1.68				
PA14_RS31435	-2.12	-1.64				
PA14_RS31455	-1.68	-2.34				
PA14_RS31465	1.72	1.90	1.87		1.66	

PA14_RS31470		15.12	8.88			
PA14_RS31490		-2.60				
PA14_RS31500	3.51					
PA1410			-1.57			putative periplasmic putrescine-binding permease protein
PA1419		-1.65				putative transporter
PA1421		-1.83				guanidinobutyrase
PA1445		1.53				flagellar protein FliO
PA1448	1.58					flagellar biosynthetic protein FliR
PA1468		-1.55				hypothetical protein
PA1488		1.51				putative oxidoreductase
PA1489			-1.52			putative oxidoreductase
PA1490	-1.60					putative transcriptional regulator
PA1499		1.82				putative hydroxypyruvate reductase
PA1517	-1.69	-1.99				hypothetical protein
PA1518	-1.59	-1.52				putative transthyretin family protein
PA1533	-1.59	-1.93				conserved hypothetical protein
PA1540	1.70	1.56	1.60			putative membrane transporter of cations and cationic drugs
PA1541	1.85	1.55	2.33			putative drug efflux transporter
PA1545	-1.91	-2.46				conserved hypothetical protein
PA1555		2.75				putative cytochrome c oxidase, cbb3-type, subunit III
PA1556		2.93			-1.51	putative cytochrome c oxidase subunit
PA1557		1.66			-1.78	putative cytochrome oxidase subunit (cbb3-type)
PA1564	-1.58	-1.76				putative redox protein
PA1565	1.73					putative

						oxidoreductase
PA1574	-2.02	-1.99				conserved hypothetical protein
PA1582	1.50	1.68				succinate dehydrogenase (D subunit)
PA1586					-1.51	dihydrolipoamide succinyltransferase
PA1591	1.52					conserved hypothetical protein
PA1592	-1.57					conserved hypothetical protein
PA1593	-1.50					putative thioesterase
PA1596		4.06				heat shock protein HtpG
PA1597		3.42				putative dienelactone hydrolase family protein
PA1602		-1.90				putative oxidoreductase
PA1624	1.54					conserved hypothetical protein
PA1627	-1.51					putative transcriptional regulator, GntR family
PA1633					-1.96	potassium-transporting ATPase, A chain
PA1634					-1.64	potassium-transporting ATPase, B chain
PA1657		1.69				conserved hypothetical protein
PA1658		1.82				conserved hypothetical protein
PA1659	1.52	2.13				conserved hypothetical protein
PA1660		2.05				conserved hypothetical protein
PA1661		1.56				conserved hypothetical protein
PA1662		1.52				putative ClpA/B-type protease
PA1663		1.67				putative sigma-54 dependent transcriptional

						regulator
PA1665		1.62				conserved hypothetical protein
PA1670	1.64	1.71				serine/threonine protein phosphatase
PA1671		1.60				serine-threonine kinase Stk1
PA1673	-1.70					putative hemerythrin
PA1690		-2.49				translocation protein in type III secretion
PA1691		-1.94				translocation protein in type III secretion
PA1692		-2.91				putative translocation protein in type III secretion
PA1693		-2.67				translocation protein in type III secretion
PA1694		-2.37				type III secretion system protein
PA1695	-1.51	-2.42	-1.52			translocation protein in type III secretion
PA1696		-1.54	-1.58			translocation protein in type III secretion
PA1697		-1.65				ATP synthase in type III secretion system
PA1698		-2.09				Type III secretion outer membrane protein PopN precursor
PA1699		-1.87				putative protein in type III secretion
PA1700		-1.63				putative type III secretion protein
PA1701		-1.82				conserved hypothetical protein
PA1703		-2.20				type III secretory apparatus protein PcrD
PA1704		-1.79				transcriptional regulator protein PcrR
PA1705		-2.64				regulator in type III secretion
PA1706		-2.10				type III secretion protein PcrV
PA1707		-2.75				regulatory protein PcrH

PA1708		-2.13				translocator protein PopB
PA1709		-2.47				translocator outer membrane protein PopD precursor
PA1710		-2.27				exoenzyme S synthesis protein C precursor
PA1711	1.90					hypothetical protein
PA1712		-1.60				exoenzyme S synthesis protein B
PA1713		-2.65				transcriptional regulator ExsA
PA1714		-1.64				conserved hypothetical protein
PA1716		-1.71				Type III secretion outer membrane protein PscC precursor
PA1717		-1.79				type III export protein PscD
PA1718		-2.08				type III export protein PscE
PA1719		-2.57				type III export protein PscF
PA1720		-1.65				type III export protein PscG
PA1721	1.58					type III export protein PscH
PA1722		-2.18				type III export protein PscI
PA1723		-2.25				pscJ type III export protein
PA1724		-1.54				PscK type III export protein
PA1725		-2.35				type III export protein PscL
PA1738				-1.61		putative transcriptional regulator
PA1760	1.56					putative transcriptional regulator
PA1764	1.59		1.69		1.81	putative outer membrane protein transport protein
PA1781					-2.01	assimilatory nitrite reductase large

						subunit
PA1782			1.55			putative serine/threonine-protein kinase
PA1793		-1.55				peptidyl-prolyl cis-trans isomerase B
PA1815		-1.63				ribonuclease H
PA1817		-1.68				conserved hypothetical protein
PA1830	-2.05	-2.25				putative sterol carrier protein
PA1831		-1.63				putative phosphoglycerate mutase
PA1837	-1.54	2.11				conserved hypothetical protein
PA1838	-1.57	2.05	-1.54			sulfite reductase
PA1840		-1.63				conserved hypothetical protein
PA1845		-2.67				hypothetical protein
PA1847		-1.78				conserved hypothetical protein
PA1848	1.56					putative MFS transporter
PA1852	-1.94	-2.53				conserved hypothetical protein
PA1854				-2.31		putative CBS-domain-containing membrane protein
PA1864			-1.52			putative transcriptional regulator, TetR family
PA1867				-2.59		conserved hypothetical protein
PA1869					1.55	putative acyl carrier protein
PA1873	2.01		1.74			putative cation transporter
PA1876		1.52				putative ATP-binding/permease fusion ABC transporter
PA1880		1.62				putative exported oxidoreductase
PA1882		-1.98	1.53			putative transporter
PA1891		2.10				conserved hypothetical protein

PA1892		1.73				hypothetical protein
PA1893		2.84				putative penicillin acylase
PA1894		2.62				putative enzyme
PA1896		3.49				hypothetical protein
PA1897		1.88				putative desaturase
PA1899	-1.69	1.54	-1.74			probable phenazine biosynthesis protein
PA1900		2.05				probable phenazine biosynthesis protein
PA1901		2.76				phenazine biosynthesis protein PhzC
PA1901		3.56				phenazine biosynthesis protein PhzC
PA1902		2.33		3.38		phenazine biosynthesis protein PhzD
PA1902		3.03				phenazine biosynthesis protein PhzD
PA1903		3.55				phenazine biosynthesis protein PhzE
PA1904		2.46				probable phenazine biosynthesis protein
PA1904		2.75				probable phenazine biosynthesis protein
PA1905		1.88				probable pyridoxamine 5'-phosphate oxidase
PA1905		3.21				probable pyrodoxamine 5'-phosphate oxidase
PA1918			1.86			putative amino acid oxidase
PA1919	1.64	1.95	1.73			putative radical-activating enzyme
PA1920		1.53	1.54			putative ribonucleotide reductase
PA1934	-1.86	-1.76				conserved hypothetical protein
PA1945	1.51	1.61				putative sigma-54 dependent transcriptional regulator

PA1949	1.55					ribose operon repressor RbsR
PA1951		1.59				conserved hypothetical protein
PA1965		-1.63				hypothetical protein
PA1967		-1.70				hypothetical protein
PA1969	-1.82	-2.10				conserved hypothetical protein
PA1972	2.09					putative membrane protein
PA1978		-1.66				putative glycerol regulatory protein
PA1981			-5.02			conserved hypothetical protein
PA1990		1.58				putative dipeptidyl aminopeptidase
PA2008		1.71				fumarylacetoacetase
PA2012		1.53				alpha subunit of geranoyl-CoA carboxylase, GnyA
PA2016		-1.54				Regulatory gene of gnyRDBHAL cluster, GnyR
PA2022	1.97					putative UDP-glucose 6-dehydrogenas
PA2026	-1.92		-1.65			putative transporter, bile acid/Na+ symporter family
PA2029	-1.68					conserved hypothetical protein
PA2030	-1.83					hypothetical protein
PA2034	1.84					putative methylase
PA2038	1.56	1.77			1.57	putative membrane protein
PA2050		3.01				putative sigma-70 factor, ECF subfamily
PA2051		2.90				putative Fe2+-dicitrate sensor, membrane component
PA2053		2.12				carbonate dehydratase
PA2062		2.57		1.56		putative pyridoxal-phosphate dependent enzyme
PA2066		2.34			1.57	conserved hypothetical protein

PA2067		2.16				putative hydrolase
PA2068		2.60				putative MFS transporter
PA2069		1.97				probable carbamoyl transferase
PA2077		1.60				conserved hypothetical protein
PA2079		1.54				putative amino acid permease
PA2080		1.60				putative kynureninase
PA2081	-1.69					kynurenine formamidase, KynB
PA2084		2.47				asparagine synthetase, glutamine-hydrolysing
PA2085		2.88				putative ring-hydroxylating dioxygenase small subunit
PA2086		3.13				putative hydrolase
PA2087		4.30				hypothetical protein
PA2088		2.55				conserved hypothetical protein
PA2089		1.65				putative TonB-dependent receptor
PA2090		1.54				putative flavin-dependent oxidoreductase
PA2091		1.98				putative permease
PA2094		1.73				putative transmembrane sensor protein
PA2109					1.51	putative outer membrane protein
PA2110		1.79				putative allophanate hydrolase subunit 2
PA2125		1.55				putative aldehyde dehydrogenase
PA2126	1.60	1.76			-1.70	putative transcriptional regulator
PA2127					-1.64	putative phosphoadenosine phosphosulfate sulfotransferase
PA2129					-2.60	chaperone CupA2

PA2129	1.74					putative pili assembly chaperone
PA2132		3.50	3.19			chaperone CupA5
PA2142	2.94					putative short-chain dehydrogenase
PA2143	-4.60					hypothetical protein
PA2145		-1.93				hypothetical protein
PA2148		2.67			2.82	putative Mg(2+) transporter
PA2159			1.72			conserved hypothetical protein
PA2166	-2.11				1.58	hypothetical protein
PA2174		-2.11				hypothetical protein
PA2175	1.57	1.63				hypothetical protein
PA2179	-1.90					putative methylase
PA2191		-2.13				adenylate cyclase ExoY
PA2193	-1.75					hydrogen cyanide synthase HcnA
PA2194		2.13				hydrogen cyanide synthase HcnB
PA2195		2.52				hydrogen cyanide synthase HcnC
PA2201			-1.50			hypothetical protein
PA2202	-2.03	3.63				putative amino acid transport system permease
PA2203	-2.35	5.16	-1.68			putative amino acid permease
PA2204	-1.64	4.42	-1.50			putative binding protein component of ABC transporter
PA2209	-1.58	-1.65				conserved hypothetical protein
PA2211	1.88					putative hydrolase
PA2238		1.52				possible glycosyltransferase
PA2252		-2.55	-1.50			putative sodium/alanine symporter
PA2254	-1.66	-1.86				pyoverdine biosynthesis protein PvcA
PA2256	1.53					pyoverdine biosynthesis protein PvcC

PA2257		-1.92				pyoverdine biosynthesis protein PvcD
PA2259		-1.50				transcriptional regulator PtxS
PA2262					-1.65	putative 2-ketogluconate transporter
PA2265					-1.77	gluconate dehydrogenase
PA2266					-1.54	putative cytochrome c precursor
PA2274	-1.59					phenazine-utilizing monooxygenase A
PA2277	-1.81					arsenic resistance transcriptional regulator
PA2282		-2.04				conserved hypothetical protein
PA2292		4.82				conserved hypothetical protein
PA2297	2.18					putative ferredoxin
PA2299	-1.51					putative transcriptional regulator, GntR family
PA2300		1.64				chitinase
PA2302		1.73				putative non-ribosomal peptide synthetase
PA2303		1.52				putative regulatory protein
PA2304		1.57				putative regulatory protein
PA2308		2.14				putative ABC transporter ATP-binding component
PA2309		2.30				putative ABC transporter, periplasmic binding protein
PA2312		3.30				putative transcriptional regulator, XRE family
PA2315			-2.10			putative beta lactamase
PA2321	-1.92	-2.01				gluconokinase

PA2324					-1.78	putative flavin reductase dependent enzyme
PA2325					-1.55	putative flavin reductase dependent enzyme
PA2326		1.59				putative xenobiotic compound monooxygenase, DszA family
PA2327		2.52				putative sulfonate ABC transporter, permease protein
PA2328		2.43				putative sulfonate ABC transporter, periplasmic sulfonate-binding protein
PA2329		2.74				putative ATP-binding component of ABC transporter
PA2330		2.46				putative acyl-CoA dehydrogenase
PA2331		2.25				putative alkylhydroperoxidase
PA2341	1.76					putative ATP-binding component of ABC maltose/mannitol transporter
PA2343	2.11					xylulose kinase
PA2350	2.57					putative ATP-binding component of ABC transporter
PA2352			-1.50			putative glycerophosphoryl diester phosphodiesterase
PA2357	3.52	4.95	5.30			NADH-dependent FMN reductase
PA2358	-1.90	-2.25				hypothetical protein
PA2359		2.72		1.75		putative sigma54-dependent transcriptional regulator
PA2360	1.64	2.14				conserved hypothetical protein
PA2362		1.53				conserved hypothetical protein

PA2366		2.03				conserved hypothetical protein
PA2368	4.18	3.30				conserved hypothetical protein
PA2369	-1.80		-1.58		-2.12	conserved hypothetical protein
PA2370		2.37				conserved hypothetical protein
PA2371		2.15	1.61			probable ClpA/B-type protease
PA2376			1.68			putative transcriptional regulator
PA2380		-1.52				hypothetical protein
PA2381			1.59			conserved hypothetical protein
PA2404			-1.81			conserved hypothetical protein
PA2405		1.90				conserved hypothetical protein
PA2406					-1.98	conserved hypothetical protein
PA2407					-1.67	putative adhesion protein
PA2408		1.67				putative ATP-binding component of ABC transporter
PA2410	-1.58					putative ABC transporter, periplasmic substrate-binding protein
PA2422		-3.03				hypothetical protein
PA2426		-5.47				sigma factor PvdS
PA2428	-1.85					hypothetical protein
PA2433	-1.68	-2.14				hypothetical protein
PA2436	-1.50	-1.78				hypothetical protein
PA2440		1.50				hypothetical protein
PA2441		1.52				hypothetical protein
PA2453	-2.42	-1.60				hypothetical protein
PA2465		-2.44				hypothetical protein
PA2466		-1.76				probable TonB-dependent receptor
PA2468		-1.64				probable sigma-70 factor, ECF subfamily
PA2470	-1.68		-1.74			gentisate 1,2-dioxygenase

PA2474	3.23					hypothetical protein
PA2481		-2.04				hypothetical protein
PA2482		-2.46				putative cytochrome c
PA2484		-1.50				putative TetR-family transcriptional regulator
PA2501	-2.19	-1.95				hypothetical protein
PA2508	-2.76					muconolactone delta-isomerase
PA2536		1.66				putative phosphatidate cytidylyltransferase
PA2547		-1.59	-1.62			putative transcriptional regulator, LysR family
PA2558		-1.56				putative transport protein
PA2562		-1.65				conserved hypothetical protein
PA2565	1.70	1.68				hypothetical protein
PA2569		-1.62				hypothetical protein
PA2594		2.17				putative periplasmic aliphatic sulfonate-binding protein
PA2597		1.84				putative acyl-CoA dehydrogenase
PA2598		1.97				putative lavin-dependent oxidoreductase
PA2599		2.01				putative periplasmic aliphatic sulfonate-binding protein
PA2600		1.66				putative flavin-dependent oxidoreductase
PA2619	-1.76					translation initiation factor IF-1
PA2621		-1.57				ATP-dependent Clp protease adaptor protein clpS
PA2622	-2.32	-2.66				cold-shock protein CspD
PA2625	-1.54					putative NUDIX hydrolase
PA2646		1.67				NADH dehydrogenase I chain K

PA2655	-1.63					hypothetical protein
PA2659		-1.74				conserved hypothetical protein
PA2662	2.06	-1.96				putative membraine protein
PA2663	1.59	-2.06				hypothetical protein
PA2664		-2.64				flavohemoprotein
PA2667	-1.85	-2.42				putative transcriptional regulator
PA2675	1.82		2.51	2.38	1.82	putative type II secretion system protein
PA2676	1.56					putative type II secretion system protein
PA2694		1.68				putative thioredoxin
PA2699	-1.52					putative hydrolase
PA2700		3.15				putative porin
PA2714		1.75				putative molybdopterin oxidoreductase
PA2723	1.95	2.09				hypothetical protein
PA2743	-1.90	-2.14				translation initiation factor IF-3
PA2746a		-1.57	1.56			conserved hypothetical protein
PA2746a	-1.98	-1.83				hypothetical protein
PA2747	-1.55					conserved hypothetical protein
PA2754a		-1.68				hypothetical protein
PA2755	-2.25	-2.37				ecotin precursor
PA2759	-1.56					hypothetical protein
PA2761	-1.51	-1.55				conserved hypothetical protein
PA2787	1.87	2.10	1.54			carboxypeptidase G2 precursor
PA2788	1.72		1.52			putative methyl-accepting chemotaxis protein
PA2805	-1.73	-1.73				conserved hypothetical protein
PA2807		-2.96				putative copper-binding protein
PA2810		1.52				putative sensor histidine kinase
PA2817	-1.69	-1.74				conserved

						hypothetical protein
PA2827		-1.73				putative PilB-related protein
PA2837		1.68				putative outer membrane protein precursor
PA2840	1.83					putative ATP-dependent RNA helicase, DEAD box family
PA2849	-1.70	-1.63				putative transcriptional regulator, MarR family
PA2850	-1.69					organic hydroperoxide resistance protein
PA2851	-1.56	-1.57				translation elongation factor P
PA2856		-1.63				acyl-CoA thioesterase I precursor
PA2860		-1.58				conserved hypothetical protein
PA2863	-1.68					lipase modulator protein
PA2864	-1.93	-2.03				putative membrane protein
PA2880		-3.11				putative membrane protein
PA2883	-1.86	-1.53				hypothetical protein
PA2885	-1.56					putative transcriptional regulator
PA2888		1.58				putative biotin-dependent carboxylase
PA2890		1.69				putative enoyl-CoA hydratase
PA2891		1.77				putative biotin carboxylase/biotin carboxyl carrier protein
PA2894		-1.52				conserved hypothetical protein
PA2921		1.51				transcriptional regulator
PA2932		1.67				morphinone

						reductase
PA2939		2.08				putative aminopeptidase
PA2941	1.57	1.58				putative magnesium chelatase
PA2966	-2.28	-2.01				acyl carrier protein
PA3006					1.59	transcriptional regulator PsrA
PA3009		-1.62				conserved hypothetical protein
PA3022		1.51				conserved hypothetical protein
PA3031	-2.01	-2.38				putative lipoprotein
PA3033		-1.52				conserved hypothetical protein
PA3035	-1.74					putative glutathione S-transferase
PA3041	1.56	1.82				putative membrane protein
PA3042	1.99	2.02				conserved hypothetical protein
PA3044	1.55					putative two-component sensor
PA3046		-1.60				conserved hypothetical protein
PA3054		1.60			-1.55	putative carboxypeptidase
PA3056		-1.65				hypothetical protein
PA3077	-1.54					putative two-component system regulatory protein
PA3100		1.50				general secretion pathway outer membrane protein H precursor
PA3123	-1.50					putative translation initiation inhibitor
PA3126		3.91	1.52			putative small heat shock protein
PA3133	-1.52		-1.58			putative transcriptional regulator
PA3140	-1.80	-1.88				putative competence protein
PA3178	-1.51	-1.57				hypothetical protein
PA3180		-1.51				putative 7,8-dihydro-8-oxoguanine-

						triphosphatase
PA3182	1.63	1.75				6-phosphogluconolactonase
PA3192		1.55				two-component response regulator GltR
PA3207	1.60					hypothetical protein
PA3221		-1.85				CsaA protein
PA3224	-1.52	-1.80				hypothetical protein
PA3232	1.58					putative nuclease
PA3235	-1.87	-2.08				putative membrane protein
PA3253					-1.75	putative permease of ABC transporter
PA3254					-1.58	putative ATP-binding component of ABC transporter
PA3260		-1.69				putative transcriptional regulator
PA3266		-2.14				cold acclimation protein B
PA3268		-2.03	-1.50			putative TonB-dependent receptor
PA3272		1.59				putative ATP-dependent DNA helicase
PA3274			1.94			conserved hypothetical protein
PA3276	-1.81	-2.31				hypothetical protein
PA3278	-1.77					hypothetical protein
PA3295	-1.82	-1.75				putative HIT family protein
PA3302		-1.50				(R)-specific enoyl-CoA hydratase
PA3313	-1.55					putative ABC-type phosphate/phosphonate transport system, periplasmic component
PA3314		1.56				probable ABC transporter ATP-binding component
PA3324	1.75					putative short-chain dehydrogenase
PA3325	1.50	1.58	1.50			putative hydrolase

PA3327		1.67				putative non-ribosomal peptide synthetase
PA3328		1.73				putative FAD-dependent monooxygenase
PA3329		1.81				hypothetical protein
PA3330		2.15				putative short chain dehydrogenas
PA3331		2.16				cytochrome P450
PA3332		1.69				putativ isomerase
PA3333		1.86				3-oxoacyl-[acyl-carrier-protein] synthase III
PA3335		2.18				hypothetical protein
PA3336		1.80				putative MFS transporter
PA3338	-1.96	-2.03				conserved hypothetical protein
PA3360		1.65				putative HlyD family secretion protein
PA3367	-1.71					hypothetical protein
PA3376		2.26				putative phosphonate ABC transporter, ATP-binding protein
PA3378		2.26				putative phosphonate metabolism protein
PA3384		-1.78				ATP-binding component of ABC phosphonate transporter
PA3385		-1.77				DNA binding-protein
PA3386	1.61					conserved hypothetical protein
PA3389		-2.12				putative ring-cleaving dioxygenase
PA3392	1.75		1.57			nitrous-oxide reductase precursor
PA3393	2.19		1.87			copper ABC transporter periplasmic substrate-binding protein
PA3394	2.63		1.97			ATP/GTP binding protein NosF'

PA3395	1.67		1.52			nitrous-oxide reductase, nosY component
PA3396	1.72		1.62			putative nitrous oxide reductase protein
PA3399	-1.51	-1.64				hypothetical protein
PA3403a	-1.58	-2.21				conserved hypothetical protein
PA3405		2.10				metalloprotease secretion protein
PA3412	-2.38					conserved hypothetical protein
PA3415	1.75					putative dihydrolipoamide acetyltransferase
PA3416	1.58	1.62				putative pyruvate dehydrogenase E1 component, beta subunit
PA3417		1.67				putative pyruvate dehydrogenase E1 component, alpha subunit
PA3428					2.01	hypothetical protein
PA3429	2.68	1.50				putative hydrolase, alpha/beta fold family
PA3431	1.72					putative murein hydrolase export regulator
PA3436	1.55					putative membrane protein
PA3437		-1.71				oxidoreductase, short chain dehydrogenase/reductase
PA3441		3.86				putative molybdopterin-binding protein
PA3442		7.27				putative aliphatic sulfonate transport ATP-binding protein
PA3443	-1.86	6.03	-1.65		-1.56	putative aliphatic sulfonates transport permease protein
PA3444	-1.86	7.25			-1.75	putative sulfonate monooxygenase

PA3445	-1.76	3.47				putative ABC-type transporter periplasmic sulfonate-binding protein
PA3446	-1.98	3.71				putative NADH-dependent FMN reductase
PA3447		3.51				putative sulfonate transport system, ATP-binding protein
PA3448		3.39				putative aliphatic sulfonates ABC transporter
PA3449		3.91				putative sulfonate binding protein
PA3450	-2.37	2.34		1.51		putative thiol-specific antioxidant protein
PA3467	-1.59					putative MFS transporter
PA3478		1.72				rhamnosyltransferase chain B
PA3496			-2.06			conserved hypothetical protein
PA3518	3.22	2.53	2.45		2.38	hypothetical protein
PA3524	-1.62	-2.33				lactoylglutathione lyase
PA3533	-1.56	-2.51				glutaredoxin-related protein
PA3536		-1.51				hypothetical protein
PA3540	-1.61					GDP-mannose 6-dehydrogenase AlgD
PA3547			2.02			poly(beta-d-mannuronate) lyase precursor AlgL
PA3552					-1.75	putative aminotransferease
PA3553					-1.72	putative glycosyl transferase
PA3554					-1.77	putative transformylase
PA3555					-1.63	putative polysaccharide deacetylase
PA3556					-1.69	4-amino-4-deoxy-L-arabinose transferase

PA3557					-1.63	putative inner membrane protein
PA3558					-1.57	putative membrane protein
PA3559					-1.76	putative nucleotide sugar dehydrogenase
PA3569		-1.58				3-hydroxyisobutyrate dehydrogenase
PA3570		-1.76				methylmalonate-semialdehyde dehydrogenase
PA3578	1.61					putative phenazine biosynthesis protein, PhzF family
PA3580		-2.12				conserved hypothetical protein
PA3581		-1.56				glycerol uptake facilitator protein
PA3582		-1.60				glycerol kinase
PA3583		-1.97				glycerol-3-phosphate regulon repressor
PA3584	1.72	-1.69				glycerol-3-phosphate dehydrogenase
PA3585		-1.57				membrane protein GlpM
PA3596		1.63				putative methylated-DNA--protein-cysteine methyltransferase
PA3597		-1.58				putative amino acid/amine transport protein
PA3603	-1.53	-1.58				diacylglycerol kinase
PA3607	-2.14					polyamine transport protein PotA
PA3609	-1.65					polyamine transport protein PotC
PA3611	-1.53	-1.74				putative secreted protein
PA3613					-1.64	conserved hypothetical protein
PA3621	-2.57	-1.97				ferredoxin I
PA3622		1.59				sigma factor RpoS
PA3626		1.50				putative tRNA pseudouridine

						synthase D
PA3657		-1.50				methionine aminopeptidase, type I
PA3662		-1.53				hypothetical protein
PA3671		1.72			1.57	putative permease of ABC transporter
PA3674	-1.62	-1.53				putative lipoprotein
PA3717	-1.58					putative FkbP-type peptidyl-prolyl cis-trans isomerase
PA3720		-1.59				conserved hypothetical protein
PA3722		-1.59				conserved hypothetical protein
PA3724		1.51				elastase LasB
PA3728		1.51				hypothetical protein
PA3730		1.59				hypothetical protein
PA3733a		-1.52				conserved hypothetical protein
PA3742	-1.63	-2.04				50S ribosomal protein L19
PA3747		-1.64				putative ABC-type transport permease
PA3750	1.72	1.69				putative Lysophospholipase
PA3752	2.21	2.17				conserved hypothetical protein
PA3755		-1.53				MutT/nudix family protein
PA3759		1.51				putative glucosamine-fructose-6-phosphate aminotransferase
PA3762	-1.52					conserved hypothetical protein
PA3776	-1.68		-1.66			putative transcriptional regulator, LysR family
PA3784		1.54				conserved hypothetical protein
PA3787		-1.56				putative peptidase
PA3789		1.59				putative iron-regulated membrane protein
PA3793	-1.84	-1.94				hypothetical protein

PA3794		-1.58				hypothetical protein
PA3807		-1.67				nucleoside diphosphate kinase
PA3808	1.61					conserved hypothetical protein
PA3812	1.57					putative iron-binding protein IscA
PA3815	1.62	-1.79				putative Rrf2 family protein
PA3826		-1.74				putative membrane protein
PA3835	-2.63					hypothetical protein
PA3840					-1.61	conserved hypothetical protein
PA3842	-1.76	-2.26				probable chaperone
PA3847		-1.66				conserved hypothetical protein
PA3859	-1.79				-1.59	carboxylesterase
PA3859		-1.89				hypothetical protein
PA3870	3.32	1.60	2.29			molybdenum cofactor biosynthesis protein A
PA3871	3.05	1.66	2.21			putative peptidyl-prolyl cis-trans isomerase
PA3872	2.07		1.67			respiratory nitrate reductase gamma chain
PA3873	2.46	1.52	1.83			respiratory nitrate reductase delta chain
PA3874	2.35		1.94		-1.58	respiratory nitrate reductase beta subuni
PA3875	1.56		1.66		-2.01	putative respiratory nitrate reductase alpha subun
PA3876	1.51		1.51		-1.65	nitrite extrusion protein
PA3884	1.63	1.62				hypothetical protein
PA3898		-1.56				putative transcriptional regulator, AraC family
PA3899		-1.58			1.51	putative RNA polymerase sigma-70 factor, ECF subfa
PA3902	-1.56	-1.66				conserved hypothetical protein

PA3905		1.52				hypothetical protein
PA3906		1.64				hypothetical protein
PA3907		1.62				hypothetical protein
PA3911	1.50					Putative lipid carrier protein
PA3914	1.79	1.60	1.52			MoeA1, Molybdopterin biosynthesis enzyme
PA3917	1.51	1.57				molybdopterin converting factor, small subunit
PA3920	2.10	1.63				probable metal transporting P-type ATPase
PA3929		1.62				CioB, cyanide insensitive terminal oxidase
PA3930		1.59				CioA, cyanide insensitive terminal oxidase
PA3931	-1.92	4.05				conserved hypothetical protein
PA3932	-1.69	5.25				probable transcriptional regulator
PA3935		2.96				TauD
PA3936		2.80				probable permease of ABC taurine transporter
PA3937		2.41				probable ATP-binding component of ABC taurine tran
PA3938		1.81				probable ABC-type taurine transporter, periplasmic component
PA3940	-2.12	-1.91				histone-like protein HU form N
PA3952		1.93				conserved hypothetical protein
PA3953	-1.67					possible isochorismatase family protein
PA3962	-1.57	-1.52				hypothetical protein
PA3965		-1.69				probable AsnC-family transcriptional regulator
PA3971	1.75					conserved

						hypothetical protein
PA3979		-1.53				conserved hypothetical protein
PA3997	1.51					lipoate-protein ligase B
PA4006	1.50	1.55				NadD nicotinic acid mononucleotide adenylyltransferase
PA4031	-1.80	-1.68				PPase
PA4033	-1.59	-1.96	-1.59		-1.98	hypothetical protein
PA4055	1.52					riboflavin synthase subunit alpha
PA4080	1.61					putative regulator of capsule synthesis
PA4087		-2.20				conserved hypothetical protein
PA4090	-2.27	-3.02				conserved hypothetical protein
PA4096			1.68			putative major facilitator family transporter
PA4099	-1.87					putative porin
PA4121	-2.56					putative 4-hydroxyphenylacetate degradation bifunctional isomerase
PA4127		1.84				2-oxo-hepta-3-ene-1,7-dioic acid hydratase
PA4128	1.55	3.07				putative 2,4-dihydroxyhept-2-ene-1,7-dioic acid aldolase
PA4129		2.35				conserved hypothetical protein
PA4130		1.76				putative sulfite or nitrite reductas
PA4131		1.89				putative iron-sulfur cluster-binding protein
PA4132		2.24				putative transcriptional regulator, GntR family
PA4133		3.35				cytochrome c oxidase subunit (cbb3-type)

PA4134		3.80				hypothetical protein
PA4136		1.89				putative MFS transporter
PA4139	-1.76					hypothetical protein
PA4142		1.51				putative secretion protein
PA4143		1.61				putative toxin transporter
PA4144		1.63				putative outer membrane protein precursor
PA4151		-1.74				acetoin catabolism protein AcoB
PA4152		1.52				putative hydrolase
PA4175		1.70				Pvds-regulated endoprotease, lysyl class
PA4188					-1.57	putative dihydrodipicolinate synthase
PA4198		-1.73				putative AMP-binding enzyme
PA4205	-1.75					putative membrane protein
PA4208	1.50	1.71				outer membrane protein
PA4209		2.08				probable phenazine-specific methyltransferase
PA4210		2.83				probable phenazine biosynthesis protein
PA4211		2.39				probable phenazine biosynthesis protein
PA4217		2.69				hypothetical protein
PA4218					-1.50	putative transporter
PA4222		2.01			-1.61	putative ATP-binding component of ABC transporter
PA4223		1.73			-1.76	putative ATP-binding component of ABC transporter
PA4224		1.89			-1.70	pyochelin biosynthetic protein PchG
PA4225					-1.58	pyochelin synthetase PchF
PA4238		1.51				DNA-directed RNA polymerase subunit

						alpha
PA4245	1.58	2.02				50S ribosomal protein L30
PA4256					-1.50	50S ribosomal protein L16
PA4261	1.55	1.77				50S ribosomal protein L23
PA4264		-1.51				30S ribosomal protein S10
PA4267		1.50				30S ribosomal protein S7
PA4290		-1.63				putative chemotaxis transducer
PA4295					1.70	putative pilus assembly protein
PA4300	1.70	1.83				putative pilus assembly protein
PA4313	1.62					putative membrane protein
PA4315	-1.97	-2.59				transcriptional regulator MvaT, P16 subunit
PA4326		-1.99				putative lipoprotein
PA4327	-1.51					hypothetical protein
PA4343	-1.80					putative MFS transporter
PA4349	1.51	1.60				conserved hypothetical protein
PA4350	1.82	1.96	1.80			putative hemolysin
PA4351	1.60	1.84				putative acyltransferase
PA4354	-2.30	-2.09				putative transcriptional regulator
PA4365	-1.64	-2.12				putative permease
PA4367		-1.58				putative GGDEF domain/EAL domain protein
PA4371		-1.69				putative thiol oxidoreductase
PA4377		-1.50				conserved hypothetical protein
PA4383		-1.96				putative integral membrane protein
PA4385		4.46				GroEL protein
PA4386		3.27				Hsp10 protein
PA4387		2.18				putative membrane

						protein
PA4390					1.51	conserved hypothetical protein
PA4428		1.56				stringent starvation protein A
PA4430		1.83				putative cytochrome b
PA4431	-1.69					putative cytochrome c reductase, iron-sulfur subun
PA4441		-2.06				conserved hypothetical protein
PA4442		2.74				ATP sulfurylase GTP-binding subunit/APS kinase
PA4443		1.76				ATP sulfurylase small subunit
PA4452		1.58				conserved hypothetical protein
PA4464		1.53				nitrogen regulatory IIA protein
PA4467					-1.65	putative heavy-metal transporter
PA4468		1.62				superoxide dismutase
PA4472		1.51				PmbA protein
PA4473		-1.63				conserved hypothetical protein
PA4474		1.65				putative tldD protein
PA4488		1.58				conserved hypothetical protein
PA4490		1.53				conserved hypothetical protein
PA4503		1.51				putative dipeptide ABC transport system permease
PA4512		-1.66				lipopolysaccharide biosynthetic protein LpxO1
PA4514		-1.71				putative outer membrane ferric siderophore receptor
PA4515		-1.96			2.05	putative iron-regulated protein
PA4516					1.69	conserved hypothetical protein
PA4522		-1.64				beta-lactamase expression regulator

PA4532		1.54				conserved hypothetical protein
PA4537	-1.50					conserved hypothetical protein
PA4545		-1.54				competence lipoprotein ComL
PA4550		-2.41				type 4 fimbrial biogenesis protein FimU
PA4563	-2.28	-2.57				ribosomal protein S20
PA4567		-1.50				50S ribosomal subunit protein L27
PA4569		-1.51				octaprenyl-diphosphate synthase
PA4571					-1.64	putative cytochrome c precursor
PA4597		1.92				outer membrane protein OprJ
PA4598					-1.65	multidrug efflux RND transporter MexD
PA4600	-1.51					transcriptional regulatory protein NfxB
PA4605	1.92	1.88				conserved hypothetical protein
PA4610	-1.68					conserved hypothetical protein
PA4611	-1.59		1.52			conserved hypothetical protein
PA4614	-2.37	-2.83				large conductance mechanosensitive channel
PA4618	1.58					putative xanthine dehydrogenase accessory factor X
PA4620	1.74					putative oxidoreductase, small subunit
PA4637	-1.56					conserved hypothetical protein
PA4639	-1.66	-1.74				putative lipoprotein
PA4643		-1.50				conserved hypothetical protein
PA4644		1.51				conserved hypothetical protein
PA4650	-2.15					conserved

						hypothetical protein
PA4654			1.57			putative MFS transporter
PA4659					-1.54	putative transcriptional regulator, MerR family
PA4669		-1.52				isopentenyl monophosphate kinase
PA4674	1.79	1.99				putative virulence-associated protein
PA4675		-1.82				putative TonB-dependent receptor
PA4687		-1.69				ferric iron-binding periplasmic protein HitA
PA4697	-1.83	-2.20				conserved hypothetical protein
PA4706	1.64	1.72				putative ATP-binding component of ABC transporter
PA4723	-2.16	-2.23				suppressor protein DksA
PA4731	-1.59					aspartate 1-decarboxylase precursor
PA4737		1.54				conserved hypothetical protein
PA4738	-1.75				1.65	conserved hypothetical protein
PA4739					1.62	conserved hypothetical protein
PA4750	1.54					dihydropteroate synthase
PA4753	-1.65	-1.98				putative RNA-binding protein
PA4757	1.50	1.60				putative transmembrane protein
PA4759		4.02				dihydrodipicolinate reductase
PA4760		3.69				chaperone protein DnaJ
PA4761		4.01				putative heat shock protein
PA4762		3.43				heat shock protein GrpE

PA4765	-1.79	-1.88				outer membrane lipoprotein OmlA precursor
PA4766	1.72	1.69				conserved hypothetical protein
PA4773			-1.57		-1.50	putative S-adenosylmethionine decarboxylase proenzyme
PA4774			-1.81		-1.72	putative spermidine synthase
PA4775			-1.69		-1.81	conserved hypothetical protein
PA4776			-1.64		-1.81	two-component response regulator
PA4777					-1.72	two-component sensor
PA4793	-1.55	-1.83				putative lipoprotein
PA4801		-1.69				hypothetical protein
PA4806		-1.60				putative transcriptional regulator
PA4823					-5.53	putative transcriptional regulator
PA4831	-1.57					transcriptional regulator
PA4841	1.71	1.55				putative isopentenyldiphosphate isomerase
PA4844	1.69		1.67			putative chemotaxis transducer
PA4853			-1.54			DNA-binding protein Fis
PA4863	-1.65					putative acetyltransferase
PA4866		1.65				putative phosphinothricin N-acetyltransferase
PA4867		1.77				urease subunit beta
PA4874	-1.70	-1.56				putative phosphate starvation-inducible protein
PA4876	-1.89	-2.21				osmotically inducible lipoprotein OsmE
PA4881					1.91	hypothetical protein
PA4885			1.89			two-component response regulator

PA4888	1.71	-1.60				putative fatty acid desaturase
PA4889	1.82					putative oxidoreductase
PA4890		-1.70				putative transcriptional regulator, TetR family
PA4891		-1.52				urease accessory protein UreE
PA4893		-1.92	-1.80		-1.52	urease accessory protein UreG
PA4894		-1.61	-1.51			urease accessory protein
PA4900	1.54					putative MFS transporter
PA4907		-1.51				putative oxidoreductase
PA4916	1.52					putative ADP-ribose pyrophosphatase
PA4922	-1.51					azurin precursor
PA4933		1.64				putative membrane protein
PA4934		1.50				30S ribosomal protein S18
PA4935	-1.61					30S ribosomal protein S6
PA4943		1.57				putative GTP-binding protein
PA4980		-1.78				putative enoyl-CoA hydratase/isomerase
PA4989	-1.52					putative transcriptional regulator
PA4990	-1.80					putative SMR multidrug efflux transporter
PA5016		1.58				dihydrolipoamide acetyltransferase
PA5020					-1.53	putative acyl-CoA dehydrogenase
PA5023	1.59					conserved hypothetical protein
PA5024		2.15			1.55	putative membrane protein
PA5053		3.01				heat shock protein HslV
PA5054		4.00				heat shock protein HslU

PA5055	-1.52					conserved hypothetical protein
PA5059		1.56				putative transcriptional regulator, TetR family
PA5061	-1.61	-1.76				putative poly(hydroxyalcanoate) granule associated protein
PA5062	-1.60	-1.70				conserved hypothetical protein
PA5082	1.69		1.78			putative binding protein component of ABC transporter
PA5083	1.60		1.79			putative translation initiation inhibitor
PA5084	2.42		2.06			putative amino acid oxidase
PA5093		1.58				probable histidine/phenylalanine ammonia-lyase
PA5101		2.48				putative ABC-type phosphate/phosphonate transport system, periplasmic component
PA5102		2.78				putative fatty acid desaturase
PA5103		1.55				putative ABC transporter, periplasmic substrate-binding protein
PA5104	1.62					conserved hypothetical protein
PA5125	1.58					two-component response regulator NtrC
PA5130		-1.52				putative rhodanese-like domain protein
PA5157	-1.63					putative multiple antibiotic resistance protein MarR
PA5158	-1.61					putative outer membrane protein precursor
PA5160		-1.69				drug efflux transporter

PA5168	2.04	1.65				probable dicarboxylate transporter
PA5169	1.69					probable C4-dicarboxylate transporter
PA5171		1.85	1.51		-1.74	arginine deiminase
PA5172		1.97	1.76		-1.60	ornithine carbamoyltransferase, catabolic
PA5173	1.60	2.36	1.79			carbamate kinase
PA5176		-1.61				putative DP compound hydrolase
PA5183a	-3.00	-2.36				conserved hypothetical protein
PA5191	-1.54	-1.76				hypothetical protein
PA5195	-2.07	-2.87			-1.55	putative ribosome-associated heat shock protein
PA5196	-1.56					conserved hypothetical protein
PA5202			-1.51			conserved hypothetical protein
PA5207					-1.57	probable phosphate transporter
PA5208	-1.56					putative phosphate transport regulator
PA5212		-1.77				conserved hypothetical protein
PA5214	-1.52					glycine cleavage system protein H1
PA5217		-1.65			1.51	putative iron ABC transporter, periplasmic iron-binding protein
PA5219	-1.69					putative permease
PA5233		-1.61				putative flagellar protein FliL
PA5235		-2.06				glycerol-3-phosphate transporter
PA5240	-2.18	-2.21				thioredoxin
PA5252a		-1.77				conserved hypothetical protein
PA5266	2.02	1.81				conserved hypothetical protein
PA5274	-1.70	-1.64				nucleoside diphosphate kinase

						regulator
PA5275		-2.26				putative CyaY protein
PA5285	-2.77	-2.21				conserved hypothetical protein
PA5287	1.53					ammonium transporter AmtB
PA5289	-1.56	-1.77				conserved hypothetical protein
PA5298	-1.83	-1.62				xanthine phosphoribosyltransferase
PA5300	-1.85	-1.73				cytochrome c5
PA5303	-1.53					putative endoribonuclease L-PSP family protein
PA5308	-1.52	-1.61				leucine responsive regulatory protein
PA5315		2.11			2.05	50S ribosomal protein L33
PA5316	-2.17	-2.34				50S ribosomal protein L28
PA5318		1.60				hypothetical protein
PA5339	-1.62	-1.54				putative endoribonuclease L-PSP
PA5347		-1.84				conserved hypothetical protein
PA5348	-2.38	-2.63				putative DNA-binding protein HU family
PA5351	-2.02	-2.52				rubredoxin 1
PA5354	1.52					glycolate oxidase subunit GlcE
PA5371	-1.76	-1.76				putative long-chain acyl-CoA thioester hydrolase
PA5388	-2.51					putative glycine betaine/L-proline ABC transporter, periplasmic substrate-binding protein
PA5395		-1.51				conserved hypothetical protein
PA5401		1.50				putative electron transfer flavoprotein, beta subunit

PA5406	electron transfer flavoprotein beta subunit					K03521
PA5419		1.50				sarcosine oxidase gamma subunit
PA5424	1.68	1.58				putative membrane protein
PA5429	-1.54	-1.57				aspartate ammonia-lyase
PA5435	1.52					putative transcarboxylase subunit
PA5440a	1.59					hypothetical protein
PA5446		1.62				conserved hypothetical protein
PA5461	-1.85	-2.21				conserved hypothetical protein
PA5465		-1.68				conserved hypothetical protein
PA5471	1.52					conserved hypothetical protein
PA5482		3.13				conserved hypothetical protein
PA5496		1.63	1.55			conserved hypothetical protein
PA5506	-1.63	-1.57				putative transcriptional regulator
PA5531					1.65	periplasmic protein tonB
PA5533	-1.50	-1.81				conserved hypothetical protein
PA5537		-1.77				conserved hypothetical protein
PA5558		1.53				ATP synthase B chain

B.2 R scripts

B.2.1 R code for generating the GO terms

```
BiocManager::install('KEGGREST',force = TRUE)
```

```
library(KEGGREST)

library(stringr)

org<-keggList('organism')

head(org)

org[str_detect(org[,3],'Pseudomonas aeruginosa UCBPP')]

pau_path<-keggLink('pathway','pau')

length(unique(names(pau_path))) # 1993

length(unique((pau_path))) # 123


pau.kegg<-data.frame(term=unname(pau_path),

                     gene=names(pau_path))

pau.kegg$gene<-str_replace_all(pau.kegg$gene,'pau:','')

pau.kegg.description<-read.table('/Users/yihuawang/Downloads/pau00001.txt',

                                 header = F,sep = '\t')

pau.kegg.description$Decribption <- gsub("^.{0,6}", "", pau.kegg.description$V1)

pau.kegg.description<-pau.kegg.description[,2:3]

colnames(pau.kegg.description)[1]<-'term'

pau.kegg.description$term<-gsub('PATH','path',pau.kegg.description$term)

pau.kegg.description<-pau.kegg.description[grepl('path',pau.kegg.description$term),]

#intersect(pau.kegg.description$term,pau.kegg$term)

#unique(pau.kegg$term)

pau.kegg<-merge(pau.kegg,pau.kegg.description,by='term')

library(clusterProfiler)

genesets<-pau.kegg
```

```
egmt<-GSEA(genelist, TERM2GENE = genesets,
        verbose = T,pvalueCutoff =1)
gene_list<-read.xlsx('/Users/yihuawang/Downloads/Total-1.xlsx')


gene_list_hptA_up<-gene_list[gene_list$hptA>0,]
KEGG_result_hptA_up<-enricher(gene_list_hptA_up$old_locus_tag,
                      TERM2GENE = genesets[,1:2],
                      TERM2NAME =genesets[,c(1,3)])
head(KEGG_result_hptA_up)



gene_list_hptA_down<-gene_list[gene_list$hptA<0,]
KEGG_result_hptA_down<-enricher(gene_list_hptA_down$old_locus_tag,
                       TERM2GENE = genesets[,1:2],
                       TERM2NAME =genesets[,c(1,3)])
head(KEGG_result_hptA_down)
gene_list_hptB_up<-gene_list[gene_list$hptB>0,]
KEGG_result_hptB_up<-enricher(gene_list_hptB_up$old_locus_tag,
                      TERM2GENE = genesets[,1:2],
                      TERM2NAME =genesets[,c(1,3)])
head(KEGG_result_hptB_up)


gene_list_hptB_down<-gene_list[gene_list$hptB<0,]
KEGG_result_hptB_down<-enricher(gene_list_hptB_down$old_locus_tag,
```

```
                    TERM2GENE = genesets[,1:2],
                    TERM2NAME =genesets[,c(1,3)])
head(KEGG_result_hptB_down)
gene_list_hptC_up<-gene_list[gene_list$hptC>0,]
KEGG_result_hptC_up<-enricher(gene_list_hptC_up$old_locus_tag,
                    TERM2GENE = genesets[,1:2],
                    TERM2NAME =genesets[,c(1,3)])
head(KEGG_result_hptC_up)
gene_list_hptC_down<-gene_list[gene_list$hptC<0,]
KEGG_result_hptC_down<-enricher (gene_list_hptC_down$old_locus_tag,
                    TERM2GENE = genesets[,1:2],
                    TERM2NAME =genesets[, c(1,3)])
head(KEGG_result_hptC_down)
save(pau.kegg,pau.kegg.description,gene_list,
    gene_list_hptB_up,gene_list_hptB_up,gene_list_hptC_up,
KEGG_result_hptA_down,KEGG_result_hptB_down,KEGG_result_hptC_down,file='Huying.RData')
rm(pau.kegg,pau.kegg.description,gene_list,egmt,org,pau_path,genesets,gene_list,
  gene_list_hptB_up,gene_list_hptB_up,gene_list_hptC_up,
  KEGG_result,
  KEGG_result_hptA_up, KEGG_result_hptB_up,KEGG_result_hptC_up,
  KEGG_result_hptA_down, KEGG_result_hptB_down,KEGG_result_hptC_down,
  gene_list_hptA_up,gene_list_hptB_up,gene_list_hptC_up,
  gene_list_hptA_down,gene_list_hptB_down,gene_list_hptC_down
)
```

Appendix C Supplementary information for chapter 4

C.1 Tables

C.1.1 Natural compounds list which effects on the bacterial growth selected from bacterial cell-based screen model

No.	Name of Natural Compound	MWt	Z-score$_{lux}$
HY103	Hematoxylin	302.28	-3.949
HY082	Erythromycin*	733.93	-3.436
HY188	Tetracycline hydrochloride*	480.9	-3.241
HY153	Parthenolide	248.32	-2.776
HY076	Doxycycline Hyclate*	512.94	-2.680
HY099	Gossypol	518.55	-2.565
HY178	Shikonin	288.3	-2.512
HY038	Azomycin*	113.07	-2.510
HY064	cis-5,8,11,14,17-Eicosapentaenoic acid	302.45	-2.375
HY073	Dimethylfumarate	144.13	-2.358
HY057	Chloramphenicol*	323.13	-2.281
HY171	Rifampicin*	822.94	-2.210
HY146	Oleamide	281.48	-2.200

*Antibiotic

C.1.2 Natural product extracts list which effects on the bacterial growth selected from bacterial cell-based screen model

No.	Natural compond name	Extract Type	Z-score$_{lux}$
CB105	*Citrus limetta*	Polar	2.003
CB160	*Fragaria vesca*	Polar	2.008
CB065	*Brassica nigra*	Polar	2.024
CB233	*Mitchella repens*	Polar	2.033
CB348	*Stachys betonica*	Polar	2.222
CB145	*Epilobium parviflorum*	Polar	2.242
CB346	*Solidago virgaurea*	Polar	2.392
CB379	*Vanilla planifolia*	Polar	2.430
CB358	*Taraxacum officinale*	Polar	2.541
CB024	*Anemone pulsatilla*	Polar	2.626
CB315	*Ribes nigrum*	Polar	2.628
CB371	*Ulva prolifera*	Polar	2.681
CB228	*Melissa officinalis*	Polar	3.008
CB182	*Hibiscus sabdariffa*	Polar	3.174
CB273	*Piscidia piscipula*	Polar	3.183

CB388	*Vinca major*	Polar	3.357
CB132	*Cynara cardunculus*	Polar	3.398
CB204	*Lavandula angustifolia*	Polar	3.481
CB009	*Alchemilla vulgaris*	Polar	4.945
CB620	*Malva vulgaris*	Nonpolar	-3.852
CB512	*Cnicus benedictus*	Nonpolar	-3.782
CB661	*Peumus boldus*	Nonpolar	-3.683
CB590	*Inula helenium*	Nonpolar	-3.668
CB419	*Althaea officinalis*	Nonpolar	-3.126
CB653	*Papaver somniferum*	Nonpolar	-2.891
CB659	*Persea americana*	Nonpolar	-2.711
CB672	*Piper nigrum*	Nonpolar	-2.359
CB735	*Sanguinaria canadensis*	Nonpolar	-2.068
CB658	*Paullinia cupana*	Nonpolar	-2.000
CB779	*Vanilla planifolia*	Nonpolar	2.054
CB405	*Aesculus hippocastanum*	Nonpolar	2.423
CB763	*Thymus vulgaris*	Nonpolar	2.575
CB403	*Acorus calamus*	Nonpolar	2.849
CB787	*Vigna radiata*	Nonpolar	2.932
CB441	*Artemisia dracunculus*	Nonpolar	3.024
CB771	*Ulva prolifera*	Nonpolar	3.205
CB530	*Curcuma longa*	Nonpolar	3.539
CB484	*Carum carvi*	Nonpolar	4.012

C.1.3 Natural compounds list which influence c-di-GMP level selected from bacterial cell-based screen model

No.	Name of Natural Compound	MWt	%Inhibition$_{GFP}$ (nomolized LUX)	Z-score$_{lux}$
HY188	Tetracycline hydrochloride*	480.9	51%	-3.241
HY135	Myricetin	302.24	51%	-0.699
HY127	Magnolol	266.32	56%	1.930
HY187	Tanshinone IIA	294.34	59%	2.036
HY169	Resveratrol	228.24	59%	-0.254
HY078	Ellagic acid	302.19	61%	-0.729
HY076	Doxycycline Hyclate*	512.94	91%	-2.680
HY171	Rifampicin*	822.94	194%	-2.210

C.1.4 Natural product extracts list which influence c-di-GMP level selected from bacterial cell-based screen model

No.	Name of Natural Product Extract	Extract Type	%Inhibition$_{GFP}$ (nomolized LUX)	Z-score$_{lux}$

CB137	*Diospyros virginiana*	Polar	50%	0.247
CB008	*Agropyron repens*	Polar	50%	1.185
CB363	*Thymus vulgaris*	Polar	50%	0.329
CB087	*Cassia senna*	Polar	50%	1.218
CB210	*Garcinia mangostana*	Polar	50%	-0.151
CB294	*Prunus domestica*	Polar	51%	0.556
CB148	*Eruca sativa*	Polar	52%	1.332
CB393	*Vitis vinifera*	Polar	52%	-0.321
CB316	*Ribes rubrum*	Polar	52%	-0.280
CB365	*Trifolium pratense*	Polar	52%	0.066
CB046	*Asparagus racemosus*	Polar	52%	0.326
CB356	*Tanacetum vulgare*	Polar	52%	0.433
CB277	Passiflora ligularis	Polar	52%	1.020
CB192	*Iris versicolor*	Polar	52%	1.005
CB362	*Thymus citriodorus*	Polar	53%	0.248
CB373	*Urtica dioica*	Polar	54%	0.227
CB170	*Ginkgo biloba*	Polar	54%	0.942
CB054	*Acca sellowiana*	Polar	54%	-0.638
CB159	*Fragaria × ananassa*	Polar	54%	-0.136
CB369	*Tussilago farfara*	Polar	54%	-0.055
CB161	*Fraxinus excelsior*	Polar	55%	0.852
CB350	*Stillingia sylvatica*	Polar	55%	0.110
CB146	*Equisetum arvense*	Polar	55%	0.017
CB033	*Apium graveolens*	Polar	55%	1.149
CB150	*Eupatorium perfoliatum*	Polar	55%	1.294
CB317	*Ribes uva-crispa*	Polar	55%	-0.038
CB273	*Piscidia piscipula*	Polar	56%	3.183
CB025	*Anethum graveolens*	Polar	56%	1.386
CB323	*Rubus idaeus*	Polar	56%	-0.456
CB292	*Prunus avium*	Polar	56%	1.578
CB381	*Verbascum thapsus*	Polar	56%	0.657
CB266	*Quassia amara*	Polar	57%	1.557
CB118	*Collinsonia canadensis*	Polar	57%	0.470
CB147	*Eriodictiyo californicum*	Polar	57%	1.924
CB107	*Citrus limon*	Polar	57%	0.426
CB024	*Anemone pulsatilla*	Polar	57%	2.626
CB189	*Indigofera tinctoria*	Polar	58%	1.527
CB023	*Anemone pulsatilla*	Polar	58%	1.943
CB361	*Thuja occidentalis*	Polar	58%	0.318
CB364	*Tilia platyphyllos*	Polar	58%	0.773
CB255	*Passiflora edulis*	Polar	58%	-0.245
CB190	*Inula helenium*	Polar	58%	1.421
CB233	*Mitchella repens*	Polar	59%	2.033
CB182	*Hibiscus sabdariffa*	Polar	59%	3.174
CB132	*Cynara cardunculus*	Polar	59%	3.398
CB012	*Allium cepa*	Polar	59%	1.694
CB338	*Scutellaria lateriflora*	Polar	60%	0.459
CB021	*Ananas comosus*	Polar	60%	0.337
CB315	*Ribes nigrum*	Polar	61%	2.628
CB188	*Ilex paraguariensis*	Polar	62%	1.912

CB145	*Epilobium parviflorum*	Polar	63%	2.242
CB390	*Viola tricolor*	Polar	64%	0.154
CB106	*Citrus limon*	Polar	64%	-0.114
CB204	*Lavandula angustifolia*	Polar	64%	3.481
CB105	*Citrus limetta*	Polar	64%	2.003
CB314	*Ribes nigrum*	Polar	64%	0.844
CB278	Pelvetia canaliculata	Polar	65%	1.193
CB228	*Melissa officinalis*	Polar	65%	3.008
CB357	*Taraxacum officinale*	Polar	67%	0.850
CB065	*Brassica nigra*	Polar	67%	2.024
CB135	Fucus spiralis	Polar	68%	1.309
CB396	*Zanthoxylum americanum*	Polar	68%	1.917
CB237	*Myrica cerifera*	Polar	70%	0.379
CB009	*Alchemilla vulgaris*	Polar	71%	4.945
CB348	*Stachys betonica*	Polar	71%	2.222
CB398	*Zea mays*	Polar	71%	1.439
CB104	*Citrus limetta*	Polar	72%	1.022
CB388	*Vinca major*	Polar	73%	3.357
CB355	*Tanacetum parthenium*	Polar	76%	1.856
CB387	*Vigna radiata*	Polar	77%	1.136
CB346	*Solidago virgaurea*	Polar	77%	2.392
CB358	*Taraxacum officinale*	Polar	79%	2.541
CB379	*Vanilla planifolia*	Polar	80%	2.430
CB371	*Ulva prolifera*	Polar	84%	2.681
CB441	*Artemisia dracunculus*	Non-polar	56%	3.024
CB763	*Thymus vulgaris*	Non-polar	59%	2.575
CB570	*Ginkgo biloba*	Non-polar	66%	0.353
CB462	*Bixa orellana*	Non-polar	92%	-1.259

C.1.5 Row data of the dose-response test for the "hits" selected from bacterial cell-based screen model

Con. (uM)	**Log[nM]**	**%Inhibition$_{GFP}$**								
		Myricetin			Resveratrol			Ellagic acid		
2000000	6.30103	109%	110%	114%	92%	91%	93%	76%	72%	79%
1000000	6	99%	101%	100%	95%	95%	95%	84%	70%	80%
500000	5.69897	79%	79%	79%	89%	88%	86%	72%	66%	70%
250000	5.39794	61%	61%	61%	74%	72%	71%	65%	67%	68%
125000	5.09691	43%	41%	39%	64%	66%	59%	69%	69%	69%
62500	4.79588	28%	28%	27%	55%	60%	56%	68%	69%	64%
31250	4.49485	13%	19%	14%	52%	55%	51%	69%	69%	67%
15625	4.19382	13%	12%	10%	52%	52%	56%	53%	56%	54%
7812.5	3.89279	20%	20%	15%	51%	53%	44%	41%	41%	42%
3906.25	3.59176	11%	5%	6%	43%	40%	35%	36%	29%	31%

C.1.6 Output data of the quantified the 3D biofilm images

Biovolume (μm^3)	Live	Dead	Total
WT	57418.8	265.15	57683.95
	66313	614.89	66927.89
	75891	640.36	76531.36
WT+ Myricetin	39695.2	187.97	39883.17
	46990.7	261.59	47252.29
	58982.5	181.68	59164.18
WT+ Myricetin+ TB	3662.62	18053	21715.62
	4562.19	21823.2	26385.39
	4333.3	19617.9	23951.2
WT+TB	16228.7	23166.8	39395.5
	22133.7	26329.1	48462.8
	24748.6	29755.6	54504.2
WT	34248.7	794.764	35043.46
	31712	667.547	32379.55
	41408.9	461.287	41870.19
WT+ Resveratrol	23933.5	455.13	24388.63
	24995.9	300.893	25296.79
	23955.1	323.115	24278.21
WT+ Resveratrol+ TB	1161.41	3117.27	4278.68
	1257.22	3307.94	4565.16
	1221.64	3417.06	4638.7
WT+TB	5295.75	10582.1	15877.85
	7558.29	13072.4	20630.69
	7623.62	11738.7	19362.32
WT	57783.3	798.65	58581.95
	52280.6	617.89	52898.49
	54035.2	432.98	54468.18
WT+ Ellagic acid	27465.5	1075.2	28540.7
	27095	976.26	28071.26
	23465.4	751.16	24216.56
WT+ Ellagic acid+ TB	2329.44	47362	49691.44
	3059.38	49006.3	52065.68
	3366.05	47624.3	50990.35
WT+TB	6378.74	12195.3	18574.04
	4395.6	12569.7	16965.3
	5730.97	13396.1	19127.07

C.1.7 Natural compounds list which effects on the bacterial growth selected from human bronchial epithelial cell-based screen model

No.	Name of Natural Compound	MWt	Z-score$_{lux}$
HY158	Piceatannol	244.24	-3.459
HY163	Propyl gallate	212.2	-3.350

HY082	Erythromycin*	733.93	-3.218
HY103	Hematoxylin	302.28	-3.034
HY090	Gallic acid	170.12	-2.990
HY001	(-)-Epigallocatechin gallate (EGCG)	458.37	-2.933
HY039	Baicalein	270.24	-2.779
HY135	Myricetin	302.24	-2.578
HY178	Shikonin	288.3	-2.465
HY075	Dopamine	189.64	-2.398
HY076	Doxycycline Hyclate*	512.94	-2.192
HY099	Gossypol	518.55	-2.186
HY167	Quercetin (Sophoretin)	302.24	-2.185
HY040	Baicalin	446.37	-2.143
HY041	Berberine hydrochloride	371.81	-2.138
HY181	Solanesol	631.07	2.033

C.1.8 Natural product extracts list which effects on the bacterial growth selected from human bronchial epithelial cell-based screen model

No.	Name of Natural Product Extract	Extract Type	Z-score$_{lux}$
CB037	*Arctostaphylos uva ursi*	Polar	-5.057
CB237	*Myrica cerifera*	Polar	-3.630
CB076	*Camellia sinensis*	Polar	-3.221
CB145	*Epilobium parviflorum*	Polar	-3.164
CB178	*Hamamelis virginiana*	Polar	-3.160
CB284	*Polygonum bistorta*	Polar	-3.145
CB102	*Cinnamomum verum*	Polar	-2.901
CB144	*Emblica officinalis*	Polar	-2.892
CB168	*Geranium maculatum*	Polar	-2.849
CB250	*Paeonia lactiflora*	Polar	-2.704
CB075	*Calluna vulgaris*	Polar	-2.641
CB331	*Salix alba*	Polar	-2.580
CB311	*Rheum palmatum*	Polar	-2.310
CB320	*Rosa spp*	Polar	-2.290
CB353	*Syzygium aromaticum*	Polar	-2.069
CB372	*Uncaria tomentosa*	Polar	-2.063
CB211	*Liriosma ovata*	Polar	2.135
CB342	*Smilax ornata*	Polar	2.171
CB410	*Alkenna tinctoria*	Non-polar	-3.745
CB721	*Rosmarinus officinalis*	Non-polar	-3.591
CB530	*Curcuma longa*	Non-polar	-3.449
CB547	*Eriodictiyo californicum*	Non-polar	-3.115
CB610	*Garcinia mangostana*	Non-polar	-3.062
CB576	*Guaiacum officinale*	Non-polar	-2.834
CB502	*Cinnamomum verum*	Non-polar	-2.677
CB573	*Glycyrrhiza glabra*	Non-polar	-2.549
CB431	*Anthemis nobilis*	Non-polar	-2.541

CB401	*Acacia senegal*	Non-polar	-2.509
CB799	*Zingiber officinale*	Non-polar	-2.427
CB735	*Sanguinaria canadensis*	Non-polar	-2.414
CB549	*Eucalyptus globulus*	Non-polar	-2.227
CB609	*Lepidium sativum*	Non-polar	-2.003
CB515	*Codonopsis pilosula*	Non-polar	2.041
CB458	*Berberis vulgaris*	Non-polar	2.224
CB507	*Citrus limon*	Non-polar	2.417
CB730	*Sabal serrulata*	Non-polar	2.992

C.1.9 Natural compounds list which influence c-di-GMP level selected from human bronchial epithelial cell-based screen model

No.	Name of Natural Compound	MWt		Z-score$_{lux}$
HY103	Hematoxylin	302.28	-906%	-3.034
HY025	Alpha-Mangostin	410.47	-258%	-1.534
HY067	Curcumin	368.38	-255%	-1.107
HY178	Shikonin	288.3	-134%	-2.465
HY099	Gossypol	518.55	-114%	-2.186
HY078	Ellagic acid	302.19	-104%	-1.520
HY007	10-Hydroxycamptothecin	364.36	-82%	0.056
HY064	cis-5,8,11,14,17-Eicosapentaenoic acid	302.45	-79%	-1.586
HY002	(-)-Scopolamine N-butyl bromide	440.37	-76%	-0.455
HY001	(-)-Epigallocatechin gallate (EGCG)	458.37	-52%	-2.933
HY010	3-hydroxy myristic acid	244.37	-50%	-0.092
HY046	Biochanin A (4-Methylgenistein)	284.26	51%	0.359
HY130	Methyl anthranilate	151.16	53%	-0.006
HY016	6,7-Dihydroxycoumarin	178.14	68%	1.368
HY188	Tetracycline hydrochloride*	480.9	78%	-0.422
HY076	Doxycycline Hyclate*	512.94	87%	-2.192
HY082	Erythromycin*	733.93	108%	-3.218
HY158	Piceatannol	244.24	110%	-3.459

C.1.10 Natural product extracts list which influence c-di-GMP level selected from human bronchial epithelial cell-based screen model

No.	Name of Natural Product Extract	Extract Type		Z-score$_{lux}$
CB005	*Aesculus hippocastanum*	Polar	-173%	-1.366
CB076	*Camellia sinensis*	Polar	-165%	-3.221
CB327	*Rumex crispus*	Polar	-151%	-1.053
CB385	*Viburnum prunifolium*	Polar	-151%	-1.768

CB054	*Acca sellowiana*	Polar	-148%	-1.442
CB117	*Cola vera, also Cola nitida*	Polar	-140%	-1.375
CB102	*Cinnamomum verum*	Polar	-132%	-2.901
CB075	*Calluna vulgaris*	Polar	-132%	-2.641
CB123	*Crataegus oxycanthoides*	Polar	-131%	-0.559
CB062	*Bixa orellana*	Polar	-126%	-0.135
CB160	*Fragaria vesca*	Polar	-120%	-1.328
CB007	*Agrimonia eupatoria*	Polar	-120%	-1.528
CB009	*Alchemilla vulgaris*	Polar	-119%	-1.517
CB325	*Rubus fruticosus*	Polar	-117%	-1.525
CB155	*Filipendula ulmaria*	Polar	-114%	-1.992
CB101	*Cinnamomum aromaticum*	Polar	-113%	-1.862
CB153	*Fallopia multiflora*	Polar	-113%	-1.317
CB023	*Anemone pulsatilla*	Polar	-113%	-0.405
CB145	*Epilobium parviflorum*	Polar	-112%	-3.164
CB091	*Ceanothus americanus*	Polar	-112%	-1.487
CB122	*Crataegus oxyacanthoides*	Polar	-110%	-0.423
CB326	*Rumex acetosella*	Polar	-108%	-0.230
CB149	*Eucalyptus globulus*	Polar	-106%	-1.032
CB010	*Alkenna tinctoria*	Polar	-105%	-1.101
CB109	*Citrus sinensis*	Polar	-94%	-0.011
CB097	*Chimaphila umbellata*	Polar	-94%	-0.769
CB139	*Echinacea purpurea*	Polar	-88%	-0.550
CB052	*Azadirachta indica*	Polar	-87%	-0.455
CB110	*Citrus sinensis*	Polar	-82%	-0.042
CB085	*Carya illinoinensis*	Polar	-81%	-0.514
CB024	*Anemone pulsatilla*	Polar	-81%	0.286
CB150	*Eupatorium perfoliatum*	Polar	-79%	0.822
CB143	*Eleutherococcus senticosus*	Polar	-79%	-0.377
CB372	*Uncaria tomentosa*	Polar	-79%	-2.063
CB129	*Cuminum cyminum*	Polar	-78%	-0.199
CB121	*Corylus avellana*	Polar	-77%	-0.188
CB169	*Geum urbanum*	Polar	-77%	-1.924
CB144	*Emblica officinalis*	Polar	-75%	-2.892
CB120	*Coriandrum sativum*	Polar	-73%	-0.761
CB017	*Alpinia officinarum*	Polar	-72%	-0.895
CB034	*Arachis hypogaea*	Polar	-72%	-0.542
CB353	*Syzygium aromaticum*	Polar	-72%	-2.069
CB376	*Vaccinium myrtillus*	Polar	-72%	-1.679
CB346	*Solidago virgaurea*	Polar	-70%	-0.720
CB360	*Theobroma cacao*	Polar	-68%	-1.299
CB108	*Aspalathus linearis*	Polar	-68%	-1.177
CB159	*Fragaria × ananassa*	Polar	-68%	0.283
CB141	*Eclipta alba*	Polar	-66%	0.118
CB331	*Salix alba*	Polar	-66%	-2.580
CB146	*Equisetum arvense*	Polar	-66%	0.022
CB006	*Agaricus bisporus*	Polar	-65%	-0.162
CB151	*Eupatorium purpureum*	Polar	-64%	0.850

CB178	*Hamamelis virginiana*	Polar	-64%	-3.160
CB237	*Myrica cerifera*	Polar	-63%	-3.630
CB137	*Diospyros virginiana*	Polar	-63%	-0.710
CB196	*Juglans regia*	Polar	-62%	-1.178
CB156	*Chrysanthemum morifolium*	Polar	-62%	-0.267
CB036	*Arctium lappa*	Polar	-61%	-0.510
CB324	*Rubus idaeus*	Polar	-61%	-0.022
CB168	*Geranium maculatum*	Polar	-60%	-2.849
CB183	*Humulus lupulus*	Polar	-60%	-0.942
CB098	*Artemisia annua*	Polar	-60%	-0.150
CB185	*Hypericum perforatum*	Polar	-60%	-0.899
CB118	*Collinsonia canadensis*	Polar	-59%	-0.163
CB084	*Carum carvi*	Polar	-58%	0.542
CB157	*Foeniculum vulgare*	Polar	-58%	1.015
CB148	*Eruca sativa*	Polar	-58%	0.861
CB301	*Pygeum africanum*	Polar	-57%	-1.427
CB179	*Hamamelis virginiana*	Polar	-57%	-1.533
CB147	*Eriodictiyo californicum*	Polar	-57%	-1.135
CB229	*Mentha piperita*	Polar	-56%	-0.823
CB364	*Tilia platyphyllos*	Polar	-55%	-1.149
CB380	*Viburnum opulus*	Polar	-54%	-1.012
CB061	*Betula alba*	Polar	-54%	1.142
CB192	*Iris versicolor*	Polar	-53%	-1.783
CB338	*Scutellaria lateriflora*	Polar	-52%	-0.563
CB119	*Coriandrum sativum*	Polar	-51%	0.127
CB008	*Agropyron repens*	Polar	-51%	0.119
CB308	*Rehmannia glutinosa*	Polar	51%	0.504
CB307	*Raphanus sativus longipinnatus*	Polar	53%	1.909
CB055	*Baptisia tinctoria*	Polar	56%	-0.143
CB278	Pelvetia canaliculata	Polar	96%	1.285
CB610	*Garcinia mangostana*	Non-polar	-522%	-3.062
CB530	*Curcuma longa*	Non-polar	-303%	-3.449
CB410	*Alkenna tinctoria*	Non-polar	-286%	-3.745
CB573	*Glycyrrhiza glabra*	Non-polar	-250%	-2.549
CB609	*Lepidium sativum*	Non-polar	-235%	-2.003
CB463	*Boletus edulis*	Non-polar	-197%	-1.517
CB617	*Macadamia integrifolia*	Non-polar	-178%	-1.521
CB547	*Eriodictiyo californicum*	Non-polar	-160%	-3.115
CB639	*Myristica fragrans*	Non-polar	-153%	-0.143
CB549	*Eucalyptus globulus*	Non-polar	-152%	-2.227
CB799	*Zingiber officinale*	Non-polar	-137%	-2.427
CB417	*Alpinia officinarum*	Non-polar	-128%	-1.814
CB693	*Prunus avium*	Non-polar	-119%	-0.844
CB637	*Myrica cerifera*	Non-polar	-113%	-1.579
CB735	*Sanguinaria canadensis*	Non-polar	-108%	-2.414
CB557	*Foeniculum vulgare*	Non-polar	-101%	-1.229
CB618	*Malus domestica*	Non-polar	-95%	0.886
CB796	*Zanthoxylum americanum*	Non-polar	-94%	-1.424

CB721	*Rosmarinus officinalis*	Non-polar	-90%	-3.591
CB631	*Mentha spicata*	Non-polar	-88%	-0.558
CB638	*Myristica fragrans*	Non-polar	-87%	-1.178
CB574	*Aframomum melegueta*	Non-polar	-86%	-1.303
CB520	*Coriandrum sativum*	Non-polar	-83%	-0.830
CB682	*Pogostemon cablin*	Non-polar	-82%	-1.491
CB529	*Cuminum cyminum*	Non-polar	-81%	-1.241
CB737	*Scrophularia nodosa*	Non-polar	-75%	-0.894
CB464	*Borago officinalis*	Non-polar	-71%	-0.577
CB407	*Agrimonia eupatoria*	Non-polar	-70%	-1.528
CB681	*Mandragora officinarum*	Non-polar	-67%	-1.069
CB704	*Quercus robur*	Non-polar	-67%	-1.186
CB502	*Cinnamomum verum*	Non-polar	-66%	-2.677
CB512	*Cnicus benedictus*	Non-polar	-66%	-1.502
CB629	*Mentha piperita*	Non-polar	-66%	-0.636
CB775	*Stevia rebaudiana*	Non-polar	-64%	-0.965
CB570	*Ginkgo biloba*	Non-polar	-63%	-0.861
CB550	*Eupatorium perfoliatum*	Non-polar	-63%	-0.021
CB448	*Astragalus propinquus*	Non-polar	-59%	-0.795
CB640	*Nepeta cataria*	Non-polar	-58%	-0.730
CB741	*Sinapis alba*	Non-polar	-58%	-1.334
CB545	*Epilobium parviflorum*	Non-polar	-57%	0.083
CB583	*Humulus lupulus*	Non-polar	-54%	-0.291
CB552	*Euphrasia officinalis*	Non-polar	-54%	0.351
CB523	*Crataegus oxycanthoides*	Non-polar	-54%	0.467
CB779	*Vanilla planifolia*	Non-polar	-54%	-1.052
CB761	*Thuja occidentalis*	Non-polar	-53%	-0.581
CB409	*Alchemilla vulgaris*	Non-polar	-53%	-0.090
CB522	*Crataegus oxyacanthoides*	Non-polar	-52%	0.248
CB729	*Ruta graveolens*	Non-polar	-51%	-0.545
CB740	*Silybum marianum*	Non-polar	-50%	-0.721
CB462	*Bixa orellana*	Non-polar	61%	-0.480

C.1.11 Natural compounds list which influence cytotoxicity level selected from human bronchial epithelial cell-based screen model

No.	Name of Natural Compound	MWt	$\%Inhibition_{Cytotoxicity}$ （nomolized LUX）	$Z\text{-}score_{lux}$
HY197	Vanillin	152.15	50%	0.675
HY148	Orotic acid (6-Carboxyuracil)	156.1	51%	0.620
HY126	Luteolin	286.24	52%	-0.029
HY157	Phylloquinone	450.7	53%	0.607
HY103	Hematoxylin	302.28	54%	-3.034
HY060	Chrysin	254.24	54%	0.720
HY200	Xylitol	152.15	58%	-0.181

HY181	Solanesol	631.07	59%	2.033
HY104	Hesperetin	302.28	60%	0.233
HY155	Phloretin	247.27	62%	0.492
HY127	Magnolol	266.32	63%	-0.098
HY085	Ethyl maltol	140.14	64%	-0.672
HY187	Tanshinone IIA	294.34	64%	-0.056
HY018	Abietic acid	302.46	67%	0.322
HY199	Xanthone	196.2	70%	0.396
HY118	Isoliquiritigenin	256.25	74%	1.027
HY139	Naringin	580.53	76%	0.964
HY094	Genistein	270.24	78%	0.291
HY119	Kaempferol	286.24	83%	-0.033
HY087	Fisetin (Fustel)	286.24	84%	-1.563
HY164	Pterostilbene	256.3	92%	-0.657
HY016	6,7-Dihydroxycoumarin	178.14	92%	1.368
HY175	Sclareol	308.5	96%	-0.442
HY178	Shikonin	288.3	97%	-2.465
HY005	(+)-Usniacin	344.32	107%	-0.144
HY153	Parthenolide	248.32	114%	-1.190
HY025	Alpha-Mangostin	410.47	114%	-1.534
HY108	Honokiol	266.23	120%	-1.092
HY099	Gossypol	518.55	122%	-2.186
HY083	Escin	1131.26	122%	-0.904

C.1.12 Natural product extracts list which influence cytotoxicity level selected from human bronchial epithelial cell-based screen model

No.	Name of Natural Product Extract	Extract Type	%Inhibition$_{Cytotoxicity}$ （nomolized LUX）	Z-score$_{lux}$
CB037	*Arctostaphylos uva ursi*	Polar	99%	-5.057
CB346	*Solidago virgaurea*	Polar	124%	-0.720
CB740	*Silybum marianum*	Non-polar	50%	-0.721
CB495	*Cetraria islandica*	Non-polar	51%	-0.841
CB779	*Vanilla planifolia*	Non-polar	51%	-1.052
CB768	*Triticum aestivum*	Non-polar	52%	-0.575
CB752	*Symphytum officinale*	Non-polar	52%	0.355
CB767	*Trigonella foenum-graecum*	Non-polar	52%	0.241
CB777	*Vigna angularis*	Non-polar	53%	0.220
CB745	*Solanum tuberosum*	Non-polar	53%	-0.273
CB757	*Taraxacum officinale*	Non-polar	54%	-0.044
CB753	*Syzygium aromaticum*	Non-polar	55%	-0.601
CB741	*Sinapis alba*	Non-polar	57%	-1.334
CB733	*Sambucus nigra*	Non-polar	57%	-0.105
CB764	*Tilia platyphyllos*	Non-polar	57%	1.157
CB780	*Viburnum opulus*	Non-polar	58%	0.082

CB758	*Taraxacum officinale*	Non-polar	59%	0.312
CB765	*Trifolium pratense*	Non-polar	60%	0.807
CB778	*Valeriana officinalis*	Non-polar	61%	0.528
CB742	*Smilax ornata*	Non-polar	61%	0.188
CB718	*Rosa canina*	Non-polar	61%	-0.864
CB774	*Vaccinium cyanococcus*	Non-polar	62%	0.389
CB782	*Verbena officinalis*	Non-polar	63%	1.085
CB773	*Urtica dioica*	Non-polar	64%	1.051
CB776	*Vaccinium myrtillus*	Non-polar	65%	-0.368
CB749	*Stellaria media*	Non-polar	65%	-0.626
CB759	*Teucrium scorodonia*	Non-polar	66%	0.496
CB750	*Stillingia sylvatica*	Non-polar	67%	-0.214
CB673	*Piscidia piscipula*	Non-polar	70%	-1.894
CB800	*Ziziphus jujuba*	Non-polar	73%	0.285
CB766	*Trigonella foenum-graecum*	Non-polar	73%	0.500
CB791	*Viscum album*	Non-polar	75%	-0.237
CB784	*Veronicastrum virginicum*	Non-polar	77%	-0.782
CB790	*Viola tricolor*	Non-polar	81%	-0.571
CB610	*Garcinia mangostana*	Non-polar	86%	-3.062
CB431	*Anthemis nobilis*	Non-polar	99%	-2.541
CB502	*Cinnamomum verum*	Non-polar	108%	-2.677
CB565	*Galium aparine*	Non-polar	109%	-0.126
CB590	*Inula helenium*	Non-polar	110%	-1.294
CB638	*Myristica fragrans*	Non-polar	110%	-1.178
CB736	*Schisandra chinensis*	Non-polar	119%	-1.702
CB589	*Indigofera tinctoria*	Non-polar	120%	0.861
CB615	*Lycopus europaeus*	Non-polar	120%	-0.251
CB597	*Juniperus communis*	Non-polar	122%	1.481
CB606	*Lens culinaris*	Non-polar	122%	0.989
CB582	*Hibiscus sabdariffa*	Non-polar	124%	0.437
CB612	*Litchi chinensis*	Non-polar	124%	1.496
CB618	*Malus domestica*	Non-polar	125%	0.886
CB619	*Malva sylvestris*	Non-polar	126%	1.997
CB623	*Morus alba*	Non-polar	127%	0.174
CB633	*Mitchella repens*	Non-polar	128%	-0.523
CB611	*Liriosma ovata*	Non-polar	128%	0.582
CB640	*Nepeta cataria*	Non-polar	128%	-0.730
CB631	*Mentha spicata*	Non-polar	130%	-0.558
CB564	*Galega officinalis*	Non-polar	131%	-0.020
CB577	*Gymnema sylvestre*	Non-polar	133%	0.067
CB573	*Glycyrrhiza glabra*	Non-polar	133%	-2.549
CB594	*Jateorhiza palmata*	Non-polar	134%	1.024
CB598	*Lactuca sativa*	Non-polar	135%	-0.941
CB584	*Hydrangea arborescens*	Non-polar	137%	-0.405
CB599	*Lactuca virosa*	Non-polar	138%	0.293
CB595	*Juglans regia*	Non-polar	138%	0.604
CB607	*Lentinula edodes*	Non-polar	139%	0.126
CB635	*Murraya koenigii*	Non-polar	139%	0.540

CB563	*Fumaria officinalis*	Non-polar	139%	-0.068
CB628	*Melissa officinalis*	Non-polar	140%	0.160
CB626	*Medicago sativa*	Non-polar	140%	1.230
CB591	*Iris florentina*	Non-polar	141%	-0.165
CB578	*Hamamelis virginiana*	Non-polar	142%	1.305
CB614	*Ipomoea batatas*	Non-polar	143%	0.145
CB579	*Hamamelis virginiana*	Non-polar	143%	1.189
CB608	*Leonurus cardiaca*	Non-polar	145%	-0.448
CB580	*Harpagophytum procumbens*	Non-polar	146%	1.166
CB616	*Lycopus virginicus*	Non-polar	146%	-0.634
CB592	*Iris versicolor*	Non-polar	146%	-0.637
CB625	*Matricaria recutita*	Non-polar	147%	0.229
CB634	*Morchella esculenta*	Non-polar	148%	0.493
CB624	*Marrubium vulgare*	Non-polar	148%	-0.418
CB566	*Galium verum*	Non-polar	149%	0.023
CB613	*Lycium barbarum*	Non-polar	149%	0.543
CB627	*Melilotus officinalis*	Non-polar	150%	1.747
CB602	*Lamium galeobdolon*	Non-polar	150%	0.687
CB600	*Lagenaria siceraria*	Non-polar	151%	-0.434
CB576	*Guaiacum officinale*	Non-polar	151%	-2.834
CB569	*Geum urbanum*	Non-polar	152%	0.138
CB568	*Geranium maculatum*	Non-polar	153%	-0.661
CB572	Psidium guajava	Non-polar	154%	0.966
CB629	*Mentha piperita*	Non-polar	154%	-0.636
CB586	*Hyssopus officinalis*	Non-polar	154%	0.988
CB567	*Gentiana lutea*	Non-polar	155%	-0.487
CB562	*Fucus vesiculosus*	Non-polar	156%	0.064
CB622	*Lablab purpureus*	Non-polar	156%	0.947
CB587	*Illicium verum*	Non-polar	157%	0.502
CB621	*Mangifera indica*	Non-polar	161%	1.501
CB637	*Myrica cerifera*	Non-polar	161%	-1.579
CB571	*Glechoma hederacea*	Non-polar	161%	0.823
CB639	*Myristica fragrans*	Non-polar	163%	-0.143
CB561	*Fraxinus excelsior*	Non-polar	164%	-0.328
CB605	*Lawsonia inermis*	Non-polar	165%	0.659
CB632	*Menyanthes trifoliata*	Non-polar	167%	-0.335
CB575	*Grindelia camporum*	Non-polar	169%	-0.671
CB604	*Lavandula angustifolia*	Non-polar	170%	-0.567
CB581	*Helianthus annuus*	Non-polar	170%	1.608
CB620	*Malva vulgaris*	Non-polar	170%	0.354
CB630	*Mentha pulegium*	Non-polar	174%	0.521
CB609	*Lepidium sativum*	Non-polar	175%	-2.003
CB601	*Lamium album*	Non-polar	176%	-0.368
CB583	*Humulus lupulus*	Non-polar	176%	-0.291
CB636	*Musa acuminata*	Non-polar	179%	0.434
CB588	*Ilex paraguariensis*	Non-polar	181%	-0.757
CB596	*Juglans regia*	Non-polar	185%	-0.358
CB603	*Laurus nobilis*	Non-polar	195%	0.854

CB617	*Macadamia integrifolia*	Non-polar	197%	-1.521
CB574	*Aframomum melegueta*	Non-polar	199%	-1.303
CB570	*Ginkgo biloba*	Non-polar	207%	-0.861
CB585	*Hypericum perforatum*	Non-polar	233%	-0.135
CB593	*Jasminum officinale*	Non-polar	239%	-0.557

C.1.13 Row data of the dose-response test for the 6,7-Dihydroxycoumarin

Con. (uM)	Log[nM]	%Inhibition$_{GFP}$			%Inhibition$_{Cytotoxicity}$		
2000000	6.30103	75%	76%	80%	49%	64%	57%
1000000	6	76%	75%	73%	50%	49%	55%
500000	5.69897	74%	76%	77%	40%	55%	47%
250000	5.39794	77%	78%	77%	39%	46%	34%
125000	5.09691	79%	78%	78%	25%	26%	26%
62500	4.79588	76%	78%	74%	12%	24%	13%
31250	4.49485	71%	67%	72%	13%	19%	18%
15625	4.19382	61%	65%	56%	11%	21%	19%
7812.5	3.89279	36%	30%	28%	13%	11%	15%
3906.25	3.59176	24%	18%	13%	9%	1%	20%

C.1.14 Output data of the quantified the 3D biofilm images for 6,7-Dihydroxycoumarin

Biovolume (μm^3)	Live
WT	13484
	13773.4
	15264.4
WT+6,7-Dihydroxycoumarin	9447.68
	12662
	9600.59
WT+6,7-Dihydroxycoumarin+TB	1917.45
	1191.31
	1886.3
WT+TB	2681.23
	2924.36
	2262.5

C.1.15 %Inhibition of cytotoxicity for the hit compounds selected by first screen model

Name	MWt	%Inhibition$_{GFP}$ (normalized lux)	(	Z-score$_{lux}$
Myricetin				
Resveratrol				
Ellagic acid	302.19	-103.7%	-115.4%	-152.0%

C.1.16 The Mortality percentage of the larvae at 16 hours after treating

Treatment	The %Mortality of larvae		
Control	100%	100%	100%
6,7-Dihydroxycoumarin	100%	100%	100%
TB+6,7-Dihydroxycoumarin	80%	80%	80%
6,7-Dihydroxycoumarin+TB	20%	30%	40%
PBS	0%	0%	0%

C.2 Figure

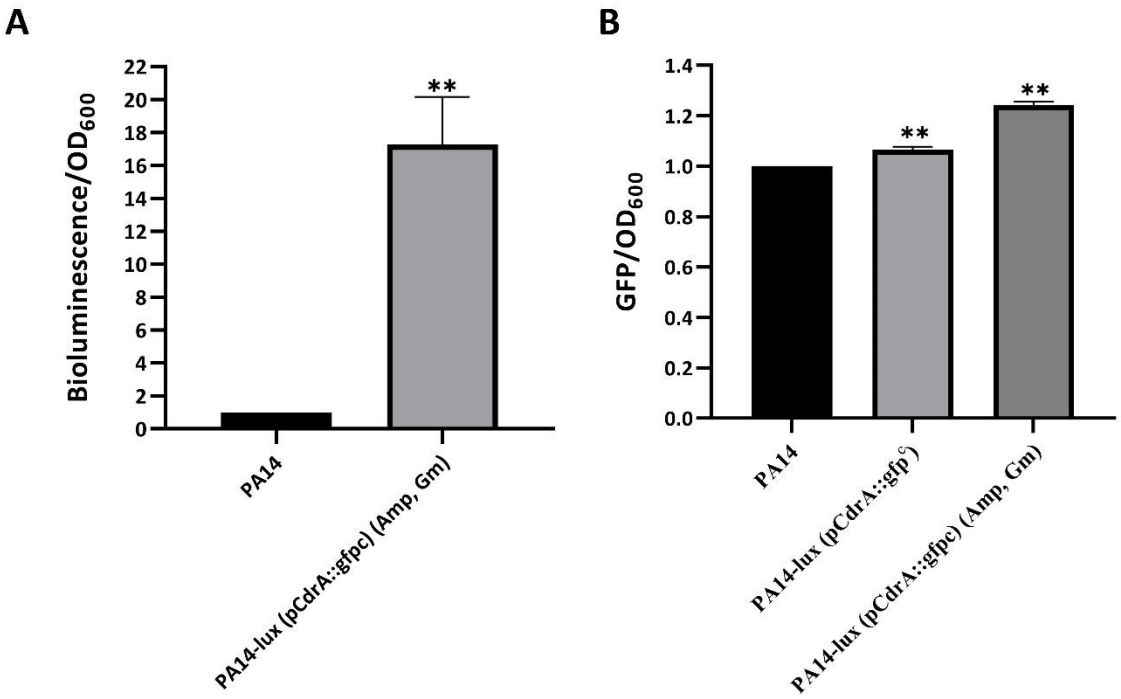

Figure C.2.2 Validation of dual labeled reporter strain PA14-lux (pCdrA::*gfp*^{c}). (A) Relative Light Unit (RLU) of PA14, PA14-lux (pCdrA::*gfp*^{C}). (B) Relative GFP intensity of PA14, PA14-lux (pCdrA::*gfp*^{C}) and PA14-lux (pCdrA::*gfp*^{C}) grown under selection (antibiotics Amp and Gm), normalized to growth (RLU) and WT PA14. Note WT PA14 does not grow under selection.

List of References

A, M. E., R, B. R. and R. Radhakrishnan (2011) 'High - Throughput Screening : The Hits and Leads of Drug Discovery - An Overview', *Journal of Applied Pharmaceutical Science*, 01(2011), pp. 2–10. Available at: https://www.researchgate.net/profile/Elvis_Martis/publication/210666871_High-Throughput_Screening_The_Hits_and_Leads_of_Drug_Discovery-_An_Overview/links/0f9845a7e00e20552af346d7/High-Throughput-Screening-The-Hits-and-Leads-of-Drug-Discovery-An-Overview.p.

Adrian, L. and Löffler, F. E. (2016) *Organohalide-respiring bacteria*, *Organohalide-Respiring Bacteria*. doi: 10.1007/978-3-662-49875-0.

ALTUN, İbrahim *et al.* (2023) 'Production Of Tetracycline Hydrochloride-Collagen-Doped Chitosan Nanofiber Scaffolds And Investigation Of Their Antibacterial Properties', *International Journal of Life Sciences and Biotechnology*, 6(1), pp. 37–60. doi: 10.38001/ijlsb.1180026.

Alvarez-Ortega, C. *et al.* (2011) 'The intrinsic resistome of *Pseudomonas aeruginosa* to β-lactams', *Virulence*, 2(2), pp. 144–146. doi: 10.4161/viru.2.2.15014.

Amikam, D., Weinhouse, H. and Galperin, M. Y. (2014) 'Moshe Benziman and the Discovery of Cyclic Di-GMP', *The Second Messenger Cyclic Di-GMP*, pp. 9–23. doi: 10.1128/9781555816667.ch2.

Amina, A. (2017) 'Pseudomonas Chemotaxis, Motility and Host-Pathogen Interactions', *MOJ Immunology*, 5(5). doi: 10.15406/moji.2017.05.00167.

An, S. Q. *et al.* (2020) 'An improved bind-n-seq strategy to determine protein-DNA interactions validated using the bacterial transcriptional regulator YipR', *BMC Microbiology*. BMC Microbiology, 20(1), pp. 1–11. doi: 10.1186/s12866-019-1672-7.

An, S. Q. and Ryan, R. P. (2016) 'Combating chronic bacterial infections by manipulating cyclic nucleotide-regulated biofilm formation', *Future Medicinal Chemistry*. doi: 10.4155/fmc-2015-0002.

An, S. qi *et al.* (2014) 'Novel Cyclic di-GMP Effectors of the YajQ Protein Family Control Bacterial Virulence', *PLoS Pathogens*, 10(10). doi: 10.1371/journal.ppat.1004429.

An, S. qi *et al.* (2019) 'Modulation of antibiotic sensitivity and biofilm formation in *Pseudomonas aeruginosa* by interspecies signal analogues', *Nature Communications*. Springer US, 10(1), pp. 1–11. doi: 10.1038/s41467-019-10271-4.

Andersen, J. B. *et al.* (2021) 'Identification of small molecules that interfere with c-di-GMP signaling and induce dispersal of *Pseudomonas aeruginosa* biofilms', *npj Biofilms and Microbiomes*. Springer US, 7(1). doi: 10.1038/s41522-021-00225-4.

Andrejko, M., Zdybicka-Barabas, A. and Cytryńska, M. (2014) 'Diverse effects of Galleria mellonella infection with entomopathogenic and clinical strains of *Pseudomonas aeruginosa*', *Journal of Invertebrate Pathology*, 115(1), pp. 14–25. doi: 10.1016/j.jip.2013.10.006.

Anisa, A. N. *et al.* (2021) 'Antimicrobial effect of roselle (Hibiscus sabdariffa l.) water fraction against *Pseudomonas aeruginosa* using drosophila infection model', *Biointerface Research in Applied Chemistry*, 11(5), pp. 12877–12885. doi: 10.33263/BRIAC115.1287712885.

Atanasov, A. G. *et al.* (2015) 'Discovery and resupply of pharmacologically active plant-derived natural products: A review', *Biotechnology Advances*. The Authors, 33(8), pp. 1582–1614. doi: 10.1016/j.biotechadv.2015.08.001.

AU - Moreau-Marquis, S. *et al.* (2010) 'Co-culture Models of *Pseudomonas aeruginosa* Biofilms Grown on Live Human Airway Cells', *JoVE*. MyJoVE Corp, (44), p. e2186. doi: doi:10.3791/2186.

Ayerbe-Algaba, R. *et al.* (2019) 'The anthelmintic oxyclozanide restores the activity of colistin against colistin-resistant Gram-negative bacilli', *International Journal of Antimicrobial Agents*. Elsevier B.V., 54(4), pp. 507–512. doi: 10.1016/j.ijantimicag.2019.07.006.

Azam, M. W. and Khan, A. U. (2019) 'Updates on the pathogenicity status of *Pseudomonas aeruginosa*', *Drug Discovery Today*. Elsevier Ltd, 24(1), pp. 350–359. doi: 10.1016/j.drudis.2018.07.003.

Barber, C. E. *et al.* (1997) 'A novel regulatory system required for pathogenicity of Xanthomonas campestris is mediated by a small diffusible signal molecule', *Molecular Microbiology*. doi: 10.1046/j.1365-2958.1997.3721736.x.

Baynham, P. J. *et al.* (2006) 'The *Pseudomonas aeruginosa* ribbon-helix-helix DNA-binding protein AlgZ (AmrZ) controls twitching motility and biogenesis of type IV pili', *Journal of Bacteriology*, 188(1), pp. 132–140. doi: 10.1128/JB.188.1.132-140.2006.

Beckert, U. *et al.* (2014) 'ExoY from *Pseudomonas aeruginosa* is a nucleotidyl cyclase with preference for cGMP and cUMP formation', *Biochemical and Biophysical Research Communications*. Elsevier Inc., 450(1), pp. 870–874. doi: 10.1016/j.bbrc.2014.06.088.

Belanger, C. R. *et al.* (2020) 'Identification of novel targets of azithromycin activity against *Pseudomonas aeruginosa* grown in physiologically relevant media', *Proceedings of the National*

Academy of Sciences of the United States of America, 117(52), pp. 33519–33529. doi: 10.1073/pnas.2007626117.

De Bentzmann, S. and Plésiat, P. (2011) 'The *Pseudomonas aeruginosa* opportunistic pathogen and human infections', *Environmental Microbiology*. doi: 10.1111/j.1462-2920.2011.02469.x.

Bao Y, Lies DP, Fu H, Roberts GP (1991) An improved Tn7-based system for the single copy insertion of cloned genes into chromosomes of Gram-negative bacteria. Gene, 109, 167–168.

Berg, H. C. (2003) 'The rotary motor of bacterial flagella', *Annual Review of Biochemistry*. doi: 10.1146/annurev.biochem.72.121801.161737.

Bhuwan, M. *et al.* (2012) 'Histidine-containing phosphotransfer protein-B (HptB) regulates swarming motility through partner-switching system in *Pseudomonas aeruginosa* PAO1 strain', *Journal of Biological Chemistry*. Â© 2012 ASBMB. Currently published by Elsevier Inc; originally published by American Society for Biochemistry and Molecular Biology., 287(3), pp. 1903–1914. doi: 10.1074/jbc.M111.256586.

Blair, J. M. A. *et al.* (2015) 'Molecular mechanisms of antibiotic resistance', *Nature Reviews Microbiology*. doi: 10.1038/nrmicro3380.

Boldrick, J. C. *et al.* (2002) 'Stereotyped and specific gene expression programs in human innate immune responses to bacteria', *Proceedings of the National Academy of Sciences of the United States of America*. doi: 10.1073/pnas.231625398.

Boon, C. *et al.* (2008) 'A novel DSF-like signal from Burkholderia cenocepacia interferes with Candida albicans morphological transition', *ISME Journal*, 2(1), pp. 27–36. doi: 10.1038/ismej.2007.76.

Bottomley, M. J. *et al.* (2007) 'Molecular insights into quorum sensing in the human pathogen *Pseudomonas aeruginosa* from the structure of the virulence regulator LasR bound to its autoinducer', *Journal of Biological Chemistry*, 282(18), pp. 13592–13600. doi: 10.1074/jbc.M700556200.

Breathnach, A. S. *et al.* (2012) 'Multidrug-resistant *Pseudomonas aeruginosa* outbreaks in two hospitals: Association with contaminated hospital waste-water systems', *Journal of Hospital Infection*. doi: 10.1016/j.jhin.2012.06.007.

Breidenstein, E. B. M., de la Fuente-Núñez, C. and Hancock, R. E. W. (2011) '*Pseudomonas aeruginosa*: All roads lead to resistance', *Trends in Microbiology*, 19(8), pp. 419–426. doi: 10.1016/j.tim.2011.04.005.

Brindhadevi, K. *et al.* (2020) 'Biofilm and Quorum sensing mediated pathogenicity in *Pseudomonas aeruginosa*', *Process Biochemistry*. Elsevier, 96(September 2019), pp. 49–57. doi: 10.1016/j.procbio.2020.06.001.

Brown, S. *et al.* (2022) 'Doxycycline for the treatment of breast cancer-related lymphedema', *Frontiers in Pharmacology*, 13(October). doi: 10.3389/fphar.2022.1028926.

Brown, S. E. *et al.* (2009) 'A peptidomics study reveals the impressive antimicrobial peptide arsenal of the wax moth Galleria mellonella', *Insect Biochemistry and Molecular Biology*. Elsevier Ltd, 39(11), pp. 792–800. doi: 10.1016/j.ibmb.2009.09.004.

Bruchmann, S. *et al.* (2013) 'Quantitative contributions of target alteration and decreased drug accumulation to *Pseudomonas aeruginosa* fluoroquinolone resistance', *Antimicrobial Agents and Chemotherapy*, 57(3), pp. 1361–1368. doi: 10.1128/AAC.01581-12.

Burrows, L. L. (2012) '*Pseudomonas aeruginosa* twitching motility: Type IV pili in action', *Annual Review of Microbiology*, 66, pp. 493–520. doi: 10.1146/annurev-micro-092611-150055.

Byrd, M. S. *et al.* (2009) 'Genetic and biochemical analyses of the *Pseudomonas aeruginosa* Psl exopolysaccharide reveal overlapping roles for polysaccharide synthesis enzymes in Psl and LPS production', *Molecular Microbiology*, 73(4), pp. 622–638. doi: 10.1111/j.1365-2958.2009.06795.x.

Calixto, J. B. (2019) 'The role of natural products in modern drug discovery.Calixto, J. B. (2019). The role of natural products in modern drug discovery. Anais Da Academia Brasileira de Ciencias, 91, 1–7. https://doi.org/10.1590/0001-3765201920190105', *Anais da Academia Brasileira de Ciencias*, 91, pp. 1–7. doi: 10.1590/0001-3765201920190105.Abstract.

Cannatelli, A. *et al.* (2018) 'Synergistic activity of colistin in combination with resveratrol against colistin-resistant gram-negative pathogens', *Frontiers in Microbiology*, 9(AUG). doi: 10.3389/fmicb.2018.01808.

Chaudhary, N. *et al.* (2022) 'Polyaspartate-derived synthetic antimicrobial polymer enhances the activity of rifampicin against multidrug-resistant *Pseudomonas aeruginosa* infections', *Biomaterials Science*. Royal Society of Chemistry, 10(18), pp. 5158–5171. doi: 10.1039/d2bm00524g.

Chen, Y. T. *et al.* (2004) 'Evolutionary analysis of the two-component systems in *Pseudomonas aeruginosa* PAO1', *Journal of Molecular Evolution*, 59(6), pp. 725–737. doi: 10.1007/s00239-004-2663-2.

Chiang, C. Y. *et al.* (2018) 'Mitigating the impact of antibacterial drug resistance through host-directed therapies: Current progress, outlook, and challenges', *mBio*. doi: 10.1128/mBio.01932-17.

Christensen, L. D. *et al.* (2013) 'Clearance of *Pseudomonas aeruginosa* foreign-body biofilm infections through reduction of the cyclic di-gmp level in the bacteria', *Infection and Immunity*, 81(8), pp. 2705–2713. doi: 10.1128/IAI.00332-13.

Chugani, S. and Greenberg, E. P. (2014) 'An evolving perspective on the *Pseudomonas aeruginosa* orphan quorum sensing regulator QscR', *Frontiers in Cellular and Infection Microbiology*, 4(OCT), pp. 1–7. doi: 10.3389/fcimb.2014.00152.

Clatworthy, A. E. *et al.* (2009) '*Pseudomonas aeruginosa* infection of zebrafish involves both host and pathogen determinants', *Infection and Immunity*, 77(4), pp. 1293–1303. doi: 10.1128/IAI.01181-08.

Claudine, B. and Harwood, C. S. (2013) 'Cyclic diguanosine monophosphate represses bacterial flagella synthesis by interacting with the Walker a motif of the enhancer-binding protein FleQ', *Proceedings of the National Academy of Sciences of the United States of America*, 110(46), pp. 18478–18483. doi: 10.1073/pnas.1318972110.

Coleman, S. R. *et al.* (2020) 'Multidrug adaptive resistance of *Pseudomonas aeruginosa* swarming cells', *Antimicrobial Agents and Chemotherapy*. doi: 10.1128/AAC.01999-19.

Colvin, K. M. *et al.* (2011) 'The pel polysaccharide can serve a structural and protective role in the biofilm matrix of *Pseudomonas aeruginosa*', *PLoS Pathogens*, 7(1). doi: 10.1371/journal.ppat.1001264.

Conrad, J. C. *et al.* (2011) 'Flagella and pili-mediated near-surface single-cell motility mechanisms in *P. aeruginosa*', *Biophysical Journal*. Biophysical Society, 100(7), pp. 1608–1616. doi: 10.1016/j.bpj.2011.02.020.

Cutuli, M. A. *et al.* (2019) 'Galleria mellonella as a consolidated in vivo model hosts: New developments in antibacterial strategies and novel drug testing', *Virulence*. Taylor & Francis, 10(1), pp. 527–541. doi: 10.1080/21505594.2019.1621649.

Cytryńska, M. *et al.* (2007) 'Purification and characterization of eight peptides from Galleria mellonella immune hemolymph', *Peptides*, 28(3), pp. 533–546. doi: 10.1016/j.peptides.2006.11.010.

D'Angelo, F. *et al.* (2018) 'Identification of FDA-Approved Drugs as Antivirulence Agents', *Antimicrobial Agents and Chemotherapy*, pp. 1–20. Available at: https://www.ncbi.nlm.nih.gov/pmc/articles/PMC6201120/pdf/e01296-18.pdf.

D'Argenio, D. A. *et al.* (2002) 'Autolysis and autoaggregation in *Pseudomonas aeruginosa* colony morphology mutants', *Journal of Bacteriology*, 184(23), pp. 6481–6489. doi: 10.1128/JB.184.23.6481-6489.2002.

Dai, L. *et al.* (2019) 'Ibuprofen-mediated potential inhibition of biofilm development and quorum sensing in *Pseudomonas aeruginosa*', *Life Sciences*. Elsevier, 237(September), p. 116947. doi: 10.1016/j.lfs.2019.116947.

Damron, F. H. *et al.* (2013a) 'Construction of mobilizable mini-Tn7 vectors for bioluminescent detection of gram-negative bacteria and single-copy promoter lux reporter analysis', *Applied and Environmental Microbiology*. doi: 10.1128/AEM.00640-13.

Damron, F. H. *et al.* (2013b) 'Construction of mobilizable mini-Tn7 vectors for bioluminescent detection of gram-negative bacteria and single-copy promoter lux reporter analysis', *Applied and Environmental Microbiology*, 79(13), pp. 4149–4153. doi: 10.1128/AEM.00640-13.

Das, M. C. *et al.* (2016) 'Attenuation of *Pseudomonas aeruginosa* biofilm formation by Vitexin: A combinatorial study with azithromycin and gentamicin', *Scientific Reports*. Nature Publishing Group, 6(March), pp. 1–13. doi: 10.1038/srep23347.

Davies, D. G. and Marques, C. N. H. (2009) 'A fatty acid messenger is responsible for inducing dispersion in microbial biofilms', *Journal of Bacteriology*, 191(5), pp. 1393–1403. doi: 10.1128/JB.01214-08.

Deng, Y. *et al.* (2010) 'Structural and functional characterization of diffusible signal factor family quorum-sensing signals produced by members of the burkholderia cepacia complex', *Applied and Environmental Microbiology*, 76(14), pp. 4675–4683. doi: 10.1128/AEM.00480-10.

Deng, Y. *et al.* (2012) 'Cis-2-dodecenoic acid receptor RpfR links quorum-sensing signal perception with regulation of virulence through cyclic dimeric guanosine monophosphate turnover', *Proceedings of the National Academy of Sciences of the United States of America*, 109(38), pp. 15479–15484. doi: 10.1073/pnas.1205037109.

Deng, Y., Lim, A., *et al.* (2013) 'Cis-2-dodecenoic acid quorum sensing system modulates N-acyl homoserine lactone production through RpfR and cyclic di-GMP turnover in Burkholderia cenocepacia', *BMC Microbiology*, 13(1). doi: 10.1186/1471-2180-13-148.

Deng, Y., Boon, C., *et al.* (2013) 'Cis-2-dodecenoic acid signal modulates virulence of *Pseudomonas aeruginosa* through interference with quorum sensing systems and T3SS Tracy Raivio', *BMC Microbiology*, 13(1). doi: 10.1186/1471-2180-13-231.

Deng, Y. *et al.* (2016) 'Diffusible signal factor family signals provide a fitness advantage to Xanthomonas campestris pv. campestris in interspecies competition', *Environmental Microbiology*. doi: 10.1111/1462-2920.13244.

Devi, K. P. *et al.* (2015) 'Molecular mechanisms underlying anticancer effects of myricetin', *Life Sciences*. Elsevier Inc., 142, pp. 19–25. doi: 10.1016/j.lfs.2015.10.004.

Diepold, A. and Armitage, J. P. (2015) 'Type III secretion systems: The bacterial flagellum and the injectisome', *Philosophical Transactions of the Royal Society B: Biological Sciences*. doi: 10.1098/rstb.2015.0020.

Döring, G. (2010) 'Prevention of *Pseudomonas aeruginosa* infection in cystic fibrosis patients', *International Journal of Medical Microbiology*, 300(8), pp. 573–577. doi: 10.1016/j.ijmm.2010.08.010.

Dow, J. M. *et al.* (2003) 'Biofilm dispersal in Xanthomonas campestris is controlled by cell-cell signaling and is required for full virulence to plants', *Proceedings of the National Academy of Sciences of the United States of America*, 100(19), pp. 10995–11000. doi: 10.1073/pnas.1833360100.

Dyshlovoy, S. A. and Honecker, F. (2018) 'Marine compounds and cancer: 2017 updates', *Marine Drugs*, 16(2), pp. 2017–2019. doi: 10.3390/md16020041.

Dzobo, K. (2022) 'The Role of Natural Products as Sources of Therapeutic Agents for Innovative Drug Discovery', *Comprehensive Pharmacology*, 2(January), pp. 408–422. doi: 10.1016/B978-0-12-820472-6.00041-4.

Elshaer, S. L. and Shaaban, M. I. (2021) 'Inhibition of Quorum Sensing and Virulence Factors of *Pseudomonas aeruginosa* by Biologically Synthesized Gold and Selenium Nanoparticles', *Antibiotics*, 10(12). doi: 10.3390/ANTIBIOTICS10121461.

Ermer, J. and Vogel, M. (2000) 'Applications of hyphenated LC-MS techniques in pharmaceutical analysis', *Biomedical Chromatography*, 14(6), pp. 373–383. doi: 10.1002/1099-0801(200010)14:6<373::AID-BMC29>3.0.CO;2-S.

Ferrières, L. and Clarke, D. J. (2003) 'The RcsC sensor kinase is required for normal biofilm formation in Escherichia coli K-12 and controls the expression of a regulon in response to growth on a solid surface', *Molecular Microbiology*. doi: 10.1046/j.1365-2958.2003.03815.x.

Filloux, A. (2011) 'Protein secretion systems in *Pseudomonas aeruginosa*: An essay on diversity, evolution, and function', *Frontiers in Microbiology*. doi: 10.3389/fmicb.2011.00155.

Filloux, A. (no date) *Pseudomonas*.

Fouhy, Y. *et al.* (2007) 'Diffusible signal factor-dependent cell-cell signaling and virulence in the nosocomial pathogen Stenotrophomonas maltophilia', *Journal of Bacteriology*, 189(13), pp. 4964–4968. doi: 10.1128/JB.00310-07.

Friedman, L. and Kolter, R. (2004) 'Genes involved in matrix formation in *Pseudomonas aeruginosa* PA14 biofilms', *Molecular Microbiology*, 51(3), pp. 675–690. doi: 10.1046/j.1365-2958.2003.03877.x.

Galperin, M. Y. (2006) 'Structural classification of bacterial response regulators: Diversity of output domains and domain combinations', *Journal of Bacteriology*, 188(12), pp. 4169–4182. doi: 10.1128/JB.01887-05.

Gao, R. and Stock, A. M. (2009) 'Biological insights from structures of two-component proteins', *Annual Review of Microbiology*, 63, pp. 133–154. doi: 10.1146/annurev.micro.091208.073214.

Geng, F. *et al.* (2017) 'Persistent exposure to Porphyromonas gingivalis promotes proliferative and invasion capabilities, and tumorigenic properties of human immortalized oral epithelial cells', *Frontiers in Cellular and Infection Microbiology*, 7(FEB), pp. 1–16. doi: 10.3389/fcimb.2017.00057.

Gerber, F. *et al.* (2004) 'Practical aspects of fast reversed-phase high-performance liquid chromatography using 3 µm particle packed columns and monolithic columns in pharmaceutical development and production working under current good manufacturing practice', *Journal of Chromatography A*, 1036(2), pp. 127–133. doi: 10.1016/j.chroma.2004.02.056.

Ghafoor, A., Hay, I. D. and Rehm, B. H. A. (2011) 'Role of exopolysaccharides in *Pseudomonas aeruginosa* biofilm formation and architecture', *Applied and Environmental Microbiology*, 77(15), pp. 5238–5246. doi: 10.1128/AEM.00637-11.

Ghosh, S. *et al.* (2022) 'Analysis of Antibiofilm Activities of Bioactive Compounds from Honeyweed (Leonurus sibiricus) Against *P. aeruginosa*: an In Vitro and In Silico Approach', *Applied Biochemistry and Biotechnology*. Springer US, (0123456789). doi: 10.1007/s12010-021-03797-1.

Guan, C. et al. (2024) 'FIhF affects the subcellular clustering of WspR through HsbR in *Pseudomonas aeruginosa*', *Microbial Pathogenesis*, 10.1128/aem.01548-23.

Guła, G. *et al.* (2018) 'Complex Signaling Networks Controlling Dynamic Molecular Changes in *Pseudomonas aeruginosa* Biofilm', *Current Medicinal Chemistry*, 26(11), pp. 1979–1993. doi: 10.2174/0929867325666180912110151.

Guo, Y. *et al.* (no date) 'Deciphering bacterial interactions via DSF-regulated public goods in an anammox community', *Research Square*, pp. 1–25. Available at: https://www.researchsquare.com/article/e3496e1c-daa3-4fa8-a444-f1e17519d749/v1?utm_source=researcher_app&utm_medium=referral&utm_campaign=RESR_MRKT_Researcher_inbound.

Guragain, M. *et al.* (2016) 'The *Pseudomonas aeruginosa* PAO1 two-component regulator CarSR regulates calcium homeostasis and calciuminduced virulence factor production through its regulatory targets CarO and CarP', *Journal of Bacteriology*, 198(6), pp. 951–963. doi: 10.1128/JB.00963-15.

Ha, D. G. and O'Toole, G. A. (2015) 'c-di-GMP and its effects on biofilm formation and dispersion: A *Pseudomonas aeruginosa* review', *Microbial Biofilms*, pp. 301–317. doi: 10.1128/9781555817466.ch15.

Han, Y. *et al.* (2019) 'A *Pseudomonas aeruginosa* type VI secretion system regulated by CueR facilitates copper acquisition', *PLoS Pathogens*, 15(12), pp. 1–25. doi: 10.1371/journal.ppat.1008198.

Hasan, T. H. and Al-Harmoosh, R. A. (2020) 'Mechanisms of antibiotics resistance in bacteria', *Systematic Reviews in Pharmacy*, 11(6), pp. 817–823. doi: 10.31838/srp.2020.6.118.

Hay, I. D., Remminghorst, U. and Rehm, B. H. A. (2009) 'MucR, a novel membrane-associated regulator of alginate biosynthesis in *Pseudomonas aeruginosa*', *Applied and Environmental Microbiology*, 75(4), pp. 1110–1120. doi: 10.1128/AEM.02416-08.

He, Y. W. *et al.* (2023) 'DSF-family quorum sensing signal-mediated intraspecies, interspecies, and inter-kingdom communication', *Trends in Microbiology*. The Author(s), 31(1), pp. 36–50. doi: 10.1016/j.tim.2022.07.006.

Henrichfreise, B. *et al.* (2007) 'Resistance mechanisms of multiresistant *Pseudomonas aeruginosa* strains from Germany and correlation with hypermutation', *Antimicrobial Agents and Chemotherapy*, 51(11), pp. 4062–4070. doi: 10.1128/AAC.00148-07.

Hentzer, M. *et al.* (2001) 'Alginate overproduction affects *Pseudomonas aeruginosa* biofilm structure and function', *Journal of Bacteriology*, 183(18), pp. 5395–5401. doi: 10.1128/JB.183.18.5395-5401.2001.

Hentzer, M. *et al.* (2003) 'Attenuation of *Pseudomonas aeruginosa* virulence by quorum sensing inhibitors', *EMBO Journal*, 22(15), pp. 3803–3815. doi: 10.1093/emboj/cdg366.

Hernandez, R. E., Gallegos-Monterrosa, R. and Coulthurst, S. J. (2020) 'Type VI secretion system effector proteins: Effective weapons for bacterial competitiveness', *Cellular Microbiology*, 22(9), pp. 1–9. doi: 10.1111/cmi.13241.

Hickman, J. W., Tifrea, D. F. and Harwood, C. S. (2005) 'A chemosensory system that regulates biofilm formation through modulation of cyclic diguanylate levels', *Proceedings of the National Academy of Sciences of the United States of America*, 102(40), pp. 14422–14427. doi: 10.1073/pnas.0507170102.

Hirakawa, H. *et al.* (2020) 'Progress overview of bacterial two-component regulatory systems as potential targets for antimicrobial chemotherapy', *Antibiotics*, 9(10), pp. 1–15. doi: 10.3390/antibiotics9100635.

Hoang, T. T., Karkhoff-Schweizer, R. R., Kutchma, A. J., & Schweizer, H. P. (1998). A broad-host-range Flp-FRT recombination system for site-specific excision of chromosomally-located DNA sequences: application for isolation of unmarked *Pseudomonas aeruginosa* mutants. Gene, 212(1), 77–86. https://doi.org/10.1016/s0378-1119(98)00130-9

Hoffman, L. R. *et al.* (2005) 'Aminoglycoside antibiotics induce bacterial biofilm formation', *Nature*, 436(7054), pp. 1171–1175. doi: 10.1038/nature03912.

Hoggarth, A. *et al.* (2019) 'Mechanistic research holds promise for bacterial vaccines and phage therapies for *Pseudomonas aeruginosa*', *Drug Design, Development and Therapy*, 13, pp. 909–924. doi: 10.2147/DDDT.S189847.

Høiby, N. *et al.* (2001) '*Pseudomonas aeruginosa* and the in vitro and in vivo biofilm mode of growth', *Microbes and Infection*, 3(1), pp. 23–35. doi: 10.1016/S1286-4579(00)01349-6.

Holland-Crimmin, S., Gosnell, P. and Quinn, C. (2011) 'Compound Management: Guidelines for Compound Storage, Provision, and Quality Control', *Current Protocols in Chemical Biology*. doi: 10.1002/9780470559277.ch110095.

Horna, G. and Ruiz, J. (2021) 'Type 3 secretion system of *Pseudomonas aeruginosa*', *Microbiological Research*. Elsevier GmbH, 246(August 2020), p. 126719. doi: 10.1016/j.micres.2021.126719.

Hou, L. *et al.* (2019) 'AmrZ Regulates Swarming Motility Through Cyclic di-GMP-Dependent Motility Inhibition and Controlling Pel Polysaccharide Production in *Pseudomonas aeruginosa* PA14', *Frontiers in Microbiology*, 10(August). doi: 10.3389/fmicb.2019.01847.

Huygens, J. *et al.* (2023) 'The impact of antibiotic residues on resistance patterns in leek at harvest', *Heliyon*. Elsevier Ltd, 9(5), p. e16052. doi: 10.1016/j.heliyon.2023.e16052.

Idowu, T. *et al.* (2019) 'Heterodimeric Rifampicin–Tobramycin conjugates break intrinsic resistance of *Pseudomonas aeruginosa* to doxycycline and chloramphenicol in vitro and in a Galleria mellonella in vivo model', *European Journal of Medicinal Chemistry*. Elsevier Masson SAS, 174, pp. 16–32. doi: 10.1016/j.ejmech.2019.04.034.

Imai, Y. *et al.* (2019) 'A new antibiotic selectively kills Gram-negative pathogens', *Nature*, 576(7787), pp. 459–464. doi: 10.1038/s41586-019-1791-1.

Intile, P. J. *et al.* (2014) 'The AlgZR two-component system recalibrates the RsmAYZ posttranscriptional regulatory system to inhibit expression of the *Pseudomonas aeruginosa* type III secretion system', *Journal of Bacteriology*, 196(2), pp. 357–366. doi: 10.1128/JB.01199-13.

Irie, Y. *et al.* (2012) 'Self-produced exopolysaccharide is a signal that stimulates biofilm formation in *Pseudomonas aeruginosa*', *Proceedings of the National Academy of Sciences of the United States of America*, 109(50), pp. 20632–20636. doi: 10.1073/pnas.1217993109.

Isles, A. *et al.* (1984) 'Pseudomonas cepacia infection in cystic fibrosis: An emerging problem', *The Journal of Pediatrics*. doi: 10.1016/S0022-3476(84)80993-2.

Jayaraman, P. *et al.* (2010) 'Activity and interactions of antibiotic and phytochemical combinations against *Pseudomonas aeruginosa* in vitro', *International Journal of Biological Sciences*, 6(6), pp. 556–568. doi: 10.7150/ijbs.6.556.

Jennings, L. K. *et al.* (2015) 'Pel is a cationic exopolysaccharide that cross-links extracellular DNA in the *Pseudomonas aeruginosa* biofilm matrix', *Proceedings of the National Academy of Sciences of the United States of America*, 112(36), pp. 11353–11358. doi: 10.1073/pnas.1503058112.

Johnston, P. A. *et al.* (2012) 'Development and validation of a high-content screening assay to identify inhibitors of cytoplasmic dynein-mediated transport of glucocorticoid receptor to the

nucleus', *Assay and Drug Development Technologies*, 10(5), pp. 432–456. doi: 10.1089/adt.2012.456.

Jouault, A., Saliba, A. M. and Touqui, L. (2022) 'Modulation of the immune response by the *Pseudomonas aeruginosa* type-III secretion system', *Frontiers in Cellular and Infection Microbiology*, 12(November), pp. 1–8. doi: 10.3389/fcimb.2022.1064010.

Juan, C., Peña, C. and Oliver, A. (2017) 'Host and pathogen biomarkers for severe *Pseudomonas aeruginosa* infections', *Journal of Infectious Diseases*, 215(Suppl 1), pp. S44–S51. doi: 10.1093/infdis/jiw299.

Kaihami, G. H. *et al.* (2014) 'Involvement of a 1-Cys Peroxiredoxin in Bacterial Virulence', *PLoS Pathogens*, 10(10). doi: 10.1371/journal.ppat.1004442.

Kaminski, A. *et al.* (2018) '*Pseudomonas aeruginosa* ExoS Induces Intrinsic Apoptosis in Target Host Cells in a Manner That is Dependent on its GAP Domain Activity', *Scientific Reports*. Springer US, 8(1), pp. 1–15. doi: 10.1038/s41598-018-32491-2.

Kang, J. *et al.* (2016) 'Improving drug discovery with high-content phenotypic screens by systematic selection of reporter cell lines', *Nature Biotechnology*, 34(1), pp. 70–77. doi: 10.1038/nbt.3419.

Kaufman, M. R. *et al.* (2000) '*Pseudomonas aeruginosa* mediated apoptosis requires the ADP-ribosylating activity of ExoS', *Microbiology*, 146(10), pp. 2531–2541. doi: 10.1099/00221287-146-10-2531.

Kavanagh, K. and Sheehan, G. (2018) 'The use of galleria mellonella larvae to identify novel antimicrobial agents against fungal species of medical interest', *Journal of Fungi*, 4(3). doi: 10.3390/jof4030113.

Kessler, B., de Lorenzo, V. and Timmis, K. N. (1992) 'A general system to integrate lacZ fusions into the chromosomes of gram-negative eubacteria: regulation of the Pm promoter of the TOL plasmid studied with all controlling elements in monocopy', *MGG Molecular & General Genetics*, 233(1–2), pp. 293–301. doi: 10.1007/BF00587591.

Khalifa, S. A. M. *et al.* (2019) 'Marine natural products: A source of novel anticancer drugs', *Marine Drugs*, 17(9). doi: 10.3390/md17090491.

Killough, M., Rodgers, A. M. and Ingram, R. J. (2022) '*Pseudomonas aeruginosa*: Recent Advances in Vaccine Development', *Vaccines*, 10(7). doi: 10.3390/vaccines10071100.

Kilmury, S. L. N. and Burrows, L. L. (2018) 'The *Pseudomonas aeruginosa* pilSR two-component system regulates both twitching and swimming motilities', *mBio*, 9(4). doi: 10.1128/mBio.01310-18.

Kim, H. S. *et al.* (2021) 'Linoleic acid inhibits *Pseudomonas aeruginosa* biofilm formation by activating diffusible signal factor-mediated quorum sensing', *Biotechnology and Bioengineering*, 118(1), pp. 82–93. doi: 10.1002/bit.27552.

Kim, S. K. and Lee, J. H. (2016) 'Biofilm dispersion in *Pseudomonas aeruginosa*', *Journal of Microbiology*, 54(2), pp. 71–85. doi: 10.1007/s12275-016-5528-7.

Klockgether, T. (2011) 'Update on degenerative ataxias', *Current Opinion in Neurology*, pp. 339–345. doi: 10.1097/WCO.0b013e32834875ba.

Koeppen, K. *et al.* (2021) 'Let-7b-5p in vesicles secreted by human airway cells reduces biofilm formation and increases antibiotic sensitivity of *P. aeruginosa*', *Proceedings of the National Academy of Sciences of the United States of America*, 118(28). doi: 10.1073/pnas.2105370118.

Kuchma, S. L. *et al.* (2007) 'BifA, a cyclic-di-GMP phosphodiesterase, inversely regulates biofilm formation and swarming motility by *Pseudomonas aeruginosa* PA14', *Journal of Bacteriology*, 189(22), pp. 8165–8178. doi: 10.1128/JB.00586-07.

Kulasekara, H. D. *et al.* (2005) 'A novel two-component system controls the expression of *Pseudomonas aeruginosa* fimbrial cup genes', *Molecular Microbiology*, 55(2), pp. 368–380. doi: 10.1111/j.1365-2958.2004.04402.x.

Kulesekara, H. *et al.* (2006) 'Analysis of *Pseudomonas aeruginosa* diguanylate cyclases and phosphodiesterases reveals a role for bis-(3'-5')-cyclic-GMP in virulence', *Proceedings of the National Academy of Sciences of the United States of America*, 103(8), pp. 2839–2844. doi: 10.1073/pnas.0511090103.

Kumar, R. A. and Clark, D. S. (2006) 'High-throughput screening of biocatalytic activity: Applications in drug discovery', *Current Opinion in Chemical Biology*, 10(2), pp. 162–168. doi: 10.1016/j.cbpa.2006.02.033.

Kurnik, M. *et al.* (2018) 'Potent α-Synuclein Aggregation Inhibitors, Identified by High-Throughput Screening, Mainly Target the Monomeric State', *Cell Chemical Biology*. Elsevier Ltd., 25(11), pp. 1389-1402.e9. doi: 10.1016/j.chembiol.2018.08.005.

Lee, D. G. *et al.* (2006) 'Genomic analysis reveals that *Pseudomonas aeruginosa* virulence is combinatorial', *Genome Biology*. doi: 10.1186/gb-2006-7-10-r90.

Lee, J. H. *et al.* (2011) 'Apple flavonoid phloretin inhibits Escherichia coli O157:H7 biofilm formation and ameliorates colon inflammation in rats', *Infection and Immunity*, 79(12), pp. 4819–4827. doi: 10.1128/IAI.05580-11.

Lee, V. T. *et al.* (2007) 'A cyclic-di-GMP receptor required for bacterial exopolysaccharide production', *Molecular Microbiology*, 65(6), pp. 1474–1484. doi: 10.1111/j.1365-2958.2007.05879.x.

Li, L. *et al.* (2019) 'Diffusible signal factor (DSF)-mediated quorum sensing modulates expression of diverse traits in Xanthomonas citri and responses of citrus plants to promote disease', *BMC Genomics*. BMC Genomics, 20(1), pp. 1–22. doi: 10.1186/s12864-018-5384-4.

Li, Y. *et al.* (2013) 'NO-induced biofilm dispersion in *Pseudomonas aeruginosa* is mediated by an MHYT domain-coupled phosphodiesterase', *Journal of Bacteriology*, 195(16), pp. 3531–3542. doi: 10.1128/JB.01156-12.

Li, Y. *et al.* (2014) 'BdlA, DipA and Induced Dispersion Contribute to Acute Virulence and Chronic Persistence of *Pseudomonas aeruginosa*', *PLoS Pathogens*, 10(6). doi: 10.1371/journal.ppat.1004168.

Liao, J., Schurr, M. J. and Sauera, K. (2013) 'The merR-like regulator brlR confers biofilm tolerance by activating multidrug efflux pumps in *Pseudomonas aeruginosa* biofilms', *Journal of Bacteriology*, 195(15), pp. 3352–3363. doi: 10.1128/JB.00318-13.

Lieberman, O. J. *et al.* (2014) 'High-throughput screening using the differential radial capillary action of ligand assay identifies ebselen as an inhibitor of diguanylate cyclases', *ACS Chemical Biology*. doi: 10.1021/cb400485k.

Lin, C. T. *et al.* (2006) 'Identification of an HptB-mediated multi-step phosphorelay in *Pseudomonas aeruginosa* PAO1', *Research in Microbiology*, 157(2), pp. 169–175. doi: 10.1016/j.resmic.2005.06.012.

Liu, Q. *et al.* (2022) 'Reversion of Ceftazidime Resistance in *Pseudomonas aeruginosa* under Clinical Setting', *Microorganisms*, 10(12). doi: 10.3390/microorganisms10122395.

Liu, Z. *et al.* (2022) 'CzcR Is Essential for Swimming Motility in *Pseudomonas aeruginosa* during Zinc Stress', *Microbiology Spectrum*. American Society for Microbiology, 10(6). doi: 10.1128/spectrum.02846-22.

Luscher, A. *et al.* (2020) 'Combined Bacteriophage and Antibiotic Treatment Prevents *Pseudomonas aeruginosa* Infection of Wild Type and cftr- Epithelial Cells', *Frontiers in Microbiology*, 11(August). doi: 10.3389/fmicb.2020.01947.

Ma, L. *et al.* (2009) 'Assembly and development of the *Pseudomonas aeruginosa* biofilm matrix', *PLoS Pathogens*, 5(3). doi: 10.1371/journal.ppat.1000354.

Macfarlane, E. L. A., Kwasnicka, A. and Hancock, R. E. W. (2009) 'Microbiology (Reading Engl) 2000 Macfarlane', pp. 1–12. Available at: papers2://publication/uuid/DEFC8853-3211-4422-8F9D-03540C52603A.

Madziara-Borusiewicz, K. and Lysenko, O. (1971) 'The mechanism of pathogenicity of *Pseudomonas aeruginosa*', *Journal of Invertebrate Pathology*, 17(1), pp. 138–140. doi: 10.1016/0022-2011(71)90139-x.

Mahamad Maifiah, M. H. *et al.* (2022) 'Integrated metabolomic and transcriptomic analyses of the synergistic effect of polymyxin–rifampicin combination against *Pseudomonas aeruginosa*', *Journal of Biomedical Science*. BioMed Central, 29(1), pp. 1–19. doi: 10.1186/s12929-022-00874-3.

Malet, J. K. *et al.* (2022) 'A Model of Intracellular Persistence of *Pseudomonas aeruginosa* in Airway Epithelial Cells', *Cellular Microbiology*, 2022. doi: 10.1155/2022/5431666.

Mattick, J. S. (2002) 'Type IV pili and twitching motility', *Annual Review of Microbiology*, 56, pp. 289–314. doi: 10.1146/annurev.micro.56.012302.160938.

McBride, K. F. J. & M. J. (no date) 'The surprisingly diverse ways that prokaryotes move'.

McCarthy, M. W. (2019) 'Teixobactin: a novel anti-infective agent', *Expert Review of Anti-Infective Therapy*. Taylor & Francis, 17(1), pp. 1–3. doi: 10.1080/14787210.2019.1550357.

McPhee, J. B. *et al.* (2006) 'Contribution of the PhoP-PhoQ and PmrA-PmrB two-component regulatory systems to Mg2+-induced gene regulation in *Pseudomonas aeruginosa*', *Journal of Bacteriology*, 188(11), pp. 3995–4006. doi: 10.1128/JB.00053-06.

Medzhitov, R., Preston-Hurlburt, P. and Janeway, C. A. (1997) 'A human homologue of the Drosophila toll protein signals activation of adaptive immunity', *Nature*. doi: 10.1038/41131.

Meirelles, L. A. and Newman, D. K. (2018) 'Both toxic and beneficial effects of pyocyanin contribute to the lifecycle of *Pseudomonas aeruginosa*', *Molecular Microbiology*, 110(6), pp. 995–1010. doi: 10.1111/mmi.14132.

Merritt, J. H. *et al.* (2007) 'SadC reciprocally influences biofilm formation and swarming motility via modulation of exopolysaccharide production and flagellar function', *Journal of Bacteriology*, 189(22), pp. 8154–8164. doi: 10.1128/JB.00585-07.

Michel, G. P. F., Durand, E. and Filloux, A. (2007) 'XphA/XqhA, a novel GspCD subunit for type II secretion in *Pseudomonas aeruginosa*', *Journal of Bacteriology*, 189(10), pp. 3776–3783. doi: 10.1128/JB.00205-07.

Miller, V. L. and Mekalanos, J. J. (1988) 'A novel suicide vector and its use in construction of insertion mutations: Osmoregulation of outer membrane proteins and virulence determinants in Vibrio cholerae requires toxR', *Journal of Bacteriology*, 170(6), pp. 2575–2583. doi: 10.1128/jb.170.6.2575-2583.1988.

Miyata, S. *et al.* (2003) 'Use of the Galleria mellonella caterpillar as a model host to study the role of the type III secretion system in *Pseudomonas aeruginosa* pathogenesis', *Infection and Immunity*, 71(5), pp. 2404–2413. doi: 10.1128/IAI.71.5.2404-2413.2003.

Mizgerd, J. P. and Skerrett, S. J. (2008) 'Animal models of human pneumonia', *American Journal of Physiology - Lung Cellular and Molecular Physiology*, 294(3). doi: 10.1152/ajplung.00330.2007.

Mohammed, N. S. and Ali, E. H. (2021) 'Extraction, Purification, and Characterization of Chloramphenicol Acetyltransferase from *Pseudomonas aeruginosa*', *International Journal of Drug Delivery Technology*, 11(4), pp. 1429–1434. doi: 10.25258/ijddt.11.4.52.

Moreau-Marquis, S. *et al.* (2010) 'Co-culture models of *Pseudomonas aeruginosa* biofilms grown on live human airway cells', *Journal of Visualized Experiments*, (44). doi: 10.3791/2186.

Morgan, R. *et al.* (2006) 'BdlA, a chemotaxis regulator essential for biofilm dispersion in *Pseudomonas aeruginosa*', *Journal of Bacteriology*, 188(21), pp. 7335–7343. doi: 10.1128/JB.00599-06.

Morita, Y., Tomida, J. and Kawamura, Y. (2013) 'Responses of *Pseudomonas aeruginosa* to antimicrobials', *Frontiers in Microbiology*, 4(JAN), pp. 1–8. doi: 10.3389/fmicb.2013.00422.

Mosaei, H. *et al.* (2018) 'Mode of Action of Kanglemycin A, an Ansamycin Natural Product that Is Active against Rifampicin-Resistant Mycobacterium tuberculosis', *Molecular Cell*. Elsevier Inc., 72(2), pp. 263-274.e5. doi: 10.1016/j.molcel.2018.08.028.

Mulcahy, L. R. *et al.* (2010) 'Emergence of *Pseudomonas aeruginosa* strains producing high levels of persister cells in patients with cystic fibrosis', *Journal of Bacteriology*. doi: 10.1128/JB.01651-09.

Murray, T. S. and Kazmierczak, B. I. (2008) '*Pseudomonas aeruginosa* exhibits sliding motility in the absence of type IV pili and flagella', *Journal of Bacteriology*, 190(8), pp. 2700–2708. doi: 10.1128/JB.01620-07.

Nadanaciva, S. *et al.* (2011) 'A high content screening assay for identifying lysosomotropic compounds', *Toxicology in Vitro*. Elsevier Ltd, 25(3), pp. 715–723. doi: 10.1016/j.tiv.2010.12.010.

Naguib, M. M. and Valvano, M. A. (2018) 'Vitamin E Increases Antimicrobial Sensitivity by Inhibiting Bacterial Lipocalin Antibiotic Binding', *mSphere*, 3(6). doi: 10.1128/msphere.00564-18.

Narayanaswamy, V. P. *et al.* (2018) 'Novel glycopolymer eradicates antibiotic- and CCCP-induced persister cells in *Pseudomonas aeruginosa*', *Frontiers in Microbiology*, 9(AUG), pp. 1–12. doi: 10.3389/fmicb.2018.01724.

Ng, W. L. *et al.* (2012) 'Broad spectrum pro-quorum-sensing molecules as inhibitors of virulence in vibrios', *PLoS Pathogens*, 8(6). doi: 10.1371/journal.ppat.1002767.

Nikolaidis, M. *et al.* (2020) 'Comparative analysis of the core proteomes among the Pseudomonas major evolutionary groups reveals species-specific adaptations for *Pseudomonas aeruginosa* and Pseudomonas chlororaphis', *Diversity*, 12(8). doi: 10.3390/D12080289.

Nolan, C. and Behrends, V. (2021) 'Sub-inhibitory antibiotic exposure and virulence in *Pseudomonas aeruginosa*', *Antibiotics*, 10(11). doi: 10.3390/antibiotics10111393.

O'Callaghan, D. and Vergunst, A. (2010) 'Non-mammalian animal models to study infectious disease: worms or fly fishing?', *Current Opinion in Microbiology*, 13(1), pp. 79–85. doi: 10.1016/j.mib.2009.12.005.

Olszak, T. *et al.* (2015) 'In vitro and in vivo antibacterial activity of environmental bacteriophages against *Pseudomonas aeruginosa* strains from cystic fibrosis patients', *Applied Microbiology and Biotechnology*, 99(14), pp. 6021–6033. doi: 10.1007/s00253-015-6492-6.

Orr, M. W. *et al.* (2015) 'Oligoribonuclease is the primary degradative enzyme for pGpG in *Pseudomonas aeruginosa* that is required for cyclic-di-GMP turnover', *Proceedings of the National Academy of Sciences of the United States of America*, 112(36), pp. E5048–E5057. doi: 10.1073/pnas.1507245112.

Osipov, A. *et al.* (2019) 'Small molecule immunomodulation: The tumor microenvironment and overcoming immune escape', *Journal for ImmunoTherapy of Cancer*. doi: 10.1186/s40425-019-0667-0.

Oyardi, O., Savage, P. B. and Guzel, C. B. (2022) 'Effects of Ceragenins and Antimicrobial Peptides on the A549 Cell Line and an In Vitro Co-Culture Model of A549 Cells and *Pseudomonas aeruginosa*', *Pathogens*, 11(9). doi: 10.3390/pathogens11091044.

Ozer, E. A. *et al.* (2019) 'The Population Structure of *Pseudomonas aeruginosa* Is Characterized by Genetic Isolation of exoU+ and exoS+ Lineages', *Genome Biology and Evolution*, 11(7), pp. 1780–1796. doi: 10.1093/gbe/evz119.

Pang, Z. *et al.* (2019) 'Antibiotic resistance in *Pseudomonas aeruginosa*: mechanisms and alternative therapeutic strategies', *Biotechnology Advances*. Elsevier, 37(1), pp. 177–192. doi: 10.1016/j.biotechadv.2018.11.013.

Di Paola, M. *et al.* (2017) 'SLC6A14 is a genetic modifier of cystic fibrosis that regulates *Pseudomonas aeruginosa* attachment to human bronchial epithelial cells', *mBio*, 8(6). doi: 10.1128/mBio.02073-17.

Pesci, E. C. *et al.* (1999) 'Quinolone signaling in the cell-to-cell communication system of *Pseudomonas aeruginosa*', *Proceedings of the National Academy of Sciences of the United States of America*, 96(20), pp. 11229–11234. doi: 10.1073/pnas.96.20.11229.

Petrova, O. E., Cherny, K. E. and Sauer, K. (2015) 'The diguanylate cyclase GcbA facilitates *Pseudomonas aeruginosa* biofilm dispersion by activating BdlA', *Journal of Bacteriology*, 197(1), pp. 174–187. doi: 10.1128/JB.02244-14.

Piddock, L. J. V. (2015) 'Teixobactin, the first of a new class of antibiotics discovered by ichip technology?', *Journal of Antimicrobial Chemotherapy*, 70(10), pp. 2679–2680. doi: 10.1093/jac/dkv175.

Pier, G. B. *et al.* (2001) 'Role of alginate O acetylation in resistance of mucoid *Pseudomonas aeruginosa* to opsonic phagocytosis', *Infection and Immunity*, 69(3), pp. 1895–1901. doi: 10.1128/IAI.69.3.1895-1901.2001.

Pires, D. P. *et al.* (2015) 'Phage Therapy: a Step Forward in the Treatment of *Pseudomonas aeruginosa* Infections', *Journal of Virology*, 89(15), pp. 7449–7456. doi: 10.1128/jvi.00385-15.

Qi, L. *et al.* (2022) 'Resveratrol Improves The Antimicrobial Properties Of Polymyxin B Against Multidrug-Resistant *Pseudomonas aeruginosa*', *Res Sq*, pp. 1–22. Available at: https://doi.org/10.21203/rs.3.rs-1359376/v1.

Rahme, L. G. *et al.* (1995) 'Common virulence factors for bacterial pathogenicity in plants and animals', *Science*, 268(5219), pp. 1899–1902. doi: 10.1126/science.7604262.

Ramirez, D. M. *et al.* (2022) 'Guanidinylated Polymyxins as Outer Membrane Permeabilizers Capable of Potentiating Rifampicin, Erythromycin, Ceftazidime and Aztreonam against Gram-Negative Bacteria', *Antibiotics*, 11(10). doi: 10.3390/antibiotics11101277.

Rasamiravaka, T. *et al.* (2015) 'The Formation of Biofilms by *Pseudomonas aeruginosa*', *BioMed Research International*, 2015, pp. 1–17. Available at: http://dx.doi.org/10.1155/2015/759348%0A.

Rasmussen, T. B. and Givskov, M. (2006) 'Quorum-sensing inhibitors as anti-pathogenic drugs', *International Journal of Medical Microbiology*, 296(2–3), pp. 149–161. doi: 10.1016/j.ijmm.2006.02.005.

Rather, M. A., Gupta, K. and Mandal, M. (2021) 'Inhibition of biofilm and quorum sensing-regulated virulence factors in *Pseudomonas aeruginosa* by Cuphea carthagenensis (Jacq.) J. F. Macbr. Leaf extract: An in vitro study', *Journal of Ethnopharmacology*. Elsevier B.V., 269(October 2020), p. 113699. doi: 10.1016/j.jep.2020.113699.

Reis, R. S. *et al.* (2011) 'Gene regulation of rhamnolipid production in *Pseudomonas aeruginosa* - A review', *Bioresource Technology*. Elsevier Ltd, 102(11), pp. 6377–6384. doi: 10.1016/j.biortech.2011.03.074.

Reuter, K., Steinbach, A. and Helms, V. (2016) 'Interfering with bacterial quorum sensing', *Perspectives in Medicinal Chemistry*, 8, pp. 1–15. doi: 10.4137/PMc.s13209.

Romling, U., Galperin, M. Y. and Gomelsky, M. (2013) 'Cyclic di-GMP: the First 25 Years of a Universal Bacterial Second Messenger', *Microbiology and Molecular Biology Reviews*, 77(1), pp. 1–52. doi: 10.1128/mmbr.00043-12.

Römling, U., Gomelsky, M. and Galperin, M. Y. (2005) 'C-di-GMP: The dawning of a novel bacterial signalling system', *Molecular Microbiology*, 57(3), pp. 629–639. doi: 10.1111/j.1365-2958.2005.04697.x.

Ross, P. *et al.* (1987) 'Regulation of cellulose synthesis in Acetobacter xylinum by cyclic diguanylic acid', *Nature*, 325(6101), pp. 279–281. doi: 10.1038/325279a0.

Ross, P., Mayer, R. and Benziman, M. (1991) 'Cellulose biosynthesis and function in bacteria', *Microbiological Reviews*, 55(1), pp. 35–58. doi: 10.1128/mmbr.55.1.35-58.1991.

Rudzite, M. *et al.* (2023) *Effectiveness of Pseudomonas aeruginosa type VI secretion system relies on toxin potency and type IV pili-dependent interaction*, *PLOS Pathogens*. doi: 10.1371/journal.ppat.1011428.

Rugjee, K. N., An, S. Q. and Ryan, R. P. (2016) 'Establishment of a high-throughput setup for screening small molecules that modulate c-di-GMP signaling in *Pseudomonas aeruginosa*', *Journal of Visualized Experiments*, 2016(112), pp. 1–7. doi: 10.3791/54115.

Rutherford, S. T. and Bassler, B. L. (2012) 'Bacterial quorum sensing: Its role in virulence and possibilities for its control', *Cold Spring Harbor Perspectives in Medicine*, 2(11), pp. 1–26. doi: 10.1101/cshperspect.a012427.

Ryan, R. P. *et al.* (2006) 'Cell-cell signaling in Xanthomonas campestris involves an HD-GYP domain protein that functions in cyclic di-GMP turnover', *Proceedings of the National Academy of Sciences of the United States of America*. doi: 10.1073/pnas.0600345103.

Ryan, R. P. *et al.* (2008) 'Interspecies signalling via the Stenotrophomonas maltophilia diffusible signal factor influences biofilm formation and polymyxin tolerance in *Pseudomonas aeruginosa*', *Molecular Microbiology*, 68(1), pp. 75–86. doi: 10.1111/j.1365-2958.2008.06132.x.

Ryan, R. P. *et al.* (2010) 'Cell-cell signal-dependent dynamic interactions between HD-GYP and GGDEF domain proteins mediate virulence in Xanthomonas campestris', *Proceedings of the National Academy of Sciences of the United States of America*. doi: 10.1073/pnas.0912839107.

Ryan, R. P. (2013) 'Cyclic di-GMP signalling and the regulation of bacterial virulence', *Microbiology (United Kingdom)*, 159(PART7), pp. 1286–1297. doi: 10.1099/mic.0.068189-0.

Ryan, R. P. *et al.* (2015) 'The DSF Family of Cell–Cell Signals: An Expanding Class of Bacterial Virulence Regulators', *PLoS Pathogens*, 11(7), pp. 1–14. doi: 10.1371/journal.ppat.1004986.

Ryan, R. P. and Dow, J. M. (2008) 'Diffusible signals and interspecies communication in bacteria', *Microbiology*. doi: 10.1099/mic.0.2008/017871-0.

Ryan, R. P. and Dow, J. M. (2011) 'Communication with a growing family: Diffusible signal factor (DSF) signaling in bacteria', *Trends in Microbiology*. doi: 10.1016/j.tim.2010.12.003.

Ryan, R. P., Tolker-Nielsen, T. and Dow, J. M. (2012) 'When the PilZ don't work: Effectors for cyclic di-GMP action in bacteria', *Trends in Microbiology*. Elsevier Ltd, 20(5), pp. 235–242. doi: 10.1016/j.tim.2012.02.008.

Rybtke, M. T. *et al.* (2012) 'Fluorescence-based reporter for gauging cyclic Di-GMP levels in *Pseudomonas aeruginosa*', *Applied and Environmental Microbiology*, 78(15), pp. 5060–5069. doi: 10.1128/AEM.00414-12.

Ryder, C., Byrd, M. and Wozniak, D. J. (2007) 'Role of polysaccharides in *Pseudomonas aeruginosa* biofilm development', *Current Opinion in Microbiology*. doi: 10.1016/j.mib.2007.09.010.

Ryder, C., Byrd, M. and Wozniak, D. J. (2016) 'development', 10(6), pp. 644–648.

Saga, Y. *et al.* (2005) 'Bacteriochlorophyll-c homolog composition in green sulfur photosynthetic bacterium Chlorobium vibrioforme dependent on the concentration of sodium sulfide in liquid cultures', in *Photosynthesis Research*. doi: 10.1007/s11120-005-5301-y.

Sambanthamoorthy, K. *et al.* (2012) 'Identification of small molecules that antagonize diguanylate cyclase enzymes to inhibit biofilm formation', *Antimicrobial Agents and Chemotherapy*. doi: 10.1128/AAC.01396-12.

Sambanthamoorthy, K. *et al.* (2014) 'Identification of small molecules inhibiting diguanylate cyclases to control bacterial biofilm development', *Biofouling*. doi: 10.1080/08927014.2013.832224.

Sana, T. G., Berni, B. and Bleves, S. (2016) 'The T6SSs of *Pseudomonas aeruginosa* strain pao1 and their effectors: Beyond bacterial-cell targeting', *Frontiers in Cellular and Infection Microbiology*, 6(JUN). doi: 10.3389/fcimb.2016.00061.

Sandoval-Motta, S. and Aldana, M. (2016) 'Adaptive resistance to antibiotics in bacteria: A systems biology perspective', *Wiley Interdisciplinary Reviews: Systems Biology and Medicine*, 8(3), pp. 253–267. doi: 10.1002/wsbm.1335.

Santos, J. F. (2012) 'Business or Fun?: Similarities and Differences between Portuguese and International Wine Bloggers', *Management*, 2(1), pp. 1–9. doi: 10.5923/j.mm.20120201.01.

Sarkar, S. (2020) 'Release mechanisms and molecular interactions of *Pseudomonas aeruginosa* extracellular DNA', *Applied Microbiology and Biotechnology*, 104(15), pp. 6549–6564. doi: 10.1007/s00253-020-10687-9.

Sauer, K. *et al.* (2002) 'Displays Multiple Phenotypes during Development as a Biofilm', *Society*, 184(4), pp. 1140–1154. doi: 10.1128/JB.184.4.1140.

Schmidt, A. *et al.* (2016) 'Oxygen-dependent regulation of c-di-GMP synthesis by SadC controls alginate production in *Pseudomonas aeruginosa*', *Environmental Microbiology*, 18(10), pp. 3390–3402. doi: 10.1111/1462-2920.13208.

Schuster, M. and Greenberg, E. P. (2007) 'Early activation of quorum sensing in *Pseudomonas aeruginosa* reveals the architecture of a complex regulon', *BMC Genomics*, 8, pp. 1–11. doi: 10.1186/1471-2164-8-287.

Semwal, D. K. *et al.* (2016) 'Myricetin: A dietary molecule with diverse biological activities', *Nutrients*, 8(2), pp. 1–31. doi: 10.3390/nu8020090.

Sermet-Gaudelus, I. (2013) 'Ivacaftor treatment in patients with cystic fibrosis and the G551D-CFTR mutation', *European Respiratory Review*, 22(127), pp. 66–71. doi: 10.1183/09059180.00008512.

Shen, B. (2015) 'A New Golden Age of Natural Products Drug Discovery', *Cell*. Elsevier Inc., 163(6), pp. 1297–1300. doi: 10.1016/j.cell.2015.11.031.

Simm, R. *et al.* (2004) 'GGDEF and EAL domains inversely regulate cyclic di-GMP levels and transition from sessibility to motility', *Molecular Microbiology*, 53(4), pp. 1123–1134. doi: 10.1111/j.1365-2958.2004.04206.x.

Skerker, J. M. and Berg, H. C. (2001) 'Direct observation of extension and retraction of type IV pili', *Proceedings of the National Academy of Sciences of the United States of America*. doi: 10.1073/pnas.121171698.

Slater, H. *et al.* (2000) 'A two-component system involving an HD-GYP domain protein links cell-cell signalling to pathogenicity gene expression in Xanthomonas campestris', *Molecular Microbiology*. doi: 10.1046/j.1365-2958.2000.02196.x.

De Smet, J. *et al.* (2017) 'Pseudomonas predators: Understanding and exploiting phage-host interactions', *Nature Reviews Microbiology*. doi: 10.1038/nrmicro.2017.61.

Smith, R. S. and Iglewski, B. H. (2003) '*P. aeruginosa* quorum-sensing systems and virulence', *Current Opinion in Microbiology*, 6(1), pp. 56–60. doi: 10.1016/S1369-5274(03)00008-0.

Stoltz, D. A. *et al.* (2008) 'Are Protected From', *The Journal of Clinical Investigation*, 118(9), pp. 3123–3131. doi: 10.1172/JCI35147DS1.

Sultan, M., Arya, R. and Kim, K. K. (2021) 'Roles of two-component systems in *Pseudomonas aeruginosa* virulence', *International Journal of Molecular Sciences*, 22(22). doi: 10.3390/ijms222212152.

Sun, B. *et al.* (2021) 'Inhibition of Quorum Sensing and Biofilm Formation of Esculetin on Aeromonas Hydrophila', *Frontiers in Microbiology*, 12(September). doi: 10.3389/fmicb.2021.737626.

Szamosvári, D. *et al.* (2016) 'Synthetic quinolone signal analogues inhibiting the virulence factor elastase of *Pseudomonas aeruginosa*', *Chemical Communications*, 52(92), pp. 13440–13443. doi: 10.1039/c6cc06295d.

Szymański, P., Markowicz, M. and Mikiciuk-Olasik, E. (2012) 'Adaptation of high-throughput screening in drug discovery-toxicological screening tests', *International Journal of Molecular Sciences*, 13(1), pp. 427–452. doi: 10.3390/ijms13010427.

Taccetti, G. *et al.* (2020) 'A critical review of definitions used to describe *Pseudomonas aeruginosa* microbiological status in patients with cystic fibrosis for application in clinical trials', *Journal of Cystic Fibrosis*, 19(1), pp. 52–67. doi: 10.1016/j.jcf.2019.08.014.

Tamma, P. D., Cosgrove, S. E. and Maragakis, L. L. (2012) 'Combination therapy for treatment of infections with gram-negative bacteria', *Clinical Microbiology Reviews*. doi: 10.1128/CMR.05041-11.

Tan, B. and Vanitha, J. (2012) 'Immunomodulatory and Antimicrobial Effects of Some Traditional Chinese Medicinal Herbs: A Review', *Current Medicinal Chemistry*. doi: 10.2174/0929867043365161.

Tart, A. H., Blanks, M. J. and Wozniak, D. J. (2006) 'The AlgT-dependent transcriptional regulator AmrZ (AlgZ) inhibits flagellum biosynthesis in mucoid, nonmotile *Pseudomonas aeruginosa* cystic fibrosis isolates', *Journal of Bacteriology*, 188(18), pp. 6483–6489. doi: 10.1128/JB.00636-06.

Thi, M. T. T., Wibowo, D. and Rehm, B. H. A. (2020) '*Pseudomonas aeruginosa* biofilms', *International Journal of Molecular Sciences*, 21(22), pp. 1–25. doi: 10.3390/ijms21228671.

Tischler, A. D. and Camilli, A. (2009) 'formation', 53(3), pp. 857–869. doi: 10.1111/j.1365-2958.2004.04155.x.Cyclic.

Torrens, G. *et al.* (2019) 'Regulation of AmpC-Driven -Lactam Resistance in', 4(6), pp. 1–14.

Toyofuku, M. *et al.* (2016) 'Environmental factors that shape biofilm formation', *Bioscience, Biotechnology and Biochemistry*, pp. 7–12. doi: 10.1080/09168451.2015.1058701.

Tran, C. S. *et al.* (2014) 'The *Pseudomonas aeruginosa* Type III Translocon Is Required for Biofilm Formation at the Epithelial Barrier', *PLoS Pathogens*, 10(11). doi: 10.1371/journal.ppat.1004479.

Trapnell, C. *et al.* (2012) 'Differential gene and transcript expression analysis of RNA-seq experiments with TopHat and Cufflinks', *Nature Protocols*, 7(3), pp. 562–578. doi: 10.1038/nprot.2012.016.

Tsai, C. J. Y., Loh, J. M. S. and Proft, T. (2016) 'Galleria mellonella infection models for the study of bacterial diseases and for antimicrobial drug testing', *Virulence*. Taylor & Francis, 7(3), pp. 214–229. doi: 10.1080/21505594.2015.1135289.

Twomey, K. B. *et al.* (2012) 'Bacterial cis-2-unsaturated fatty acids found in the cystic fibrosis airway modulate virulence and persistence of *Pseudomonas aeruginosa*', *ISME Journal*. doi: 10.1038/ismej.2011.167.

Uddin, T. M. *et al.* (2021) 'Antibiotic resistance in microbes: History, mechanisms, therapeutic strategies and future prospects', *Journal of Infection and Public Health*, 14(12), pp. 1750–1766. doi: 10.1016/j.jiph.2021.10.020.

Ulloa, E. R. and Sakoulas, G. (2022) 'Azithromycin: An Underappreciated Quinolone-Sparing Oral Treatment for *Pseudomonas aeruginosa* Infections', *Antibiotics*, 11(4), pp. 10–15. doi: 10.3390/antibiotics11040515.

Valentini, M. and Filloux, A. (2016a) 'Biofilms and Cyclic di-GMP (c-di-GMP) signaling: Lessons from *Pseudomonas aeruginosa* and other bacteria', *Journal of Biological Chemistry*, 291(24), pp. 12547–12555. doi: 10.1074/jbc.R115.711507.

Valentini, M. and Filloux, A. (2016b) 'Biofilms and Cyclic di-GMP (c-di-GMP) signaling: Lessons from *Pseudomonas aeruginosa* and other bacteria', *Journal of Biological Chemistry*. Â© 2016 ASBMB. Currently published by Elsevier Inc; originally published by American Society for Biochemistry and Molecular Biology, 291(24), pp. 12547–12555. doi: 10.1074/jbc.R115.711507.

Vasavi, H. S. *et al.* (2017) 'Bioavailability-enhanced Resveramax™ modulates quorum sensing and inhibits biofilm formation in *Pseudomonas aeruginosa* PAO1', *Microbial Pathogenesis*. Elsevier Ltd, 104, pp. 64–71. doi: 10.1016/j.micpath.2017.01.015.

Vasquez-Rifo, A. *et al.* (2019) 'The *Pseudomonas aeruginosa* accessory genome elements influence virulence towards Caenorhabditis elegans', *Genome Biology*. Genome Biology, 20(1), pp. 1–22. doi: 10.1186/s13059-019-1890-1.

Vernooij, L. *et al.* (2021) 'High-throughput screening identifies idasanutlin as a resensitizing drug for venetoclax-resistant neuroblastoma cells', *Molecular Cancer Therapeutics*, 20(6), pp. 1161–1172. doi: 10.1158/1535-7163.MCT-20-0666.

Vitro, I. *et al.* (2023) 'Resveratrol Increases Sensitivity of Clinical Colistin-Resistant'. American Society for Microbiology, 11(1), pp. 1–13.

Wagner, V. E., Gillis, R. J. and Iglewski, B. H. (2004) 'Transcriptome analysis of quorum-sensing regulation and virulence factor expression in *Pseudomonas aeruginosa*', *Vaccine*, 22(SUPPL. 1). doi: 10.1016/j.vaccine.2004.08.011.

Walsh, V. and Goodman, J. (1999) 'Cancer chemotherapy, biodiversity, public and private property: The case of the anti-cancer drug Taxol', *Social Science and Medicine*, 49(9), pp. 1215–1225. doi: 10.1016/S0277-9536(99)00161-6.

Wang, H., Liao, L. and Chen, S. (2020) 'crossm Substrate-Inducible Genes Conferring Degradation of Diffusible Signal Factor', 86(7), pp. 1–18.

Wang, L. H. *et al.* (2004) 'A bacterial cell-cell communication signal with cross-kingdom structural analogues', *Molecular Microbiology*, 51(3), pp. 903–912. doi: 10.1046/j.1365-2958.2003.03883.x.

Wang, M. *et al.* (2022) 'The cis -2-Dodecenoic Acid (BDSF) Quorum Sensing System in'. American Society for Microbiology, (19).

Wang, Z. H. *et al.* (2010) 'Myricetin suppresses oxidative stress-induced cell damage via both direct and indirect antioxidant action', *Environmental Toxicology and Pharmacology*, 29(1), pp. 12–18. doi: 10.1016/j.etap.2009.08.007.

Warchal, S. J. *et al.* (2020) 'High content phenotypic screening identifies serotonin receptor modulators with selective activity upon breast cancer cell cycle and cytokine signaling pathways', *Bioorganic and Medicinal Chemistry*. Elsevier, 28(1), p. 115209. doi: 10.1016/j.bmc.2019.115209.

Watnick, P. and Kolter, R. (2000) 'Biofilm, city of microbes', *Journal of Bacteriology*, 182(10), pp. 2675–2679. doi: 10.1128/JB.182.10.2675-2679.2000.

Weichert, S. *et al.* (2013) 'Bioengineered 2'-fucosyllactose and 3-fucosyllactose inhibit the adhesion of *Pseudomonas aeruginosa* and enteric pathogens to human intestinal and respiratory cell lines', *Nutrition Research*. Elsevier Inc., 33(10), pp. 831–838. doi: 10.1016/j.nutres.2013.07.009.

WHO (2017) 'Global priority list of antibiotic-resistant batceria to guide research, discovery, and development of new antibiotics', *Who*.

Winstanley, C., O'Brien, S. and Brockhurst, M. A. (2016) '*Pseudomonas aeruginosa* Evolutionary Adaptation and Diversification in Cystic Fibrosis Chronic Lung Infections', *Trends in Microbiology*. Elsevier Ltd, 24(5), pp. 327–337. doi: 10.1016/j.tim.2016.01.008.

Wood, T. E. *et al.* (2019) 'The *Pseudomonas aeruginosa* T6SS Delivers a Periplasmic Toxin that Disrupts Bacterial Cell Morphology', *Cell Reports*, 29(1), pp. 187-201.e7. doi: 10.1016/j.celrep.2019.08.094.

Wu, W. *et al.* (2014) *Pseudomonas aeruginosa*, *Molecular Medical Microbiology*. Elsevier Ltd. doi: 10.1016/B978-0-12-397169-2.00041-X.

Xie, Y. *et al.* (2022) 'Inhibition of Quorum-Sensing Regulator from *Pseudomonas aeruginosa* Using a Flavone Derivative', *Molecules*, 27(8), pp. 1–13. doi: 10.3390/molecules27082439.

Xu, L. *et al.* (2016) 'A cyclic di-GMP-binding adaptor protein interacts with histidine kinase to regulate two-component signaling', *Journal of Biological Chemistry*, 291(31), pp. 16112–16123. doi: 10.1074/jbc.M116.730887.

Yang, A. *et al.* (2017) 'Influence of Physical Effects on the Swarming Motility of *Pseudomonas aeruginosa*', *Biophysical Journal*. Biophysical Society, 112(7), pp. 1462–1471. doi: 10.1016/j.bpj.2017.02.019.

Yang, L. *et al.* (2016) 'New insights into the antibacterial activity of hydroxycoumarins against ralstonia solanacearum', *Molecules*, 21(4), pp. 1–13. doi: 10.3390/molecules21040468.

Yang, Y. *et al.* (2022) 'H3-T6SS of *Pseudomonas aeruginosa* PA14 contributes to environmental adaptation via secretion of a biofilm-promoting effector', *Stress Biology*, 2(1). doi: 10.1007/s44154-022-00078-7.

Yazdanian, M. *et al.* (2023) 'The comparative effects of erythromycin and amikacin on acute respiratory *Pseudomonas aeruginosa* infection', *Veterinary Medicine and Science*, 9(2), pp. 867–875. doi: 10.1002/vms3.991.

Zanella, F., Lorens, J. B. and Link, W. (2010) 'High content screening: Seeing is believing', *Trends in Biotechnology*. Elsevier Ltd, 28(5), pp. 237–245. doi: 10.1016/j.tibtech.2010.02.005.

Zdybicka-Barabas, A. *et al.* (2012) 'Synergistic action of Galleria mellonella anionic peptide 2 and lysozyme against Gram-negative bacteria', *Biochimica et Biophysica Acta - Biomembranes*, 1818(11), pp. 2623–2635. doi: 10.1016/j.bbamem.2012.06.008.

Zhang, L., Xie, Q. and Li, X. (2022) 'Esculetin: A review of its pharmacology and pharmacokinetics', *Phytotherapy Research*, 36(1), pp. 279–298. doi: 10.1002/ptr.7311.

Zhao, Y. hu *et al.* (2019) 'Identification and expression analysis of ceftriaxone resistance-related genes in Neisseria gonorrhoeae integrating RNA-Seq data and qRT-PCR validation', *Journal of Global Antimicrobial Resistance*. Taibah University, 16(2019), pp. 202–209. doi: 10.1016/j.jgar.2018.10.008.

Zheng, Z. *et al.* (2017) 'crossm Synergistic Efficacy of Aedes aegypti', 61(7), pp. 1–15.

Zhou, T. *et al.* (2022) 'The Two-Component System FleS / FleR Represses H1-T6SS via', *Applied and environmental microbiology*. American Society for Microbiology, 88(2), pp. e01655-21.

Zscherp, R. *et al.* (2023) 'Design of non-cytotoxic 6,7-dihydroxycoumarin-5-carboxylates with antibiofilm activity against Staphylococcus aureus and Candida albicans', *Organic and Biomolecular Chemistry*. Royal Society of Chemistry, 21. doi: 10.1039/d3ob00303e.

A, M. E., R, B. R. and R. Radhakrishnan (2011) 'High - Throughput Screening : The Hits and Leads of Drug Discovery - An Overview', *Journal of Applied Pharmaceutical Science*, 01(2011), pp. 2–10. Available at: https://www.researchgate.net/profile/Elvis_Martis/publication/210666871_High-Throughput_Screening_The_Hits_and_Leads_of_Drug_Discovery-_An_Overview/links/0f9845a7e00e20552af346d7/High-Throughput-Screening-The-Hits-and-Leads-of-Drug-Discovery-An-Overview.p.

Adrian, L. and Löffler, F. E. (2016) *Organohalide-respiring bacteria*, *Organohalide-Respiring Bacteria*. doi: 10.1007/978-3-662-49875-0.

ALTUN, İbrahim *et al.* (2023) 'Production Of Tetracycline Hydrochloride-Collagen-Doped Chitosan Nanofiber Scaffolds And Investigation Of Their Antibacterial Properties', *International Journal of Life Sciences and Biotechnology*, 6(1), pp. 37–60. doi: 10.38001/ijlsb.1180026.

Alvarez-Ortega, C. *et al.* (2011) 'The intrinsic resistome of *Pseudomonas aeruginosa* to β-lactams', *Virulence*, 2(2), pp. 144–146. doi: 10.4161/viru.2.2.15014.

Amikam, D., Weinhouse, H. and Galperin, M. Y. (2014) 'Moshe Benziman and the Discovery of Cyclic Di-GMP', *The Second Messenger Cyclic Di-GMP*, pp. 9–23. doi: 10.1128/9781555816667.ch2.

Amina, A. (2017) 'Pseudomonas Chemotaxis, Motility and Host-Pathogen Interactions', *MOJ Immunology*, 5(5). doi: 10.15406/moji.2017.05.00167.

An, S. Q. *et al.* (2020) 'An improved bind-n-seq strategy to determine protein-DNA interactions validated using the bacterial transcriptional regulator YipR', *BMC Microbiology*. BMC Microbiology, 20(1), pp. 1–11. doi: 10.1186/s12866-019-1672-7.

An, S. Q. and Ryan, R. P. (2016) 'Combating chronic bacterial infections by manipulating cyclic nucleotide-regulated biofilm formation', *Future Medicinal Chemistry*. doi: 10.4155/fmc-2015-0002.

An, S. qi *et al.* (2014) 'Novel Cyclic di-GMP Effectors of the YajQ Protein Family Control Bacterial Virulence', *PLoS Pathogens*, 10(10). doi: 10.1371/journal.ppat.1004429.

An, S. qi *et al.* (2019) 'Modulation of antibiotic sensitivity and biofilm formation in *Pseudomonas aeruginosa* by interspecies signal analogues', *Nature Communications*. Springer US, 10(1), pp. 1–11. doi: 10.1038/s41467-019-10271-4.

Andersen, J. B. *et al.* (2021) 'Identification of small molecules that interfere with c-di-GMP signaling and induce dispersal of *Pseudomonas aeruginosa* biofilms', *npj Biofilms and Microbiomes*. Springer US, 7(1). doi: 10.1038/s41522-021-00225-4.

Andrejko, M., Zdybicka-Barabas, A. and Cytryńska, M. (2014) 'Diverse effects of Galleria mellonella infection with entomopathogenic and clinical strains of *Pseudomonas aeruginosa*', *Journal of Invertebrate Pathology*, 115(1), pp. 14–25. doi: 10.1016/j.jip.2013.10.006.

Anisa, A. N. *et al.* (2021) 'Antimicrobial effect of roselle (Hibiscus sabdariffa l.) water fraction against *Pseudomonas aeruginosa* using drosophila infection model', *Biointerface Research in Applied Chemistry*, 11(5), pp. 12877–12885. doi: 10.33263/BRIAC115.1287712885.

Atanasov, A. G. *et al.* (2015) 'Discovery and resupply of pharmacologically active plant-derived natural products: A review', *Biotechnology Advances*. The Authors, 33(8), pp. 1582–1614. doi: 10.1016/j.biotechadv.2015.08.001.

AU - Moreau-Marquis, S. *et al.* (2010) 'Co-culture Models of *Pseudomonas aeruginosa* Biofilms Grown on Live Human Airway Cells', *JoVE*. MyJoVE Corp, (44), p. e2186. doi: doi:10.3791/2186.

Ayerbe-Algaba, R. *et al.* (2019) 'The anthelmintic oxyclozanide restores the activity of colistin against colistin-resistant Gram-negative bacilli', *International Journal of Antimicrobial Agents*. Elsevier B.V., 54(4), pp. 507–512. doi: 10.1016/j.ijantimicag.2019.07.006.

Azam, M. W. and Khan, A. U. (2019) 'Updates on the pathogenicity status of *Pseudomonas aeruginosa*', *Drug Discovery Today*. Elsevier Ltd, 24(1), pp. 350–359. doi: 10.1016/j.drudis.2018.07.003.

Barber, C. E. *et al.* (1997) 'A novel regulatory system required for pathogenicity of Xanthomonas campestris is mediated by a small diffusible signal molecule', *Molecular Microbiology*. doi: 10.1046/j.1365-2958.1997.3721736.x.

Baynham, P. J. *et al.* (2006) 'The *Pseudomonas aeruginosa* ribbon-helix-helix DNA-binding protein AlgZ (AmrZ) controls twitching motility and biogenesis of type IV pili', *Journal of Bacteriology*, 188(1), pp. 132–140. doi: 10.1128/JB.188.1.132-140.2006.

Beckert, U. *et al.* (2014) 'ExoY from *Pseudomonas aeruginosa* is a nucleotidyl cyclase with preference for cGMP and cUMP formation', *Biochemical and Biophysical Research Communications*. Elsevier Inc., 450(1), pp. 870–874. doi: 10.1016/j.bbrc.2014.06.088.

Belanger, C. R. *et al.* (2020) 'Identification of novel targets of azithromycin activity against *Pseudomonas aeruginosa* grown in physiologically relevant media', *Proceedings of the National Academy of Sciences of the United States of America*, 117(52), pp. 33519–33529. doi: 10.1073/pnas.2007626117.

De Bentzmann, S. and Plésiat, P. (2011) 'The *Pseudomonas aeruginosa* opportunistic pathogen and human infections', *Environmental Microbiology*. doi: 10.1111/j.1462-2920.2011.02469.x.

Berg, H. C. (2003) 'The rotary motor of bacterial flagella', *Annual Review of Biochemistry*. doi: 10.1146/annurev.biochem.72.121801.161737.

Bhuwan, M. *et al.* (2012) 'Histidine-containing phosphotransfer protein-B (HptB) regulates swarming motility through partner-switching system in *Pseudomonas aeruginosa* PAO1 strain', *Journal of Biological Chemistry*. Â© 2012 ASBMB. Currently published by Elsevier Inc; originally published by American Society for Biochemistry and Molecular Biology., 287(3), pp. 1903–1914. doi: 10.1074/jbc.M111.256586.

Blair, J. M. A. *et al.* (2015) 'Molecular mechanisms of antibiotic resistance', *Nature Reviews Microbiology*. doi: 10.1038/nrmicro3380.

Boldrick, J. C. *et al.* (2002) 'Stereotyped and specific gene expression programs in human innate immune responses to bacteria', *Proceedings of the National Academy of Sciences of the United States of America*. doi: 10.1073/pnas.231625398.

Boon, C. *et al.* (2008) 'A novel DSF-like signal from Burkholderia cenocepacia interferes with Candida albicans morphological transition', *ISME Journal*, 2(1), pp. 27–36. doi: 10.1038/ismej.2007.76.

Bottomley, M. J. *et al.* (2007) 'Molecular insights into quorum sensing in the human pathogen *Pseudomonas aeruginosa* from the structure of the virulence regulator LasR bound to its autoinducer', *Journal of Biological Chemistry*, 282(18), pp. 13592–13600. doi: 10.1074/jbc.M700556200.

Breathnach, A. S. *et al.* (2012) 'Multidrug-resistant *Pseudomonas aeruginosa* outbreaks in two hospitals: Association with contaminated hospital waste-water systems', *Journal of Hospital Infection*. doi: 10.1016/j.jhin.2012.06.007.

Breidenstein, E. B. M., de la Fuente-Núñez, C. and Hancock, R. E. W. (2011) '*Pseudomonas aeruginosa*: All roads lead to resistance', *Trends in Microbiology*, 19(8), pp. 419–426. doi: 10.1016/j.tim.2011.04.005.

Brindhadevi, K. *et al.* (2020) 'Biofilm and Quorum sensing mediated pathogenicity in *Pseudomonas aeruginosa*', *Process Biochemistry*. Elsevier, 96(September 2019), pp. 49–57. doi: 10.1016/j.procbio.2020.06.001.

Brown, S. *et al.* (2022) 'Doxycycline for the treatment of breast cancer-related lymphedema', *Frontiers in Pharmacology*, 13(October). doi: 10.3389/fphar.2022.1028926.

Brown, S. E. *et al.* (2009) 'A peptidomics study reveals the impressive antimicrobial peptide arsenal of the wax moth Galleria mellonella', *Insect Biochemistry and Molecular Biology*. Elsevier Ltd, 39(11), pp. 792–800. doi: 10.1016/j.ibmb.2009.09.004.

Bruchmann, S. *et al.* (2013) 'Quantitative contributions of target alteration and decreased drug accumulation to *Pseudomonas aeruginosa* fluoroquinolone resistance', *Antimicrobial Agents and Chemotherapy*, 57(3), pp. 1361–1368. doi: 10.1128/AAC.01581-12.

Burrows, L. L. (2012) '*Pseudomonas aeruginosa* twitching motility: Type IV pili in action', *Annual Review of Microbiology*, 66, pp. 493–520. doi: 10.1146/annurev-micro-092611-150055.

Byrd, M. S. *et al.* (2009) 'Genetic and biochemical analyses of the *Pseudomonas aeruginosa* Psl exopolysaccharide reveal overlapping roles for polysaccharide synthesis enzymes in Psl and LPS production', *Molecular Microbiology*, 73(4), pp. 622–638. doi: 10.1111/j.1365-2958.2009.06795.x.

Calixto, J. B. (2019) 'The role of natural products in modern drug discovery.Calixto, J. B. (2019). The role of natural products in modern drug discovery. Anais Da Academia Brasileira de Ciencias, 91, 1–7. https://doi.org/10.1590/0001-3765201920190105', *Anais da Academia Brasileira de Ciencias*, 91, pp. 1–7. doi: 10.1590/0001-3765201920190105.Abstract.

Cannatelli, A. *et al.* (2018) 'Synergistic activity of colistin in combination with resveratrol against colistin-resistant gram-negative pathogens', *Frontiers in Microbiology*, 9(AUG). doi: 10.3389/fmicb.2018.01808.

Chaudhary, N. *et al.* (2022) 'Polyaspartate-derived synthetic antimicrobial polymer enhances the activity of rifampicin against multidrug-resistant *Pseudomonas aeruginosa* infections', *Biomaterials Science*. Royal Society of Chemistry, 10(18), pp. 5158–5171. doi: 10.1039/d2bm00524g.

Chen, Y. T. *et al.* (2004) 'Evolutionary analysis of the two-component systems in *Pseudomonas aeruginosa* PAO1', *Journal of Molecular Evolution*, 59(6), pp. 725–737. doi: 10.1007/s00239-004-2663-2.

Chiang, C. Y. *et al.* (2018) 'Mitigating the impact of antibacterial drug resistance through host-directed therapies: Current progress, outlook, and challenges', *mBio*. doi: 10.1128/mBio.01932-17.

Christensen, L. D. *et al.* (2013) 'Clearance of *Pseudomonas aeruginosa* foreign-body biofilm infections through reduction of the cyclic di-gmp level in the bacteria', *Infection and Immunity*, 81(8), pp. 2705–2713. doi: 10.1128/IAI.00332-13.

Chugani, S. and Greenberg, E. P. (2014) 'An evolving perspective on the *Pseudomonas aeruginosa* orphan quorum sensing regulator QscR', *Frontiers in Cellular and Infection Microbiology*, 4(OCT), pp. 1–7. doi: 10.3389/fcimb.2014.00152.

Clatworthy, A. E. *et al.* (2009) '*Pseudomonas aeruginosa* infection of zebrafish involves both host and pathogen determinants', *Infection and Immunity*, 77(4), pp. 1293–1303. doi: 10.1128/IAI.01181-08.

Claudine, B. and Harwood, C. S. (2013) 'Cyclic diguanosine monophosphate represses bacterial flagella synthesis by interacting with the Walker a motif of the enhancer-binding protein FleQ', *Proceedings of the National Academy of Sciences of the United States of America*, 110(46), pp. 18478–18483. doi: 10.1073/pnas.1318972110.

Coleman, S. R. *et al.* (2020) 'Multidrug adaptive resistance of *Pseudomonas aeruginosa* swarming cells', *Antimicrobial Agents and Chemotherapy*. doi: 10.1128/AAC.01999-19.

Colvin, K. M. *et al.* (2011) 'The pel polysaccharide can serve a structural and protective role in the biofilm matrix of *Pseudomonas aeruginosa*', *PLoS Pathogens*, 7(1). doi: 10.1371/journal.ppat.1001264.

Conrad, J. C. *et al.* (2011) 'Flagella and pili-mediated near-surface single-cell motility mechanisms in *P. aeruginosa*', *Biophysical Journal*. Biophysical Society, 100(7), pp. 1608–1616. doi: 10.1016/j.bpj.2011.02.020.

Cutuli, M. A. *et al.* (2019) 'Galleria mellonella as a consolidated in vivo model hosts: New developments in antibacterial strategies and novel drug testing', *Virulence*. Taylor & Francis, 10(1), pp. 527–541. doi: 10.1080/21505594.2019.1621649.

Cytryńska, M. *et al.* (2007) 'Purification and characterization of eight peptides from Galleria mellonella immune hemolymph', *Peptides*, 28(3), pp. 533–546. doi: 10.1016/j.peptides.2006.11.010.

D'Angelo, F. *et al.* (2018) 'Identification of FDA-Approved Drugs as Antivirulence Agents', *Antimicrobial Agents and Chemotherapy*, pp. 1–20. Available at: https://www.ncbi.nlm.nih.gov/pmc/articles/PMC6201120/pdf/e01296-18.pdf.

D'Argenio, D. A. *et al.* (2002) 'Autolysis and autoaggregation in *Pseudomonas aeruginosa* colony morphology mutants', *Journal of Bacteriology*, 184(23), pp. 6481–6489. doi: 10.1128/JB.184.23.6481-6489.2002.

Dai, L. *et al.* (2019) 'Ibuprofen-mediated potential inhibition of biofilm development and quorum sensing in *Pseudomonas aeruginosa*', *Life Sciences*. Elsevier, 237(September), p. 116947. doi: 10.1016/j.lfs.2019.116947.

Damron, F. H. *et al.* (2013a) 'Construction of mobilizable mini-Tn7 vectors for bioluminescent detection of gram-negative bacteria and single-copy promoter lux reporter analysis', *Applied and Environmental Microbiology*. doi: 10.1128/AEM.00640-13.

Damron, F. H. *et al.* (2013b) 'Construction of mobilizable mini-Tn7 vectors for bioluminescent detection of gram-negative bacteria and single-copy promoter lux reporter analysis', *Applied and Environmental Microbiology*, 79(13), pp. 4149–4153. doi: 10.1128/AEM.00640-13.

Das, M. C. *et al.* (2016) 'Attenuation of *Pseudomonas aeruginosa* biofilm formation by Vitexin: A combinatorial study with azithromycin and gentamicin', *Scientific Reports*. Nature Publishing Group, 6(March), pp. 1–13. doi: 10.1038/srep23347.

Davies, D. G. and Marques, C. N. H. (2009) 'A fatty acid messenger is responsible for inducing dispersion in microbial biofilms', *Journal of Bacteriology*, 191(5), pp. 1393–1403. doi: 10.1128/JB.01214-08.

Deng, Y. *et al.* (2010) 'Structural and functional characterization of diffusible signal factor family quorum-sensing signals produced by members of the burkholderia cepacia complex', *Applied and Environmental Microbiology*, 76(14), pp. 4675–4683. doi: 10.1128/AEM.00480-10.

Deng, Y. *et al.* (2012) 'Cis-2-dodecenoic acid receptor RpfR links quorum-sensing signal perception with regulation of virulence through cyclic dimeric guanosine monophosphate turnover', *Proceedings of the National Academy of Sciences of the United States of America*, 109(38), pp. 15479–15484. doi: 10.1073/pnas.1205037109.

Deng, Y., Lim, A., *et al.* (2013) 'Cis-2-dodecenoic acid quorum sensing system modulates N-acyl homoserine lactone production through RpfR and cyclic di-GMP turnover in Burkholderia cenocepacia', *BMC Microbiology*, 13(1). doi: 10.1186/1471-2180-13-148.

Deng, Y., Boon, C., *et al.* (2013) 'Cis-2-dodecenoic acid signal modulates virulence of *Pseudomonas aeruginosa* through interference with quorum sensing systems and T3SS Tracy Raivio', *BMC Microbiology*, 13(1). doi: 10.1186/1471-2180-13-231.

Deng, Y. *et al.* (2016) 'Diffusible signal factor family signals provide a fitness advantage to Xanthomonas campestris pv. campestris in interspecies competition', *Environmental Microbiology*. doi: 10.1111/1462-2920.13244.

Devi, K. P. *et al.* (2015) 'Molecular mechanisms underlying anticancer effects of myricetin', *Life Sciences*. Elsevier Inc., 142, pp. 19–25. doi: 10.1016/j.lfs.2015.10.004.

Diepold, A. and Armitage, J. P. (2015) 'Type III secretion systems: The bacterial flagellum and the injectisome', *Philosophical Transactions of the Royal Society B: Biological Sciences*. doi: 10.1098/rstb.2015.0020.

Döring, G. (2010) 'Prevention of *Pseudomonas aeruginosa* infection in cystic fibrosis patients', *International Journal of Medical Microbiology*, 300(8), pp. 573–577. doi: 10.1016/j.ijmm.2010.08.010.

Dow, J. M. *et al.* (2003) 'Biofilm dispersal in Xanthomonas campestris is controlled by cell-cell signaling and is required for full virulence to plants', *Proceedings of the National Academy of Sciences of the United States of America*, 100(19), pp. 10995–11000. doi: 10.1073/pnas.1833360100.

Dyshlovoy, S. A. and Honecker, F. (2018) 'Marine compounds and cancer: 2017 updates', *Marine Drugs*, 16(2), pp. 2017–2019. doi: 10.3390/md16020041.

Dzobo, K. (2022) 'The Role of Natural Products as Sources of Therapeutic Agents for Innovative Drug Discovery', *Comprehensive Pharmacology*, 2(January), pp. 408–422. doi: 10.1016/B978-0-12-820472-6.00041-4.

Elshaer, S. L. and Shaaban, M. I. (2021) 'Inhibition of Quorum Sensing and Virulence Factors of *Pseudomonas aeruginosa* by Biologically Synthesized Gold and Selenium Nanoparticles', *Antibiotics*, 10(12). doi: 10.3390/ANTIBIOTICS10121461.

Ermer, J. and Vogel, M. (2000) 'Applications of hyphenated LC-MS techniques in pharmaceutical analysis', *Biomedical Chromatography*, 14(6), pp. 373–383. doi: 10.1002/1099-0801(200010)14:6<373::AID-BMC29>3.0.CO;2-S.

Ferrières, L. and Clarke, D. J. (2003) 'The RcsC sensor kinase is required for normal biofilm formation in Escherichia coli K-12 and controls the expression of a regulon in response to growth on a solid surface', *Molecular Microbiology*. doi: 10.1046/j.1365-2958.2003.03815.x.

Filloux, A. (2011) 'Protein secretion systems in *Pseudomonas aeruginosa*: An essay on diversity, evolution, and function', *Frontiers in Microbiology*. doi: 10.3389/fmicb.2011.00155.

Filloux, A. (no date) *Pseudomonas*.

Fouhy, Y. *et al.* (2007) 'Diffusible signal factor-dependent cell-cell signaling and virulence in the nosocomial pathogen Stenotrophomonas maltophilia', *Journal of Bacteriology*, 189(13), pp. 4964–4968. doi: 10.1128/JB.00310-07.

Friedman, L. and Kolter, R. (2004) 'Genes involved in matrix formation in *Pseudomonas aeruginosa* PA14 biofilms', *Molecular Microbiology*, 51(3), pp. 675–690. doi: 10.1046/j.1365-2958.2003.03877.x.

Galperin, M. Y. (2006) 'Structural classification of bacterial response regulators: Diversity of output domains and domain combinations', *Journal of Bacteriology*, 188(12), pp. 4169–4182. doi: 10.1128/JB.01887-05.

Gao, R. and Stock, A. M. (2009) 'Biological insights from structures of two-component proteins', *Annual Review of Microbiology*, 63, pp. 133–154. doi: 10.1146/annurev.micro.091208.073214.

Geng, F. *et al.* (2017) 'Persistent exposure to Porphyromonas gingivalis promotes proliferative and invasion capabilities, and tumorigenic properties of human immortalized oral epithelial cells', *Frontiers in Cellular and Infection Microbiology*, 7(FEB), pp. 1–16. doi: 10.3389/fcimb.2017.00057.

Gerber, F. *et al.* (2004) 'Practical aspects of fast reversed-phase high-performance liquid chromatography using 3 µm particle packed columns and monolithic columns in pharmaceutical development and production working under current good manufacturing practice', *Journal of Chromatography A*, 1036(2), pp. 127–133. doi: 10.1016/j.chroma.2004.02.056.

Ghafoor, A., Hay, I. D. and Rehm, B. H. A. (2011) 'Role of exopolysaccharides in *Pseudomonas aeruginosa* biofilm formation and architecture', *Applied and Environmental Microbiology*, 77(15), pp. 5238–5246. doi: 10.1128/AEM.00637-11.

Ghosh, S. *et al.* (2022) 'Analysis of Antibiofilm Activities of Bioactive Compounds from Honeyweed (Leonurus sibiricus) Against *P. aeruginosa*: an In Vitro and In Silico Approach', *Applied Biochemistry and Biotechnology*. Springer US, (0123456789). doi: 10.1007/s12010-021-03797-1.

Guła, G. *et al.* (2018) 'Complex Signaling Networks Controlling Dynamic Molecular Changes in *Pseudomonas aeruginosa* Biofilm', *Current Medicinal Chemistry*, 26(11), pp. 1979–1993. doi: 10.2174/0929867325666180912110151.

Guo, Y. *et al.* (no date) 'Deciphering bacterial interactions via DSF-regulated public goods in an anammox community', *Research Square*, pp. 1–25. Available at: https://www.researchsquare.com/article/e3496e1c-daa3-4fa8-a444-f1e17519d749/v1?utm_source=researcher_app&utm_medium=referral&utm_campaign=RESR_MRKT_Researcher_inbound.

Guragain, M. *et al.* (2016) 'The *Pseudomonas aeruginosa* PAO1 two-component regulator CarSR regulates calcium homeostasis and calciuminduced virulence factor production through its regulatory targets CarO and CarP', *Journal of Bacteriology*, 198(6), pp. 951–963. doi: 10.1128/JB.00963-15.

Ha, D. G. and O'Toole, G. A. (2015) 'c-di-GMP and its effects on biofilm formation and dispersion: A *Pseudomonas aeruginosa* review', *Microbial Biofilms*, pp. 301–317. doi: 10.1128/9781555817466.ch15.

Han, Y. *et al.* (2019) 'A *Pseudomonas aeruginosa* type VI secretion system regulated by CueR facilitates copper acquisition', *PLoS Pathogens*, 15(12), pp. 1–25. doi: 10.1371/journal.ppat.1008198.

Hasan, T. H. and Al-Harmoosh, R. A. (2020) 'Mechanisms of antibiotics resistance in bacteria', *Systematic Reviews in Pharmacy*, 11(6), pp. 817–823. doi: 10.31838/srp.2020.6.118.

Hay, I. D., Remminghorst, U. and Rehm, B. H. A. (2009) 'MucR, a novel membrane-associated regulator of alginate biosynthesis in *Pseudomonas aeruginosa*', *Applied and Environmental Microbiology*, 75(4), pp. 1110–1120. doi: 10.1128/AEM.02416-08.

He, Y. W. *et al.* (2023) 'DSF-family quorum sensing signal-mediated intraspecies, interspecies, and inter-kingdom communication', *Trends in Microbiology*. The Author(s), 31(1), pp. 36–50. doi: 10.1016/j.tim.2022.07.006.

Henrichfreise, B. *et al.* (2007) 'Resistance mechanisms of multiresistant *Pseudomonas aeruginosa* strains from Germany and correlation with hypermutation', *Antimicrobial Agents and Chemotherapy*, 51(11), pp. 4062–4070. doi: 10.1128/AAC.00148-07.

Hentzer, M. *et al.* (2001) 'Alginate overproduction affects *Pseudomonas aeruginosa* biofilm structure and function', *Journal of Bacteriology*, 183(18), pp. 5395–5401. doi: 10.1128/JB.183.18.5395-5401.2001.

Hentzer, M. *et al.* (2003) 'Attenuation of *Pseudomonas aeruginosa* virulence by quorum sensing inhibitors', *EMBO Journal*, 22(15), pp. 3803–3815. doi: 10.1093/emboj/cdg366.

Hernandez, R. E., Gallegos-Monterrosa, R. and Coulthurst, S. J. (2020) 'Type VI secretion system effector proteins: Effective weapons for bacterial competitiveness', *Cellular Microbiology*, 22(9), pp. 1–9. doi: 10.1111/cmi.13241.

Hickman, J. W., Tifrea, D. F. and Harwood, C. S. (2005) 'A chemosensory system that regulates biofilm formation through modulation of cyclic diguanylate levels', *Proceedings of the National Academy of Sciences of the United States of America*, 102(40), pp. 14422–14427. doi: 10.1073/pnas.0507170102.

Hirakawa, H. *et al.* (2020) 'Progress overview of bacterial two-component regulatory systems as potential targets for antimicrobial chemotherapy', *Antibiotics*, 9(10), pp. 1–15. doi: 10.3390/antibiotics9100635.

Hoffman, L. R. *et al.* (2005) 'Aminoglycoside antibiotics induce bacterial biofilm formation', *Nature*, 436(7054), pp. 1171–1175. doi: 10.1038/nature03912.

Hoggarth, A. *et al.* (2019) 'Mechanistic research holds promise for bacterial vaccines and phage therapies for *Pseudomonas aeruginosa*', *Drug Design, Development and Therapy*, 13, pp. 909–924. doi: 10.2147/DDDT.S189847.

Høiby, N. *et al.* (2001) '*Pseudomonas aeruginosa* and the in vitro and in vivo biofilm mode of growth', *Microbes and Infection*, 3(1), pp. 23–35. doi: 10.1016/S1286-4579(00)01349-6.

Holland-Crimmin, S., Gosnell, P. and Quinn, C. (2011) 'Compound Management: Guidelines for Compound Storage, Provision, and Quality Control', *Current Protocols in Chemical Biology*. doi: 10.1002/9780470559277.ch110095.

Horna, G. and Ruiz, J. (2021) 'Type 3 secretion system of *Pseudomonas aeruginosa*', *Microbiological Research*. Elsevier GmbH, 246(August 2020), p. 126719. doi: 10.1016/j.micres.2021.126719.

Hou, L. *et al.* (2019) 'AmrZ Regulates Swarming Motility Through Cyclic di-GMP-Dependent Motility Inhibition and Controlling Pel Polysaccharide Production in *Pseudomonas aeruginosa* PA14', *Frontiers in Microbiology*, 10(August). doi: 10.3389/fmicb.2019.01847.

Huygens, J. *et al.* (2023) 'The impact of antibiotic residues on resistance patterns in leek at harvest', *Heliyon*. Elsevier Ltd, 9(5), p. e16052. doi: 10.1016/j.heliyon.2023.e16052.

Idowu, T. *et al.* (2019) 'Heterodimeric Rifampicin–Tobramycin conjugates break intrinsic resistance of *Pseudomonas aeruginosa* to doxycycline and chloramphenicol in vitro and in a Galleria mellonella in vivo model', *European Journal of Medicinal Chemistry*. Elsevier Masson SAS, 174, pp. 16–32. doi: 10.1016/j.ejmech.2019.04.034.

Imai, Y. *et al.* (2019) 'A new antibiotic selectively kills Gram-negative pathogens', *Nature*, 576(7787), pp. 459–464. doi: 10.1038/s41586-019-1791-1.

Intile, P. J. *et al.* (2014) 'The AlgZR two-component system recalibrates the RsmAYZ posttranscriptional regulatory system to inhibit expression of the *Pseudomonas aeruginosa* type III secretion system', *Journal of Bacteriology*, 196(2), pp. 357–366. doi: 10.1128/JB.01199-13.

Irie, Y. *et al.* (2012) 'Self-produced exopolysaccharide is a signal that stimulates biofilm formation in *Pseudomonas aeruginosa*', *Proceedings of the National Academy of Sciences of the United States of America*, 109(50), pp. 20632–20636. doi: 10.1073/pnas.1217993109.

Isles, A. *et al.* (1984) 'Pseudomonas cepacia infection in cystic fibrosis: An emerging problem', *The Journal of Pediatrics*. doi: 10.1016/S0022-3476(84)80993-2.

Jayaraman, P. *et al.* (2010) 'Activity and interactions of antibiotic and phytochemical combinations against *Pseudomonas aeruginosa* in vitro', *International Journal of Biological Sciences*, 6(6), pp. 556–568. doi: 10.7150/ijbs.6.556.

Jennings, L. K. *et al.* (2015) 'Pel is a cationic exopolysaccharide that cross-links extracellular DNA in the *Pseudomonas aeruginosa* biofilm matrix', *Proceedings of the National Academy of Sciences of the United States of America*, 112(36), pp. 11353–11358. doi: 10.1073/pnas.1503058112.

Johnston, P. A. *et al.* (2012) 'Development and validation of a high-content screening assay to identify inhibitors of cytoplasmic dynein-mediated transport of glucocorticoid receptor to the nucleus', *Assay and Drug Development Technologies*, 10(5), pp. 432–456. doi: 10.1089/adt.2012.456.

Jouault, A., Saliba, A. M. and Touqui, L. (2022) 'Modulation of the immune response by the *Pseudomonas aeruginosa* type-III secretion system', *Frontiers in Cellular and Infection Microbiology*, 12(November), pp. 1–8. doi: 10.3389/fcimb.2022.1064010.

Juan, C., Peña, C. and Oliver, A. (2017) 'Host and pathogen biomarkers for severe *Pseudomonas aeruginosa* infections', *Journal of Infectious Diseases*, 215(Suppl 1), pp. S44–S51. doi: 10.1093/infdis/jiw299.

Kaihami, G. H. *et al.* (2014) 'Involvement of a 1-Cys Peroxiredoxin in Bacterial Virulence', *PLoS Pathogens*, 10(10). doi: 10.1371/journal.ppat.1004442.

Kaminski, A. *et al.* (2018) '*Pseudomonas aeruginosa* ExoS Induces Intrinsic Apoptosis in Target Host Cells in a Manner That is Dependent on its GAP Domain Activity', *Scientific Reports*. Springer US, 8(1), pp. 1–15. doi: 10.1038/s41598-018-32491-2.

Kang, J. *et al.* (2016) 'Improving drug discovery with high-content phenotypic screens by systematic selection of reporter cell lines', *Nature Biotechnology*, 34(1), pp. 70–77. doi: 10.1038/nbt.3419.

Kaufman, M. R. *et al.* (2000) '*Pseudomonas aeruginosa* mediated apoptosis requires the ADP-ribosylating activity of ExoS', *Microbiology*, 146(10), pp. 2531–2541. doi: 10.1099/00221287-146-10-2531.

Kavanagh, K. and Sheehan, G. (2018) 'The use of galleria mellonella larvae to identify novel antimicrobial agents against fungal species of medical interest', *Journal of Fungi*, 4(3). doi: 10.3390/jof4030113.

Kessler, B., de Lorenzo, V. and Timmis, K. N. (1992) 'A general system to integrate lacZ fusions into the chromosomes of gram-negative eubacteria: regulation of the Pm promoter of the TOL plasmid studied with all controlling elements in monocopy', *MGG Molecular & General Genetics*, 233(1–2), pp. 293–301. doi: 10.1007/BF00587591.

Khalifa, S. A. M. *et al.* (2019) 'Marine natural products: A source of novel anticancer drugs', *Marine Drugs*, 17(9). doi: 10.3390/md17090491.

Killough, M., Rodgers, A. M. and Ingram, R. J. (2022) '*Pseudomonas aeruginosa*: Recent Advances in Vaccine Development', *Vaccines*, 10(7). doi: 10.3390/vaccines10071100.

Kilmury, S. L. N. and Burrows, L. L. (2018) 'The *Pseudomonas aeruginosa* pilSR two-component system regulates both twitching and swimming motilities', *mBio*, 9(4). doi: 10.1128/mBio.01310-18.

Kim, H. S. *et al.* (2021) 'Linoleic acid inhibits *Pseudomonas aeruginosa* biofilm formation by activating diffusible signal factor-mediated quorum sensing', *Biotechnology and Bioengineering*, 118(1), pp. 82–93. doi: 10.1002/bit.27552.

Kim, S. K. and Lee, J. H. (2016) 'Biofilm dispersion in *Pseudomonas aeruginosa*', *Journal of Microbiology*, 54(2), pp. 71–85. doi: 10.1007/s12275-016-5528-7.

Klockgether, T. (2011) 'Update on degenerative ataxias', *Current Opinion in Neurology*, pp. 339–345. doi: 10.1097/WCO.0b013e32834875ba.

Koeppen, K. *et al.* (2021) 'Let-7b-5p in vesicles secreted by human airway cells reduces biofilm formation and increases antibiotic sensitivity of *P. aeruginosa*', *Proceedings of the National Academy of Sciences of the United States of America*, 118(28). doi: 10.1073/pnas.2105370118.

Kuchma, S. L. *et al.* (2007) 'BifA, a cyclic-di-GMP phosphodiesterase, inversely regulates biofilm formation and swarming motility by *Pseudomonas aeruginosa* PA14', *Journal of Bacteriology*, 189(22), pp. 8165–8178. doi: 10.1128/JB.00586-07.

Kulasekara, H. D. *et al.* (2005) 'A novel two-component system controls the expression of *Pseudomonas aeruginosa* fimbrial cup genes', *Molecular Microbiology*, 55(2), pp. 368–380. doi: 10.1111/j.1365-2958.2004.04402.x.

Kulesekara, H. *et al.* (2006) 'Analysis of *Pseudomonas aeruginosa* diguanylate cyclases and phosphodiesterases reveals a role for bis-(3'-5')-cyclic-GMP in virulence', *Proceedings of the National Academy of Sciences of the United States of America*, 103(8), pp. 2839–2844. doi: 10.1073/pnas.0511090103.

Kumar, R. A. and Clark, D. S. (2006) 'High-throughput screening of biocatalytic activity: Applications in drug discovery', *Current Opinion in Chemical Biology*, 10(2), pp. 162–168. doi: 10.1016/j.cbpa.2006.02.033.

Kurnik, M. *et al.* (2018) 'Potent α-Synuclein Aggregation Inhibitors, Identified by High-Throughput Screening, Mainly Target the Monomeric State', *Cell Chemical Biology*. Elsevier Ltd., 25(11), pp. 1389-1402.e9. doi: 10.1016/j.chembiol.2018.08.005.

Lee, D. G. *et al.* (2006) 'Genomic analysis reveals that *Pseudomonas aeruginosa* virulence is combinatorial', *Genome Biology*. doi: 10.1186/gb-2006-7-10-r90.

Lee, J. H. *et al.* (2011) 'Apple flavonoid phloretin inhibits Escherichia coli O157:H7 biofilm formation and ameliorates colon inflammation in rats', *Infection and Immunity*, 79(12), pp. 4819–4827. doi: 10.1128/IAI.05580-11.

Lee, V. T. *et al.* (2007) 'A cyclic-di-GMP receptor required for bacterial exopolysaccharide production', *Molecular Microbiology*, 65(6), pp. 1474–1484. doi: 10.1111/j.1365-2958.2007.05879.x.

Li, L. *et al.* (2019) 'Diffusible signal factor (DSF)-mediated quorum sensing modulates expression of diverse traits in Xanthomonas citri and responses of citrus plants to promote disease', *BMC Genomics*. BMC Genomics, 20(1), pp. 1–22. doi: 10.1186/s12864-018-5384-4.

Li, Y. *et al.* (2013) 'NO-induced biofilm dispersion in *Pseudomonas aeruginosa* is mediated by an MHYT domain-coupled phosphodiesterase', *Journal of Bacteriology*, 195(16), pp. 3531–3542. doi: 10.1128/JB.01156-12.

Li, Y. *et al.* (2014) 'BdlA, DipA and Induced Dispersion Contribute to Acute Virulence and Chronic Persistence of *Pseudomonas aeruginosa*', *PLoS Pathogens*, 10(6). doi: 10.1371/journal.ppat.1004168.

Liao, J., Schurr, M. J. and Sauera, K. (2013) 'The merR-like regulator brlR confers biofilm tolerance by activating multidrug efflux pumps in *Pseudomonas aeruginosa* biofilms', *Journal of Bacteriology*, 195(15), pp. 3352–3363. doi: 10.1128/JB.00318-13.

Lieberman, O. J. *et al.* (2014) 'High-throughput screening using the differential radial capillary action of ligand assay identifies ebselen as an inhibitor of diguanylate cyclases', *ACS Chemical Biology*. doi: 10.1021/cb400485k.

Lin, C. T. *et al.* (2006) 'Identification of an HptB-mediated multi-step phosphorelay in *Pseudomonas aeruginosa* PAO1', *Research in Microbiology*, 157(2), pp. 169–175. doi: 10.1016/j.resmic.2005.06.012.

Liu, Q. *et al.* (2022) 'Reversion of Ceftazidime Resistance in *Pseudomonas aeruginosa* under Clinical Setting', *Microorganisms*, 10(12). doi: 10.3390/microorganisms10122395.

Liu, Z. *et al.* (2022) 'CzcR Is Essential for Swimming Motility in *Pseudomonas aeruginosa* during Zinc Stress', *Microbiology Spectrum*. American Society for Microbiology, 10(6). doi: 10.1128/spectrum.02846-22.

Luscher, A. *et al.* (2020) 'Combined Bacteriophage and Antibiotic Treatment Prevents *Pseudomonas aeruginosa* Infection of Wild Type and cftr- Epithelial Cells', *Frontiers in Microbiology*, 11(August). doi: 10.3389/fmicb.2020.01947.

Ma, L. *et al.* (2009) 'Assembly and development of the *Pseudomonas aeruginosa* biofilm matrix', *PLoS Pathogens*, 5(3). doi: 10.1371/journal.ppat.1000354.

Macfarlane, E. L. A., Kwasnicka, A. and Hancock, R. E. W. (2009) 'Microbiology (Reading Engl) 2000 Macfarlane', pp. 1–12. Available at: papers2://publication/uuid/DEFC8853-3211-4422-8F9D-03540C52603A.

Madziara-Borusiewicz, K. and Lysenko, O. (1971) 'The mechanism of pathogenicity of *Pseudomonas aeruginosa*', *Journal of Invertebrate Pathology*, 17(1), pp. 138–140. doi: 10.1016/0022-2011(71)90139-x.

Mahamad Maifiah, M. H. *et al.* (2022) 'Integrated metabolomic and transcriptomic analyses of the synergistic effect of polymyxin–rifampicin combination against *Pseudomonas aeruginosa*', *Journal of Biomedical Science*. BioMed Central, 29(1), pp. 1–19. doi: 10.1186/s12929-022-00874-3.

Malet, J. K. *et al.* (2022) 'A Model of Intracellular Persistence of *Pseudomonas aeruginosa* in Airway Epithelial Cells', *Cellular Microbiology*, 2022. doi: 10.1155/2022/5431666.

Mattick, J. S. (2002) 'Type IV pili and twitching motility', *Annual Review of Microbiology*, 56, pp. 289–314. doi: 10.1146/annurev.micro.56.012302.160938.

McBride, K. F. J. & M. J. (no date) 'The surprisingly diverse ways that prokaryotes move'.

McCarthy, M. W. (2019) 'Teixobactin: a novel anti-infective agent', *Expert Review of Anti-Infective Therapy*. Taylor & Francis, 17(1), pp. 1–3. doi: 10.1080/14787210.2019.1550357.

McPhee, J. B. *et al.* (2006) 'Contribution of the PhoP-PhoQ and PmrA-PmrB two-component regulatory systems to Mg2+-induced gene regulation in *Pseudomonas aeruginosa*', *Journal of Bacteriology*, 188(11), pp. 3995–4006. doi: 10.1128/JB.00053-06.

Medzhitov, R., Preston-Hurlburt, P. and Janeway, C. A. (1997) 'A human homologue of the Drosophila toll protein signals activation of adaptive immunity', *Nature*. doi: 10.1038/41131.

Meirelles, L. A. and Newman, D. K. (2018) 'Both toxic and beneficial effects of pyocyanin contribute to the lifecycle of *Pseudomonas aeruginosa*', *Molecular Microbiology*, 110(6), pp. 995–1010. doi: 10.1111/mmi.14132.

Merritt, J. H. *et al.* (2007) 'SadC reciprocally influences biofilm formation and swarming motility via modulation of exopolysaccharide production and flagellar function', *Journal of Bacteriology*, 189(22), pp. 8154–8164. doi: 10.1128/JB.00585-07.

Michel, G. P. F., Durand, E. and Filloux, A. (2007) 'XphA/XqhA, a novel GspCD subunit for type II secretion in *Pseudomonas aeruginosa*', *Journal of Bacteriology*, 189(10), pp. 3776–3783. doi: 10.1128/JB.00205-07.

Miller, V. L. and Mekalanos, J. J. (1988) 'A novel suicide vector and its use in construction of insertion mutations: Osmoregulation of outer membrane proteins and virulence determinants in Vibrio cholerae requires toxR', *Journal of Bacteriology*, 170(6), pp. 2575–2583. doi: 10.1128/jb.170.6.2575-2583.1988.

Miyata, S. *et al.* (2003) 'Use of the Galleria mellonella caterpillar as a model host to study the role of the type III secretion system in *Pseudomonas aeruginosa* pathogenesis', *Infection and Immunity*, 71(5), pp. 2404–2413. doi: 10.1128/IAI.71.5.2404-2413.2003.

Mizgerd, J. P. and Skerrett, S. J. (2008) 'Animal models of human pneumonia', *American Journal of Physiology - Lung Cellular and Molecular Physiology*, 294(3). doi: 10.1152/ajplung.00330.2007.

Mohammed, N. S. and Ali, E. H. (2021) 'Extraction, Purification, and Characterization of Chloramphenicol Acetyltransferase from *Pseudomonas aeruginosa*', *International Journal of Drug Delivery Technology*, 11(4), pp. 1429–1434. doi: 10.25258/ijddt.11.4.52.

Moreau-Marquis, S. *et al.* (2010) 'Co-culture models of *Pseudomonas aeruginosa* biofilms grown on live human airway cells', *Journal of Visualized Experiments*, (44). doi: 10.3791/2186.

Morgan, R. *et al.* (2006) 'BdlA, a chemotaxis regulator essential for biofilm dispersion in *Pseudomonas aeruginosa*', *Journal of Bacteriology*, 188(21), pp. 7335–7343. doi: 10.1128/JB.00599-06.

Morita, Y., Tomida, J. and Kawamura, Y. (2013) 'Responses of *Pseudomonas aeruginosa* to antimicrobials', *Frontiers in Microbiology*, 4(JAN), pp. 1–8. doi: 10.3389/fmicb.2013.00422.

Mosaei, H. *et al.* (2018) 'Mode of Action of Kanglemycin A, an Ansamycin Natural Product that Is Active against Rifampicin-Resistant Mycobacterium tuberculosis', *Molecular Cell*. Elsevier Inc., 72(2), pp. 263-274.e5. doi: 10.1016/j.molcel.2018.08.028.

Mulcahy, L. R. *et al.* (2010) 'Emergence of *Pseudomonas aeruginosa* strains producing high levels of persister cells in patients with cystic fibrosis', *Journal of Bacteriology*. doi: 10.1128/JB.01651-09.

Murray, T. S. and Kazmierczak, B. I. (2008) '*Pseudomonas aeruginosa* exhibits sliding motility in the absence of type IV pili and flagella', *Journal of Bacteriology*, 190(8), pp. 2700–2708. doi: 10.1128/JB.01620-07.

Nadanaciva, S. *et al.* (2011) 'A high content screening assay for identifying lysosomotropic compounds', *Toxicology in Vitro*. Elsevier Ltd, 25(3), pp. 715–723. doi: 10.1016/j.tiv.2010.12.010.

Naguib, M. M. and Valvano, M. A. (2018) 'Vitamin E Increases Antimicrobial Sensitivity by Inhibiting Bacterial Lipocalin Antibiotic Binding', *mSphere*, 3(6). doi: 10.1128/msphere.00564-18.

Narayanaswamy, V. P. *et al.* (2018) 'Novel glycopolymer eradicates antibiotic- and CCCP-induced persister cells in *Pseudomonas aeruginosa*', *Frontiers in Microbiology*, 9(AUG), pp. 1–12. doi: 10.3389/fmicb.2018.01724.

Ng, W. L. *et al.* (2012) 'Broad spectrum pro-quorum-sensing molecules as inhibitors of virulence in vibrios', *PLoS Pathogens*, 8(6). doi: 10.1371/journal.ppat.1002767.

Nikolaidis, M. *et al.* (2020) 'Comparative analysis of the core proteomes among the Pseudomonas major evolutionary groups reveals species-specific adaptations for *Pseudomonas aeruginosa* and Pseudomonas chlororaphis', *Diversity*, 12(8). doi: 10.3390/D12080289.

Nolan, C. and Behrends, V. (2021) 'Sub-inhibitory antibiotic exposure and virulence in *Pseudomonas aeruginosa*', *Antibiotics*, 10(11). doi: 10.3390/antibiotics10111393.

O'Callaghan, D. and Vergunst, A. (2010) 'Non-mammalian animal models to study infectious disease: worms or fly fishing?', *Current Opinion in Microbiology*, 13(1), pp. 79–85. doi: 10.1016/j.mib.2009.12.005.

Olszak, T. *et al.* (2015) 'In vitro and in vivo antibacterial activity of environmental bacteriophages against *Pseudomonas aeruginosa* strains from cystic fibrosis patients', *Applied Microbiology and Biotechnology*, 99(14), pp. 6021–6033. doi: 10.1007/s00253-015-6492-6.

Orr, M. W. *et al.* (2015) 'Oligoribonuclease is the primary degradative enzyme for pGpG in *Pseudomonas aeruginosa* that is required for cyclic-di-GMP turnover', *Proceedings of the National Academy of Sciences of the United States of America*, 112(36), pp. E5048–E5057. doi: 10.1073/pnas.1507245112.

Osipov, A. *et al.* (2019) 'Small molecule immunomodulation: The tumor microenvironment and overcoming immune escape', *Journal for ImmunoTherapy of Cancer*. doi: 10.1186/s40425-019-0667-0.

Oyardi, O., Savage, P. B. and Guzel, C. B. (2022) 'Effects of Ceragenins and Antimicrobial Peptides on the A549 Cell Line and an In Vitro Co-Culture Model of A549 Cells and *Pseudomonas aeruginosa*', *Pathogens*, 11(9). doi: 10.3390/pathogens11091044.

Ozer, E. A. *et al.* (2019) 'The Population Structure of *Pseudomonas aeruginosa* Is Characterized by Genetic Isolation of exoU+ and exoS+ Lineages', *Genome Biology and Evolution*, 11(7), pp. 1780–1796. doi: 10.1093/gbe/evz119.

Pang, Z. *et al.* (2019) 'Antibiotic resistance in *Pseudomonas aeruginosa*: mechanisms and alternative therapeutic strategies', *Biotechnology Advances*. Elsevier, 37(1), pp. 177–192. doi: 10.1016/j.biotechadv.2018.11.013.

Di Paola, M. *et al.* (2017) 'SLC6A14 is a genetic modifier of cystic fibrosis that regulates *Pseudomonas aeruginosa* attachment to human bronchial epithelial cells', *mBio*, 8(6). doi: 10.1128/mBio.02073-17.

Pesci, E. C. *et al.* (1999) 'Quinolone signaling in the cell-to-cell communication system of *Pseudomonas aeruginosa*', *Proceedings of the National Academy of Sciences of the United States of America*, 96(20), pp. 11229–11234. doi: 10.1073/pnas.96.20.11229.

Petrova, O. E., Cherny, K. E. and Sauer, K. (2015) 'The diguanylate cyclase GcbA facilitates *Pseudomonas aeruginosa* biofilm dispersion by activating BdlA', *Journal of Bacteriology*, 197(1), pp. 174–187. doi: 10.1128/JB.02244-14.

Piddock, L. J. V. (2015) 'Teixobactin, the first of a new class of antibiotics discovered by ichip technology?', *Journal of Antimicrobial Chemotherapy*, 70(10), pp. 2679–2680. doi: 10.1093/jac/dkv175.

Pier, G. B. *et al.* (2001) 'Role of alginate O acetylation in resistance of mucoid *Pseudomonas aeruginosa* to opsonic phagocytosis', *Infection and Immunity*, 69(3), pp. 1895–1901. doi: 10.1128/IAI.69.3.1895-1901.2001.

Pires, D. P. *et al.* (2015) 'Phage Therapy: a Step Forward in the Treatment of *Pseudomonas aeruginosa* Infections', *Journal of Virology*, 89(15), pp. 7449–7456. doi: 10.1128/jvi.00385-15.

Qi, L. *et al.* (2022) 'Resveratrol Improves The Antimicrobial Properties Of Polymyxin B Against Multidrug-Resistant *Pseudomonas aeruginosa*', *Res Sq*, pp. 1–22. Available at: https://doi.org/10.21203/rs.3.rs-1359376/v1.

Rahme, L. G. *et al.* (1995) 'Common virulence factors for bacterial pathogenicity in plants and animals', *Science*, 268(5219), pp. 1899–1902. doi: 10.1126/science.7604262.

Ramirez, D. M. *et al.* (2022) 'Guanidinylated Polymyxins as Outer Membrane Permeabilizers Capable of Potentiating Rifampicin, Erythromycin, Ceftazidime and Aztreonam against Gram-Negative Bacteria', *Antibiotics*, 11(10). doi: 10.3390/antibiotics11101277.

Rasamiravaka, T. *et al.* (2015) 'The Formation of Biofilms by *Pseudomonas aeruginosa*', *BioMed Research International*, 2015, pp. 1–17. Available at: http://dx.doi.org/10.1155/2015/759348%0A.

Rasmussen, T. B. and Givskov, M. (2006) 'Quorum-sensing inhibitors as anti-pathogenic drugs', *International Journal of Medical Microbiology*, 296(2–3), pp. 149–161. doi: 10.1016/j.ijmm.2006.02.005.

Rather, M. A., Gupta, K. and Mandal, M. (2021) 'Inhibition of biofilm and quorum sensing-regulated virulence factors in *Pseudomonas aeruginosa* by Cuphea carthagenensis (Jacq.) J. F. Macbr. Leaf extract: An in vitro study', *Journal of Ethnopharmacology*. Elsevier B.V., 269(October 2020), p. 113699. doi: 10.1016/j.jep.2020.113699.

Reis, R. S. *et al.* (2011) 'Gene regulation of rhamnolipid production in *Pseudomonas aeruginosa* - A review', *Bioresource Technology*. Elsevier Ltd, 102(11), pp. 6377–6384. doi: 10.1016/j.biortech.2011.03.074.

Reuter, K., Steinbach, A. and Helms, V. (2016) 'Interfering with bacterial quorum sensing', *Perspectives in Medicinal Chemistry*, 8, pp. 1–15. doi: 10.4137/PMc.s13209.

Romling, U., Galperin, M. Y. and Gomelsky, M. (2013) 'Cyclic di-GMP: the First 25 Years of a Universal Bacterial Second Messenger', *Microbiology and Molecular Biology Reviews*, 77(1), pp. 1–52. doi: 10.1128/mmbr.00043-12.

Römling, U., Gomelsky, M. and Galperin, M. Y. (2005) 'C-di-GMP: The dawning of a novel bacterial signalling system', *Molecular Microbiology*, 57(3), pp. 629–639. doi: 10.1111/j.1365-2958.2005.04697.x.

Ross, P. *et al.* (1987) 'Regulation of cellulose synthesis in Acetobacter xylinum by cyclic diguanylic acid', *Nature*, 325(6101), pp. 279–281. doi: 10.1038/325279a0.

Ross, P., Mayer, R. and Benziman, M. (1991) 'Cellulose biosynthesis and function in bacteria', *Microbiological Reviews*, 55(1), pp. 35–58. doi: 10.1128/mmbr.55.1.35-58.1991.

Rudzite, M. *et al.* (2023) *Effectiveness of Pseudomonas aeruginosa type VI secretion system relies on toxin potency and type IV pili-dependent interaction*, *PLOS Pathogens*. doi: 10.1371/journal.ppat.1011428.

Rugjee, K. N., An, S. Q. and Ryan, R. P. (2016) 'Establishment of a high-throughput setup for screening small molecules that modulate c-di-GMP signaling in *Pseudomonas aeruginosa*', *Journal of Visualized Experiments*, 2016(112), pp. 1–7. doi: 10.3791/54115.

Rutherford, S. T. and Bassler, B. L. (2012) 'Bacterial quorum sensing: Its role in virulence and possibilities for its control', *Cold Spring Harbor Perspectives in Medicine*, 2(11), pp. 1–26. doi: 10.1101/cshperspect.a012427.

Ryan, R. P. *et al.* (2006) 'Cell-cell signaling in Xanthomonas campestris involves an HD-GYP domain protein that functions in cyclic di-GMP turnover', *Proceedings of the National Academy of Sciences of the United States of America*. doi: 10.1073/pnas.0600345103.

Ryan, R. P. *et al.* (2008) 'Interspecies signalling via the Stenotrophomonas maltophilia diffusible signal factor influences biofilm formation and polymyxin tolerance in *Pseudomonas aeruginosa*', *Molecular Microbiology*, 68(1), pp. 75–86. doi: 10.1111/j.1365-2958.2008.06132.x.

Ryan, R. P. *et al.* (2010) 'Cell-cell signal-dependent dynamic interactions between HD-GYP and GGDEF domain proteins mediate virulence in Xanthomonas campestris', *Proceedings of the National Academy of Sciences of the United States of America*. doi: 10.1073/pnas.0912839107.

Ryan, R. P. (2013) 'Cyclic di-GMP signalling and the regulation of bacterial virulence', *Microbiology (United Kingdom)*, 159(PART7), pp. 1286–1297. doi: 10.1099/mic.0.068189-0.

Ryan, R. P. *et al.* (2015) 'The DSF Family of Cell–Cell Signals: An Expanding Class of Bacterial Virulence Regulators', *PLoS Pathogens*, 11(7), pp. 1–14. doi: 10.1371/journal.ppat.1004986.

Ryan, R. P. and Dow, J. M. (2008) 'Diffusible signals and interspecies communication in bacteria', *Microbiology*. doi: 10.1099/mic.0.2008/017871-0.

Ryan, R. P. and Dow, J. M. (2011) 'Communication with a growing family: Diffusible signal factor (DSF) signaling in bacteria', *Trends in Microbiology*. doi: 10.1016/j.tim.2010.12.003.

Ryan, R. P., Tolker-Nielsen, T. and Dow, J. M. (2012) 'When the PilZ don't work: Effectors for cyclic di-GMP action in bacteria', *Trends in Microbiology*. Elsevier Ltd, 20(5), pp. 235–242. doi: 10.1016/j.tim.2012.02.008.

Rybtke, M. T. *et al.* (2012) 'Fluorescence-based reporter for gauging cyclic Di-GMP levels in *Pseudomonas aeruginosa*', *Applied and Environmental Microbiology*, 78(15), pp. 5060–5069. doi: 10.1128/AEM.00414-12.

Ryder, C., Byrd, M. and Wozniak, D. J. (2007) 'Role of polysaccharides in *Pseudomonas aeruginosa* biofilm development', *Current Opinion in Microbiology*. doi: 10.1016/j.mib.2007.09.010.

Ryder, C., Byrd, M. and Wozniak, D. J. (2016) 'development', 10(6), pp. 644–648.

Saga, Y. *et al.* (2005) 'Bacteriochlorophyll-c homolog composition in green sulfur photosynthetic bacterium Chlorobium vibrioforme dependent on the concentration of sodium sulfide in liquid cultures', in *Photosynthesis Research*. doi: 10.1007/s11120-005-5301-y.

Sambanthamoorthy, K. *et al.* (2012) 'Identification of small molecules that antagonize diguanylate cyclase enzymes to inhibit biofilm formation', *Antimicrobial Agents and Chemotherapy*. doi: 10.1128/AAC.01396-12.

Sambanthamoorthy, K. *et al.* (2014) 'Identification of small molecules inhibiting diguanylate cyclases to control bacterial biofilm development', *Biofouling*. doi: 10.1080/08927014.2013.832224.

Sana, T. G., Berni, B. and Bleves, S. (2016) 'The T6SSs of *Pseudomonas aeruginosa* strain pao1 and their effectors: Beyond bacterial-cell targeting', *Frontiers in Cellular and Infection Microbiology*, 6(JUN). doi: 10.3389/fcimb.2016.00061.

Sandoval-Motta, S. and Aldana, M. (2016) 'Adaptive resistance to antibiotics in bacteria: A systems biology perspective', *Wiley Interdisciplinary Reviews: Systems Biology and Medicine*, 8(3), pp. 253–267. doi: 10.1002/wsbm.1335.

Santos, J. F. (2012) 'Business or Fun?: Similarities and Differences between Portuguese and International Wine Bloggers', *Management*, 2(1), pp. 1–9. doi: 10.5923/j.mm.20120201.01.

Sarkar, S. (2020) 'Release mechanisms and molecular interactions of *Pseudomonas aeruginosa* extracellular DNA', *Applied Microbiology and Biotechnology*, 104(15), pp. 6549–6564. doi: 10.1007/s00253-020-10687-9.

Sauer, K. *et al.* (2002) 'Displays Multiple Phenotypes during Development as a Biofilm', *Society*, 184(4), pp. 1140–1154. doi: 10.1128/JB.184.4.1140.

Schmidt, A. *et al.* (2016) 'Oxygen-dependent regulation of c-di-GMP synthesis by SadC controls alginate production in *Pseudomonas aeruginosa*', *Environmental Microbiology*, 18(10), pp. 3390–3402. doi: 10.1111/1462-2920.13208.

Schuster, M. and Greenberg, E. P. (2007) 'Early activation of quorum sensing in *Pseudomonas aeruginosa* reveals the architecture of a complex regulon', *BMC Genomics*, 8, pp. 1–11. doi: 10.1186/1471-2164-8-287.

Semwal, D. K. *et al.* (2016) 'Myricetin: A dietary molecule with diverse biological activities', *Nutrients*, 8(2), pp. 1–31. doi: 10.3390/nu8020090.

Sermet-Gaudelus, I. (2013) 'Ivacaftor treatment in patients with cystic fibrosis and the G551D-CFTR mutation', *European Respiratory Review*, 22(127), pp. 66–71. doi: 10.1183/09059180.00008512.

Shen, B. (2015) 'A New Golden Age of Natural Products Drug Discovery', *Cell*. Elsevier Inc., 163(6), pp. 1297–1300. doi: 10.1016/j.cell.2015.11.031.

Simm, R. *et al.* (2004) 'GGDEF and EAL domains inversely regulate cyclic di-GMP levels and transition from sessibility to motility', *Molecular Microbiology*, 53(4), pp. 1123–1134. doi: 10.1111/j.1365-2958.2004.04206.x.

Skerker, J. M. and Berg, H. C. (2001) 'Direct observation of extension and retraction of type IV pili', *Proceedings of the National Academy of Sciences of the United States of America*. doi: 10.1073/pnas.121171698.

Slater, H. *et al.* (2000) 'A two-component system involving an HD-GYP domain protein links cell-cell signalling to pathogenicity gene expression in Xanthomonas campestris', *Molecular Microbiology*. doi: 10.1046/j.1365-2958.2000.02196.x.

De Smet, J. *et al.* (2017) 'Pseudomonas predators: Understanding and exploiting phage-host interactions', *Nature Reviews Microbiology*. doi: 10.1038/nrmicro.2017.61.

Smith, R. S. and Iglewski, B. H. (2003) '*P. aeruginosa* quorum-sensing systems and virulence', *Current Opinion in Microbiology*, 6(1), pp. 56–60. doi: 10.1016/S1369-5274(03)00008-0.

Stoltz, D. A. *et al.* (2008) 'Are Protected From', *The Journal of Clinical Investigation*, 118(9), pp. 3123–3131. doi: 10.1172/JCI35147DS1.

Sultan, M., Arya, R. and Kim, K. K. (2021) 'Roles of two-component systems in *Pseudomonas aeruginosa* virulence', *International Journal of Molecular Sciences*, 22(22). doi: 10.3390/ijms222212152.

Sun, B. *et al.* (2021) 'Inhibition of Quorum Sensing and Biofilm Formation of Esculetin on Aeromonas Hydrophila', *Frontiers in Microbiology*, 12(September). doi: 10.3389/fmicb.2021.737626.

Szamosvári, D. *et al.* (2016) 'Synthetic quinolone signal analogues inhibiting the virulence factor elastase of *Pseudomonas aeruginosa*', *Chemical Communications*, 52(92), pp. 13440–13443. doi: 10.1039/c6cc06295d.

Szymański, P., Markowicz, M. and Mikiciuk-Olasik, E. (2012) 'Adaptation of high-throughput screening in drug discovery-toxicological screening tests', *International Journal of Molecular Sciences*, 13(1), pp. 427–452. doi: 10.3390/ijms13010427.

Taccetti, G. *et al.* (2020) 'A critical review of definitions used to describe *Pseudomonas aeruginosa* microbiological status in patients with cystic fibrosis for application in clinical trials', *Journal of Cystic Fibrosis*, 19(1), pp. 52–67. doi: 10.1016/j.jcf.2019.08.014.

Tamma, P. D., Cosgrove, S. E. and Maragakis, L. L. (2012) 'Combination therapy for treatment of infections with gram-negative bacteria', *Clinical Microbiology Reviews*. doi: 10.1128/CMR.05041-11.

Tan, B. and Vanitha, J. (2012) 'Immunomodulatory and Antimicrobial Effects of Some Traditional Chinese Medicinal Herbs: A Review', *Current Medicinal Chemistry*. doi: 10.2174/0929867043365161.

Tart, A. H., Blanks, M. J. and Wozniak, D. J. (2006) 'The AlgT-dependent transcriptional regulator AmrZ (AlgZ) inhibits flagellum biosynthesis in mucoid, nonmotile *Pseudomonas aeruginosa* cystic fibrosis isolates', *Journal of Bacteriology*, 188(18), pp. 6483–6489. doi: 10.1128/JB.00636-06.

Thi, M. T. T., Wibowo, D. and Rehm, B. H. A. (2020) '*Pseudomonas aeruginosa* biofilms', *International Journal of Molecular Sciences*, 21(22), pp. 1–25. doi: 10.3390/ijms21228671.

Tischler, A. D. and Camilli, A. (2009) 'formation', 53(3), pp. 857–869. doi: 10.1111/j.1365-2958.2004.04155.x.Cyclic.

Torrens, G. *et al.* (2019) 'Regulation of AmpC-Driven -Lactam Resistance in', 4(6), pp. 1–14.

Toyofuku, M. *et al.* (2016) 'Environmental factors that shape biofilm formation', *Bioscience, Biotechnology and Biochemistry*, pp. 7–12. doi: 10.1080/09168451.2015.1058701.

Tran, C. S. *et al.* (2014) 'The *Pseudomonas aeruginosa* Type III Translocon Is Required for Biofilm Formation at the Epithelial Barrier', *PLoS Pathogens*, 10(11). doi: 10.1371/journal.ppat.1004479.

Trapnell, C. *et al.* (2012) 'Differential gene and transcript expression analysis of RNA-seq experiments with TopHat and Cufflinks', *Nature Protocols*, 7(3), pp. 562–578. doi: 10.1038/nprot.2012.016.

Tsai, C. J. Y., Loh, J. M. S. and Proft, T. (2016) 'Galleria mellonella infection models for the study of bacterial diseases and for antimicrobial drug testing', *Virulence*. Taylor & Francis, 7(3), pp. 214–229. doi: 10.1080/21505594.2015.1135289.

Twomey, K. B. *et al.* (2012) 'Bacterial cis-2-unsaturated fatty acids found in the cystic fibrosis airway modulate virulence and persistence of *Pseudomonas aeruginosa*', *ISME Journal*. doi: 10.1038/ismej.2011.167.

Uddin, T. M. *et al.* (2021) 'Antibiotic resistance in microbes: History, mechanisms, therapeutic strategies and future prospects', *Journal of Infection and Public Health*, 14(12), pp. 1750–1766. doi: 10.1016/j.jiph.2021.10.020.

Ulloa, E. R. and Sakoulas, G. (2022) 'Azithromycin: An Underappreciated Quinolone-Sparing Oral Treatment for *Pseudomonas aeruginosa* Infections', *Antibiotics*, 11(4), pp. 10–15. doi: 10.3390/antibiotics11040515.

Valentini, M. and Filloux, A. (2016a) 'Biofilms and Cyclic di-GMP (c-di-GMP) signaling: Lessons from *Pseudomonas aeruginosa* and other bacteria', *Journal of Biological Chemistry*, 291(24), pp. 12547–12555. doi: 10.1074/jbc.R115.711507.

Valentini, M. and Filloux, A. (2016b) 'Biofilms and Cyclic di-GMP (c-di-GMP) signaling: Lessons from *Pseudomonas aeruginosa* and other bacteria', *Journal of Biological Chemistry*. Â© 2016 ASBMB. Currently published by Elsevier Inc; originally published by American Society for Biochemistry and Molecular Biology, 291(24), pp. 12547–12555. doi: 10.1074/jbc.R115.711507.

Vasavi, H. S. *et al.* (2017) 'Bioavailability-enhanced Resveramax™ modulates quorum sensing and inhibits biofilm formation in *Pseudomonas aeruginosa* PAO1', *Microbial Pathogenesis*. Elsevier Ltd, 104, pp. 64–71. doi: 10.1016/j.micpath.2017.01.015.

Vasquez-Rifo, A. *et al.* (2019) 'The *Pseudomonas aeruginosa* accessory genome elements influence virulence towards Caenorhabditis elegans', *Genome Biology*. Genome Biology, 20(1), pp. 1–22. doi: 10.1186/s13059-019-1890-1.

Vernooij, L. *et al.* (2021) 'High-throughput screening identifies idasanutlin as a resensitizing drug for venetoclax-resistant neuroblastoma cells', *Molecular Cancer Therapeutics*, 20(6), pp. 1161–1172. doi: 10.1158/1535-7163.MCT-20-0666.

Vitro, I. *et al.* (2023) 'Resveratrol Increases Sensitivity of Clinical Colistin-Resistant'. American Society for Microbiology, 11(1), pp. 1–13.

Wagner, V. E., Gillis, R. J. and Iglewski, B. H. (2004) 'Transcriptome analysis of quorum-sensing regulation and virulence factor expression in *Pseudomonas aeruginosa*', *Vaccine*, 22(SUPPL. 1). doi: 10.1016/j.vaccine.2004.08.011.

Walsh, V. and Goodman, J. (1999) 'Cancer chemotherapy, biodiversity, public and private property: The case of the anti-cancer drug Taxol', *Social Science and Medicine*, 49(9), pp. 1215–1225. doi: 10.1016/S0277-9536(99)00161-6.

Wang, H., Liao, L. and Chen, S. (2020) 'crossm Substrate-Inducible Genes Conferring Degradation of Diffusible Signal Factor', 86(7), pp. 1–18.

Wang, L. H. *et al.* (2004) 'A bacterial cell-cell communication signal with cross-kingdom structural analogues', *Molecular Microbiology*, 51(3), pp. 903–912. doi: 10.1046/j.1365-2958.2003.03883.x.

Wang, M. *et al.* (2022) 'The cis -2-Dodecenoic Acid (BDSF) Quorum Sensing System in'. American Society for Microbiology, (19).

Wang, Z. H. *et al.* (2010) 'Myricetin suppresses oxidative stress-induced cell damage via both direct and indirect antioxidant action', *Environmental Toxicology and Pharmacology*, 29(1), pp. 12–18. doi: 10.1016/j.etap.2009.08.007.

Warchal, S. J. *et al.* (2020) 'High content phenotypic screening identifies serotonin receptor modulators with selective activity upon breast cancer cell cycle and cytokine signaling pathways', *Bioorganic and Medicinal Chemistry*. Elsevier, 28(1), p. 115209. doi: 10.1016/j.bmc.2019.115209.

Watnick, P. and Kolter, R. (2000) 'Biofilm, city of microbes', *Journal of Bacteriology*, 182(10), pp. 2675–2679. doi: 10.1128/JB.182.10.2675-2679.2000.

Weichert, S. *et al.* (2013) 'Bioengineered 2'-fucosyllactose and 3-fucosyllactose inhibit the adhesion of *Pseudomonas aeruginosa* and enteric pathogens to human intestinal and respiratory cell lines', *Nutrition Research*. Elsevier Inc., 33(10), pp. 831–838. doi: 10.1016/j.nutres.2013.07.009.

WHO (2017) 'Global priority list of antibiotic-resistant batceria to guide research, discovery, and development of new antibiotics', *Who*.

Winstanley, C., O'Brien, S. and Brockhurst, M. A. (2016) '*Pseudomonas aeruginosa* Evolutionary Adaptation and Diversification in Cystic Fibrosis Chronic Lung Infections', *Trends in Microbiology*. Elsevier Ltd, 24(5), pp. 327–337. doi: 10.1016/j.tim.2016.01.008.

Wood, T. E. *et al.* (2019) 'The *Pseudomonas aeruginosa* T6SS Delivers a Periplasmic Toxin that Disrupts Bacterial Cell Morphology', *Cell Reports*, 29(1), pp. 187-201.e7. doi: 10.1016/j.celrep.2019.08.094.

Wu, W. *et al.* (2014) *Pseudomonas aeruginosa*, *Molecular Medical Microbiology*. Elsevier Ltd. doi: 10.1016/B978-0-12-397169-2.00041-X.

Xie, Y. *et al.* (2022) 'Inhibition of Quorum-Sensing Regulator from *Pseudomonas aeruginosa* Using a Flavone Derivative', *Molecules*, 27(8), pp. 1–13. doi: 10.3390/molecules27082439.

Xu, L. *et al.* (2016) 'A cyclic di-GMP-binding adaptor protein interacts with histidine kinase to regulate two-component signaling', *Journal of Biological Chemistry*, 291(31), pp. 16112–16123. doi: 10.1074/jbc.M116.730887.

Yang, A. *et al.* (2017) 'Influence of Physical Effects on the Swarming Motility of *Pseudomonas aeruginosa*', *Biophysical Journal*. Biophysical Society, 112(7), pp. 1462–1471. doi: 10.1016/j.bpj.2017.02.019.

Yang, L. *et al.* (2016) 'New insights into the antibacterial activity of hydroxycoumarins against ralstonia solanacearum', *Molecules*, 21(4), pp. 1–13. doi: 10.3390/molecules21040468.

Yang, Y. *et al.* (2022) 'H3-T6SS of *Pseudomonas aeruginosa* PA14 contributes to environmental adaptation via secretion of a biofilm-promoting effector', *Stress Biology*, 2(1). doi: 10.1007/s44154-022-00078-7.

Yazdanian, M. *et al.* (2023) 'The comparative effects of erythromycin and amikacin on acute respiratory *Pseudomonas aeruginosa* infection', *Veterinary Medicine and Science*, 9(2), pp. 867–875. doi: 10.1002/vms3.991.

Zanella, F., Lorens, J. B. and Link, W. (2010) 'High content screening: Seeing is believing', *Trends in Biotechnology*. Elsevier Ltd, 28(5), pp. 237–245. doi: 10.1016/j.tibtech.2010.02.005.

Zdybicka-Barabas, A. *et al.* (2012) 'Synergistic action of Galleria mellonella anionic peptide 2 and lysozyme against Gram-negative bacteria', *Biochimica et Biophysica Acta - Biomembranes*, 1818(11), pp. 2623–2635. doi: 10.1016/j.bbamem.2012.06.008.

Zhang, L., Xie, Q. and Li, X. (2022) 'Esculetin: A review of its pharmacology and pharmacokinetics', *Phytotherapy Research*, 36(1), pp. 279–298. doi: 10.1002/ptr.7311.

Zhao, Y. hu *et al.* (2019) 'Identification and expression analysis of ceftriaxone resistance-related genes in Neisseria gonorrhoeae integrating RNA-Seq data and qRT-PCR validation', *Journal of Global Antimicrobial Resistance*. Taibah University, 16(2019), pp. 202–209. doi: 10.1016/j.jgar.2018.10.008.

Zheng, Z. *et al.* (2017) 'crossm Synergistic Efficacy of Aedes aegypti', 61(7), pp. 1–15.

Zhou, T. *et al.* (2022) 'The Two-Component System FleS / FleR Represses H1-T6SS via', *Applied and environmental microbiology*. American Society for Microbiology, 88(2), pp. e01655-21.

Zscherp, R. *et al.* (2023) 'Design of non-cytotoxic 6,7-dihydroxycoumarin-5-carboxylates with antibiofilm activity against Staphylococcus aureus and Candida albicans', *Organic and Biomolecular Chemistry*. Royal Society of Chemistry, 21. doi: 10.1039/d3ob00303e.